

AD734762

AFOSR FINAL SCIENTIFIC REPORT  
AFOSR TR 71-3003

COMPLEX MIXING MODELS FOR CHEMICAL REACTION SYSTEMS

by

Reuel Shinnar and Stanley Katz  
Department of Chemical Engineering  
The City College, The City University of New York

Research Sponsored by the  
Air Force Office of Scientific Research  
Grant No. AF AFOSR 67-0921

DDC  
RECORDED  
JAN 11 1972  
LIBRARY

Reproduced by  
NATIONAL TECHNICAL  
INFORMATION SERVICE  
Springfield, Va. 22151



THE CITY COLLEGE  
RESEARCH FOUNDATION  
THE CITY COLLEGE of  
THE CITY UNIVERSITY of NEW YORK

Approved for public release  
distribution unlimited.

135

## DOCUMENT CONTROL DATA - R &amp; D

(Security classification of title, body of abstract or indexing annotation must be entered when the overall report is classified)

1. ORIGINATING ACTIVITY (Corporate author) THE CITY COLLEGE RESEARCH FOUNDATION THE CITY COLLEGE OF THE CITY UNIVERSITY OF NEW YORK CONVENT AVENUE AT 138TH STREET NEW YORK, NEW YORK 10031		2a. REPORT SECURITY CLASSIFICATION UNCLASSIFIED	
3. REPORT TITLE COMPLEX MIXING MODELS FOR CHEMICAL REACTION SYSTEMS		2b. GROUP	
4. DESCRIPTIVE NOTES (Type of report and inclusive dates) Scientific Final			
5. AUTHOR(S) (First name, middle initial, last name) REUEL SHINNAR STANLEY KATZ			
6. REPORT DATE Dec 1971	7a. TOTAL NO. OF PAGES 141	7b. NO. OF REFS 12	
8a. CONTRACT OR GRANT NO AFOSR-921-67		8b. ORIGINATOR'S REPORT NUMBER(S)	
b. PROJECT NO 9711-02	9b. OTHER REPORT NO(S) (Any other numbers that may be assigned this report)		
c. 61102F	AFOSR-TR-71-3003		
d. 681308			
10. DISTRIBUTION STATEMENT Approved for public release; distribution unlimited.			
11. SUPPLEMENTARY NOTES TECH, OTHER		12. SPONSORING MILITARY ACTIVITY AF Office of Scientific Research (NAE) 1400 Wilson Boulevard Arlington, Virginia 22209	
13. ABSTRACT This investigation encompasses research to evaluate the possible effect of the stochastic and non-uniform nature of the transport processes on nonisothermal nonlinear reactions. It is especially in fast exothermic reactions that the magnitude of these effects could be considerable, as the concentration and temperature gradients are often steep as compared to the scale of the stochastic processes. New approaches to the evaluation of the magnitude of these interactions are made, and phenomenological models for turbulent flows are proposed, and related to real flows by tracer experiments. The use of tracer experiments in the design and study by turbulent combustion reactors is discussed and a theoretical framework for the evaluation of tracer experiments in fluctuating quasi-steady flow systems is presented. The advantages of using reacting tracers in reactor modeling is discussed. This results in the Laplace transform of the sojourn time distributions and provides sensitive criteria for reactor design for complex reactions. Design criteria for stirred combustors are given and the effects of imperfect mixing and fluctuating inputs on such reactors is described. Design and modeling of fluidized bed reactors is also treated.			

AFOSR FINAL SCIENTIFIC REPORT  
AFOSR TR 71-3003

"COMPLEX MIXING MODELS FOR CHEMICAL REACTION SYSTEMS"

by

Reuel Shinnar and Stanley Katz  
Department of Chemical Engineering  
The City College, The City University of New York

Research Sponsored by the  
Air Force Office of Scientific Research  
Grant No. AF AFOER 67-0921  
To The City College Research Foundation

Approved for public release  
distribution unlimited.

ABSTRACT

In the study of chemical reactions in turbulent flows and packed and fluidized beds, the flow itself is too complicated to allow an accurate analytical description. In the analytical study of these reactions, some strongly simplified idealized flow models are commonly used to allow an analytical treatment. In these idealizations the stochastic nature of the transport processes as well as their spatial inhomogeneity are usually neglected. This investigation encompasses research to evaluate the possible effect of the stochastic and non-uniform nature of the transport processes on nonisothermal nonlinear reactions. It is especially in fast exothermic reactions that the magnitude of these effects could be considerable, as the concentration and temperature gradients are often steep as compared to the scale of the stochastic processes. New approaches to the evaluation of the magnitude of these interactions are made, and phenomenological models for turbulent flows are proposed, and related to real flows by tracer experiments. The use of tracer experiments in the design and study of turbulent combustion reactors is discussed.

The results of this study of the effect of the random and non-uniform nature of transport processes on nonisothermal nonlinear chemical reactions in turbulent flows and the behavior of energetic chemical reactions under transient and oscillating conditions should aid in understanding the start-up and control of chemical reaction and propulsion systems, unstable burning in rocket motors, and design of supersonic combustors.



FINAL REPORT

A difficult problem that faces the design of any combustion equipment is the fact that the flows are turbulent and often complex and defy a complete analytical description. Mixing processes are very important in any fast reaction and often they are the dominant factor.

There have been historically several approaches to the problem.

- 1) Modeling of the flow system by some simplified solution of the Navier Stokes equations, making some strong assumption about the average properties of the turbulent fluctuations. An example of this approach is the work of Corsin (1, 2), and Spelding's recent work on modeling of combustors.
- 2) Modeling of the flow system by some simple phenomenological models such as stirred tank or a network of stirred tanks, and plug flow reactors (3, 4), or simple diffusional models such as eddy diffusivity (5).
- 3) Modeling techniques based on tracer experiments (21). In some sense this leads to a better formulation of the simple models mentioned, but it also allows some direct conclusions as to effect of mixing processes on chemical reactions.

This final report summarizes a six year effort in this area. Our approach centered mainly on the third approach on phenomenological models, based on tracer experiments. As we

had no experimental program our main goal was to provide better tools for the experimentalist and the designer, and to provide a theoretical base for an understanding of the effects that turbulent mixing processes have on combustion reactions and the way this effects proper design procedures. The special and central features of our work in contrast to others, was that we made an attempt to include the stochastic and fluctuating nature of turbulent flows. Most simple phenomenological models simply neglect this feature and replace the non-steady mixing processes with steady state models, which describe the average behavior of the system.

It might be useful to divide the description of our results into two main areas.

1) Use of tracer experiments in the study of reactors and flow system.

The first publication (ref. 6) still dealt with tracer experiments in steady flow systems and tried to show the relation and similarity between eddy diffusion and models built on networks of stirred tanks. It showed that networks of stirred tanks can describe diffusional process to a very good approximation. Such models are mathematically far simpler to treat than models based on eddy diffusion. In complex turbulent flows eddy diffusion itself is only a very approximate description, and the added complexity introduced by the use of diffusion models as compared to networks of stirred tanks is very seldom justified. Ref. 6 also introduces methods to increase local age and antiage distributions, and discusses their application to reactor modeling.

In ref. 7 an attempt was made to include the stochastic nature of the mixing processes in such stirred tank models by allowing the flows between the stages of the network to vary with time in a random fashion. The main flow in and out of the system was still kept steady. In ref. 8 the main flow was also allowed to vary. In these two papers we tried to elucidate two things. One is the effect of the quasi steady fluctuating behavior of the mixing process on the overall behavior of the system, and second, how to evaluate and perform tracer experiments in a fluctuating flow. An understanding of the latter is important if we want to use tracer experiments to model a turbulent flow. The problem is not only important in reactor design but also in physiology, ref. 9. A useful concept in Modeling <sup>reactors</sup> / on the basis of tracer experiments is the residence time distribution, and age distribution as well as local age and antiage distributions. These concepts derived for steady flow is generalized in these two publications for randomly varying quasi steady flows, and can be very helpful in studying such reactors.

A theoretical framework is presented for the interpretation of tracer experiments in quasi steady-flow systems, where the inflow and outflow, as well as the internal flows, exhibit stationary fluctuations about fixed central values. The fluctuating throughput leads to the consideration of different types of sojourn time distribution of material in the system. These are discussed in detail, and related to different ways of carrying out tracer experiments on the system. The standard experiment, in which a known amount of tracer is injected quickly into the inlet and its concentration measured

in the outlet, leads to none of these distributions. Ref. 7 and 8 also discuss methods that enable one to compute the probability distribution of the outlet concentration for such networks with random interstage flows. For first order reactions the results are analytical and can also be directly computed from tracer experiments. For second order and adiabatic systems, numerical solutions are required, but this is still simpler than simulation methods. For a single stirred tank with fluctuating throughput or fluctuating outlet concentration, analytical solutions are possible for any system in which the reaction rate is expressible as a function of a single state variable. This therefore allows analytical treatment of adiabatic irreversible n-th order reactions. This result is used in ref. 16 which will be discussed later. Understanding of random mixing processes is also important in quality control in the preparation of propellants. Application of our methods to such problems is discussed in ref. 10.

A different approach to tracer experiments in modeling flow reactors is the use of a reactive tracer. Two experimental methods have been proposed. The first was by Orcutt (11) who used a simple first order reaction (decomposition of ozone on a catalyst) and varied the reaction rate by varying the temperature. Another more promising approach was formulated by Zahner (12) who used a complex consecutive reaction (exchange of neopentan with deuterium). In both cases one obtains a Laplace transform of the residence time distribution. This is of special advantage if one deals with multiphase system where the reaction occurs only in one phase as one obtains directly sojourn time distribution only in the

active phase. The difficulty is that one obtains a Laplace transform instead of the more commonly used residence time distribution. Inversion of experimentally determined Laplace transforms is difficult. In ref. 13 which is available in preprint form, a method was developed which circumvents this difficulty. It is shown that the information needed for purposes of reactor modeling and design can be directly obtained from the experimentally measured Laplace transform, without any inversion. In fact, in many cases this information might be more useful than a regular tracer experiment with a non-reactive tracer. Till now, the method has only been applied to fluidized beds, but it could be a powerful tool in the study of complex flows occurring in combustion reactors.

The methods described in (7) and (8) can also be applied to the description of particulate systems. Particulate systems, involving distribution of particle sizes, and simultaneous nucleation and growth are quite important in combustion. (Metal oxides in solid propellants, soot formation in jet engines, combustion of droplets in rocket motors, etc.). There is an advantage in using probability theory in describing such processes as it often leads to simpler formulation of the equations. This is discussed in more detail in ref. 14.

The basic methods described previously, especially in ref. 7 and 8 were applied to practical problems in reactor design and modeling of combustion reactors.

## 2) Design and Modeling of Combustion Reactors.

Ref. 15 deals with fluidized beds which recently are

becoming more and more important as combustion reactors. Solid particles can be burned in fluidized beds, but there is also an advantage of combusting gaseous and liquid fluids in fluidized beds of inert particles, or solid particles containing a catalyst. The bed keeps the temperature uniform and provides a large constant temperature sink, allowing stable combustion to be carried out at lower temperatures, which reduces nitrogen oxide emission. One of the disadvantages of fluidized beds that the gas solid contact is quite non-uniform, as the gas forms large bubbles. The local transport processes are therefore highly fluctuating in time as the time scale of the fluctuations is of the same order as the residence time. Using the modeling methods discussed in (7) and (8) it could be shown that the net result of this fluctuation is to reduce the effective volume of the reactor. Only part of the particles are reacting in it at any time. This helps to understand and explain some of the known behavior of fluidized beds.

Ref. 16 deals with a completely different problem. In some combustors the feed rate is varied, and fluctuates for different reasons either due to control or disturbances. If one looks at a small region on a turbulent combustor one can also look at it as a mixed region in which the inflow and outflow rate, as well as inflow and outflow composition changes. Now if we consider a single stirred tank with fluctuating throughput (or fluctuating inlet concentration or temperature) the method described in 7 and 8, allows one to obtain analytical solutions, even for exothermic reactions. What one obtains is not just the average outlet concentration and temperature but the whole probability distri-

bution. This gives one an understanding of the effect of random fluctuations on a combustor, especially with respect to stability, apparent activation energy and average conversion. For some combustors where the disturbances are in the feed rate, this is a quite realistic modeling of the process. For real turbulent mixing, this is a strong over-simplification, but still it has the advantage of giving an analytical solution for complex reaction systems. The methods derived could also be useful to study the effect of unstable burning.

A completely different approach was taken in ref. 17 and 18, in dealing with stirred combustors. Intensely stirred combustors have played an important role in the study of combustion kinetics (3, 4). They are also used as highly compact efficient combustion devices. Mostly such ideally stirred combustors are treated as if they were ideally stirred tanks of completely uniform concentration. In reality, this is seldom true as the residence time in combustion is very short. In (17) and (18) the following method is used to estimate the effect of imperfect mixing on combustion. The feed is assumed to consist of small droplets or pockets, which maintain their identity. If two such pockets or droplets collide they mix completely and separate immediately into two droplets of the same average concentration and temperature. A mathematical machinery is set up which allows one to follow the distribution of concentration and temperature in time. The mixing rate of droplets can be measured from a tracer experiment and can also be approximately estimated from theoretical considerations. We can now estimate the minimum mixing rate necessary for the results to be well approximated by an ideally mixed

reactor. We can also see in what direction incomplete mixing effects the results. In ref. 18 some guidance is also given as how to design and scale up an efficiently mixed stirred combustor for gaseous reactants. It is also shown that many of the kinetic data reported in the literature were taken under conditions where the assumption of an ideally stirred reactor is not justified, and mixing effects cannot be neglected.

In ref. 19 the effect of transport processes on the heterogeneous combustion of solid ammonium perchlorate is discussed. It is shown that some commonly used theoretical models for the combustion process of AP lead to totally unrealistic reaction rates and diffusion rates.

Ref. 20 (available in preprint) deals with the design of nonisothermal reactors. It shows that for any first order reaction a plug flow reactor with a prescribed temperature profile is as good or better than any other reactor configuration. This is not true for adiabatic reactors but only for a reactor in which the temperature can be imposed from the outside. While this is in itself an important result in chemical reactor design the method by which this is proven may be of more general interest for the combustion researcher. Complex first order reactions can be looked at as Markov processes, in which the concentration of a species is interpreted as the probability of a molecule to be in state  $i$ . Reaction rates are then equivalent to the transition probability of a molecule to go from state  $i$  to  $j$ . This gives one some powerful tool for studying nonisothermal reactions, as the mixing history (where history means the distribution of successive sojourn times in



each temperature region) completely describes the composition at the outlet.

References

1. Corsin, S. p. 105, Proc. 1961, Symp. on Fluid Dyn. and Appl. Math., U. of Maryland, Gordon and Breach Publ.
2. Corsin, S., Journal of Fluid Dynamics II, Part 3, 407, (1961).
3. Longwell, J.P. and Weiss, M.A., Ind. Eng. Chem. 47, 1634 (1955).
4. Essenhigh, R.H., Technical Report FS67-1(W), Combustion Laboratory, Pennsylvania State University, March 1967.
5. Wehner, J.R. and Wilhelm, R.H., Chem. Eng. Sci., 6, 89 (1956).
6. Shinnar, R. and Naor, P., "Residence Time Distributions in Systems with Internal Reflux," Chem. Eng. Sci., 22, 1369 (1967).
7. Krambeck, F.J., Shinnar, R. and Katz, S., "Stochastic Mixing Models for Chemical Reactors," In. and Eng. Chem. Fundamentals, 6, 276 (1967).
8. Krambeck, F.J., Shinnar, R. and Katz, S., "Interpretation of Tracer Experiments in Systems with Fluctuating Throughput," Ind. and Eng. Chem., 8, 431 (1969).
9. Bassingthwaite, J.B., Science, 167, 1347 (1970).
10. Krambeck, F.J., Shinnar, R. and Katz, S., "Analysis of Some Random Blending Processes," The Canadian Journ. of Chem. Engr., 45, 203 (1967).
11. Orcutt, J.C., Davidson, J.F. and Pigford, R.L., Chem. Eng. Prog. Symp. Ser., 58, 381 (1962).
12. Zahner, J.C., Proc. of the 1st International (5th European) Reaction Engineering Symposium, ACS (1971).
13. Glasser, D., Katz, S. and Shinnar, R., "The Measurement and Interpretation of Contact Time Distribution for Catalytic Reactor Characterization" submitted for publication.

14. Katz, S. and Shinnar, R., "Particulate Methods in Probability Systems," Ind. and Eng. Chem., 61, 60 (1969).
15. Krambeck, F.J., Katz, S. and Shinnar, R., "A Stochastic Model for Fluidized Bed," Chem. Eng. Sci., 24, 1437 (1969).
16. Krambeck, F.J., Katz, S. and Shinnar, R., "The Effects of Perturbations in Flow-Rate on a Stirred Combustor," accepted for publication in Combustion Science and Technology.
17. Evangelista, J.J., Katz, S. and Shinnar, R., "Scale-Up Criteria for Stirred Tank Reactors," AIChE Jour., 15, 843 (1969).
18. Evangelista, J.J., Shinnar, R. and Katz, S., "The Effect of Imperfect Mixing on Stirred Combustion Reactors," 12th Symp. (International) on Combustion, The Combustion Institute, Pittsburgh, Pennsylvania (1969).
19. Wenograd, J. and Shinnar, R., "Combustion of Ammonium Perchlorate - Some Negative Conclusions," AIAA Jour., 6, 964 (1968).
20. Shinnar, R., Glasser, D. and Katz, S., "First Order Kinetics in Continuous Reactors," submitted for publication.
21. Naor, P. and Shinnar, R., Ind. and Eng. Chem. Fundamentals, 2, 278 (1963).

List of Publications for AFOSR Grant No. 921-67 and 921-65.

1. Shinnar, R. and Naor, P., "Residence Time Distributions in Systems with Internal Reflux", Chem. Eng. Sci., 22, 1369 (1967).
2. Krambeck, F.J., Shinnar, R. and Katz, S., "Stochastic Mixing Models for Chemical Reactors", Ind. and Eng. Chem. Fundamentals, 6, 276 (1967).
3. Krambeck, F.J., Shinnar, R. and Katz, S., "Interpretation of Tracer Experiments in Systems with Fluctuating Throughput", Ind. and Eng. Chem. 8, 431 (1969).
4. Krambeck, F.J., Shinnar, R. and Katz, S., "Analysis of Some Random Blending Processes", the Canadian Jour. of Chem. Eng., 45, 203 (1967).
5. Katz, S. and Shinnar, R., "Particulate Methods in Probability Systems", Ind. and Eng. Chem., 61, 60 (1969).
6. Krambeck, F.J., Katz, S. and Shinnar, R., "A Stochastic Model for Fluidized Bed", Chem. Eng. Sci., 24, 1497 (1969).
7. Evangelista, J.J., Katz, S. and Shinnar, R., "Scale-Up Criteria for Stirred Tank Reactors", AIChE Jour., 15, 843 (1969).
8. Evangelista, J.J., Shinnar, R. and Katz, S., "The Effect of Imperfect Mixing on Stirred Combustion Reactors", 12th Symp. (International) on Combustion, The Combustion Institute, Pittsburgh, Pennsylvania (1969).
9. Wenograd, J. and Shinnar, R., "Combustion of Ammonium Perchlorate - Some Negative Conclusions", AIAA Jour., 6, 964 (1968).
10. Krambeck, F.J., Katz, S. and Shinnar, R., "The Effects of Perturbations in Flow-Rate on a Stirred Combustor", accepted for publication in Combustion Science and Technology.

List of Publications (cont.)

2.

11. Glasser, D., Katz, S. and Shinnar, R., "The Measurement and Interpretation of Contact Time Distribution for Catalytic Reactor Characterization" submitted for publication.
12. Shinnar, R., Glasser, D. and Katz, S., "First Order Kinetics in Continuous Reactors", submitted for publication.

*Reprinted from*

*Chemical Engineering Science*, 1967, Vol. 22, pp. 1369-1381. Pergamon Press Ltd., Oxford. Printed in Great Britain.

**Residence time distributions in systems with internal reflux**

**REUEL SHINNAR and PINHAS NAOR\***

City University of New York, New York 10051

and

University of North Carolina, Chapel Hill, N.C. 27515

*(Received 8 October 1966; in revised form 1 February 1967)*

**Abstract**—A general method for calculating residence time distributions for systems with internal



**PERGAMON PRESS**  
OXFORD NEW YORK LONDON PARIS

**Residence time distributions in systems with internal reflux**

REUEL SHINNAR and PINHAS NAOR\*

City University of New York, New York 10051

and

University of North Carolina, Chapel Hill, N.C. 27515

(Received 8 October 1966; in revised form 1 February 1967)

**Abstract**—A general method for calculating residence time distributions for systems with internal reflux is described. The method allows the derivation of the Laplace transform of any system composed of mixed vessels with both forward and backward flow between them. In particular, the properties of a linear cascade of mixed vessels with forward and backward flow between the vessels is discussed.

**INTRODUCTION**

Flow systems with internal back-flow or reflux are frequently encountered by the chemical engineer. In many cases this reflux is induced intentionally, whereas in others it is inherent in the properties of the flow system used.

In many complicated flow processes the engineer uses some simplified flow models to describe the fluid-dynamic behavior of the system. Such an approach has been especially fruitful in reactor design, where it allows an approximate analytical treatment of the kinetic processes in the reactor. One such flow model, which is of very general interest, is a network of mixed vessels with both forward and backward flow between them [1-3]. The advantage of this model is that with a large number of vessels it approximates molecular or eddy diffusion.

As there is some similarity in their residence time, such networks with a forward flow only have also been proposed as a model for packed beds [3, 4].

As mentioned in a previous publication [5], measurement of residence time distributions often allows a good evaluation of the suitability of a specific model to a specific process equipment. However, only few residence time distributions for systems with internal reflux have been published [6-8].

In the following, a method suitable for the calculation of the residence time distribution of any system with internal backflow is described, residence

time distributions for networks of mixed vessels are given and the general properties of such systems are discussed.

**GENERAL METHOD**

Consider a system composed of  $n$  stages in series (see Fig. 1). It is not necessary to assume that various stages and/or flows are equal but all stages are assumed to be ideally mixed vessels. For a complete definition of each stage it is necessary to know:

- the volume of the stage  $V_i$
- the four streams  $u_i$ ,  $w_i$ ,  $u_{i-1}$ , and  $w_{i+1}$ .

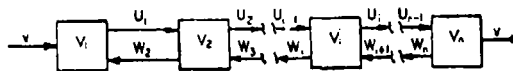


FIG. 1. Schematic diagram of system.

While the link velocities  $u_i$  are not necessarily equal, the law of conservation of mass renders

$$u_{i-1} + w_{i+1} = u_i + w_i \quad (1a)$$

and

$$u_{i-1} - w_i = u_i - w_{i+1} = v \quad (1b)$$

where  $v$  is the forward drift velocity of the fluid, a constant characteristic of the whole system, and pertaining to each stage. The average residence time in the total system is given by

$$E(t) = \sum \frac{V_i}{v} \quad (1c)$$

\* On leave of absence from Technion, Israel Institute of Technology, Haifa, Israel.

All problems dealing with residence time distribution can either be formulated by defining the different flows and transport processes of the system, or, alternatively, may be approached (and defined) by viewing a single particle and describing its passage through the system in terms of probabilities.

For the system described in Fig. 1 the latter approach can be exhibited in the following fashion. A particle starts its residence time in the system by entering the first vessel. It stays there for a random time and moves forward into the second vessel. After an additional random time, during which it stays in the second vessel, it can either move forward into the third vessel, or backward into the first with prescribed probabilities for each of these alternatives. However, it can move to a neighboring vessel only or, in the nomenclature of the theory of stochastic processes, to a neighboring state. This type of process is usually referred to as "birth-and-death process". We note that the first vessel is different from the others as a particle in it can move forward only; the last vessel is also unique, as a particle leaving it in the forward direction, cannot return to the system. This is the termination of the process and in the nomenclature of birth-and-death (as well as diffusion) processes the time elapsing between entry into some state (in our case: the first vessel) and absorption on entering another state (in our case: a fictitious  $(n+1)$ th vessel from which no return to the  $n$ -th vessel is possible) is termed a *first-passage-time*. Thus, for instance, in other areas of birth-and-death process applications, the *busy period of a server* (in queueing theory), the *time to first emptiness* (in dam theory), etc., are first-passage times. The residence time of a particle in a system of connected agitated vessels is a first passage time and it is worthwhile to analyze it as such so as to make use of well-established theory and lines of research. To define the system on these terms one now has to specify:

(a) The probability distributions for the sojourn times  $e_i(t)$  in each stage (the sojourn time being the uninterrupted time a particle remains in each state). The *average* sojourn time in any state is obviously equal to

$$E_i\{t\} = \frac{V_i}{u_i + w_i} \quad (2)$$

If we assume the vessel under consideration to be ideally mixed the sojourn time is an exponentially distributed random variable

$$e_i(t) = \eta_i e^{-\eta_i t} \quad (3)$$

where  $\eta_i$  is the reciprocal average sojourn time

$$\eta_i = [E_i\{t\}]^{-1} \quad (4)$$

(b) The probabilities of a particle associated with forward and backward movement into a neighboring state. Clearly in our case of ideal mixing such probability is independent of the realized sojourn time and can be derived from the flow velocities. The probability of moving backward equals

$$p_i = \frac{w_i}{u_i + w_i} \quad (5)$$

and the complementary probability of moving forward is obviously given by  $1 - p_i$ .

Let us fix attention on a particle in the  $i$ -th state and inquire into the characteristics of the random variable "future residence time" (as measured from the present instant) of the particle in the system. It is convenient to refer to this random variable as "anti-age" since it is completely analogous to "age of the particle in the system".

On considering the physical significance of the two concepts "anti-age of a particle residing in the first state" and "total residence time" one draws the conclusion that *one* density function,  $f_1(t)$  say, is representative of both. It is connected with the density function of anti-age in the second state through a simple convolutional relationship

$$f_1(t) = \int_0^t e_1(t-x)f_2(x)dx = e_1(t)*f_2(t) \quad (6a)$$

The density function of anti-age in an intermediate state (i.e., other than the first and the last) is related to those of both its neighbors

$$f_i(t) = p_i e_i(t)*f_{i-1}(t) + (1-p_i)e_i(t)*f_{i+1}(t) \quad (6b)$$

$$(i = 2, 3, \dots, n-1)$$

† In some studies (e.g. [19]) this is referred to as "life expectation". However, in the statistical literature the term "expectation" is used to denote an average; hence we prefer the notion of "anti-age".



## Residence time distributions in systems with internal reflux

The interpretation of the right-hand side of Eq. (6b) is the following: The duration of sojourn in the  $i$ -th state is associated with the density  $e_i$  regardless of the particle's future course; a transition to the  $(i-1)$ th state will take place with probability  $p_i$ ; and the additional future residence time (as measured from time of entry into that state) is governed by the density  $f_{i-1}(t)$ ; the alternative transition to the  $(i+1)$ th state possesses probability  $(1-p_i)$  and in that case it is  $f_{i+1}(t)$  which represents the density of the future residence time.

Analogously the anti-age density function of the last state is given by

$$f_n(t) = p_n e_n(t) * f_{n-1}(t) + (1-p_n) e_n(t) \quad (6c)$$

We have then a set of  $n$  equations in  $n$  unknown functions. Let us now apply the Laplace transformation on the set (6); we define

$$L_i(s) = \int_0^\infty e^{-st} f_i(t) dt \quad (7)$$

On designating the Laplace transform  $e_i(t)$  by  $\bar{e}_i(s)$  and making use of the fact that the Laplace transform of the convolution of two functions is the product of the Laplace transforms of the contributing functions the set (6) can be transformed into a set of  $n$  linear equations with  $n$  unknowns  $L_i$ .

$$L_1 = \bar{e}_1(s) L_2 \quad (8a)$$

$$L_i = p_i \bar{e}_i(s) L_{i-1} + (1-p_i) \bar{e}_i(s) L_{i+1} \quad (1 < i < n) \quad (8b)$$

$$L_n = p_n \bar{e}_n(s) L_{n-1} + (1-p_n) \bar{e}_n(s) \quad (8c)$$

In principle this can be solved in an elementary fashion. The residence time distribution is obtained by inverting  $L_1$ . In many cases it will be impossible to invert  $L_1$  into a (relatively) simple functional form but for practical purposes the residence time distribution can still be computed by standard numerical procedures. Moments of any order can be directly derived from the Laplace transform, which serves as a moment generating function.

The anti-age density  $f_i(t)$  for any stage can also be obtained from the above equations: the physical meaning of this is best presented as the residence time density of a particle injected at the  $i$ -th stage. This might be of special interest in the experimental evaluation of complicated flow models.

By injecting a tracer pulse or step input at different

points into the system and measuring the concentration of interest in the outflow, one can obtain a set of experimental anti-age densities and thereby get a more accurate check on the applicability of the model. Similarly, the age density in the  $i$ -th stage can be obtained by measuring the time of equivalent concentration response in the  $i$ -th stage resulting from a tracer pulse added to the first stage. It may suitably be called a *local* age density. The Laplace transform  $f_i(t)$  can now be expressed in an explicit form. Since sojourn time is exponentially distributed with parameter  $\eta$  we have

$$e_i(s) = \int_0^\infty \eta_i e^{-(\eta_i+s)t} dt = \frac{\eta_i}{\eta_i+s} \quad (9)$$

Now let quantities  $\alpha_i$  and  $\alpha_i^*$  be defined as

$$\alpha_i = (1-p_i) \frac{\eta_i}{\eta_i+s} \quad (10)$$

$$\alpha_i^* = p_i \frac{\eta_i}{\eta_i+s} \quad (11)$$

We note that for the first vessel  $p_1$  is zero and  $\alpha_1$  is then  $\eta_1/\eta_1+s$  and  $\alpha_1^*=0$ . The Laplace transform,  $L_1(s)$ , of the first passage time density—the function of main-interest—can be evaluated. By introducing the above quantities into set (8) we obtain

$$L_1(s) = \frac{\Pi_i \alpha_i}{\Delta} \quad (12)$$

Where  $\Delta$  is the determinant

$$\begin{vmatrix} 1 & \alpha_1 & & & & \\ \alpha_2^* & 1 & \alpha_2 & & & \\ & \alpha_3^* & 1 & \alpha_3 & & \\ & & \alpha_4^* & 1 & \alpha_4 & \\ & & & & & \alpha_{n-1}^* & 1 & \alpha_{n-1} \\ & & & & & & \alpha_n^* & 1 \end{vmatrix}$$

(all other entries being zero). This can also be written

$$\Delta = 1 - \sum_i \alpha_i \alpha_{i+1}^* + \sum_{j>i+1} \alpha_i \alpha_{i+1}^* \alpha_j \alpha_{j+1}^* - \sum_{k>j+1>i+2} \alpha_i \alpha_{i+1}^* \alpha_j \alpha_{j+1}^* \alpha_k \alpha_{k+1}^* + \dots \quad (12a)$$

where the first sum contains  $\binom{n-1}{1}$  terms the second sum  $\binom{n-1}{2}$  terms and so on.

The other unknowns  $L_i(s)$  ( $i=2, 3, \dots, n$ ) too can be derived in terms of the above quantities  $\alpha_i$  and  $\alpha_i^*$ .

The above Laplace transform can be inverted in the following way: For any finite  $n$  the above expressions can be written in terms of polynomials of  $s$

$$J(s) = \frac{q(s)}{p(s)} \quad (13)$$

which has a standard inversion in terms of the characteristic roots  $a_k$  of the polynomial  $p(s)$

$$f(t) = \sum_{k=1}^n \frac{q(a_k) e^{a_k t}}{p'(a_k)} \quad (14)$$

We note, in passing, that the choice of the *prospective* random variable "anti-age of a particle" is arbitrary, to some extent, for the purpose of our investigation. An alternative course would be to subject the *retrospective* random variable "age of a particle" to the type of argument used in this section. A set of relations analogous to (5) would be generated and the desired result—the residence time density (or rather its Laplace transform)—would be obtained in the "guise" of the age density in the *last* state. Equation (12) pertains to the Laplace transform of three *conceptually different* densities: residence time (or first-passage time), anti-age in the first state, and age in the last state. A little reflection confirms the *logical identity* of the three concepts.

The mathematical techniques used in our analysis are a modification of Bachelier's methods—expounded, for instance, in BACHELIER [9]—combined with the application of the Laplace transformation. Alternative techniques for the (elementary) evaluation of first-passage time distributions are described by BHARUCHA-REID [10] and SAATY [11].

#### A CASCADE OF EQUAL, MIXED VESSELS WITH FORWARD AND BACKWARD FLOW

Equation (12) gives the Laplace transform of a residence time distribution for any cascade of mixed vessels without restrictions as to their relative sizes or their connecting links. In the majority of cases the chemical engineer is dealing with simpler cascades in which both the stages and the flow links can be assumed to be equal. In compartmentalized

equipment technical considerations, such as design simplicity, usually prescribe identical vessels and flow links. In cases where the cascade is just an idealized flow model, as in packed beds, these simplifying assumptions are also often justified by the nature of the system. It is therefore of interest to study in some more detail the properties of such a cascade.

At first sight it appears that there are still four parameters describing the specialized model:

- (1) the number of states,  $n$ , in the system;
- (2) the total volume of the system,  $V$ ;
- (3) the average drift velocity,  $v$ ;
- (4) the average forward flow velocity,  $u$ , between the adjacent states.

Two only of these four parameters are non-trivial. No loss of generality is incurred if we set both  $V$  and  $v$  to equal 1. However some physical insight is gained if explicit use is made in our developments of all four parameters (and of other quantities dependent on them).

We drop the general subscripts from the letters denoting various quantities in the last section. The forward and backward flow velocities in any double link are denoted by  $u$  and  $w$ , respectively. The reciprocal sojourn times—the parameters of the pertaining exponential distributions—in all intermediate (i.e. other than first and last) vessels are identical and the use of the letter  $\eta$  will be retained for their description

$$\eta = \frac{n(u+w)}{V} \quad (15)$$

For terminal vessels (both the first and the last) we introduce  $\xi$  as the reciprocal average sojourn time

$$\xi = \frac{n(v+w)}{V} = \frac{nu}{V} = \eta \frac{u}{u+w} \quad (16)$$

The probability,  $p$ , of a particle leaving an intermediate vessel in the backward direction† is given by

† In [6] a backmixing ratio  $\alpha$  is defined as

$$\alpha = w/v = \frac{w}{u-w}$$

Thus

$$p = \frac{\alpha}{1+2\alpha}$$

## Residence time distributions in systems with internal reflux

$$p = \frac{w}{u+w} = 1 - \frac{\xi}{\eta} \quad (17)$$

The analogous quantity in the first vessel equals zero. In the last vessel this probability will be denoted by  $\pi$ ; it is given by

$$\pi = \frac{w}{v+w} = \frac{w}{u} = \frac{p}{1-p} = \frac{\eta}{\xi} - 1 \quad (18)$$

This can be rewritten as

$$\frac{1}{p} - \frac{1}{\pi} = 1 \quad (19)$$

which is convenient for some purposes. It is evident that restrictions on possible values of  $\pi$  are rather mild

$$0 \leq \pi < 1 \quad (20)$$

whereas  $p$  is rather constrained

$$0 \leq p < \frac{1}{2} \quad (21)$$

Physically (20) and (21) may be interpreted as follows: At the end of the system we can "reflux" any desired fraction of the material; however, the bulk of the material—located in the first and the intermediate vessels—has to possess a forward drift movement  $(1-p) > \frac{1}{2}$ .

The expected residence time in the system (first-passage time) can be expressed in terms of the above quantities

$$\bar{z}(s) = \frac{V}{v} = \frac{nu}{\xi v} = \frac{n}{\xi \left(1 - \frac{w}{u}\right)} = \frac{n}{(1-\pi)\xi} \quad (22)$$

Next we shall derive the residence time density function—by inversion of the Laplace transform—in the simplest cases:  $n=2$  and  $n=3$ .

In the first of these cases— $n=2$ —Eq. (12) is reduced to

$$\begin{aligned} L_1(s) &= \frac{\alpha_1 \alpha_2}{1 - \alpha_1 \alpha_2^*} = \frac{\left(\frac{\xi}{\xi+s}\right)^2 (1-\pi)}{1 - \left(\frac{\xi}{\xi+s}\right)^2 \pi} \\ &= \frac{\xi^2 (1-\pi)}{\xi^2 (1-\pi) + 2\xi s + s^2} \\ &= \frac{\xi^2 (1-\pi)}{[s + (1 + \sqrt{1-\pi})\xi][s + (1 - \sqrt{1-\pi})\xi]} \end{aligned} \quad (23)$$

The inverse,  $f(t)$ , of this expression can be obtained by standard procedures

$$\begin{aligned} f(t) &= \frac{\xi(1-\pi)}{2\sqrt{\pi}} (e^{-\xi(1-\sqrt{1-\pi})t} - e^{-\xi(1+\sqrt{1-\pi})t}) \\ &= \frac{1-\pi}{\sqrt{\pi}} \xi e^{-\xi t} \sinh(\xi \sqrt{\pi} t) \end{aligned} \quad (24)$$

If we increase the number of states to the case  $n=3$  complexity is greatly increased but a closed expression for the density is still obtainable. Equation (12) becomes

$$\begin{aligned} L_1(s) &= \frac{\alpha_1 \alpha_2 \alpha_3}{1 - \alpha_1 \alpha_2^* - \alpha_2 \alpha_3^*} = \frac{\left(\frac{\xi}{\xi+s}\right)^2 \left(\frac{\eta}{\eta+s}\right) (1-p)(1-\pi)}{1 - \left(\frac{\xi}{\xi+s}\right) \left(\frac{\eta}{\eta+s}\right) p - \left(\frac{\eta}{\eta+s}\right) \left(\frac{\xi}{\xi+s}\right) (1-p)\pi} \\ &= \frac{\xi^3 (1-\pi)}{(s+\xi) \left( s + \xi \frac{2+\pi + \sqrt{(8\pi+\pi^2)}}{2} \right) \left( s + \xi \frac{2+\pi - \sqrt{(8\pi+\pi^2)}}{2} \right)} \end{aligned} \quad (25)$$

The inverse transform of (25) is given by

$$f(t) = \frac{\xi(1-\pi)e^{-\xi t}}{2} \left\{ e^{-\frac{\xi t \pi}{2}} \left[ \frac{\sinh\left(\frac{\xi t}{2} \sqrt{8\pi + \pi^2}\right)}{\sqrt{8\pi + \pi^2}} + \cosh\left(\frac{\xi t}{2} \sqrt{8\pi + \pi^2}\right) \right] - \frac{1}{\pi} \right\} \quad (26)$$

For large values of  $n$  the roots of  $p(s)$  have to be found by numerical methods.

Of course, as was stated before, approximations to the density functions can be obtained and precise values of moments, cumulants, etc. can be made available by standard methods. Without factorizing  $p(s)$  we shall derive the variance (and other quantities of interest) of the residence time for a general  $n$  by using a variant of Bachelier's procedure:

Let the expected anti-age of a particle in the  $i$ -th vessel be denoted† by  $E\{T_i\}$ . By considerations very similar to those made for deriving set (8) we obtain

$$E\{T_1\} = E\{t\} = \frac{n}{1-\pi} \frac{1}{\xi}$$

$$E\{T_i\} = \frac{1}{\eta} + pE\{T_{i-1}\} + (1-p)E\{T_{i+1}\} \quad (i \neq 1, n) \quad (27)$$

$$E\{T_n\} = \frac{1}{\xi} + \pi E\{T_{n-1}\}$$

The solution of (27) is given by

$$E\{T_i\} = \frac{1}{\xi} \left[ (n-i+1) + (n-i+2)\pi + \dots + n\pi^{i-1} + \frac{n\pi^i}{1-\pi} \right] \quad (i=1, 2, \dots, n) \quad (28)$$

† Digressing we note that in a system composed of identical vessels and of identical double links symmetry considerations generate the following relation: Expected anti-age in the  $i$ -th vessel = Expected age in  $(n-i+1)$ th vessel. Actually the symmetry reaches farther—even the distributions are identical.

The expected anti-age  $E\{T\}$ , in the system (or, what is the same, the expected age in the system) is then equal to

$$E\{T\} = \frac{1}{n} \sum_{i=1}^n E\{T_i\} = \frac{1}{n\xi} \left[ \frac{n\pi}{1-\pi} \cdot \frac{1-\pi^n}{1-\pi} + n \frac{1-\pi^n}{1-\pi} + (n-1) \frac{1-\pi^{n-1}}{1-\pi} + \dots + 2 \frac{1-\pi^2}{1-\pi} + 1 \right] = \frac{E\{t\}}{n^2} \left[ \frac{n(n+1)}{2} + \frac{\pi}{(1-\pi)^2} ((n-1) - n\pi + \pi^n) \right] \quad (29)$$

Now it is known from SMOLUCHOWSKI's work‡ [18] that the expected value of the life expectation (or age) and the moments of residence time are related as follows

$$E\{T\} = \frac{E\{t^2\}}{2E\{t\}} = \frac{E\{t\}}{2} (1 + \gamma^2) \quad (30)$$

where  $\gamma$  is the coefficient of variation‡ of the residence time distribution, (that is the ratio of the standard deviation and the average of the residence time distribution). Combination of (29) and (30) yields

$$\gamma^2 = \frac{1}{n} + \frac{2\pi}{[n(1-\pi)]^2} [(n-1) - n\pi + \pi^n] = \frac{1}{n} + \frac{2}{n^2} [\pi(n-1) + \pi^2(n-2) + \dots + \pi^{n-1}] \quad (31)$$

Since in many (but by no means all) engineering situations the performance of mixing equipment is judged by the variance‡ of the residence time distribution, relation (31) is of some importance. A useful representation of (31) is obtained by drawing contours—that is, lines of equal  $\gamma$ —on a graph whose abscissa§ and ordinate denote  $n$  and  $\pi$ , respectively (see Fig. 2).

‡ The present notion of anti-age is identical with Smoluchowski's concept of "Erwartungszeit".

§ The reciprocal of the squared coefficient of variation is sometimes described as the "equivalent" number of vessels.

¶ The quantity  $n$ , originally conceived as a natural number can easily be thought of as (i.e. generalized to) a positive, not necessarily integral, number.

Residence time distributions in systems with internal reflux

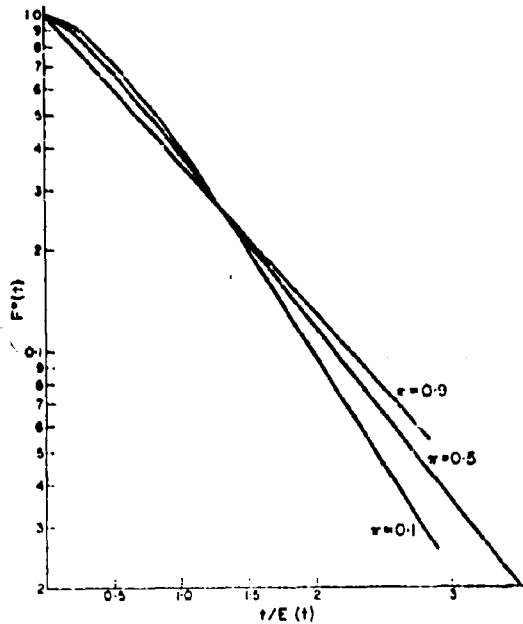


FIG. 2(a). Cumulative residence time distribution for a cascade of two identical mixed vessels with internal reflux.

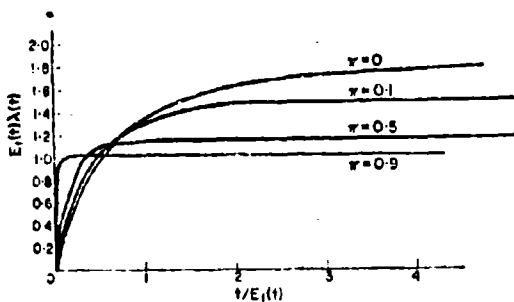


FIG. 2(b). Intensity function for a cascade of two identical mixed vessels with internal reflux.

The flexibility of the present model can be demonstrated by examining special and extreme cases:

(a) Let  $n$  equal 1; in this case there is no physical meaning to the notion of  $\pi$  but even formal use of (31) with an arbitrary  $\pi$  renders the correct result:  $\gamma^2 = 1$ . The present case simply represents the single exponential vessel.

(b) Let  $n$  equal a fixed positive integer (other than 1) and assume  $\pi = 0$ ; this corresponds to a pure birth process and indeed the correct value— $\gamma^2 = 1/n$ —of the dimensionless variance (i.e., the squared coefficient of variation) is obtained.

(c) Let again  $n$  equal a fixed positive integer (other than 1) and let  $\pi$  approach 1. Physically, it is meaningless to let  $\pi$  be equal to 1 (and  $n$  finite at the same time) since in that case material could not flow at all through the system. If, however, formally  $\pi$  is made equal to 1, we obtain

$$\begin{aligned} \gamma^2 &= \frac{1}{n} + \frac{2}{n^2} [(n-1) + (n-2) + \dots + 1] \\ &= \frac{1}{n} + \frac{2(n-1)n}{2n^2} = 1 \end{aligned}$$

i.e. that value of  $\gamma^2$  which is associated with a single exponential vessel. The physical interpretation to be attached to a situation where  $\pi$  approaches 1 arbitrarily closely is the following: the birth-and-death model of a particle flow through  $n$  vessels can be made to approach the single exponential vessel model as (arbitrarily) close as desired by making a judicious choice of the reflux parameter  $\pi$ .

(d) Let  $n$  tend to infinity and simultaneously both

$$E(t) = \left( \frac{n-1}{1-\pi\xi} \right)$$

and  $\pi (\neq 1)$  are held constant; clearly  $\gamma^2 \rightarrow 0$  and the case under consideration involves plug-flow.

(e) As a final example consider the case where  $n$  tends to  $\infty$  and simultaneously  $\pi$  approaches 1 such that

$$n(1-\pi) = \rho \tag{32}$$

where  $\rho$  is positive and finite. This is the case of diffusion and  $\gamma^2$  can be expressed as function of  $\rho$

$$\begin{aligned} \gamma^2 &= \frac{1}{n} + \frac{2}{[n(1-\pi)]^2} \left\{ -1 + n(1-\pi) \right. \\ &\quad \left. + \left[ (1-(1-\pi))^{-\frac{1}{1-\pi}} \right]^{n(1-\pi)} \right\} \\ &\quad n \rightarrow \infty, \pi \rightarrow 1, n(1-\pi) \rightarrow \rho \\ &= 2 \frac{[e^{-\rho} - (1-\rho)]}{\rho^2} \tag{33} \end{aligned}$$

Diffusion will be discussed in the next section in some more detail. It is well known that by a suitable limiting process the different equations, describing the behavior of a cascade of mixed vessels with forward and backward flow, transform into the diffusion equation. In order to illustrate both the similarity and the difference between the two cases it might be illuminating to perform this limiting process in terms of the residence time distribution for a particle.

Equations (8)—associated with the birth-and-death process—may be regarded as a set of second-order difference equations. If proper assumptions are made a second-order differential equation in the desired Laplace transform (as a function of the location of the particle under observation) can be derived. First we make the homogeneity assumption, i.e. all vessel volumes are equal and all double links connecting adjacent vessels are identical. Next we define a variable  $Z$  depending on  $i$  (and  $n$ ) by

$$Z = \frac{i-1}{n} \quad (0 \leq Z \leq 1) \quad (34)$$

The required second-order differential equation will next be set up. Under the simplifying homogeneity assumption Eq. (8b) reads (for  $i \neq 1, n$ )

$$L_i = p \frac{\eta}{\eta+s} L_{i-1} + (1-p) \frac{\eta}{\eta+s} L_{i+1} \quad (35)$$

If we introduce (in obvious notation)

$$\Delta Z = \frac{1}{n} \quad (36)$$

$$\Delta L = L_{i+1} - L_i \quad (37)$$

and

$$\Delta(\Delta L) = L_{i+1} - 2L_i + L_{i-1} \quad (38)$$

we can—on multiplying by  $(\eta+s)$  and rearranging terms—cast (35) into

$$\begin{aligned} & (1-p)\eta L_{i+1} - (\eta+s)L_i + p\eta L_{i-1} \\ &= [p\eta L_{i+1} - 2p\eta L_i + p\eta L_{i-1}] \\ & \quad + [(1-2p)\eta L_{i+1} - (1-2p\eta)L_i] - sL_i \\ &= \frac{p\eta \Delta(\Delta L)}{n^2 \Delta Z \Delta Z} + \frac{(1-2p)\Delta L}{n \Delta Z} - sL_i = 0 \end{aligned} \quad (39)$$

We take note that—on going to the limit ( $n \rightarrow \infty$ ;  $\pi \rightarrow 1$ ;  $n(1-\pi) \rightarrow \rho$ )—the coefficients  $p\eta/n^2$  and  $(1-2p)\eta/n$  tend to the following simple expressions

$$\frac{p\eta}{n^2} = \frac{\xi\pi}{n^2} = \frac{1}{E\{t\}} \frac{\pi}{n(1-\pi)} \rightarrow \frac{1}{\rho E\{t\}} \quad (40)$$

$$\frac{(1-2p)\eta}{n} = \frac{1-2p}{1-p} \frac{\xi}{n} = \frac{(1-\pi)\xi}{n} = \frac{1}{E\{t\}} \quad (41)$$

After multiplying (39) by  $\rho E\{t\}$  the differential equation is established as

$$\frac{d^2 L}{dZ^2} + \rho \frac{dL}{dZ} - \rho E\{t\} s L = 0 \quad (42)$$

and boundary conditions are set up as counterparts to the equations for  $L_1$  and  $L_n$  in the set (8)

$$\left( \frac{dL}{dZ} \right)_{(Z=0)} = 0 \quad (43)$$

$$\left( \frac{dL}{dZ} \right)_{(Z=1)} + \rho L_{(Z=1)} - \rho = 0 \quad (44)$$

It can be seen immediately that the quantity

$$\rho \equiv \frac{n(1-\pi)}{n \rightarrow \infty \quad \pi \rightarrow 1}$$

which appears in the diffusion case is equivalent to the Peclet number  $UL/D$ . It is therefore only natural to suggest that  $n(1-\pi)$  should be identified with the Peclet number also for the case of a cascade made up of a finite number of mixed vessels.

The proper boundary conditions for the flow reactor, the correct choice of which has caused some discussion in the literature [7, 12, 13], are here obtained directly. It should be remembered that  $L$  refers to the anti-age. As the anti-age in stage 1 is the analogue of age at stage  $n$ , the normally used boundary conditions are here inverted with respect to the length coordinate  $Z$ . Equation (42) together with boundary conditions (43) and (44) can be solved by standard methods, details of which will not be presented here [4, 7, 14]. Let a quantity  $\sigma$  be defined as

$$\sigma = \sqrt{(\rho^2 + 4\rho E\{t\}s)} \quad (45)$$

## Residence time distributions in systems with internal reflux

We have then the following expression as the solution of Eq. (42)

$$L = \frac{e^{s\pi(1-Z)} \left[ \rho \sinh \frac{\sigma Z}{2} + \cosh \frac{\sigma Z}{2} \right]}{\left[ \rho + 2E\{t\}s \right] \sinh \frac{\sigma}{2} + \cosh \frac{\sigma}{2}} \quad (46)$$

This is the Laplace transform of the anti-age density given that the particle under consideration is located on site  $Z$  within the interval  $(0, 1)$ . By virtue of arguments analogous to those used before, expression (46) is also the transform of the age density function of a particle located on site  $(1-Z)$ ; finally, it is the Laplace transform of the first-passage time density of a particle injected into the interval  $(0, 1)$  at location  $Z$ . The residence time density is associated with the particular choice of the parameter  $Z=0$ . The inversion of the transform into a density function of closed simple form seems to be impossible, but again precise values of all moments, cumulants, etc., can be derived by standard (though cumbersome) procedures and approximations to the density function are readily established.

We note here that the formulation of first-passage time problems in terms of second order differential equations in the Laplace transform goes back to the work of DARLING and SIEGERT [15].

#### PROPERTIES OF CASCADES OF MIXED VESSELS WITH FORWARD AND BACKWARD FLOW

In principle the methods discussed in the previous chapter allow the derivation of the Laplace transform for any system with internal reflux, provided the system is made up of elements with known residence time distribution. Specific solutions were obtained for cascades of equal mixed vessels and some typical results are given in Figs. 2-5.

In plotting the various residence time distributions, both the cumulative distribution

$$F^*(t) = \int_0^t f(t) dt$$

and the intensity function  $\lambda(t)$

$$\lambda(t) = \frac{f(t)}{F^*(t)} = \frac{-d \ln F^*(t)}{dt}$$

are given. It was shown in a previous paper [5] that the intensity function is of advantage in plotting such distributions as it allows a better physical insight into the nature of the mixing processes in the system.

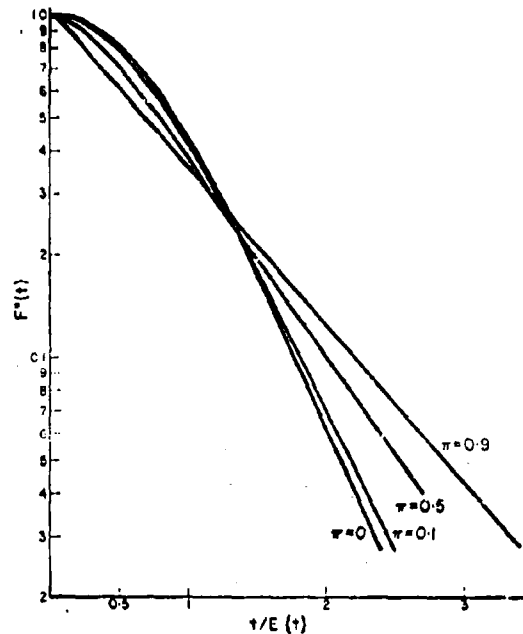


FIG. 3(a). Cumulative residence time distribution for a cascade of three identical mixed vessels with internal reflux.

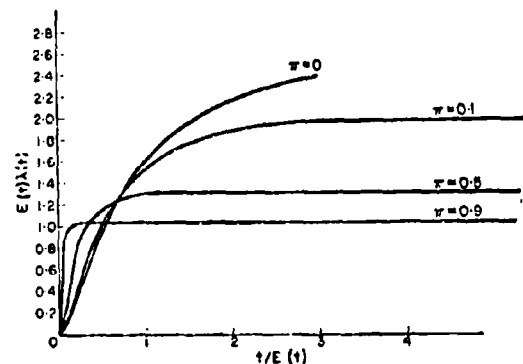


FIG. 3(b). Intensity function for a cascade of three identical vessels with internal reflux.

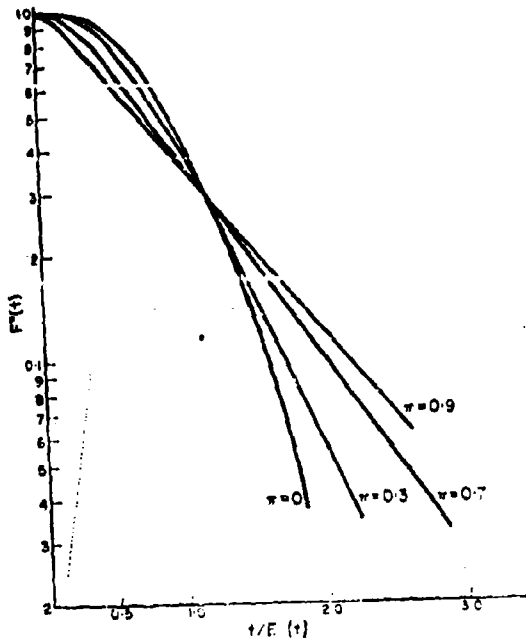


FIG. 4(a). Cumulative residence time distribution  $F^*(t)$  for a cascade of five identical mixed vessels with internal reflux.

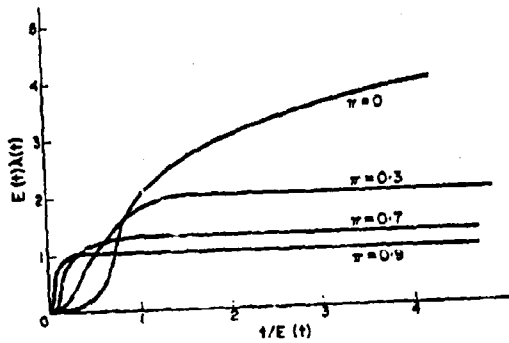


FIG. 4(b). Intensity function for a cascade of five identical mixed vessels with internal reflux.

Figure 2 gives the cumulative residence time distribution and the intensity functions for two equal mixed vessels in series and different values of  $\pi$ . Figure 3 gives the same functions for three equal vessels in series.

In Fig. 5 the intensity function (see [5]) of cascades with equal coefficients of variation but

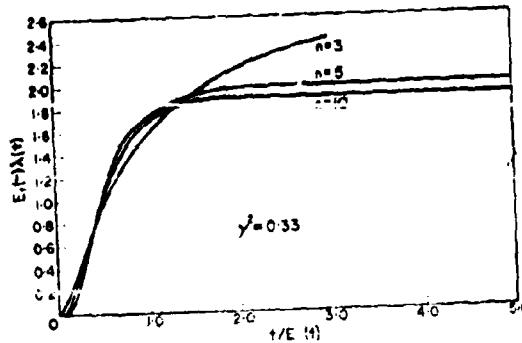


FIG. 5. Intensity function for cascades having the same coefficient of variation (0.33) but different numbers of vessels.

different values of  $n$  are compared to each other. For higher values of  $n$  the solution converges very rapidly to the solution for axial diffusion.

For equal coefficients of variation it can be seen that increasing the value of  $n$  reduces both  $\lambda_c$  and the value  $\lambda$  for very low times. The asymptotic value of  $\lambda$  is, however, approached at lower values of  $t$  than in the model with forward flow only, and the  $\lambda$  function, or in other words, the escape probability resembles a step function.†

$\lambda_c$  can be found directly from the Laplace transform. It is equal to the root of  $p(s)$  in Eq. (13) which has the lowest absolute value. In the case of a flow reactor with axial diffusion [Eq. (46)],  $\lambda_c$  is given by

$$\lambda_c = \frac{4u^2 + p^2}{4p}$$

† In our previous paper [5] it was stated erroneously that the intensity function for axial diffusion increases to infinity with  $t$ . This was due to a mistake which is corrected here. The case discussed in the previous paper (Fig. 2 of [5]) referring to [16; Eq. (19)]

$$F^*(t) \approx \frac{1}{2} \operatorname{erf} \frac{1-at}{\sqrt{bt}} + \frac{1}{2}$$

deals with a semi-open system. There is no clearly defined exit after which a particle can not diffuse back into the system. The results of tracer experiments will therefore lead to a local age distribution rather than a residence time distribution. In the case where there is an endwall through which particles can pass forward but not backward, Eq. (46) in this paper or the solutions given in [4] and [14] apply. The difference between the two cases has been discussed in [7] and [3]. The correct value for  $\lambda_c$  in this case is  $a^2/b$  which is equal to  $p^2/4$ .



Residence time distributions in systems with internal reflux

where  $a$  is the lowest root of the equation

$$\frac{a}{2} + \frac{\tan a}{2} = \frac{\rho}{4}$$

For high values of  $\rho$ ,  $\lambda_{\infty}$  becomes  $\rho/4$ .

For huge residence times the effect of diffusion is thus somewhat similar to that of a plug-flow reactor with  $n$  mixed vessels in series. In the asymptotic region both reactors behave as *single* ideally mixed vessels. This means that the particle has a high probability of being in the last vessel.

In recent chemical engineering literature (for example [14]) the similarity between a cascade of stirred tanks and molecular or eddy diffusion has often been stressed. In most cases the comparison is based on equal variance of residence time. This, for example, leads to equal dampening of low frequency concentration fluctuations in the input of the two systems.

However, even for high Peclet number (or low values of  $\gamma$ ) the two systems are still basically different. A discussion of the influence of the detailed structure of the mixing processes on chemical reactions will be given in a separate paper.

The model for the cascades under consideration in this study possesses two independent, non-dimensional parameters and we may choose several modes of representation. Thus, in one set of circumstances, we may consider  $n$  and  $\pi$  to be the underlying basic parameters; in other analyses we may wish to start out with  $\gamma^2$  and  $n(1-\pi)$ . If  $\pi \rightarrow 0$  (forward flow only)  $\gamma^2$  becomes  $1/n$  and if  $n \rightarrow \infty$ ,  $\pi \rightarrow 1$  such that  $n(1-\pi)$  remains finite,  $n(1-\pi)$  becomes the equivalent Peclet number. In Fig. 6

and 7,  $\gamma^2$  is given as a function of  $\pi$  and  $n(1-\pi)$  for various values of  $n$  and for axial diffusion ( $n \rightarrow \infty$ ).

In some physical cases there is a considerable advantage in using as a theoretical flow model a finite cascade of mixed vessels with forward and backward flow between the vessels. As an example, consider a packed bed or a turbulent flow reactor. Describing the transport processes in such a system by an overall eddy diffusivity introduces considerable difficulties when dealing with the transient behavior of highly non-linear reactions. These

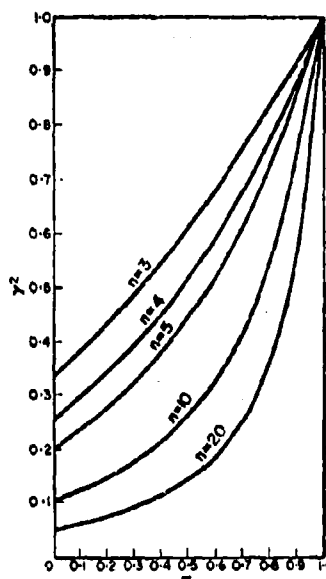


FIG. 6.  $\gamma^2$  as a function of  $\pi$  for a series of equal vessels with backflow.

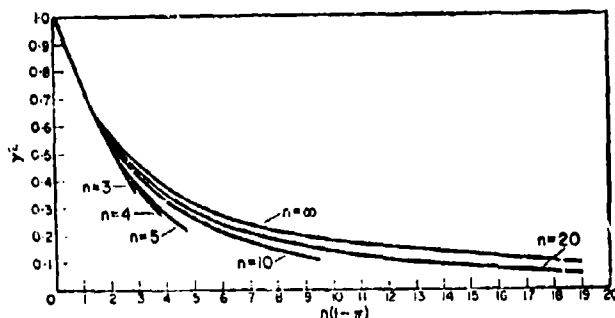


FIG. 7.  $\gamma^2$  as a function of Peclet number for a cascade of equal mixed vessels with backflow.

difficulties can be considerably reduced by substituting the above described model of a finite cascade. If one now realizes that the physical system also contains mixing zones of finite extension, then this model might even be a better approximation of the actual flow than the model of axial eddy diffusion.

A model with forward flow only, as proposed in [17] is even more simple to treat. However, such a one-parameter model is less flexible and harder to fit to an experimental residence time distribution. The two-parameter model described above should in many cases lead to a more realistic description of the transport processes.

In conclusion we would like to point out one property of flow models based on cascades of mixed vessels with internal reflux which is useful in reactor design. In reactor design it is often sufficient to estimate a minimum and maximum conversion with the help of the residence time distribution. The fact that the intensity function  $\lambda(t)$  of these models reaches an asymptotic value very fast simplifies the computational procedures considerably. From Figs. 2-4 it can further be seen that the intensity function can often be approximately represented by a step function. Many practical residence time distributions of packed beds (for example, Fig. 6B of [5]) exhibit the same property. In such cases approximating the  $\lambda$ -function by a step function tends to a further simplification. A step function in  $\lambda$  is nothing else but a plug-flow reactor in series with a single stirred tank. The residence time of the equivalent stirred tank can be found from  $\lambda_\infty$ , the asymptotic value of  $\lambda$ , as

$$E(t) \approx 1/\lambda_\infty$$

and the residence time of the plug reactor is the value of  $t$  at which the step occurs. From this simple flow model one can compute a first-order approximation of the effect of transport processes on conversion with considerable accuracy.

#### SUMMARY AND CONCLUSIONS

A method was derived which allows one to compute the residence time distribution, for any network of stirred tanks with arbitrary flows between the tanks. The method which is based on computing the probability density function of the residence

time for a single particle also allows one to compute the age distribution and anti-age distribution in any of the stirred tanks, comprising the network. These can be considered as local age and anti-age distributions and may be measured experimentally. The method gives the Laplace transform of the distributions and also allows one to obtain directly the moments of the distributions.

The method is demonstrated for a cascade of stirred tanks with reflux between them. If all the tanks are equal and the reflux is constant a special simple two parameter model is obtained, these parameters being the variance  $\gamma^2$  and a dimensionless group  $n(1-\pi)$ . If  $\pi$  is zero the model reduces to the well-known case of a cascade of stirred tanks with forward flow only. If at constant resident time the number of tanks as well as the backflow is increased then the case approaches asymptotically the case of one dimensional diffusion in a flow reactor, and  $n(1-\pi)$  becomes the well-known Peclet number.

Such a model with a finite number of tanks might be a good approximation of one dimensional eddy diffusivity. Furthermore, if  $n$  is large as compared to  $n(1-\pi)$  the intensity function is quite well approximated by a step function.

**Acknowledgment**—The work of Professor R. Shinnar was supported by the City University of New York and partly by the Air Force Office of Scientific Research under Grant No. A-F-AFOSR 971-65. Professor P. Naor was supported during this work by the Office of Naval Research under Contract No. Nonr. 355(109).

The authors want to express their gratitude for this support.

The authors also want to thank Dr. Clark Hermance for helping with the computations.

#### NOMENCLATURE

$a_k$	characteristic root
$e_i(t)$	density function of sojourn time in $i$ -th mixed vessel
$\bar{e}_i(s)$	Laplace transform of $e_i(t)$
$f_i(t)$	density function of residence time
$\bar{f}(s)$	Laplace transform of a function
$n$	number of states or vessels
$p_i$	probability of a particle in state $i$ moving into state $(i-1)$
$p(s)$	polynomial in $s$
$q(s)$	polynomial in $s$

## Residence time distributions in systems with internal reflux

$u_i$	forward velocity between vessels $i$ and $(i+1)$	$L$	Laplace transform of a residence time density function
$v$	forward drift velocity of fluid through system	$UL/D$	Peclet number
$w_i$	backward velocity between vessels $i$ and $(i-1)$	$V_i$	volume of $i$ -th vessel
$E\{t\}$	average residence time	$Z$	quantity describing location
$E\{t^2\}$	second moment of residence time	$\alpha, \alpha'$	functions associated with Laplace transform
$E_i\{t\}$	average sojourn time in $i$ -th state or vessel	$\gamma$	coefficient of variation
$E\{T\}$	average age or anti-age in system	$\lambda(t)$	intensity function
$E\{T_i\}$	average anti-age in $i$ -th vessel	$\pi$	probability of a particle in state $n$ moving backward
$F^*(t)$	distribution function (cumulative to the right)	$\rho$	constant equivalent to Peclet number
		$\sigma$	$\sqrt{(\rho^2 + 4\rho E\{t\}s)}$
		$\xi, \eta$	reciprocal average sojourn times

## REFERENCES

- [1] LATINEN F. D. and STOCKTON, A. I.Ch.E., National Meeting, St. Paul, Minn., September 1959.
- [2] MIAUCHI T. and VERMEULEN TH., *Ind. Engng Chem. Fundls* 1963 2 304.
- [3] WILHELM P. H., *Pure appl. Chem.* 1962 5 403.
- [4] BRENNER H., *Chem. Engng Sci.* 1962 17 229.
- [5] NAOR P. and SHINNAR R., *Ind. Engng Chem. Fundl* 1963 2 278.
- [6] KLINKENBERG A., *Ind. Engng Chem. Fundls* 1966 7 286.
- [7] VAN DER LAAN E. TH., *Chem. Engng Sci.* 1958 7 187.
- [8] SINCLAIR C. G. and MCNAUGHTON K. J., *Chem. Engng Sci.* 1965 20 261.
- [9] BACHLIER L., *Calcul de Probabilités*, Tome 1, Gauthier-Villars, Paris 1912.
- [10] BHARUCHA-REID A. T., *Elements of the Theory of Markov Processes and their Applications*, McGraw-Hill, New York 1960.
- [11] SAATY T. L., *Elements of Queuing Theory with Applications*, McGraw-Hill, New York 1961.
- [12] LEVENSPIEL O. and SMITH W. K., *Chem. Engng Sci.* 1957 6 227.
- [13] WEINER J. R. and WILHELM R. H., *Chem. Engng Sci.* 1956 6 89.
- [14] WESTERTEP K. R. and LANDSMAN P., *Chem. Engng Sci.* 1962 17 363.
- [15] DARLING D. A. and SIEGERT A. J. F., *Ann. math. Statist.* 1953 24 624.
- [16] DANCKWERTS P. V., *Chem. Engng Sci.* 1953 2 1.
- [17] DEAN H. A. and LAPIDUS L., *A.I.Ch.E. J.* 1960 6 656.
- [18] SMOLUCHOWSKY M. v. S.B., *Akad. Wiss Wien (IIA)* 1915 124 339.
- [19] ZWIETRING Th. N., *Chem. Engng Sci.* 1959 11 1.

**Résumé**—Une méthode générale du calcul des répartitions du temps de résidence pour des systèmes ayant un reflux interne, est décrite. La méthode permet la dérivation de la transformation de Laplace de tout système composé de récipients mixtes ayant entre eux un courant dans les deux sens. En particulier, les propriétés d'une cascade linéaire de récipients mixtes avec courant dans les deux sens entre eux, est discuté.

**Zusammenfassung**—Eine allgemeine Methode zur Berechnung der Verweilzeitverteilungen für Systeme mit innerem Rückfluss wird beschrieben. Die Methode gestattet die Ableitung der Laplace-Transformierten für jedes System, das sich aus Gefässen mit Vorwärts- und Rückwärtsfluss zwischen ihnen zusammensetzt. Im besonderen werden die Eigenschaften und das Verhalten einer Linearkaskade gemischter Gefässe mit Vorwärts- und Rückwärtsfluss zwischen den Gefässen besprochen.

REPRINTED



FROM

**FUNDAMENTALS****Stochastic Mixing Models for Chemical Reactors***F. J. Krambeck, R. Shinnar, and S. Katz*

Reprinted from I&amp;EC Fundamentals

Volume 6, May 1967, Page 276

Copyright 1967 by the American Chemical Society and reprinted by permission of the copyright owner

# STOCHASTIC MIXING MODELS FOR CHEMICAL REACTORS

F. J. KRAMBECK, R. SHINNAR, AND S. KATZ

Department of Chemical Engineering, The City College of the City University of New York, New York, N. Y. 10031

Turbulent chemical reactors are modeled by networks of stirred tanks, with the stochastic nature of the mixing introduced by taking the interstage flows to be stationary Markov processes. Some general features of tracer experiments in these quasi-steady flows are discussed, together with their relation to residence time distributions. The statistics of tracer experiments are analyzed, and related on the one hand to the estimation of mixing parameters, and on the other hand to the forecast of average yield from the reactor system under first-order kinetics. The variability of the reactor performance and the general story of more complicated kinetic mechanisms are deferred for a later report.

**T**HE first feature of a turbulent mixing system that calls for mathematical modeling is its average behavior, both as mixer and as chemical reactor. And there is of course an extensive literature of such models—for example (4, 6, 9, 10)—from arrangements of stirred tanks to eddy diffusion systems, all capturing the salient features of this average behavior.

Turbulent mixing systems, however, exhibit pronounced statistical fluctuations about their average behavior, and these fluctuations are in fact often the dominant feature of the actual performance of the system. Now the full statistical behavior of such a system is in principle opened to mathematical analysis by entering the differential equations for concentration change with suitable forms of random turbulent velocity. But the studies of Corrsin and others have shown (7, 5, 6) how hard it is to follow this line of analysis to the point where one can see working engineering results.

Another approach for dealing with turbulent flow systems as reactors is the use of residence time distributions, obtained from tracer experiments (4, 7, 10). Such residence time distributions are not only helpful in deriving a reasonable model for the average flow behavior, but they also allow the direct computation of conversion in first-order reactions, as well as the derivation of upper and lower bounds for the conversion for second-order reactions.

Obtaining a residence time distribution from a single tracer experiment implies that either the flow is completely steady or at least the residence time distribution of any small volume of fluid entering the system is constant and independent of the time the material entered the system (8). This is approximately true for the turbulent flow in a very long pipe, but does not apply to many other common flow systems. For example,

in the study of industrial fluidized beds the unsteady nature of the flow leads to considerable difficulties in determining residence time distributions, as repeated tracer experiments will give varying results.

The study of these unsteady only statistically determined properties of the flow is of twofold interest to the reactor designer. First of all, even in systems in which the fluctuations average out sufficiently to give a unique response to a tracer input, one would expect the unsteady nature of the flow processes to have strong effects on highly nonlinear reaction systems which are not described by steady-state flow models such as eddy diffusivity or a cascade of stirred tanks with forward and backward flow between them.

Secondly, one is interested in applying the methods of tracer experiments and residence time distributions to systems in which the fluctuations are strong enough to become apparent in tracer experiments, and to obtain the maximum information from such experiments about the nature of the flow.

The approach that we have chosen in this research, of which this is the first publication, is to study the properties of some ideal flow systems which on the one side show all the essential properties of a flow with strongly time-variant behavior and on the other allow one to perform exact calculations. It is hoped that this will not only allow quantitative checks on some common assumptions but also allow one to get some insight into the general properties of such systems.

What we present here is a kind of *ad hoc* engineering model for turbulent mixing systems, that permits one to make working calculations of both the average behavior of such systems and their statistical fluctuations. The model does not go back to the fundamental differential equations for a turbulent flow, but

instead separates in a pragmatic way molecular mixing effects from large scale turbulent effects, allocating the former to a number of stirred tanks and the latter to suitable interconnecting flows. Our picture of the mixing system thus appears as a network of stirred tanks, with interconnecting flows that are random functions of time. And in application, we would hope to be able to select suitable networks, and the corresponding random flows, to model chemical processing systems ranging from fluid bed reactors to turbulent flames.

We note that in the steady-state case any residence time distribution can be arbitrarily closely represented by a network of stirred tanks. Thus a cascade of stirred tanks with forward and backward flow between them approaches the one-dimensional diffusion equation in the limit, if the number of tanks approaches infinity while their total volume remains constant.

The model presented here allows one, with a very large number of tanks and interconnections, to describe both the steady and time-dependent behavior of any turbulent flow phenomenon to any desired degree of approximation. However, as such very complicated models are not easily amenable to analytical treatment, one should hopefully be able to elucidate the basic features of the behavior of such systems with a relatively simple network.

A word may be in order on the mathematical form in which we describe the random flows. We wish to consider flow systems with a quasi-steady character, and to this end, we take our flows to be, technically speaking, stationary random processes—that is, random functions of time whose statistical properties are unchanged by any shift of the time axis. Specifically, we take the flow pattern for a given system in the form of a stationary Markov process, so as to be able to take advantage of the very considerable body of knowledge about such processes—for example, (5). Since, for technical reasons, we need to control the flows to have positive values, we cannot conveniently use the familiar Gaussian processes such as arise in the description of Brownian motion, and we confine ourselves instead to the mathematically much simpler situation of flows that take only a finite number of preselected values. Indeed, the numerical calculations we present below are all for two-valued flows.

The statistical history of a Markov process is governed entirely by the probabilities of transition from one state to another. Its present alone is accordingly all that is needed to forecast its future. The concentrations that develop in our mixing-reactor systems under the influence of the Markov flows cannot by themselves form a Markov process, since the concentration patterns might change in this way or that, depending on the state of flow. The concentrations, when taken together with the state of flow, do, however, form a Markov process, and the equations describing how the joint probability distribution of concentration and flow evolves in time serve as the working equation for our mixing and reactor studies. Restricting the flows to a finite number of preselected values does not correspondingly restrict the concentrations. They go freely over the whole range of physically possible values.

In this paper, we aim to set down a fairly complete mathematical description of our system, and carry out a preliminary analysis of its behavior as mixer, and as reactor. The plan is accordingly as follows. After setting down the description of our mixing model, we construct a random walk for the passage of a particle of fluid through the system. We then develop the equations describing tracer experiments on the model, and discuss their relation with the random walk probabilities, in particular with the residence time distribution of fluid in the system. Next, we present and discuss the results

of some sample calculations of the statistics of tracer experiments. Finally, we formulate the equations describing the behavior of our mixing systems as chemical reactors, and, for first-order reactions, discuss the relation between conversion and residence time.

### The Model

To fix the description of our mixing model, we take  $n$  stirred tanks, connected, quite arbitrarily, by interstage flows (see Figure 1). We index the tanks by  $i$  (running from 1 to  $n$ ), denote the volume of the  $i$ th tank by  $v_i$  and the volumetric flow rate from the  $i$ th tank to the  $j$ th by  $w_{ij}$ . Since each tank may receive part of the feed, it is convenient to assign the index value  $i = 0$  to a feed station, and denote the feed rate to the  $j$ th tank by  $w_{0j}$ . Since each tank may contribute to the outlet stream, it is convenient to assign the index value  $i = n + 1$  to an outlet station, and denote the outlet rate from the  $j$ th tank by  $w_{j,n+1}$ . The quantity  $w_{0,n+1}$  may be taken to be the flow rate of material that bypasses the mixing system altogether.

The flow rates  $w_{ij}$  will be permitted to vary with time, but the volumes  $v_i$  are to be held constant. Accordingly, we require the equality of inlet and outlet flows, tank by tank:

$$\sum_{i=0}^n w_{ij} = \sum_{k=1}^n w_{jk}; \quad j = 1, 2, \dots, n \quad (1)$$

This entails, of course, the equality of the total inlet and outlet flow rates, so that, denoting this over-all flow rate by  $w$ , we may write

$$\sum_{j=1}^{n+1} w_{0j} = \sum_{i=0}^n w_{i,n+1} = w \quad (2)$$

We have so far not attached any meaning to the "diagonal" expressions  $w_{jj}$  but if we denote the common value of the two sides of Equation 1 by  $-w_{jj}$ , we will have filled out a square matrix ( $n + 1$  by  $n + 1$ ) of flow rates  $w_{ij}$ ,  $i = 0, 1, 2, \dots, n$ ,  $j = 1, 2, \dots, n + 1$  (see Table I), for which

$$\sum_{i=0}^n w_{ij} = \sum_{k=1}^{n+1} w_{jk} = 0; \quad j = 1, 2, \dots, n \quad (3)$$

We have so far not said anything about the random variation of the flows, and we now explicitly recognize the flows as arising from a Markov process. We consider for this purpose only Markov processes with a finite number of states, and if we

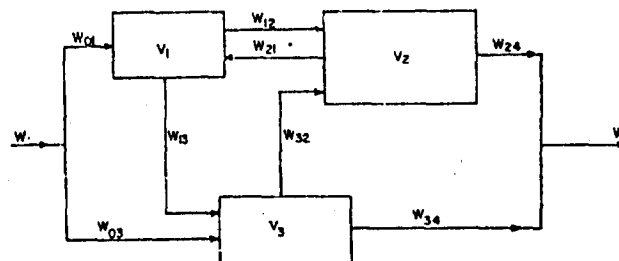


Figure 1. Typical flow network

Table I. Typical Flow Matrix for Figure 1

		Column Index			
		1	2	3	4
Row Index	0	1	0	1	0
	1	[-3]	2	1	0
	2	2	[-3]	0	1
	3	0	1	[-2]	1

index the states by  $\alpha$ , we have in the system at any moment a square matrix

$$w_{i,j}; \quad i = 0, 1, \dots, n \\ j = 1, 2, \dots, n + 1$$

representing the flows in state  $\alpha$ . Conditions 2 and 3 hold for every state  $\alpha$ , so we may write them as

$$\sum_{i=0}^n w_{i,j} = \sum_{i=1}^{n+1} w_{j,i} = 0; \quad j = 1, 2, \dots, n \quad (4)$$

$$\sum_{j=1}^{n+1} w_{j,\alpha} = \sum_{i=0}^n w_{i,\alpha+1} = w_{\alpha}; \quad \text{all } \alpha \quad (5)$$

In Equation 5,  $w_{\alpha}$  represents the total feed (take-off) rate for the system when the flows are in state  $\alpha$ . We note explicitly that the tank volumes are not subject to variation with the flows, and keep their constant values  $v_i$ .

The probability structure of the flows now resides in how we describe the transitions of the underlying Markov process from one state  $\alpha$  to another  $\beta$ . Denoting the probability of such a transition in a time  $\tau$  by  $\pi(\alpha \rightarrow \beta; \tau)$ , we may describe the behavior of  $\pi$  for small  $\tau$  by setting

$$\pi(\alpha \rightarrow \beta; \tau) = \lambda_{\alpha\beta}\tau + o(\tau); \quad \alpha \neq \beta$$

where  $\lambda_{\alpha\beta}$  is some assigned matrix of switching rates and  $o(\tau)$  is a function of  $\tau$  which goes to zero faster than  $\tau$ . Since, in a time  $\tau$ , state  $\alpha$  can either become some other state or remain unchanged, we complete the characterization of  $\pi$  for small  $\tau$  by setting the probability that state  $\alpha$  remains unchanged,

$$\pi(\alpha \rightarrow \alpha; \tau) = 1 - \left( \sum_{\beta \neq \alpha} \lambda_{\alpha\beta} \right) \tau + o(\tau)$$

If now we define the diagonal quantities  $\lambda_{\alpha\alpha}$  to make

$$\sum_{\beta} \lambda_{\alpha\beta} = 0; \quad \text{all } \alpha \quad (6)$$

we have a full square matrix of switching rates  $\lambda_{\alpha\beta}$  in terms of which we may compactly describe the transition probabilities,  $\pi$ :

$$\pi(\alpha \rightarrow \beta; \tau) = \delta_{\alpha\beta} + \lambda_{\alpha\beta}\tau + o(\tau) \quad (7)$$

where  $\delta_{\alpha\beta}$  is the Kronecker delta.

We may now describe the probability history of flow states  $\alpha$ . If we denote by  $p_{\alpha}(t)$  the probability that the flows are in state  $\alpha$  at time  $t$ , we have, from the characteristic property of Markov processes, that

$$p_{\beta}(t + \tau) = \sum_{\alpha} p_{\alpha}(t) \cdot \pi(\alpha \rightarrow \beta; \tau)$$

Applying Equation 7 gives the set of differential equations

$$\frac{dp_{\beta}(t)}{dt} = \sum_{\alpha} \lambda_{\alpha\beta} p_{\alpha}(t) \quad (8)$$

whose solution carries with it the complete evolution of the distribution of flow states with time. Now we shall be concerned in what follows only with quasi-steady flow systems—that is, only with flows in a stationary state, whose probability distribution no longer varies with time. This statistical equilibrium distribution is given from Equation 8 as those probabilities  $\hat{p}_{\alpha}$  for which

$$\sum_{\alpha} \lambda_{\alpha\beta} \hat{p}_{\alpha} = 0 \quad (9)$$

We take our Markov flow processes always to be of the well-behaved kind that have a unique stationary distribution, defined by Equation 9, together with the normalization

$$\sum_{\alpha} \hat{p}_{\alpha} = 1 \quad (10)$$

This amounts algebraically to requiring that zero, which is always an eigenvalue of the matrix  $\lambda_{\alpha\beta}$ , be only a single, not a multiple, eigenvalue.

Finally, the equilibrium corresponding to our stationary flows is a statistical equilibrium only—that is, the flows continue to exhibit random fluctuations, but the statistical character of these fluctuations does not change with time. And the system may of course exhibit other random features that do not share the stationary character of the flows. This will certainly be the case when we come to discuss tracer experiments.

### A Random Walk

The physical nature of the mixing system we have just described can be studied on two levels: in terms of the random passage through the system of a particle of tracer put initially in the feed line; or in terms of the random concentration pattern developed in the system when the tracer is fed according to an assigned schedule. The second we analyze later under the heading "Mixing Equations"; what we do here is set up the random walk for a single particle.

The system, for this purpose, consists of the  $n$  tanks plus the outlet station, and the state of a particle is accordingly described by its location index  $i$  (ranging from 1 to  $n + 1$ ). We regard each tank in the usual way as a Poisson (exponential) holdup for the particle, so that the probability that the particle goes in a short time  $\tau$  from tank  $i$  to tank  $j$  is just  $(w_{ij}/v_i)\tau$ . The probability that it stays in tank  $i$  is

$$1 - \left( \sum_{j \neq i} \frac{w_{ij}}{v_i} \right) \tau = 1 + \frac{w_{ii}}{v_i} \tau$$

the equality holding by virtue of Equation 4. And, once the particle is in the outlet state,  $i = n + 1$ , it stays there.

The flows  $w_{ij}$  must, however, be regarded as random quantities  $w_{ij\alpha}$ . Thus, the location of the tracer particle cannot alone be a Markov process, since the transition probabilities from one location to another depend on the state of the flow. However, if we lump together  $\alpha$  and  $i$ , the state of the flow and the location of the particle, we find a composite Markov process whose structure can be described in terms of the probability  $\pi(\alpha, i \rightarrow \beta, j; \tau)$  of making a transition from state  $\alpha, i$  to state  $\beta, j$  in time  $\tau$ . Following Equation 7, and the Poisson holdup character of the individual tanks, we may describe the behavior of this  $\pi$  for small  $\tau$  by setting

$$\left\{ \begin{aligned} \pi(\alpha, i \rightarrow \beta, j; \tau) &= [\delta_{\alpha\beta} + \lambda_{\alpha\beta}\tau + o(\tau)] \left[ \delta_{ij} + \frac{w_{ij\alpha}}{v_i} \tau + o(\tau) \right] \\ \pi(\alpha, n + 1 \rightarrow \beta, j; \tau) &= [\delta_{\alpha\beta} + \lambda_{\alpha\beta}\tau + o(\tau)] \delta_{n+1,j} \end{aligned} \right. \quad (11)$$

We may now describe the probability history of the composite flow-particle location states in terms of the distribution  $p_{\alpha i}(t)$ , the probability that the flow is in state  $\alpha$  and the tracer particle in location  $i$  at time  $t$ . Setting down the characteristic property of the Markov process, that

$$p_{\beta j}(t + \tau) = \sum_{\alpha} \sum_i p_{\alpha i}(t) \pi(\alpha, i \rightarrow \beta, j; \tau)$$

and applying Equation 11, gives the set of differential equations

$$\frac{d\rho_{\beta j}}{dt} = \sum_{i=1}^n \frac{w_{i\beta}}{v_i} \rho_{\beta i}(t) + \sum_{\alpha} \lambda_{\alpha j} \rho_{\beta j}(t), \quad j = 1, 2, \dots, n+1 \quad (12)$$

The particle's being initially in the input line, we describe by distributing its initial location probability over the  $n$  tanks (and the outlet) in proportion to the feed rates—that is, we take

$$\rho_{\beta j}(0) = \bar{\rho}_{\beta} \frac{w_{\alpha j \beta}}{w_{\beta}}; \quad j = 1, 2, \dots, n+1 \quad (13)$$

where  $\bar{\rho}_{\beta}$  is the stationary distribution of flow states defined by Equations 9 and 10.

The differential Equations 12, together with the initial Conditions 13, determine the whole development in time of the joint probability history of flow state and particle location. If we sum  $\rho_{\beta j}$  over  $j$ , we recover simply the probability distribution of the flow states:

$$\rho_{\beta}(t) = \sum_{j=1}^{n+1} \rho_{\beta j}(t)$$

If we sum Equations 12 and 13 over  $j$ , applying 4 and 5, we find

$$\frac{d\rho_{\beta}(t)}{dt} = \sum_{\alpha} \lambda_{\alpha \beta} \rho_{\alpha}(t) \\ \rho_{\beta}(0) = \bar{\rho}_{\alpha}$$

that is, the differential equations (8) for the flow state probabilities, with the stationary distribution as initial conditions. It then follows from our earlier discussion that the flow state probability  $\rho_{\beta}(t)$  remains at the stationary initial value  $\bar{\rho}_{\beta}$ , so that, for all time,

$$\sum_{j=1}^{n+1} \rho_{\beta j}(t) = \bar{\rho}_{\beta} \quad (14)$$

Equations 12 and 13, or rather, their solution, contain all the basic information about distribution of age and residence time in the mixing system. Thus  $\sum_{\beta} \rho_{\beta j}(t)$  is the probability that a particle, initially in the inlet, is in location  $j$  at time  $t$ . Suitably normalized

$$g_j(t) = \frac{\sum_{\beta} \rho_{\beta j}(t)}{\sum_{\beta} \int_0^{\infty} \rho_{\beta j}(t) dt} \quad (15)$$

it is simply the age distribution of material in location  $j$ , in the sense that  $\int_{t_0}^{t_1} g_j(t) dt$  is the probability that a particle in location

$j$  has been in the system a time between  $t_0$  and  $t_1$ . One can accordingly, for specified flow models, compute such over-all measures of the performance of the flow system as the local age distributions and local life expectancy distributions which again can be measured by tracer experiments.

Also,

$$F(t) = \sum_{\beta} \rho_{\beta, n+1}(t) \quad (16)$$

is the probability that a particle, initially in the inlet, has found its way to the outlet by time  $t$ —that is,  $F$  is the cumulative residence time distribution of material in the system, and will be related, in what follows, to the average response of the system to suitable tracer experiments.

We set up here the mathematical methods for studying tracer experiments in our flow systems. The mean response, as well as suitable measures of fluctuations about the mean, will satisfy certain ordinary differential equations rather like Equation 12, and their solution in illustrative cases is discussed later under the heading "Tracer Calculations."

If we arrange to load into the input lines of our mixing systems  $\varphi(t)$  moles per unit time of tracer material, then the concentration  $x_j$  (in moles per unit volume) of tracer in the  $j$ th tank develops under the influence of the random flow states  $\alpha$  according to the differential equations

$$v_j \frac{dx_j}{dt} = \frac{w_{\alpha j \alpha}}{w_{\alpha}} \varphi(t) + \sum_{i=1}^n w_{i j \alpha} x_i - \sum_{k=1}^{n+1} w_{j k \alpha} x_j$$

Introducing the pseudo-flows  $w_{i j \alpha}$ , and calling on Equation 4, this material balance may be written compactly as

$$v_j \frac{dx_j}{dt} = \frac{w_{\alpha j \alpha}}{w_{\alpha}} \varphi(t) + \sum_{i=1}^n w_{i j \alpha} x_i; \quad j = 1, 2, \dots, n \quad (17)$$

If further, we arrange that the system be initially empty of tracer material, we may add to Equation 17 the initial condition

$$x_j|_{t=0} = 0; \quad j = 1, 2, \dots, n \quad (18)$$

Now, for the reasons noted earlier, the set of concentration values

$$x = \{x_1, x_2, \dots, x_n\}$$

does not alone form a Markov process, but the composite

$$\{\alpha, x\} = \{\alpha; x_1, x_2, \dots, x_n\}$$

of flow state and concentration pattern does. The structure of this composite Markov process is governed by the transition probability density,  $\pi(\alpha, x \rightarrow \beta, y; t, \tau)$ , where

$$\int_{a_n}^{b_n} \dots \int_{a_1}^{b_1} \pi(\alpha, x \rightarrow \beta, y; t, \tau) dy_1 \dots dy_n$$

is the probability of making a transition from flow state  $\alpha$  with concentration pattern  $x = x_1, x_2, \dots, x_n$  at time  $t$ , to flow state  $\beta$  with concentration in the  $j$ th tank between  $a_j$  and  $b_j$  a time  $\tau$  later. The time  $t$  appears here explicitly in  $\pi$  because of the time dependence of the tracer feed rate,  $\varphi$ .

Following Equation 7, and the fact that the  $x_j$  are bound by the differential Equations 17, we may express this  $\pi$  for small  $\tau$  in the form

$$\pi(\alpha, x \rightarrow \beta, y; t, \tau) = [\delta_{\alpha \beta} + \lambda_{\alpha \beta} \tau + o(\tau)] \cdot \\ \delta \left[ y_1 - x_1 - \left( \frac{w_{\alpha 1 \alpha}}{w_{\alpha}} \frac{\varphi(t)}{v_1} + \sum_{i=1}^n \frac{w_{i 1 \alpha}}{v_1} x_i \right) \tau + o(\tau) \right] \cdot \\ \dots \delta \left[ y_n - x_n - \left( \frac{w_{\alpha n \alpha}}{w_{\alpha}} \frac{\varphi(t)}{v_n} + \sum_{i=1}^n \frac{w_{i n \alpha}}{v_n} x_i \right) \tau + o(\tau) \right] \quad (19)$$

where the  $\delta$ 's in the concentration variables are Dirac deltas.

We may now describe the statistical history of the composite flow-concentration states in terms of the probability density,  $p_{\alpha}(x, t)$ , where

$$\int_{a_n}^{b_n} \dots \int_{a_1}^{b_1} p_{\alpha}(x, t) dx_1 \dots dx_n$$

is the probability that at time  $t$  the flow is in state  $\alpha$ , and the concentration in the  $j$ th tank is between  $a_j$  and  $b_j$ . We set down the characteristic property of the Markov process, that



$$p_{\beta}(y, t + \tau) = \sum_{\alpha} \int \dots \int p_{\alpha}(x, t) \pi(\alpha, x \rightarrow \beta, y; t, \tau) dy_1 \dots dy_n$$

where the integrals are over all values of the  $y_j$ , just as the sum is over all flow states  $\alpha$ . Then, applying Equation 19 gives the partial differential equation

$$\frac{\partial p_{\beta}(y, t)}{\partial t} + \sum_{i=1}^n \frac{\partial}{\partial y_i} \left[ \left\{ \frac{w_{i\beta}}{v_i} \varphi(t) + \sum_{j=1}^n \frac{w_{ij}}{v_j} y_j \right\} p_{\beta}(y, t) \right] = \sum_{\alpha} \lambda_{\alpha\beta} p_{\alpha}(y, t) \quad (20)$$

Further, we may interpret the initial Conditions 18 as implying an initial condition for the distribution  $p_{\beta}(y, t)$ , in the form

$$p_{\beta}(y, 0) = \bar{p}_{\beta} \cdot \delta(y_1) \dots \delta(y_n) \quad (21)$$

where  $\bar{p}_{\beta}$  is the stationary probability distribution of flow states defined by Equations 9 and 10.

With Equations 20 and 21 in hand, we note first that, if we integrate  $p_{\beta}(y, t)$  over the  $y_j$  (the integrals running over all possible values), we find simply the probability distribution of the flow states

$$p_{\beta}(t) = \int \dots \int p_{\beta}(y, t) dy_1 \dots dy_n$$

If, similarly, we integrate Equations 20 and 21 over the  $y_j$ , we find

$$\frac{dp_{\beta}(t)}{dt} = \sum_{\alpha} \lambda_{\alpha\beta} p_{\alpha}(t); \quad p_{\beta}(0) = \bar{p}_{\beta}$$

that is, the differential Equations 8 for the flow state probabilities, with the stationary distribution as initial condition. It follows, as in our discussion for the random walk, that the flow state probabilities  $p_{\beta}(t)$  remain at their stationary initial values  $\bar{p}_{\beta}$ , so that for all time

$$\int \dots \int p_{\beta}(y, t) dy_1 \dots dy_n = \bar{p}_{\beta} \quad (22)$$

Now the partial differential Equation 20, although linear, presents in general formidable complications, and we propose accordingly to confine ourselves to a study of the leading moments of the concentration variables. We begin by defining the partial mean concentrations

$$\mu_{\beta j}(t) = \int \dots \int y_j p_{\beta}(y, t) dy_1 \dots dy_n; \quad j = 1, 2, \dots, n \quad (23)$$

Bringing this definition to Equation 20 and 21 and applying 22 we find the system of ordinary differential equations with initial conditions

$$\frac{d\mu_{\beta j}(t)}{dt} = \bar{p}_{\beta} \frac{w_{j\beta}}{v_j} \varphi(t) + \sum_{i=1}^n \frac{w_{ij}}{v_j} \mu_{\beta i}(t) + \sum_{\alpha} \lambda_{\alpha\beta} \mu_{\alpha j}(t) \quad (24)$$

$$\mu_{\beta j}(0) = 0$$

These are the equations that will be solved below for illustrative flow systems to produce the mean response to tracer inputs. The mean rate (in moles per unit time) at which tracer material leaves the system may be calculated from the solution of Equation 24 as

$$\mu(t) = \sum_{\beta} \int \dots \int \left[ \frac{w_{\beta n}}{v_n} \varphi(t) + \sum_{j=1}^{n-1} w_{j, n+\beta} v_j \right] \times p_{\beta}(y, t) dy_1 \dots dy_n$$

which we may write as

$$\mu(t) = \sum_{\beta} \left[ \bar{p}_{\beta} \frac{w_{\beta n}}{v_n} \varphi(t) + \sum_{j=1}^{n-1} w_{j, n+\beta} \mu_{\beta j}(t) \right] \quad (25)$$

It appears from Equations 24 and 25 that the functions  $\mu_{\beta j}(t)$ ,  $\mu(t)$  are related linearly and homogeneously to the tracer feed schedule  $\varphi(t)$ . They are accordingly convolutions of suitable kernels with  $\varphi$ . In particular, we may set

$$\mu(t) = \int_0^t f(t - \tau) \varphi(\tau) d\tau \quad (26)$$

where  $f(t)$  is the mean response in outlet tracer flow to a unit pulse in inlet tracer:

$$\mu(t) = f(t) \quad \text{for} \quad \varphi(t) = \delta(t)$$

That is, as far as mean values (first moments) go, the response to an arbitrary tracer feed schedule  $\varphi$  is simply the convolution of  $\varphi$  with the impulse response  $f$ , just as it is for a deterministically modeled mixing system. In particular, the mean step response is the integral of the mean impulse response.

Further, the mean response described by Equations 24 and 25 can be related directly to the random walk probability distributions (12, 13, and 16). If we enter Equation 24 with  $\varphi(t) = \delta(t)$ , and interpret the  $\delta$ -function terms suitably as initial conditions, we see that the average molar amounts of tracer  $v_j \mu_{\beta j}(t)$  are exactly the probabilities  $p_{\beta j}(t)$  for  $j = 1, 2, \dots, n$ . Also, under these circumstances, we have from Equation 25 that

$$f(t) = \sum_{\beta} \left[ \bar{p}_{\beta} \frac{w_{\beta n}}{v_n} \delta(t) + \sum_{j=1}^n \frac{w_{j, n+\beta}}{v_j} p_{\beta j}(t) \right]$$

and a comparison with the random walk equations shows that

$$f(t) = \frac{dF(t)}{dt}$$

so that the mean impulse response is just the probability density function of residence times in the system. This is simply another indication that, as far as first moments go, our stochastic mixing models behave in very much the same way as deterministically modeled systems.

We turn now to a consideration of the second moments of the concentration variables. Defining the partial mean values of the products (squares included) by

$$S_{\beta jk}(t) = \int \dots \int y_j y_k p_{\beta}(y, t) dy_1 \dots dy_n \quad (27)$$

$$j, k = 1, 2, \dots, n$$

and bringing the definitions to Equations 20 and 21, we find the system of ordinary differential equations with initial conditions

$$\frac{dS_{\beta jk}}{dt} = \left( \frac{w_{j\beta}}{v_j} \mu_{\beta k}(t) + \frac{w_{k\beta}}{v_k} \mu_{\beta j}(t) \right) \varphi(t) + \sum_{i=1}^n \left( \frac{w_{ij}}{v_j} S_{\beta ik}(t) + \frac{w_{ik}}{v_k} S_{\beta ij}(t) \right) + \sum_{\alpha} \lambda_{\alpha\beta} S_{\alpha jk}(t),$$

$$S_{\beta jk}(0) = 0 \quad j, k = 1, 2, \dots, n \quad (28)$$

with the  $\mu_{\beta j}(t)$  defined by Equation 24. These are the equations that will be solved below for illustrative flow systems to produce the variances in response to tracer input. The mean square rate at which tracer leaves the system can be calculated from the solution of Equation 28 as

$$S^2(t) = \sum_{\beta} \int \dots \int \left[ \frac{w_{\beta n}}{v_n} \varphi(t) + \sum_{j=1}^{n-1} w_{j, n+\beta} v_j \right]^2 p_{\beta}(y, t) dy_1 \dots dy_n$$

which we may write as

$$S^2(t) = \sum_n \left[ \bar{\rho}_n \left( \frac{w_{\alpha, n+1, \beta}}{w_\beta} \right)^2 \varphi^2(t) + 2 \frac{w_{\alpha, n+1, \beta}}{w_\beta} \varphi(t) \sum_{j=1}^n w_{j, n+1, \beta} \mu_{\beta j}(t) + \sum_{j=1}^n \sum_{k=1}^n w_{j, n+1, \beta} w_{k, n+1, \beta} S_{\beta j k} \right] \quad (29)$$

Finally, calling on Equation 25, we may calculate the variance of the outlet response to the tracer feed schedule  $\varphi(t)$  as

$$\sigma^2(t) = S^2(t) - \mu^2(t) \quad (30)$$

In the same way we can calculate the variance of the local concentration response in tank  $j$  to the tracer feed schedule  $\varphi(t)$ . These measures of the statistical fluctuation in the system response have of course no counterparts for deterministically modeled mixing systems.

Another statistical average that can be calculated from the results of tracer experiments is the autocorrelation function,  $\rho_i(\tau)$ , defined as follows:

$$\rho_i(\tau) = \frac{\langle z(t)z(t+\tau) \rangle - \mu(t)\mu(t+\tau)}{\sigma(t)\sigma(t+\tau)}$$

where  $z(t)$  is the rate at which tracer leaves the system at time  $t$ .

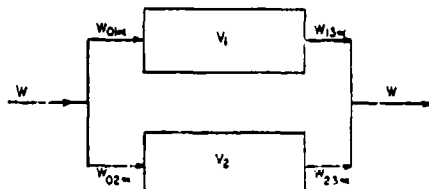


Figure 2. Parallel tank model



Figure 3. Series tank model

For a stationary random process this would be a function of  $\tau$  only, but tracer response is not stationary. To calculate this function for the model we note that

$$z(t) = \frac{w_{\alpha, n+1, \beta}}{w_\beta} \varphi(t) + \sum_{j=1}^n w_{j, n+1, \beta} v_j(t)$$

$$\langle z(t)z(t+\tau) \rangle = \varphi(t)\varphi(t+\tau) \left\langle \frac{w_{\alpha, n+1, \beta}}{w_\beta} \frac{w_{\alpha, n+1, \beta}}{w_\beta} \right\rangle + \varphi(t) \left\langle \frac{w_{\alpha, n+1, \beta}}{w_\beta} \sum_{j=1}^n w_{j, n+1, \beta} v_j(t+\tau) \right\rangle + \varphi(t+\tau) \left\langle \frac{w_{\alpha, n+1, \beta}}{w_\beta} \sum_{j=1}^n w_{j, n+1, \beta} v_j(t) \right\rangle + \left\langle \sum_{j=1}^n \sum_{k=1}^n w_{j, n+1, \beta} w_{k, n+1, \beta} v_j(t)v_k(t+\tau) \right\rangle$$

where  $\alpha$  is the flow state at time  $t$  and  $\beta$  is the flow state at time  $t + \tau$ . In case there is no direct bypassing ( $w_{\alpha, n+1, \beta} = 0$  for all  $\alpha$ ), the first three terms vanish. Otherwise they can be calculated by methods similar to that shown below for the last term. We now express the expectation in terms of the probability distribution.

$$\left\langle \sum_{j=1}^n \sum_{k=1}^n w_{j, n+1, \beta} w_{k, n+1, \beta} v_j(t)v_k(t+\tau) \right\rangle = \int \dots \int dx_1 \dots dx_n dy_1 \dots dy_n \sum_{\alpha} \sum_{\beta} \sum_{j=1}^n \sum_{k=1}^n w_{j, n+1, \beta} \times w_{k, n+1, \beta} v_j(t)v_k(t+\tau) p_\alpha(t, x) \pi(\alpha, x \rightarrow \beta, y; \tau) = \sum_{\beta} \sum_{k=1}^n w_{k, n+1, \beta} q_{k\beta}$$

where

$$q_{k\beta} = \sum_{\alpha} \sum_{j=1}^n w_{j, n+1, \alpha} \int \dots \int dx_1 \dots dx_n dy_1 \dots dy_n v_j(t) p_\alpha(t, x) \pi(\alpha, x \rightarrow \beta, y; \tau)$$

The product  $p_\alpha(t, x) \pi(\alpha, x \rightarrow \beta, y; \tau)$  above is just the joint distribution of  $(\alpha, x)$  and  $(\beta, y)$  at  $t$  and  $t + \tau$ , respectively. The transition probability  $\pi(\alpha, x \rightarrow \beta, y; \tau)$  satisfies the same differential equation as  $p_\beta(t + \tau, y)$ —namely,

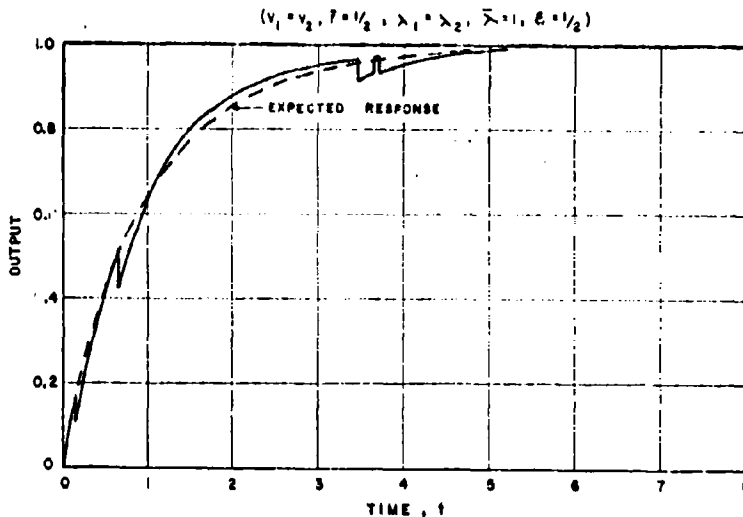


Figure 4. Typical step response for parallel case

$$(v_1 = v_2, P = 1/2, \lambda_1 = \lambda_2, \Sigma = 1)$$

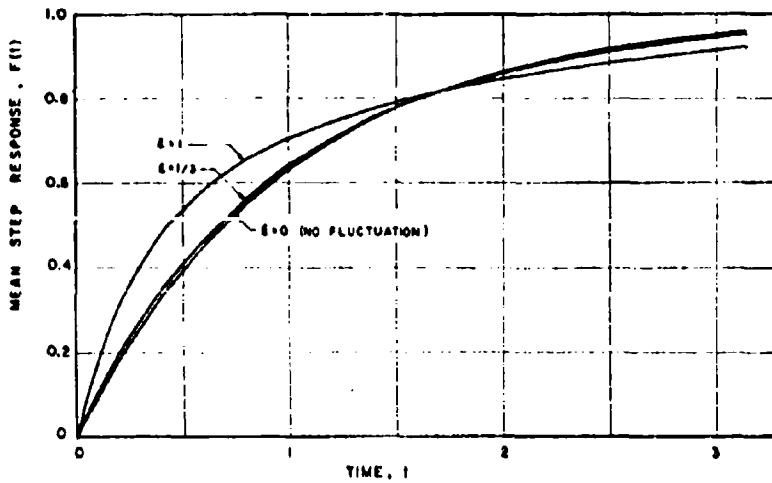


Figure 5. Effect of fluctuation magnitude on mean response to step input for parallel case

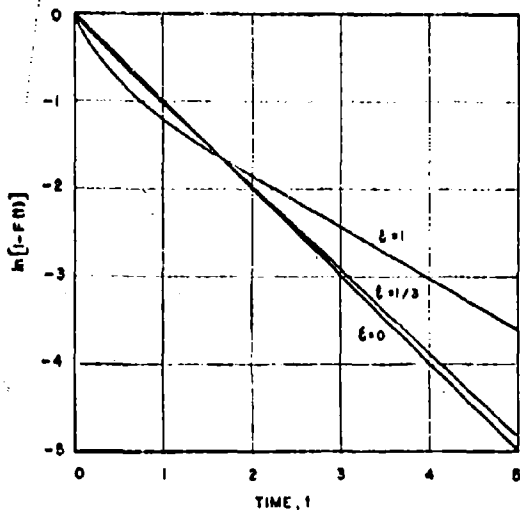


Figure 6. Effect of fluctuation magnitude on mean response to step input for parallel case (replotted)

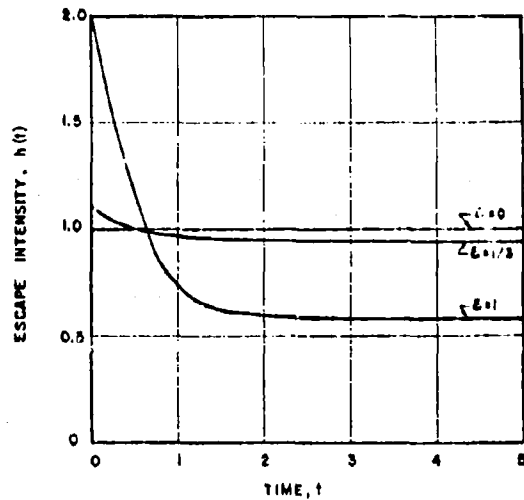


Figure 7. Effect of fluctuation magnitude on escape intensity,  $h(t)$ , for parallel case

$$v_1 = v_2, P = 1/2, \lambda_1 = \lambda_2, \lambda = 1$$

$$\frac{\partial}{\partial \tau} \pi(\alpha, \lambda \rightarrow \beta, y; \tau) + \sum_{j=1}^n \frac{\partial}{\partial y_j} \left[ \left\{ \frac{w_{\alpha, \beta} \varphi(t + \tau)}{v_j} + \sum_{l=1}^n \frac{w_{l, \beta}}{v_l} y_l \right\} \pi(\alpha, \lambda \rightarrow \beta, y; \tau) \right] = \sum_{\gamma} \lambda_{\gamma \beta} \pi(\alpha, \lambda \rightarrow \gamma, y; \tau)$$

with

$$\pi(\alpha, \lambda \rightarrow \beta, y; 0) = \delta_{\alpha \beta} \delta(y - \lambda)$$

From this equation we find that

$$\frac{dq_{\lambda \beta}}{d\tau} = \frac{w_{\alpha \beta} \varphi(t + \tau)}{v_\beta} + \sum_{\alpha} \sum_{j=1}^n \pi(\alpha \rightarrow \beta; \tau) w_{j, \alpha-1, \beta} u_{\alpha j}(t) + \sum_{j=1}^n \frac{w_{j, \beta}}{v_j} q_{j\beta} + \sum_{\gamma} \lambda_{\gamma \beta} q_{\gamma}$$

with

$$\gamma = 0; \quad q_{\lambda \beta} = \sum_{j=1}^n w_{j, \alpha-1, \beta} S_{\beta j}(t)$$

This set of equations can be solved in conjunction with the previous set for  $\mu_{\beta j}$  and  $S_{\beta j}$ .

By methods similar to the above one could compute many other statistical measures of the tracer response of the model which could be directly compared with values determined experimentally for a real system. The measures mentioned above,  $\mu(t)$ ,  $\sigma(t)$ , and  $\rho_L(\tau)$ , are probably the easiest to obtain accurate estimates of experimentally. In certain situations, however, one might want to study the effect of unsteadiness in a system for which the variance of the response, at the outlet,  $\sigma^2(t)$ , is small but sizable fluctuations occur in other parts of

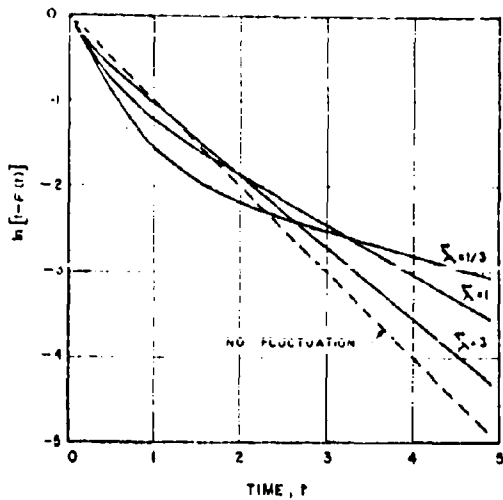


Figure 8. Effect of switching rate on mean response to step input for parallel case

$$v_1 = v_2, \bar{\tau} = 1/2, \lambda_1 = \lambda_2, \epsilon = 1$$

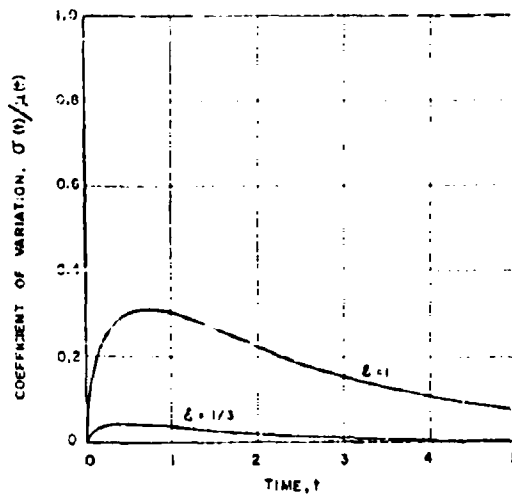


Figure 10. Effect of fluctuation magnitude on  $\sigma(t)/\mu(t)$  of step response for parallel case

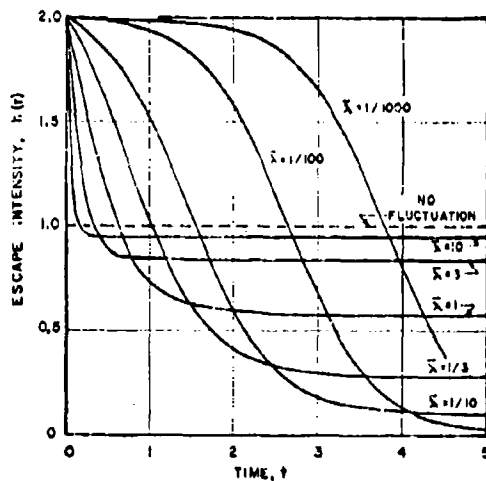


Figure 9. Effect of switching rate on escape intensity,  $h(t)$ , for parallel case

$$v_1 = v_2, \bar{\tau} = 1/2, \lambda_1 = \lambda_2, \epsilon = 1$$

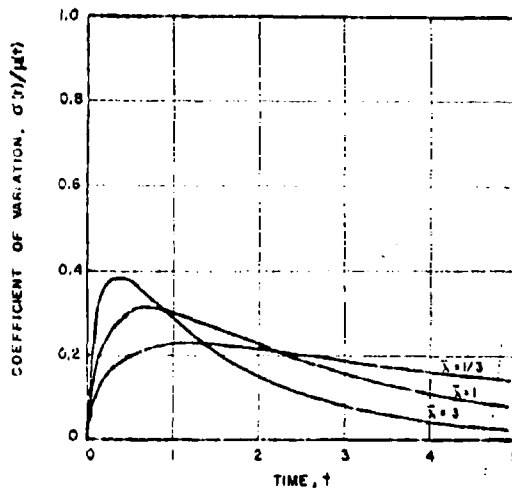


Figure 11. Effect of switching rate on  $\sigma(t)/\mu(t)$  of step response for parallel case

$$v_1 = v_2, \bar{\tau} = 1/2, \lambda_1 = \lambda_2, \epsilon = 1$$

the system. In this case one could measure statistics of the response at various points within the system and compare this with the corresponding statistics of various tanks in the model.

Once a model has been formulated and the parameters have been fixed by comparison with tracer experiments, one can proceed to study how the unsteadiness of the system affects various types of chemical reactions.

#### Tracer Calculations

We now apply the foregoing analysis to two simple mixing systems. In these examples the variable flows are assumed to take on only two values. The matrix of switching rates becomes two-by-two, and application of Equation 6 allows us to express the four elements of the matrix in terms of two quantities  $\lambda_1$  and  $\lambda_2$ , as follows:

$$\begin{aligned} \lambda_{12} &= -\lambda_{11} = \lambda_1 \\ \lambda_{21} &= -\lambda_{22} = \lambda_2 \end{aligned} \quad (31)$$

The meaning of these quantities is given by Equation 7:

$$\begin{aligned} \pi(1 \rightarrow 2; \tau) &= \lambda_1 \tau + o(\tau) \\ \pi(1 \rightarrow 1; \tau) &= 1 - \lambda_1 \tau + o(\tau) \\ \pi(2 \rightarrow 1; \tau) &= \lambda_2 \tau + o(\tau) \\ \pi(2 \rightarrow 2; \tau) &= 1 - \lambda_2 \tau + o(\tau) \end{aligned} \quad (32)$$

The equations for the probability distribution of the flow states (Equation 8) then take the form

$$\begin{aligned} \frac{d\rho_1}{dt} &= -\lambda_1 \rho_1 + \lambda_2 \rho_2 \\ \frac{d\rho_2}{dt} &= \lambda_1 \rho_1 - \lambda_2 \rho_2 \end{aligned} \quad (33)$$

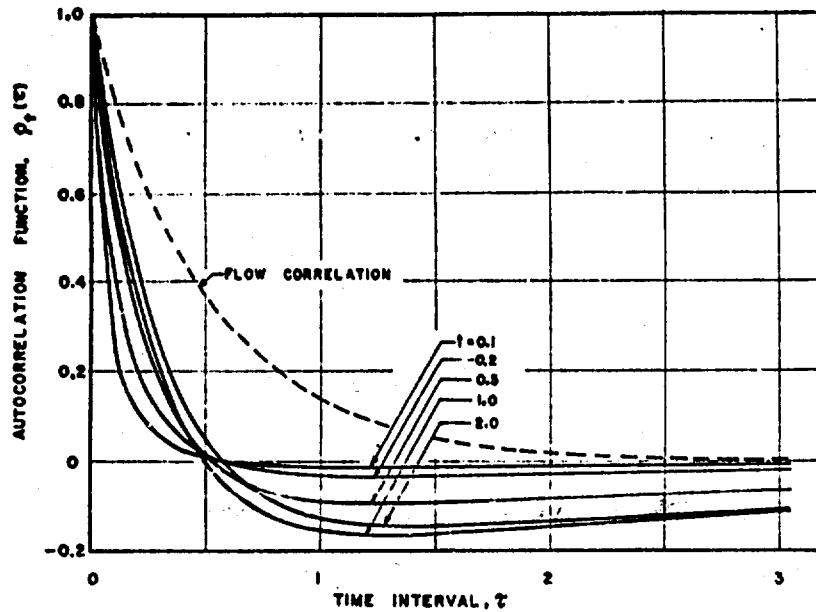


Figure 12. Typical autocorrelation of step response for parallel case

$$v_1 = v_2, \bar{r} = 1/2, \lambda_1 = \lambda_2, \epsilon = 1, \bar{\lambda} = 1$$

The stationary distribution is then given by

$$\beta_1 = \frac{\lambda_2}{\lambda_1 + \lambda_2}, \quad \beta_2 = \frac{\lambda_1}{\lambda_1 + \lambda_2} \quad (34)$$

We may define a mean switching rate,  $\bar{\lambda}$ , by

$$\bar{\lambda} = \beta_1 \lambda_1 + \beta_2 \lambda_2 = \frac{2\lambda_1 \lambda_2}{\lambda_1 + \lambda_2} \quad (35)$$

In the first of the two cases, the system consists of two tanks in parallel (Figure 2), where the total flow,  $w$ , is constant. The split of flow between the two tanks will vary, however. The flow states will be described by the fraction of the total flow entering tank 1,  $r_\alpha$ :

$$r_\alpha = \frac{w'_{1\alpha}}{w'}; \quad \alpha = 1, 2 \quad (36)$$

We then let

$$\begin{aligned} r_1 &= \bar{r} + \beta_2 \epsilon \\ r_2 &= \bar{r} - \beta_1 \epsilon \end{aligned} \quad (37)$$

where  $\bar{r}$  is the average split of flow and  $\epsilon$  is equal to  $r_1 - r_2$ , the size of the variation. Using the analysis of the previous section we may write differential equations for the tracer response of the system. The material balance (Equation 17) becomes, for this case,

$$\begin{aligned} v_1 \frac{dx_1}{dt} &= r_\alpha \varphi(t) - w r_\alpha x_1 \\ v_2 \frac{dx_2}{dt} &= (1 - r_\alpha) \varphi(t) - w(1 - r_\alpha) x_2 \end{aligned} \quad (38)$$

In the second of the two cases (Figure 3), the system consists of two tanks in series. Again the total flow,  $w$ , is constant. The variable flows in this case are those between the two tanks. In this case the flows are conveniently described by the quantity  $r_\alpha$ , where

$$r_\alpha = \frac{w_{12\alpha} - w}{w} = \frac{w_{21\alpha}}{w}; \quad \alpha = 1, 2 \quad (39)$$

In this case the material balance becomes

$$\begin{aligned} v_1 \frac{dx_1}{dt} &= \varphi(t) - w(1 + r_\alpha)x_1 + w r_\alpha x_2 \\ v_2 \frac{dx_2}{dt} &= w(1 + r_\alpha)x_1 - w(1 + r_\alpha)x_2 \end{aligned} \quad (40)$$

In both cases equations corresponding to Equations 24, 25, 27, 28, and 29 may be written describing the first and second moments of the tracer output, resulting in a system of 10 linear differential equations in each case (although the equations are not all coupled). The solutions to these were found for some typical sets of parameters. The differential equations for the autocorrelation function were also assembled and solved for typical values.

Figure 4 is a realization of the step response of the parallel system calculated by a Monte Carlo method. The time has been scaled so that the average residence time is unity. Although the expected step response is identical to the cumulative distribution of residence times, individual realizations cannot be interpreted as distributions. This particular example is not even monotone. The mean step response for various fluctuation magnitudes,  $\epsilon$ , is shown in Figure 5. Even though the mean flow distribution is the same in each case, the residence time distributions are in fact different, because the flow distribution does not affect the output of the system in a linear way. To show more clearly the nature of the difference between the various curves, the quantity  $1 - F(t)$  has been plotted on semilogarithmic coordinates in Figure 6. The negative of the slope of this curve, which, as a function of time, has been referred to as the intensity function (Equation 7), has the physical interpretation of an escape rate. Thus denoting the escape intensity function by  $h(t)$ , if a particle has been in the system a time  $t$ , its probability of escaping in the next  $dt$  seconds is  $h(t)dt$ . This quantity is plotted in

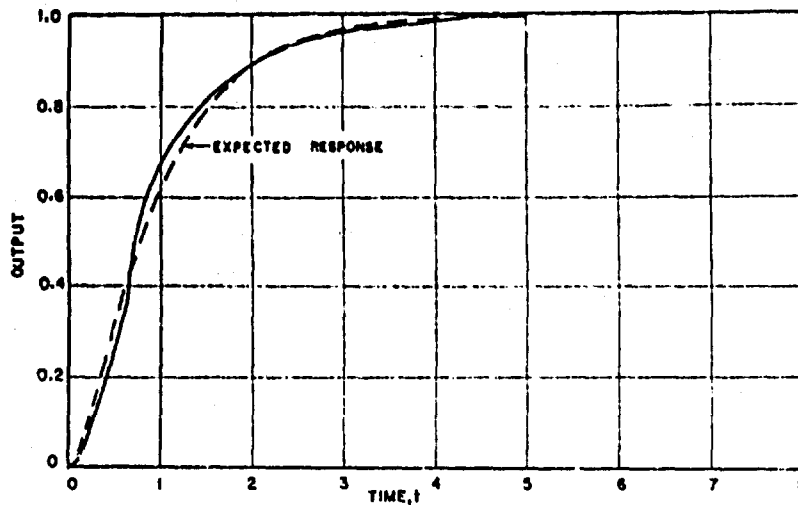


Figure 13. Typical step response for series case

$$v_1 = v_2, \bar{r} = 1, \lambda_1 = \lambda_2, \lambda = 1, \epsilon = 2$$

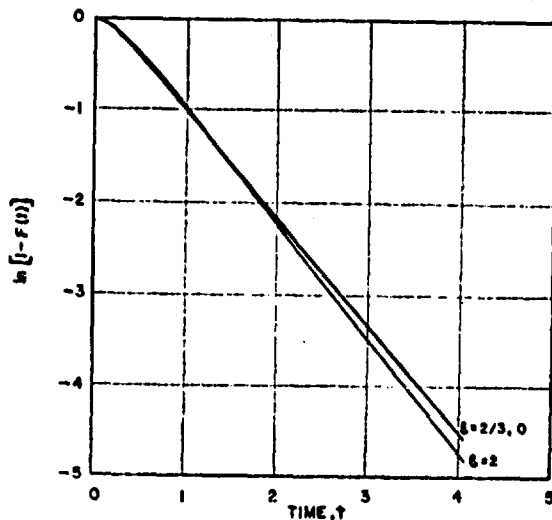


Figure 14. Effect of fluctuation magnitude on mean response to step input for series case

$$v_1 = v_2, \bar{r} = 1, \lambda_1 = \lambda_2, \lambda = 1$$

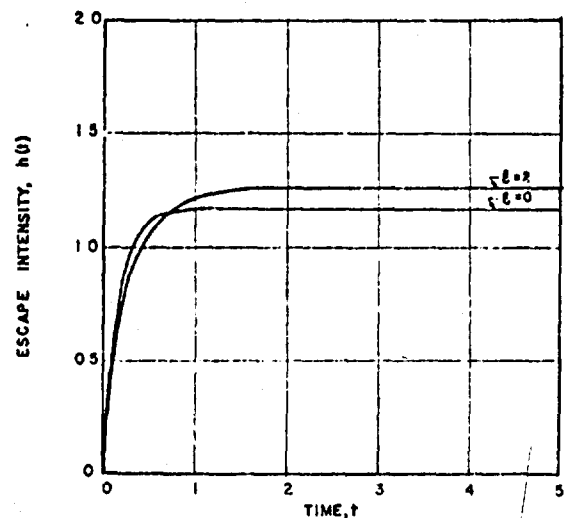


Figure 15. Effect of fluctuation magnitude on escape intensity,  $h(t)$ , for series case

$$v_1 = v_2, \bar{r} = 1, \lambda_1 = \lambda_2, \lambda = 1$$

Figure 7. We see that as the flow disturbance is increased the magnitude of  $h(t)$  decreases for large  $t$ . Generally speaking, a curve of  $h(t)$  that decreases over some interval is characteristic of systems exhibiting stagnancy or bypassing, so the effect of the flow fluctuations on the residence time distribution of the parallel model is similar to these effects.

In Figures 8 and 9 we see the effect of switching rate on the mean step response of the same system. As the switching rate increases with fixed disturbance size, the response is seen to approach that for the same mean flow with no flow fluctuation [ $h(t) \equiv 1$ ]. As the switching rate decreases, the decrease in  $h(t)$  with increasing  $t$  becomes more pronounced, suggesting a greater amount of stagnancy or bypassing.

The quantity  $\sigma(t)/\mu(t)$  for the step input has been plotted in Figure 10 for various fluctuation magnitudes and in Figure 11 for various switching rates. As could be expected,  $\sigma(t)/\mu(t)$  increases with increasing fluctuation magnitude, but the shape of the curve is relatively unaffected. In Figure 11 we see that increasing switching rate has the effect of increasing the peak

in the curve of  $\sigma(t)/\mu(t)$ , but causing the peak to occur earlier and the curve to go to zero more quickly. For very high switching rates the variance of outlet concentration goes to zero almost immediately. The autocorrelation function,  $\rho_r(\tau)$ , is shown in Figure 12. The dependence on  $t$  is different for different values of  $t$ , although for a stationary process the function would be independent of  $t$ . The autocorrelation of the fluctuating flow rate (which is stationary) is shown for comparison. The autocorrelation of the step response approaches zero rather slowly at large  $\tau$ , indicating a long "memory time" of the process compared to that of the flow. This is especially pronounced at values of  $t$  near unity, meaning that if the part of the step response in the vicinity of  $t = 1$  is on one side of the mean, there is a good chance it will be on the other side from about  $t = 2$  onward.

A realization of the step response of the series system is shown in Figure 13. It appears that the flow fluctuations have much less effect on the output than in the parallel case. This is borne out in Figures 14 and 15, where we see that even in the

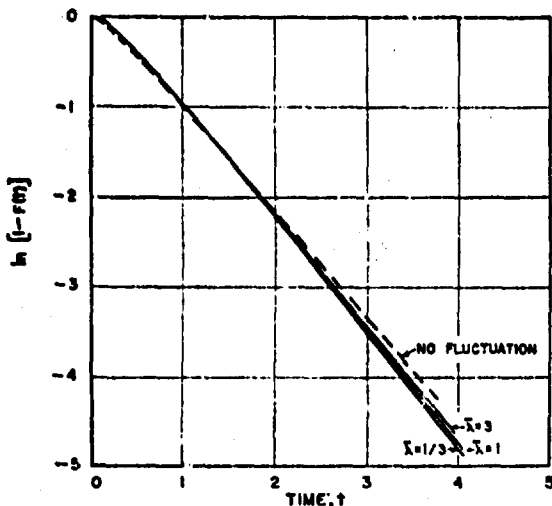


Figure 16. Effect of switching rate on mean response to step input for series case

$$v_1 = v_2, \bar{r} = 1, \lambda_1 = \lambda_2, \epsilon = 2$$

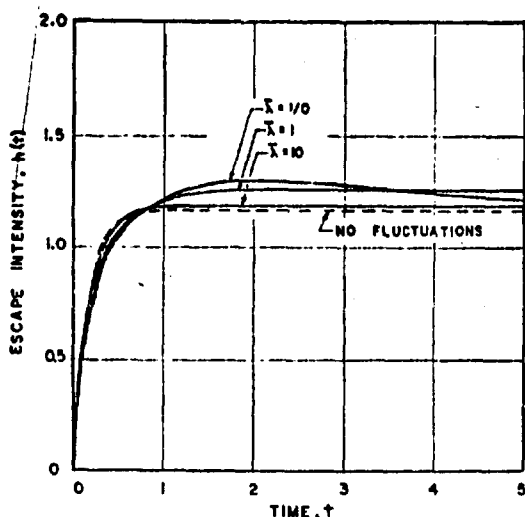


Figure 17. Effect of switching rate on escape intensity,  $h(t)$ , for series case

$$v_1 = v_2, \bar{r} = 1, \lambda_1 = \lambda_2, \epsilon = 2$$

case  $\epsilon = 2$ , which is the maximum fluctuation magnitude obtainable with the given  $\bar{r}$  and  $\lambda_1/\lambda_2$ , the effect on the mean response and the escape intensity is slight. Figures 16 and 17 show that the effect of switching rate on these curves is also slight. The effects on the coefficient of variation,  $\sigma(t)/\mu(t)$ , are shown in Figures 18 and 19. While the fluctuation magnitude affects the curve practically linearly, the switching rate just increases slightly the rate at which the curve drops to zero. The autocorrelation function for the series case (Figure 20) shows a very long memory time. For small values of  $t$ , as  $t$  increases each successive curve is lower than the one before, but for values of  $t$  greater than 1 this trend is reversed. A similar effect occurred in the parallel case, although less pronounced.

#### Reactor Equations

We set up here the mathematical methods for studying chemical reactions in our mixing systems, and apply them to

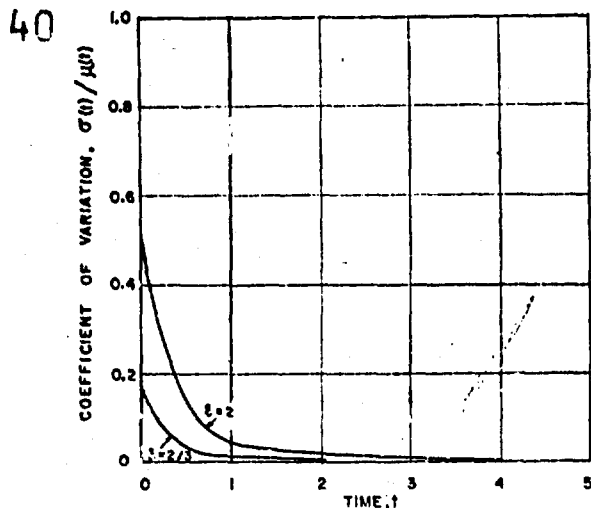


Figure 18. Effect of fluctuation magnitude on  $\sigma(t)/\mu(t)$  of step response for series case

$$v_1 = v_2, \bar{r} = 1, \lambda_1 = \lambda_2, \lambda = 1$$

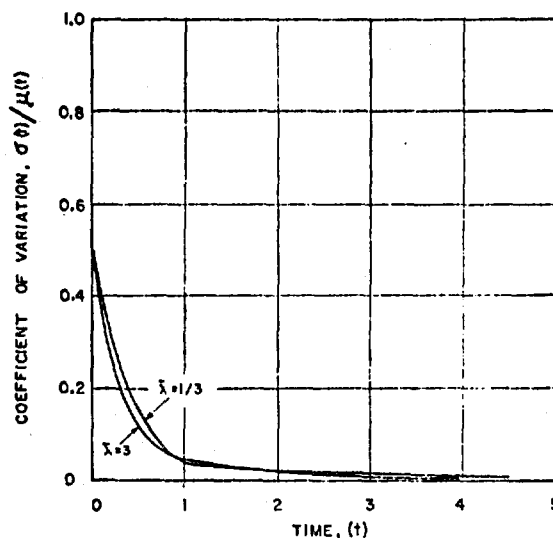


Figure 19. Effect of switching rate on  $\sigma(t)/\mu(t)$  of step response for series case

$$v_1 = v_2, \bar{r} = 1, \lambda_1 = \lambda_2, \epsilon = 2$$

first-order reactions. The methods follow closely the earlier development under the heading "Mixing Equations."

There is no particular difficulty in formulating the probability equations for complex reaction systems, but we confine ourselves here for concreteness to single reactions



which we follow in terms of the concentration of A. Denoting this concentration (in moles per unit volume) by  $x$ , we describe the rate at which reagent A is consumed (in moles per unit volume per unit time) by the rate function  $R(x)$ . If we load  $\psi$  mole of reagent per unit time into the feed line of our reactor system, the reagent concentration  $x_j$  in the  $j$ th tank satisfies, following Equation 17, the differential equation

$$v_j \frac{dx_j}{dt} = \frac{v_{j-1} v_j}{v_p} \psi + \sum_{i=1}^n v_{ij} v_i - v_j k(x_j) \quad (41)$$

$$j = 1, 2, \dots, n$$

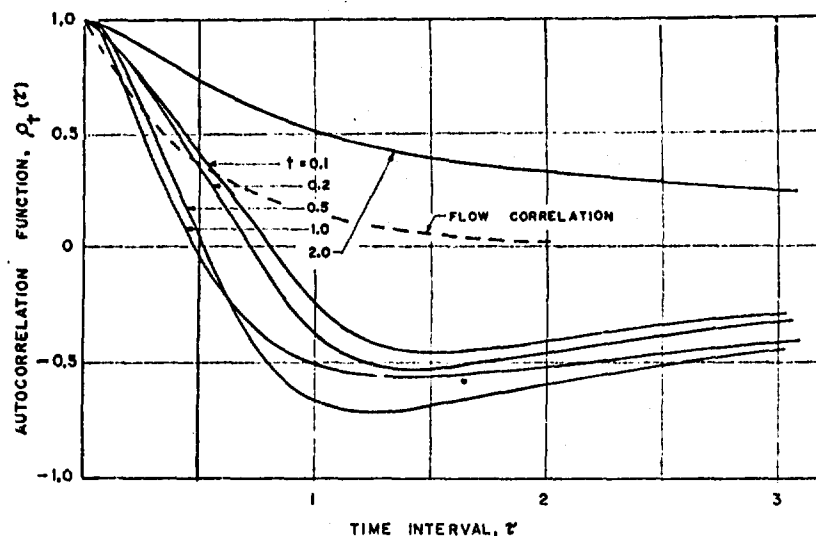


Figure 20. Typical autocorrelation of step response for series case

$$v_1 = v_2, \bar{r} = 1, \lambda_1 = \lambda_2, \bar{\lambda} = 1, \epsilon = 2$$

Now, just as in the treatment of the mixing equations, it is the composite

$$\{\alpha, x\} = \{\alpha; x_1, x_2, \dots, x_n\}$$

of flow state and concentration pattern that we may follow as a Markov process. The corresponding probability density,  $p_\alpha(x, t)$ , with

$$\int_{a_n}^{b_n} \dots \int_{a_1}^{b_1} p_\alpha(x, t) dx_1 \dots dx_n$$

giving the probability that the flow is in state  $\alpha$  and the concentration in the  $j$ th tank between  $a_j$  and  $b_j$ , satisfies, following Equation 20, the partial differential equation

$$\frac{\partial p_\alpha(y, t)}{\partial t} + \sum_{j=1}^n \frac{\partial}{\partial y_j} \left[ \left\{ \frac{w_{0j\beta} \psi}{w_\beta v_j} + \sum_{i=1}^n \frac{w_{ij\beta}}{v_j} y_i - R(y_j) \right\} p_\alpha(y, t) \right] = \sum_{\alpha} \lambda_{\alpha\beta} p_\alpha(y, t) \quad (42)$$

We are not here concerned to follow the history of the probability distribution in time, but rather to go directly to a study of the stationary distribution, which represents the quasi-steady behavior of the reactor system. Denoting this stationary distribution by  $\bar{p}_\beta(y)$ , we find from Equation 42 the defining equation

$$\sum_{j=1}^n \frac{\partial}{\partial y_j} \left[ \left\{ \frac{w_{0j\beta} \psi}{w_\beta v_j} + \sum_{i=1}^n \frac{w_{ij\beta}}{v_j} y_i - R(y_j) \right\} \bar{p}_\beta(y) \right] = \sum_{\alpha} \lambda_{\alpha\beta} \bar{p}_\alpha(y) \quad (43)$$

to which we must add the normalization condition

$$\int_{\beta} \int \dots \int \bar{p}_\beta(y) dy_1 \dots dy_n = 1 \quad (44)$$

the integration being carried out over all the values of the  $y_j$ . We note that in Equation 43, the reagent feed rate,  $\psi$ , is a constant.

If we integrate  $\bar{p}_\beta(y)$  over the  $y_j$  (the integration running over all possible values), we find simply the probability distribution of the flow states:

$$\int \dots \int \bar{p}_\beta(y) dy_1 \dots dy_n = \bar{p}_\beta \quad (45)$$

Carrying out this integration in Equations 43 and 44 gives just the defining Equations 9 and 10 for the stationary flow state probabilities, so that the  $\bar{p}_\beta$  in Equation 45 are just these stationary probabilities.

Now any general treatment of the distribution Equation 43 presents substantial analytical difficulties, and accordingly we restrict ourselves in this preliminary study to first-order reactions, with

$$R(x) = kx$$

so that Equation 43 becomes

$$\sum_{j=1}^n \frac{\partial}{\partial y_j} \left[ \left\{ \frac{w_{0j\beta} \psi}{w_\beta v_j} + \sum_{i=1}^n \frac{w_{ij\beta}}{v_j} y_i - ky_j \right\} \bar{p}_\beta(y) \right] = \sum_{\alpha} \lambda_{\alpha\beta} \bar{p}_\alpha(y) \quad (46)$$

For these first-order reaction systems, we can readily develop working equations for the leading moments of the concentration variables.

We define the partial mean concentrations as

$$m_{\beta j} = \int \dots \int y_j \bar{p}_\beta(y) dy_1 \dots dy_n; \quad j = 1, 2, \dots, n \quad (47)$$

Bringing this definition to Equation 46 gives

$$km_{\beta j} = \frac{\bar{p}_\beta w_{0j\beta} \psi}{v_j w_\beta} + \sum_{i=1}^n \frac{w_{ij\beta}}{v_j} m_{\beta i} + \sum_{\alpha} \lambda_{\alpha\beta} m_{\alpha j}; \quad j = 1, 2, \dots, n \quad (48)$$

which appears as a set of linear algebraic equations which one might solve for the  $m_{\beta j}$ . The mean rate (in moles per unit time) at which unconsumed reagent leaves the system may be calculated from these solutions as

$$m = \sum_{\beta} \int \dots \int \left[ \frac{w_{0, n+1, \beta} \psi}{w_\beta} + \sum_{j=1}^n w_{j, n+1, \beta} y_j \right] \bar{p}_\beta(y) dy_1 \dots dy_n$$



which we may write as

$$m = \sum_{\beta} \left[ \bar{r}_{\beta} \frac{w_{\beta, n+1, \beta}}{w_{\beta}} \psi + \sum_{j=1}^n w_{j, n+1, \beta} m_{\beta j} \right] \quad (49)$$

We may see now that the average conversion in first-order reactions is related to the residence time distribution of the mixing system in just the same way as for deterministically modeled systems. Specifically, Equations 48, suitably scaled on the reagent feed rate  $\psi$ , are just the Laplace transforms (with transform variable the rate constant,  $k$ ) of Equations 24 with the tracer feed rate  $\varphi(t) = \delta(t)$ —that is,

$$\frac{m_{\beta j}}{\psi} = \int_0^{\infty} e^{-kt} \mu_{\beta j}(t) dt$$

The same remark applying to outlet Equations 49 and 25, we may conclude, applying Equation 26, that

$$\frac{m}{\psi} = \int_0^{\infty} e^{-kt} f(t) dt$$

where  $f(t)$  is equivalently the mean tracer impulse response of the systems, and its residence time distribution (density function).

Such simple relationships are no longer at hand for the higher moments of the concentration variables, which express the statistical fluctuation about their mean values, and indeed these statistical fluctuations have no counterpart in deterministically modeled systems. Expressions for these higher moments

can readily be developed from Equation 43, in the same manner as for the mixing equations, but we defer these studies of the variability and the associated correlation structure of our reactor systems.

#### References

- (1) Batchelor, G. K., *J. Fluid Mech.* 5, 113-39 (1959).
- (2) Corrsin, S., *A.I.Ch.E. J.* 10, 870-7 (1964).
- (3) Corrsin, S., *Phys. Fluids* 1, 42-7 (1958).
- (4) Danckwerts, P. V., *Chem. Eng. Sci.* 8, 93-102 (1958).
- (5) Feller, W., "An Introduction to Probability Theory and Its Applications," Wiley, New York, 1966.
- (6) Kramers, H., Westerterp, K. R., "Elements of Chemical Reactor Design and Operation," Academic Press, New York, 1963.
- (7) Naor, P., Shinnar, R., *IND. ENG. CHEM. FUNDAMENTALS* 2, 278-86 (1963).
- (8) Shinnar, R., Naor, P., "Residence Time Distributions in Systems with Internal Reflux," in press.
- (9) Weinstein, H., Adler, R. J., "Effect of Mixing on Conversion in Chemical Reactors," A.I.Ch.E. meeting, Houston, Tex., December 1963.
- (10) Zwiering, Th. N., *Chem. Eng. Sci.* 11, 1-15 (1959).

RECEIVED for review June 10, 1966  
ACCEPTED February 7, 1967

Symposium on Applied Kinetics and Reaction Engineering, Division of Industrial and Engineering Chemistry, Washington, D. C., June 1966. Work supported in part under AFOSR Grant No. 921-65. Some of this work is part of the research carried out by one of the authors (F. J. Krambeck) at the City University of New York in partial fulfillment of the requirements of the degree of doctor of philosophy.

REPRINTED

FROM



# FUNDAMENTALS

## Interpretation of Tracer Experiments in Systems with Fluctuating Throughput

*Frederick J. Krambeck, Stanley Katz,  
and Reuel Shinnar*

Reprinted from I&EC Fundamentals

Volume 8, August 1969, Page 431

Copyright 1969 by the American Chemical Society and reprinted by permission of the copyright owner

**BLANK PAGE**

# INTERPRETATION OF TRACER EXPERIMENTS IN SYSTEMS WITH FLUCTUATING THROUGHPUT

FREDERICK J. KRAMBECK, STANLEY KATZ, AND REUEL SHINNAR

Department of Chemical Engineering, The City College, The City University of New York, New York, N. Y. 10031

A theoretical framework is presented for the interpretation of tracer experiments in quasisteady-flow systems, where the inflow and outflow, as well as the internal flows, exhibit stationary fluctuations about fixed central values. The fluctuating throughput leads to the consideration of different types of sojourn time distribution of material in the system. These are discussed in detail, and related to different ways of carrying out tracer experiments on the system. The standard experiment, in which a known amount of tracer is injected quickly into the inlet and its concentration measured in the outlet, leads to none of these distributions.

**I**N FLUID systems serving as chemical reactors, mixing processes have pronounced effects on reactor performance. Often, these processes involve turbulent motion of the fluid, introducing randomly fluctuating behavior into the system. In many biological flow networks, large flow fluctuations occur in a roughly periodic way. In both cases transient tracer experiments are often used to characterize the system, but the analysis of these experiments is generally based on the behavior of steady-flow systems (American Heart Association, 1962; Danckwerts, 1958; Kramers and Westerterp, 1963; Naor and Shinnar, 1963; Zweitering, 1959). When the flow distribution of the system fluctuates, the tracer response of the system is a random process, and only the statistics of this process are experimentally accessible. Even if the flows are strictly periodic, the starting time of the tracer experiment is usually random, so the same situation exists. One would like to know the relationship among the statistics of tracer response experiments, the probability distribution of particle residence time, and the statistics of the system's performance in the presence of a first-order reaction. In discussing the properties of a proposed stochastic mixing model, Krambeck *et al.* (1967) showed how the above data are related when the inlet and outlet flow rates of the system are constant but the internal flow distribution fluctuates. The same method is used in this paper to study the problem with fluctuating inlet and outlet flows. Some beginnings were made in this direction in earlier work, and are here developed further.

For a flow system with an unambiguous inlet and outlet, three different distributions of sojourn time can be defined: for a random particle, for a particle chosen at a random time from the outlet stream, and for a particle chosen at a random time from the inlet stream. These distributions differ only in respect to fluctuations in the inlet and outlet flow rates, and merge into a common residence time distribution when these flow rates become steady. In the general situation, the distribution for a random particle is to be identified with the over-all residence time distribution.

The differences among these three distributions can be shown intuitively for a situation somewhat more general than the particular mixing model which underlies the detailed calculations in this paper. Consider accordingly a mixing system of volume  $V$ , with volumetric inlet and outlet flow rates,  $u$  and  $w$ , respectively. The volume and flow rates vary with time, in a jointly stationary way, with  $\langle u \rangle$  and  $\langle w \rangle$  having the same constant values. The pointed brackets

denote probability averages, or, as may be sometimes conceptually more convenient, long-term time averages.

For such a mixing system, we may define two conditional probability densities, each with a direct interpretation in terms of idealized tracer experiments. Consider first that we inject a quantity of tracer into the inlet at time  $s$ , and measure that fraction of this inlet quantity which has emerged by time  $t$ . This fraction we may interpret as the probability that a particle of material entering the system at time  $s$  leaves it before  $t$ , and denoting it by

$$\int_0^t g(s, \tau) d\tau$$

we may accordingly interpret the differential  $g(s, t)dt$  as the probability that a particle entering the system at time  $s$  leaves it during  $t, t + dt$ . Consider next that, starting at time  $s$ , we label all the material entering the system, and at time  $t$  measure that fraction of the material in the outlet stream which is labeled. This fraction we may interpret as the probability that a particle of material leaving the system at time  $t$  has entered after  $s$ , and denoting it by

$$\int_0^t h(s, t) ds$$

we may interpret  $h(s, t)ds$  as the probability that a particle leaving the system at time  $t$  has entered it during  $s, s + ds$ .

The conditional probability density,  $g$ , may be used to define the density,  $f_e$ , of sojourn times  $t$  for a particle entering the system at a random time. We set

$$f_e(t) = \langle g(\sigma, \sigma + t) \rangle$$

where, because of the stationarity, the mean value depends only on the difference of the time arguments in  $g$ . This distribution is thus essentially the mean response in tracer outlet flow arising from the feed of a certain quantity of tracer. Similarly,  $h$  may be used to define the density,  $f_o$ , of sojourn times  $t$  for a particle leaving the system at a random time. We set

$$f_o(t) = \langle h(\tau - t, \tau) \rangle$$

and this distribution is thus essentially the mean response in tracer outlet concentration arising from a certain level of tracer concentration in the feed. The distributions  $f_e$  and  $f_o$  are just those developed for our concrete mixing model in the body of this paper; in particular,  $f_o$  is the distribution given in Equation 37.

The conditional probability densities,  $g$  and  $h$ , are of course related through the inlet and outlet flow rates,  $u$  and  $w$ . This relation arises through a natural probabilistic interpretation of these flow rates, whereby we take (up to a common constant of proportionality), the probability that an incoming particle enters during the time  $s, s + ds$  to be given by  $u(s)ds$ , and the probability that it leaves during  $t, t + dt$  to be given by  $w(t)dt$ . Recalling the formal specification of  $g(s, t)dt$  as the probability that a particle leaves during  $t, t + dt$ , given that it entered at  $s$ , we see that the probability that a particle enters during  $s, s + ds$  and leaves during  $t, t + dt$  is proportional to  $u(s)ds \cdot g(s, t)dt$ . Further, recalling the formal specification of  $h(s, t)ds$  as the probability that a particle has entered during  $s, s + ds$ , given that it leaves at  $t$ , we see that the probability that a particle enters during  $s, s + ds$  and leaves during  $t, t + dt$  is (with the same constant of proportionality) also proportional to  $h(s, t)ds \cdot w(t)dt$  so that

$$u(s)g(s, t) = h(s, t)w(t)$$

This conclusion can, of course, also be reached by a straightforward comparison of the conceptual tracer experiments underlying  $g$  and  $h$ . We may see from this relation that  $g$  and  $h$  (and hence  $f_e$  and  $f_o$ ) may be expected to be equal only when inlet and outlet flow rates  $u$  and  $w$  are steady, and hence equal to the same constant value. If, further, the mixing system itself is completely steady, without internal fluctuation,  $g$  and  $h$  are not only equal but equal to the same function of the time difference:

$$g(s, t) = h(s, t) = f(t - s)$$

Now, with the probabilistic interpretation of flow rates  $u$  and  $w$  made above, we may construct the density,  $f_s$ , of sojourn times  $t$  for a random particle (caught at the moment it enters the system) in the form

$$f_s(t) = \frac{\langle u(\sigma)g(\sigma, \sigma + t) \rangle}{\langle u(\sigma) \rangle}$$

But since  $\langle u \rangle = \langle w \rangle$ , and since all mean values depend only on time differences, we may, taking account of the relation developed above between  $g$  and  $h$ , write this as

$$f_s(t) = \frac{\langle h(\tau - t, \tau)w(\tau) \rangle}{\langle w(\tau) \rangle}$$

and so interpret it also as the density of sojourn times for a random particle caught at the moment it leaves the system. This density  $f_s$  is just the density of residence times in the system, and is precisely that developed for our concrete mixing model in this paper, using the inlet flow state distribution corresponding to Equation 16. As long as inlet and outlet flow rates  $u$  and  $w$  really fluctuate, it may be expected to differ from  $f_e$  and  $f_o$ . The sojourn times distributed according to  $f_s$ , and not according to  $f_e$  or  $f_o$ , have a mean value given in a natural way as the ratio of the mean system volume to the mean input-output flow rate. This fact is developed by explicit algebraic calculation for our concrete mixing model in Equation 25. A less precise, but somewhat more general, intuitive argument to the same conclusion appears in an Appendix.

This paper aims to take the whole line of intuitive considerations adduced above, and reduce them to precise calculations for a broad class of mixing models, making clear the connections among sojourn time distributions, tracer experiments, and the behavior of the mixing system for first-order

reactions. The mixing model chosen is that developed by Krambeck *et al.* (1967), which has a very considerable degree of flexibility, although for reasons of technical simplicity its properties have been developed for fixed mixing volumes. Specifically, the model consists of a network of well-mixed tanks, where the connecting flows fluctuate randomly in time. The number and arrangement of tanks are left arbitrary. It is assumed that the tank volumes are fixed and that the flow is incompressible. Such a model with steady flows can be used to simulate any steady mixing process by taking an appropriate arrangement of tanks and allowing the number to increase. Axial diffusion, for example, may be approximated to any degree with a sufficiently large number of tanks in cascade, with forward and backward flows between each tank. The added feature of randomly fluctuating flows should make it possible to simulate stochastic mixing processes if sufficient numbers of tanks are taken. Of course, such a large number of tanks might be required that there would be no saving in effort over a complete description of the flow process. On the other hand, if conclusions may be drawn about such a model with the number and arrangement of tanks left arbitrary, it is clear that they will apply to a very general class of mixing processes.

One additional assumption is added to make the analysis possible: that the interconnecting flow rates vary in time as finite-state Markov processes. Such processes are described in detail by Feller (1960). The fact that the states are discrete is not important, since their number is arbitrary. The fact that the process is Markov is a rather mild restriction because the dimensionality of the state space is arbitrary. This allows the state of many non-Markov processes to be redefined to include information about the history, making the new process Markov.

Krambeck *et al.* (1967) showed how this model could be analyzed in terms of the random passage of a single particle through the system or, alternatively, in terms of the randomly fluctuating concentration in the various tanks. In the present study, the same methods are used to analyze the situation with fluctuating inlet and outlet flows in more detail. The concepts developed are then illustrated by the properties of a single tank with fluctuating throughput. Some of the derivations given in the earlier work are repeated here.

#### Formulation of Model

In the most general case the model consists of  $n$  stirred tanks arbitrarily connected by interstage flows (Figure 1), where the volume of the  $i$ th tank is  $v_i$ , and the volumetric flow rate from the  $i$ th to the  $j$ th tank is  $w_{ij}$  ( $i, j = 1, 2, \dots, n$ ). The inlet stream is distributed to the tanks arbitrarily, and the feed rate to the  $j$ th tank is denoted  $w_{0j}$ . The contribution of the  $j$ th tank to the outlet stream is similarly called  $w_{j, n+1}$ . The amount bypassing the system entirely is  $w_{0, n+1}$ .

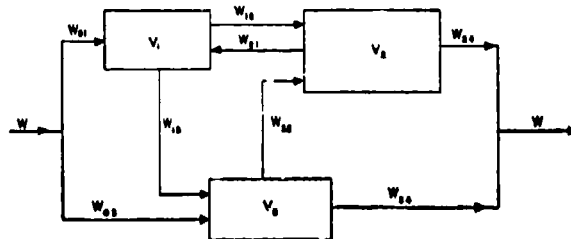


Figure 1. Typical flow network

Although the flow rates are permitted to vary with time, it is assumed that the volumes,  $v_i$ , remain constant. Thus, the total flow entering the  $j$ th tank at any instant is equal to the total flow leaving it:

$$\sum_{i=0, i \neq j}^n w_{ij} = \sum_{i=1, i \neq j}^{n+1} w_{ji}; \quad j = 1, 2, \dots, n \quad (1)$$

Also, the total flow entering the system is equal to the total leaving. Denoting this quantity by  $w$ ,

$$w = \sum_{j=1}^{n+1} w_{0j} = \sum_{j=0}^n w_{j, n+1} \quad (2)$$

It is convenient to define "diagonal" quantities of the form  $w_{jj}$  such that the total inlet flow to the  $j$ th tank (equal to the total outlet flow) is the negative of  $w_{jj}$ . Thus,

$$w_{jj} = - \sum_{i=0, i \neq j}^n w_{ij} = - \sum_{i=1, i \neq j}^{n+1} w_{ji}; \quad j = 1, 2, \dots, n \quad (3)$$

Flow rates  $w_{ij}$  so defined fill out a square matrix ( $n+1$  by  $n+1$ ) which has the property

$$\sum_{i=0}^n w_{ij} = \sum_{k=1}^{n+1} w_{jk} = 0; \quad j = 1, 2, \dots, n \quad (4)$$

and where all elements  $w_{ij}$  with  $i \neq j$  are nonnegative.

The random variation of the flow states with time is assumed to arise from a Markov process with a finite number of states. Each state of the Markov process corresponds to a given matrix of flow rates. Letting  $\alpha$  be the index of a flow state, the flow rates corresponding to  $\alpha$  are written

$$w_{i\alpha}; \quad i = 0, 1, \dots, n; \quad j = 1, 2, \dots, n+1$$

For every state  $\alpha$

$$\sum_{i=0}^n w_{i\alpha} = \sum_{k=1}^{n+1} w_{\alpha k} = 0; \quad j = 1, 2, \dots, n \quad (5)$$

$$\sum_{j=1}^{n+1} w_{\alpha j} = \sum_{i=0}^n w_{i, n+1, \alpha} = w_{\alpha}; \quad \text{all } \alpha \quad (6)$$

The probability structure of the flows resides in that of the transitions of the underlying Markov process. Denoting the probability of transition from state  $\alpha$  to state  $\beta$  in a time interval  $\tau$  by  $\pi_{\alpha\beta}(\tau)$ , one has, for small time intervals,

$$\pi_{\alpha\beta}(\tau) = \delta_{\alpha\beta} + \lambda_{\alpha\beta}\tau + o(\tau) \quad (7)$$

where the  $\lambda_{\alpha\beta}$  satisfy

$$\lambda_{\alpha\alpha} = - \sum_{\beta \neq \alpha} \lambda_{\alpha\beta} \quad (8)$$

$$\lambda_{\alpha\beta} \geq 0; \quad \alpha \neq \beta \quad (9)$$

The matrix of switching rates,  $\lambda_{\alpha\beta}$ , then defines the probabilistic behavior of the process completely.

Krambeck *et al.* (1967) showed how one may derive differential equations describing the evolution in time of various probabilities. The probabilities of being in the various states  $\beta$  at time  $t$ , denoted by functions  $p_{\beta}(t)$ , satisfy the simultaneous differential equations

$$\frac{dp_{\beta}(t)}{dt} = \sum_{\alpha} \lambda_{\alpha\beta} p_{\alpha}(t) \quad (10)$$

The equilibrium distribution of flow states,  $\bar{p}_{\alpha}$ , which obtains after long times when the process becomes stationary, then satisfies

$$\sum_{\alpha} \lambda_{\alpha\beta} \bar{p}_{\alpha} = 0 \quad (11)$$

### Model as a Random Walk

When the system is followed from the point of view of the random passage of a single particle through the system, the probability of the particle being in tank  $i$  while the flow is in state  $\alpha$  at time  $t$ ,  $p_{\alpha i}(t)$ , satisfies

$$\frac{dp_{\alpha i}(t)}{dt} = \sum_{j=1}^n \frac{w_{ij\alpha}}{v_i} p_{\alpha j}(t) + \sum_{\alpha} \lambda_{\alpha\beta} p_{\alpha j}(t); \quad j = 1, 2, \dots, n+1 \quad (12)$$

The specification of an initial probability distribution,  $p_{\alpha}(0)$ , will then determine the properties of the random passage completely.

In this case, however, the stationary distribution is of no particular interest, since the particle eventually finds its way to the outlet with probability 1. It is necessary to state explicitly the initial distribution, in order to calculate the probability structure of the random walk. If the total flow through the system,  $w_{\alpha}$ , is constant ( $w_{\alpha} = w$ ; all  $\alpha$ ), the initial distribution is given by

$$p_{\beta j}(0) = \bar{p}_{\beta} (w_{\alpha\beta} / w) \quad (13)$$

which is to say that the flow state distribution is in its stationary condition, and that the probability of starting in a certain tank, given the flow state, is proportional to the flow to that tank from the inlet stream. In case the total flow is not constant, some ambiguity arises. One could either assume that at the instant a particle enters, the flow state probabilities have their stationary values,  $\bar{p}_{\beta}$ , implying that the chance of a particle entering at a certain time is independent of the flow state, or could assume that the chance of a particle entering at a given instant is proportional to the total flow rate at that instant, so that the initial distribution of flow states, say  $p_{\beta}^c$ , is different from  $\bar{p}_{\beta}$ . In the first case the initial distribution would be given by

$$p_{\beta j}(0) = \bar{p}_{\beta} \frac{w_{\alpha\beta}}{w_{\beta}} \quad (14)$$

In the second case,

$$p_{\beta}^c = \bar{p}_{\beta} w_{\beta} / \sum_{\alpha} \bar{p}_{\alpha} w_{\alpha} \quad (15)$$

since the arrival of a particle in a short time, given that the flow state is  $\alpha$ , is proportional to  $w_{\alpha}$ , and the initial distribution of the process is then

$$p_{\beta j}(0) = p_{\beta}^c \frac{w_{\alpha\beta}}{w_{\beta}} = \bar{p}_{\beta} \frac{w_{\alpha\beta}}{w} \quad (16)$$

If all the  $w_{\alpha}$  are equal, Equations 14 and 16 are identical to Equation 13. The initial distribution (Equation 14) corresponds to tracer experiments in which the tracer is injected as a pulse at a random time or as a step function in tracer flow rate (constant flow rate of tracer fluctuating inlet concentration). The initial distribution (Equation 16) corresponds to tracer experiments in which a constant concentration of tracer is fed regardless of instantaneous total flow rate.

At any rate once the initial distribution is specified by either Equation 14 or 16, the complete time history of the probability distribution,  $p_{\beta j}(t)$ , can be calculated. The cumulative residence time distribution is then given by

$$F(t) = \sum_{\beta} p_{\beta, n+1}(t) \quad (17)$$

which is the probability that a particle entering the system at time zero will be in the outlet at time  $t$ .

It is interesting to compute the mean residence time to see how it compares with the value for a steady system in which case it would be the total volume divided by the total flow rate. To do this,

$$1 - F(t) = \sum_{\beta} \sum_{j=1}^n p_{\beta j}(t) \quad (18)$$

which simply states that  $1 - F(t)$  is the probability that a particle which entered at time zero is still in the system at time  $t$ . Then  $\theta$ , the mean residence time, is given by

$$\theta = \int_0^{\infty} [1 - F(t)] dt = \sum_{\beta} \sum_{j=1}^n \int_0^{\infty} p_{\beta j}(t) dt \quad (19)$$

Integrating Equation 12 one finds

$$p_{\beta j}(\infty) - p_{\beta j}(0) = \sum_{i=1}^n \frac{w_{ij\beta}}{v_i} \int_0^{\infty} p_{\beta i}(t) dt + \sum_{\alpha} \lambda_{\alpha\beta} \int_0^{\infty} p_{\alpha j}(t) dt; \quad j = 1, 2, \dots, n \quad (20)$$

Defining

$$\theta_{\beta j} = \int_0^{\infty} p_{\beta j}(t) dt$$

and noting that  $p_{\beta j}(\infty) = 0$  ( $j = 1, 2, \dots, n$ ), this becomes

$$-p_{\beta j}(0) = \sum_{i=1}^n \frac{w_{ij\beta}}{v_i} \theta_{\beta i} + \sum_{\alpha} \lambda_{\alpha\beta} \theta_{\alpha j}; \quad j = 1, 2, \dots, n \quad (21)$$

If Equation 21 is solved for the  $\theta_{\beta j}$ , the mean residence time can then be calculated:

$$\theta = \sum_{\beta} \sum_{j=1}^n \theta_{\beta j} \quad (22)$$

Substituting the initial distribution (Equation 16) into Equation 21,

$$-\tilde{p}_{\beta} \frac{w_{0j\beta}}{\bar{w}} = \sum_{i=1}^n \frac{w_{ij\beta}}{v_i} \theta_{\beta i} + \sum_{\alpha} \lambda_{\alpha\beta} \theta_{\alpha j}; \quad j = 1, 2, \dots, n \quad (23)$$

This equation may be solved to yield

$$\theta_{\beta j} = \frac{\tilde{p}_{\beta}}{\bar{w}} v_j \quad (24)$$

as can be seen by substitution, and by using Equations 11 and 5. Substituting 24 into 22 gives

$$\theta = \sum_{j=1}^n v_j / \bar{w} \quad (25)$$

which states that the mean residence time is just the total volume over the mean total flow. However, the initial distribution (Equation 14) does not give this result.

When discussing the significance of tracer experiments another statistical property of the random passage proved useful: the distribution of residence times for a particle chosen at a random time from the outlet of the system, called the outlet age distribution. To discuss this situation, it is useful to modify the transition probabilities slightly so as to make all the outlet states,  $(\alpha, n+1)$ , absorbing. Thus, for  $j \neq n+1$ , the probabilities again obey

$$\frac{dp_{\beta j}}{dt}(t) = \sum_{i=1}^n \frac{w_{ij\beta}}{v_i} p_{\beta i}(t) + \sum_{\alpha} \lambda_{\alpha\beta} p_{\alpha j}(t) \quad j = 1, 2, \dots, n \quad (26)$$

but the probabilities for the outlet states are given by

$$\frac{dp_{\beta, n+1}(t)}{dt} = \sum_{i=1}^n \frac{w_{i, n+1, \beta}}{v_i} p_{\beta i}(t) \quad (27)$$

The quantity  $p_{\beta, n+1}(t)$  is then the probability that at time  $t$  the particle has left the system and that when it left, the flow was in state  $\beta$ . As  $t \rightarrow \infty$ , this will just be the probability that the flow state was  $\beta$  at the instant the particle left. Thus, denoting this quantity by  $p_{\beta}^{\infty}$

$$p_{\beta}^{\infty} = p_{\beta, n+1}(\infty) \quad (28)$$

This may be expressed in terms of the  $\theta_{\alpha j}$  defined earlier and given by Equation 21. Thus

$$p_{\beta}^{\infty} = p_{\beta, n+1}(\infty) = p_{\beta, n+1}(0) + \sum_{i=1}^n \frac{w_{i, n+1, \beta}}{v_i} \int_0^{\infty} p_{\beta i}(t) dt \quad (29)$$

or

$$p_{\beta}^{\infty} = p_{\beta, n+1}(0) + \sum_{i=1}^n \frac{w_{i, n+1, \beta}}{v_i} \theta_{\beta i} \quad (30)$$

For the initial distribution Equation 16,  $\theta_{\beta j}$  is given by Equation 24 and

$$p_{\beta, n+1}(0) = \tilde{p}_{\beta} (w_{0, n+1, \beta} / \bar{w})$$

Thus

$$p_{\beta}^{\infty} = \tilde{p}_{\beta} \frac{w_{0, n+1, \beta}}{\bar{w}} + \sum_{i=1}^n \tilde{p}_{\beta} \frac{w_{i, n+1, \beta}}{\bar{w}} \quad (31)$$

which gives

$$p_{\beta}^{\infty} = \tilde{p}_{\beta} (w_{\beta} / \bar{w}) = p_{\beta}^{\infty} \quad (32)$$

This result is reasonable, since initial distribution Equation 16 corresponds to a particle chosen at random from the entire population, which would imply that the rate of leaving is proportional to the instantaneous total flow, just as is the rate of entering.

For the initial distribution Equation 14 the  $\theta_{\beta j}$  depend more on the details of the system, so the  $p_{\beta}^{\infty}$  cannot be calculated so simply.

The joint probability  $p_{\beta, n+1}(t)$  can be expressed as the product of the probability that the flow state is  $\beta$  when the particle leaves with the conditional probability that the particle has left by time  $t$  given that the flow state when it leaves is  $\beta$ . Thus

$$p_{\beta, n+1}(t) = p_{\beta}^{\infty} p_{n+1}(t | \beta) \quad (33)$$

If now a particle is chosen in the exiting stream at a random time, the distribution of the flow states is  $\tilde{p}_{\alpha}$  rather than  $p_{\alpha}^{\infty}$ . Thus the joint probability of leaving in flow state  $\alpha$  at a time less than  $t$  for a particle so chosen is given by  $p_{\alpha, n+1}^*(t)$ , where

$$p_{\alpha, n+1}^* = \tilde{p}_{\alpha} p_{n+1}(t | \alpha) \quad (34)$$

This gives

$$p_{\alpha, n+1}^*(t) = \frac{\tilde{p}_{\alpha}}{p_{\alpha}^{\infty}} p_{\alpha, n+1}(t) \quad (35)$$

For initial distribution Equation 16, this gives

$$p_{\alpha, n+1}^*(t) = \frac{\bar{w}}{w_{\alpha}} p_{\alpha, n+1}(t) \quad (36)$$

The outlet age density under these conditions becomes

$$f_o(t) = \sum_{\alpha} \tilde{p}_{\alpha} \frac{w_{0, n+1, \alpha}}{w_{\alpha}} \delta(t) + \bar{w} \sum_{\alpha} \sum_{i=1}^n \frac{w_{i, n+1, \alpha}}{w_{\alpha}} \frac{p_{\alpha i}(t)}{v_i} \quad (37)$$

Thus  $f_o(t)$  is the density function of residence times for a

particle chosen at a random time from the outlet stream, assuming that particles enter in proportion to the instantaneous total flow rate.

While it is more difficult to calculate, one can also define a sojourn time distribution for a particle chosen at a random time from the outlet, assuming that particles enter at a rate independent of the instantaneous total flow rate. This quantity,  $f_{\psi}(t)$ , is given by

$$f_{\psi}(t) = \sum_{\alpha} \frac{\bar{p}_{\alpha}^2 w_{\alpha, n+1, \alpha}}{p_{\alpha}^2 w_{\alpha}} \lambda(t) + \sum_{\alpha} \sum_{i=1}^n \frac{\bar{p}_{\alpha}}{p_{\alpha}^2} w_{i, \alpha} \frac{p_{\alpha i}(t)}{v_i} \quad (38)$$

when the initial distribution is given by Equation 14. However,  $f_{\psi}(t)$  has no clear probabilistic meaning with respect to the system as such. It refers to a specific experiment only—the case when tracer is introduced to the system at a fixed rate independent of total flow rate. In that case  $f_{\psi}(t)$  gives the sojourn time distribution of a tracer particle chosen at a random time at the outlet. All other distributions, while relating to tracer experiments, have a probabilistic interpretation for the system as such and the tracer is just a measuring device.

#### Tracer Experiments on Model

Krambeck *et al.* (1967) showed that when some process occurs in the model which obeys differential equations of the form

$$\frac{dx_i}{dt} = f_{i\alpha}(t, \mathbf{x}); \quad i = 1, 2, \dots \quad (39)$$

where  $f_{i\alpha}(\mathbf{x})$  depends on the random flow state,  $\alpha$ , as well as the set  $\{x_i\}$ , the probability density  $p_{\alpha}(t, \mathbf{x})$  will satisfy

$$\frac{\partial p_{\alpha}(t, \mathbf{x})}{\partial t} + \sum_{j=1}^n \frac{\partial}{\partial x_j} [f_{j\alpha}(t, \mathbf{x}) p_{\alpha}(t, \mathbf{x})] = \sum_{\alpha} \lambda_{\alpha} p_{\alpha}(t, \mathbf{x}) \quad (40)$$

The function  $p_{\alpha}(t, \mathbf{x})$  is defined so that the joint probability that the flow state is  $\alpha$  and the state of the system is in  $(\mathbf{x}, \mathbf{x} + d\mathbf{x})$  at time  $t$  is given by  $p_{\alpha}(t, \mathbf{x}) d\mathbf{x}$ . A tracer material balance gives

$$\frac{dx_j}{dt} = \frac{\varphi_{aj}(t)}{v_j} + \sum_{i=1}^n \frac{w_{ija}}{v_j} x_i; \quad j = 1, 2, \dots, n \quad (41)$$

where  $x_i$  is the concentration of tracer in tank  $i$  and  $\varphi_{aj}$  is the rate at which tracer is fed to tank  $j$  when the flow state is  $\alpha$ . Comparison of Equation 41 with 39 and 40 shows that, for tracer experiments,

$$\frac{\partial p_{\alpha}(t, \mathbf{x})}{\partial t} + \sum_{j=1}^n \frac{\partial}{\partial x_j} \left[ \left( \frac{\varphi_{aj}}{v_j} + \sum_{i=1}^n \frac{w_{ija}}{v_j} x_i \right) p_{\alpha}(t, \mathbf{x}) \right] = \sum_{\alpha} \lambda_{\alpha} p_{\alpha}(t, \mathbf{x}) \quad (42)$$

The inlet flow rates of tracer to the individual tanks may be expressed in terms of the inlet concentration schedule, or of the total feed rate of tracer schedule. Thus, if  $x_0(t)$  is the inlet concentration schedule and  $\varphi(t)$  is the total feed rate schedule, the two expressions are

$$\varphi_{aj}(t) = w_{aja} x_0(t) \quad (43)$$

and

$$\varphi_{aj}(t) = \frac{w_{aja}}{w_{\alpha}} \varphi(t) \quad (44)$$

In a system with fluctuating total throughput, an experiment measuring the response to a step in  $x_0(t)$  would be different

from one measuring the response to a step in  $\varphi(t)$ . In the first case the tracer inlet concentration would be fixed and the feed rate of tracer would fluctuate in time with the total flow, while in the second case the feed rate of tracer would be fixed and the inlet concentration would fluctuate. Of course, if the total throughput were constant, this ambiguity would not arise.

The case of fluctuating total throughput also raises the question of whether to measure outlet concentration or outlet tracer flow rate. Denoting the outlet concentration by  $z$  and the outlet tracer flow rate by  $\psi$  we see that

$$\psi = w_{n+1} z = \sum_{i=1}^n w_{i, n+1} x_i + \varphi_{n, n+1} \quad (45)$$

For initial conditions to Equation 42, assume that at the instant the experiment is begun the flow state probabilities have their stationary values,  $\bar{p}_{\alpha}$ . In other words, the experiment is begun at a random time independent of the flow state with the system running continuously. Thus

$$p_{\alpha}(0, \mathbf{x}) = \bar{p}_{\alpha} \delta(x_1) \delta(x_2) \dots \delta(x_n) \quad (46)$$

Once the conditions of the tracer experiment are set through either Equation 43 or Equation 44, the complete probability structure of the process is determined by Equation 42 together with the initial conditions (Equation 46). The probability structure of  $\psi$  or  $z$  can then be determined by taking appropriate combinations of the  $x$ 's, as prescribed by Equation 45.

To understand the relationship among the various possible tracer experiments and the probability structure of residence times as studied in the previous section, let us consider the first moments of  $p_{\alpha}(t, \mathbf{x})$  defined as follows:

$$\mu_{j\alpha}(t) = \int x_j p_{\alpha}(t, \mathbf{x}) d\mathbf{x} = \langle x_j \rangle_{\alpha} \quad j = 1, 2, \dots, n \quad (47)$$

Multiplying Equations 42 and 46 by  $x_j$  and integrating gives

$$\frac{d\mu_{j\alpha}}{dt} = \frac{\bar{p}_{\alpha}}{v_j} \varphi_{j\alpha}(t) + \sum_{i=1}^n \frac{w_{ija}}{v_j} \mu_{i\alpha} + \sum_{\alpha} \lambda_{\alpha} \mu_{j\alpha}; \quad j = 1, 2, \dots, n \quad (48)$$

and

$$\mu_{j\alpha}(0) = 0 \quad (49)$$

The expected outlet concentration response is given by

$$\langle z \rangle = \sum_{\alpha} \sum_{i=1}^n \frac{w_{i, n+1, \alpha}}{w_{\alpha}} \mu_{i\alpha} + \sum_{\alpha} \bar{p}_{\alpha} \frac{\varphi_{\alpha, n+1}}{w_{\alpha}} \quad (50)$$

and the expected outlet tracer flow rate by

$$\langle \psi \rangle = \sum_{\alpha} \sum_{i=1}^n w_{i, n+1, \alpha} \mu_{i\alpha} + \sum_{\alpha} \bar{p}_{\alpha} \varphi_{\alpha, n+1} \quad (51)$$

It is interesting to compare Equation 48 with Equation 12. The systems become equivalent with variables identified as in 52 to 55:

$$p_{j\alpha}(t) = v_j \mu_{j\alpha}(t); \quad j = 1, 2, \dots, n \quad (52)$$

$$p_{j\alpha}(0) \delta(t) = \bar{p}_{\alpha} \varphi_{j\alpha}(t); \quad j = 1, 2, \dots, n \quad (53)$$

$$f(t) = \frac{d}{dt} \sum_{\beta} p_{\beta, n+1}(t) = \langle \psi \rangle \quad (54)$$

$$f_0(t) = \frac{d}{dt} \sum_{\beta} p_{\beta, n+1}^*(t) = \bar{w} \langle z \rangle \quad (55)$$

where  $f(t)$  is the residence time density function for particles



chosen at random from the entire population or for particles entering the system at a random time, and  $f_o(t)$  is the residence time density for particles leaving the system at a random time, provided initial distribution Equation 16 applies. The different initial distributions, 14 and 16, can be matched by supplying the appropriate tracer inputs. Thus, to determine statistical quantities for initial distribution (Equation 14) experimentally, the tracer input must be

$$\varphi_{\beta i}(t) = \frac{w_{\alpha j \beta}}{w_{\beta}} \delta(t) \quad (56)$$

which can be achieved by an impulse in tracer feed rate:

$$\varphi(t) = \delta(t) \quad (57)$$

To determine statistical quantities for initial distribution Equation 16, the input is

$$\varphi_{\beta i}(t) = \frac{w_{\alpha j \beta}}{w_{\beta}} \delta(t) \quad (58)$$

which can be achieved with an impulse in inlet concentration:

$$x_o(t) = (1/\bar{v}) \delta(t) \quad (59)$$

The amount injected for an impulse in flow rate is the same for each realization, while for an impulse in concentration, the amount injected is proportional to the instantaneous inlet flow rate (which in practice is impractical).

Since the system of Equations 48 is linear in the  $\mu_{\beta j}$  and also in either  $\varphi(t)$  or  $x_o(t)$ , whichever is used to describe the tracer input, the expected responses to arbitrary inputs are given by the convolutions:

$$\begin{aligned} \langle \psi(t) \rangle &= \int_0^t \langle \psi_x(t-\tau) \rangle x_o(\tau) d\tau \\ \langle \psi(t) \rangle &= \int_0^t \langle \psi_{\varphi}(t-\tau) \rangle \varphi(\tau) d\tau \\ \langle z(t) \rangle &= \int_0^t \langle z_x(t-\tau) \rangle x_o(\tau) d\tau \\ \langle z(t) \rangle &= \int_0^t \langle z_{\varphi}(t-\tau) \rangle \varphi(\tau) d\tau \end{aligned} \quad (60)$$

where  $\psi_x(t)$  is the response in flow rate to an impulse in concentration,  $\psi_{\varphi}(t)$  is the response in flow rate to an impulse in flow rate,  $z_x(t)$  is the concentration response to an impulse in concentration, and  $z_{\varphi}(t)$  is the concentration response to an impulse in tracer flow rate. The various residence time densities are given by

$$\begin{aligned} f_x(t) &= (1/\bar{v}) \langle \psi_x(t) \rangle \\ f_{\varphi}(t) &= \langle \psi_{\varphi}(t) \rangle \\ f_o(t) &= \langle z_x(t) \rangle \end{aligned} \quad (61)$$

where  $f_x(t)$  is the residence time density of a particle chosen at random from the entire population,  $f_o(t)$  is that of a particle chosen at a random time at the inlet of the system, and  $f_{\varphi}(t)$  is that of a particle chosen at a random time at the outlet of the system. From Equation 60 it is clear that the response to a step input is just the integral of the corresponding impulse response. Thus, the distribution functions corresponding to  $f_x$ ,  $f_{\varphi}$ , and  $f_o$  are just the expected step responses. The impulse response  $\langle z_{\varphi}(t) \rangle$ , however, is difficult to interpret as a probability distribution.

In the presence of reaction, Equation 41 becomes

$$v_j \frac{dx_j}{dt} = \varphi_{\alpha j}(t) + \sum_{i=1}^n w_{ij} x_i - v_j R(x_j) \quad (62)$$

where  $x_j$  is now the concentration of reactant in tank  $j$ , and  $R(x)$  is the reaction rate expression. Applying Equation 40, it is found that the joint probability distribution of reaction concentration and flow state is given by

$$\frac{\partial p_{\beta}(t, \mathbf{x})}{\partial t} + \sum_{j=1}^n \frac{\partial}{\partial x_j} \left[ \left\{ \frac{\varphi_{\beta j}}{v_j} + \sum_{i=1}^n \frac{w_{ij \beta}}{v_j} x_i - R(x_j) \right\} p_{\beta}(t, \mathbf{x}) \right] = \sum_{\alpha} \lambda_{\alpha \beta} p_{\alpha}(t, \mathbf{x}) \quad (63)$$

In considering the model as a reactor, one is primarily concerned with its stationary behavior, that which prevails at some large time after startup. Such a stationary distribution will exist only if  $\varphi_{\beta j}$  is independent of  $t$ . Again, two possibilities occur, depending on whether one feeds reactant at a constant rate or at constant concentration. Thus either

$$\varphi_{\alpha j} = w_{\alpha j} x_o \quad (64)$$

or

$$\varphi_{\alpha j} = \frac{w_{\alpha j}}{w_{\alpha}} \varphi \quad (65)$$

where  $x_o$  is the constant inlet concentration and  $\varphi$  is the constant reactant feed rate. Defining  $\bar{p}_{\alpha}(\mathbf{x}) = p_{\alpha}(\infty; \mathbf{x})$ ,

$$\sum_{j=1}^n \frac{\partial}{\partial x_j} \left[ \left\{ \frac{\varphi_{\beta j}}{v_j} + \sum_{i=1}^n \frac{w_{ij \beta}}{v_j} x_i - R(x_j) \right\} \bar{p}_{\beta}(\mathbf{x}) \right] = \sum_{\alpha} \lambda_{\alpha \beta} \bar{p}_{\alpha}(\mathbf{x}) \quad (66)$$

The outlet reactant concentration and reactant flow rate will again be given by Equation 45.

To compare the reactor behavior to the tracer response behavior, define

$$m_{\beta j} = \langle x_j \rangle_{\beta} = \int_0^{\infty} x_j \bar{p}_{\beta}(\mathbf{x}) d\mathbf{x} \quad (67)$$

Then, from Equation 66,

$$\langle R(x_j) \rangle_{\beta} = \bar{p}_{\beta} \frac{\varphi_{\beta j}}{v_j} + \sum_{i=1}^n \frac{w_{ij \beta}}{v_j} m_{\beta i} + \sum_{\alpha} \lambda_{\alpha \beta} m_{\alpha j}; \quad j = 1, 2, \dots, n \quad (68)$$

The expected outlet concentration is then given by

$$\langle z \rangle = \sum_{\alpha} \sum_{i=1}^n \frac{w_{i, n+1, \alpha}}{w_{\alpha}} m_{\alpha i} + \sum_{\alpha} \bar{p}_{\alpha} \frac{\varphi_{\alpha, n+1}}{w_{\alpha}} \quad (69)$$

which corresponds to Equation 50 for tracer experiments. Similarly, the expected outlet flow rate of reactant is given by

$$\langle \psi \rangle = \sum_{\alpha} \sum_{i=1}^n w_{i, r+1, \alpha} m_{\alpha i} + \sum_{\alpha} \bar{p}_{\alpha} \varphi_{\alpha, n+1} \quad (70)$$

which corresponds in a similar way to Equation 51. The set of Equations 68 determines  $m_{\alpha i}$  completely only if  $R(x_i)$  is a linear function of  $x_i$ . Thus, let  $R(x_i) = kx_i$ . Then one obtains

$$km_{\beta j} = \bar{p}_{\beta} \frac{\varphi_{\beta j}}{v_j} + \sum_{i=1}^n \frac{w_{ij \beta}}{v_j} m_{\beta i} + \sum_{\alpha} \lambda_{\alpha \beta} m_{\alpha j}; \quad j = 1, 2, \dots, n \quad (71)$$

which is a set of algebraic equations sufficient to determine

the  $m_{\beta_j}$ . Comparing Equation 71 with Equation 48 it is seen that replacement of  $\varphi_{\beta_j}(t)$  in 48 with  $\varphi_{\beta_j}\delta(t)$ , where  $\varphi_{\beta_j}$  is constant, makes 71 the Laplace transform of 48 with transform variable  $k$ , and with

$$m_{\beta_j} = \bar{\mu}_{\beta_j} = \int_0^{\infty} e^{-kt} \mu_{\beta_j}(t) dt \quad (72)$$

Thus, the moments of reactant concentration,  $m_{\beta_j}$ , for a system with first-order reaction and with feed distribution  $\varphi_{\beta_j}$  are just the Laplace transforms of the moments of tracer concentration,  $\mu_{\beta_j}(t)$ , with tracer feed rate  $\varphi_{\beta_j}\delta(t)$ . Since the expected outlet concentration and the expected outlet flow rate of tracer and reactant are given by the same linear combination of individual moments, and since the Laplace transform operation is linear, the expected outlet concentration in the reaction case will be the Laplace transform of the expected outlet concentration for the corresponding tracer experiment, and the expected outlet reactant flow rate will be the Laplace transform of the expected outlet tracer flow rate. The tracer input that corresponds to the constant inlet concentration reactor case,

$$\varphi_{\beta_j}(t) = w_{o\beta} x_o \delta(t) \quad (73)$$

as comparison with Equation 43 shows, is an impulse in tracer inlet concentration of height  $x_o$ . Similarly, the tracer input corresponding to the constant reactant feed rate case is

$$\varphi_{\beta_j}(t) = \frac{w_{o\beta}}{w_{\beta}} \varphi \delta(t) \quad (74)$$

which is seen to be an impulse in tracer feed rate of height  $\varphi$  on comparison with Equation 44. Since  $f_x(t)$  and  $f_{\varphi}(t)$  are the expected responses in outlet tracer flow rate for an impulse in inlet tracer concentration (of height  $1/w$ ) and a unit impulse in inlet tracer flow rate, respectively, it is seen that, for a reactor with constant inlet reactant concentration  $x_o$ ,

$$\frac{\langle \psi \rangle}{w x_o} = \int_0^{\infty} e^{-kt} f_x(t) dt \quad (75)$$

and for one with a constant inlet reactant flow rate,

$$\frac{\langle \psi \rangle}{\varphi} = \int_0^{\infty} e^{-kt} f_{\varphi}(t) dt \quad (76)$$

Similarly, one can express the expected outlet concentration of reactant as the Laplace transform of the expected outlet tracer concentration for the appropriate tracer input. The terms on the left of Equations 75 and 76 are the expected fraction of reactant which leaves unconverted. The situation of Equation 75—fixed concentration of reactant in a fluctuating feed stream—is by far the more common. The situation of Equation 76—fixed flow of reactant—however, arises in certain contexts.

#### Interpretation of Tracer Experiments

Four impulse response experiments were discussed:  $\psi_x$ , the tracer flow rate response to a concentration impulse;  $\psi_{\varphi}$ , the tracer flow rate response to a flow rate impulse of tracer;  $z_x$ , the concentration response to a concentration impulse; and  $z_{\varphi}$ , the concentration response to a flow rate impulse. When the inlet and outlet flow rates are constant, all four responses are identical. In general, however, the expected values of three of these can be given a probabilistic interpre-

tation. Thus

$$\begin{aligned} (1/w) \langle \psi_x(t) \rangle &= f_x(t) \\ \langle \psi_{\varphi}(t) \rangle &= f_{\varphi}(t) \\ \langle z_x(t) \rangle &= f_o(t) \end{aligned} \quad (77)$$

where  $f_x(t)$ ,  $f_{\varphi}(t)$ , and  $f_o(t)$  are the residence time density functions for different populations of particles. Function  $f_x(t)$  is the density for the entire population of particles that pass through the system. This is the "true" residence time density. Its mean value is equal to the total volume of the system divided by the average inlet and outlet flow rate, while the other distributions do not, in general, have this property. Function  $f_{\varphi}(t)$  is the residence time density of a particle injected into the system at a random time, and  $f_o(t)$  is the residence time density of a particle taken from the outlet stream at a random time. In general, all three functions are different. However,  $f_{\varphi}(t)$  and  $f_o(t)$  are rather closely related. At point  $t = 0$ , for example, the functions can be shown to be equal [ $f_{\varphi}(0) = f_o(0)$ ]. Step experiments corresponding to the above impulse experiments can also be used to find the probability distributions. In such cases the expected step response is the distribution function of residence times.

When conventional experimental techniques are used, not all the responses are as convenient to determine. It is usual to measure tracer outlet concentration directly. Determination of tracer outlet flow rate thus requires simultaneous knowledge of total outlet flow rate and concentration. Also, it is more convenient to inject pulses of constant amount, which correspond to pulses in inlet tracer flow rate, than to vary the amounts in proportion to the instantaneous total inlet flow rate, which would correspond to pulses in inlet concentration. Of course, since the expected response of the system depends linearly on the input, the response to a concentration impulse can be determined by injecting equal pulses but multiplying the output by the total flow rate at the instant of injection before averaging the realizations together. Again, this would require knowledge of the total flow rate. The two step inputs, constant inlet tracer concentration and constant inlet tracer flow rate, can be achieved without measuring flow rate. Thus, if total flow rate is measured along with outlet concentration, all the responses, both impulse and step, can be measured. If total flow rate is not measured, however, only the impulse response  $\langle z_{\varphi}(t) \rangle$  and the step responses corresponding to  $\langle z_{\varphi}(t) \rangle$  and  $\langle z_x(t) \rangle$  can be found.  $\langle z_{\varphi}(t) \rangle$  is hard to interpret in a probabilistic sense, while  $\langle z_x(t) \rangle$  gives the residence time density for a special class of particles, those chosen, at random times from the outlet stream. The true residence time density,  $f_x(t) = \langle \psi_x(t) \rangle$ , could not be determined by such experiments.

In most cases measuring  $z_{\varphi}(t)$  is the method most convenient, and therefore generally used. It has no direct probabilistic interpretation, but provides important information about the system. If we want either to confirm or construct a simplified flow model for our process,  $z_{\varphi}$  serves this purpose as well as any of the other three functions.

When a first-order reaction occurs in the system, the mean outlet flow rate of unconverted reactant is given by the Laplace transform of  $f_x(t) = (1/w) \langle \psi_x(t) \rangle$  when reactant enters at constant concentration, and by that of  $f_{\varphi}(t) = \langle \psi_{\varphi}(t) \rangle$  when reactant enters at a constant flow rate. The mean outlet concentration of unconverted reactant is given by the Laplace transform of  $f_o(t) = \langle z_x(t) \rangle$  for the constant inlet concentration case and that of  $\langle z_{\varphi}(t) \rangle$  for the constant inlet reactant flow rate case.

### An Example

To illustrate the kind of behavior exhibited by stochastic systems, the foregoing analysis is applied to a simple example of the general stochastic model previously described—a single tank with a fluctuating throughput. It is also assumed that the flow rate assumes only two values, again for simplicity. Under these conditions, Equation 10 becomes

$$\frac{dp_1}{dt} = -\lambda_1 p_1 + \lambda_2 p_2 \quad (78)$$

$$\frac{dp_2}{dt} = \lambda_1 p_1 - \lambda_2 p_2$$

These equations can readily be solved, and the transition probabilities  $\pi_{\alpha\beta}(\tau)$ ,  $\alpha, \beta = 1, 2$ , set down explicitly by taking the appropriate initial conditions for  $p_1$  and  $p_2$ . All the probabilities go exponentially to their steady values

$$\bar{p}_1 = \frac{\lambda_2}{\lambda_1 + \lambda_2}, \quad \bar{p}_2 = \frac{\lambda_1}{\lambda_1 + \lambda_2} \quad (79)$$

as  $t \rightarrow \infty$ , with the time constant  $\lambda_1 + \lambda_2$ . With the (single) flow rate  $\omega$  taking just the two values  $\omega_\alpha$ ,  $\alpha = 1, 2$ , one may readily compute its mean

$$\bar{v} = \bar{p}_1 \omega_1 + \bar{p}_2 \omega_2 \quad (80)$$

and the covariance function may also be seen to be a simple exponential

$$\rho(\tau) = \bar{p}_1 \bar{p}_2 (\omega_1 - \omega_2)^2 e^{-(\lambda_1 + \lambda_2)|\tau|} \quad (81)$$

With the probability structure of the flow states established, one can readily investigate the tracer response of the model. For a single tank, the tracer material balance, Equation 41, becomes

$$v \frac{dx}{dt} = \varphi_\alpha(t) - \omega_\alpha x; \quad \alpha = 1, 2 \quad (82)$$

We need work here only with the probability distribution  $p_\alpha(t, x)$  for a single  $x$ , and apply the machinery of Equations 46 to 48 to give the moments

$$\mu_\alpha(t) = \int x p_\alpha(t, x) dx; \quad \alpha = 1, 2 \quad (83)$$

From Equations 50 and 51, we see that the mean outlet tracer concentration is given by

$$\langle z \rangle = \mu_1 + \mu_2 \quad (84)$$

and the mean outlet tracer flow by

$$\langle \psi \rangle = \omega_1 \mu_1 + \omega_2 \mu_2 \quad (85)$$

We may now calculate the response to an impulse in tracer concentration, where

$$\varphi_\alpha(t) = u_\alpha \delta(t); \quad \alpha = 1, 2 \quad (86)$$

and to an impulse in tracer flow, where

$$\varphi_\alpha(t) = \delta(t); \quad \alpha = 1, 2 \quad (87)$$

The general procedures noted earlier then give for the different mean responses

$$f_\alpha(t) = \frac{1}{\bar{v}} \langle \psi_\alpha(t) \rangle = \frac{\bar{p}_1 \omega_1^2 + \bar{p}_2 \omega_2^2}{\bar{v} \bar{v}} \frac{b_1 e^{b_1 t} - b_2 e^{b_2 t}}{b_1 - b_2} - \left\{ \frac{\bar{p}_1 \omega_1^2 + \bar{p}_2 \omega_2^2}{\bar{v}^2 \bar{v}} + \frac{(\omega_1 - \omega_2)^2}{\bar{v} \bar{v}} \bar{p}_1 \lambda_1 \right\} \frac{e^{b_1 t} - e^{b_2 t}}{b_1 - b_2} \quad (88)$$

$$f_\sigma(t) = \langle \psi_\sigma(t) \rangle = \frac{\bar{v} b_1 e^{b_1 t} - b_2 e^{b_2 t}}{v} - \frac{\bar{p}_1 \omega_1^2 + \bar{p}_2 \omega_2^2}{\bar{v}^2} \frac{e^{b_1 t} - e^{b_2 t}}{b_1 - b_2} \quad (89)$$

$$\bar{v} \langle z_\sigma(t) \rangle = \frac{\bar{v} b_1 e^{b_1 t} - b_2 e^{b_2 t}}{v} - \left( \frac{\bar{v}^2}{v} \right) \frac{e^{b_1 t} - e^{b_2 t}}{b_1 - b_2} \quad (90)$$

where  $b_1$  and  $b_2$  are the two roots of

$$b^2 + \left[ \frac{\omega_1}{v} + \frac{\omega_2}{v} + \lambda_1 + \lambda_2 \right] b + \frac{\omega_1 \omega_2}{v^2} + (\lambda_1 + \lambda_2) \frac{\bar{v}}{v} = 0 \quad (91)$$

The concentration-concentration response,  $f_\sigma(t) = \langle z_\sigma(t) \rangle$ , is not quoted above, since it is identically equal to  $f_\sigma(t)$ . This is not true in general. It happens here because this illustrative case, involving only a single flow state, is too thin to permit the distinction between these two sojourn time distributions.

Function  $f_\sigma(t)$  of Equation 88 is the true residence time distribution for the system—that is, the distribution for the entire population of particles. Its mean value is just equal to  $\bar{v}/\bar{v}$ . This is not true for the mean sojourn time calculated from Equation 80—that is, for a particle caught at a random moment in the inlet (or, in this example, in the outlet). Indeed, the mean value from Equation 89 is

$$\theta_\sigma = \frac{v}{\bar{v}} \left( 1 + \frac{\bar{p}_1 \bar{p}_2 (\omega_1 - \omega_2)^2}{v \bar{v} (\lambda_1 \lambda_2) + \omega_1 \omega_2} \right) \quad (92)$$

which always overstates  $v/\bar{v}$ , sometimes appreciably. If the average residence time is independently known (from direct measurements, say, of the volume and the mean flow rate), the size of the overstatement given by Equation 92 is itself valuable information. Also, if we have some preconceived notion about the flow,  $f_\sigma$  provides sufficient information to estimate the parameters for a flow model. For such estimations  $f_\sigma$  is just as good as  $f_x$  and there is therefore often no incentive to measure  $f_x$ .

The concentration response to an impulse in tracer flow rate is shown in Equation 90 multiplied by  $\bar{v}$ , to make its dimensions consistent with those of the other responses. This response corresponds to the most common kind of tracer experiment, and it is not a probability density at all. Indeed,

$$\int_0^\infty \bar{v} \langle z_\sigma(t) \rangle dt = \bar{v} \theta_\sigma / v$$

rather than unity.

In the limit of fast switching rates, the roots of Equation 91 become

$$b \approx \frac{-v}{\bar{v}}, \quad -(\lambda_1 + \lambda_2); \quad \lambda_1, \lambda_2 \rightarrow \infty \quad (93)$$

and all responses coalesce to the common exponential

$$f(t) = \frac{v}{\bar{v}} \exp\left(\frac{-v}{\bar{v}} t\right) \quad (94)$$

that is, to the response for a steady system with constant flow rate,  $\bar{v}$ . Illustrative plots of  $f_x$ ,  $f_\sigma$  from Equation 88 and 89, and the limiting  $f$  of Equation 94 are shown in Figure 2. These are all for

$$\frac{\omega_1 - \omega_2}{\bar{v}} = 1.8$$

and

$$\lambda_1 = \lambda_2 = \frac{\bar{w}}{v}$$

so that

$$\beta_1 = \beta_2 = \frac{1}{2}$$

All curves are shown with the time scale normalized on  $v/\bar{w}$ . For these values,  $\theta_p$  is 40% greater than  $v/\bar{w}$ .

A useful device for evaluating residence time distributions is to express them in terms of the escape intensity,  $h(t)$ , as defined by Naor and Shinnar (1963):

$$h(t) = f(t) / \int_0^\infty f(s) ds = \frac{f(t)}{1 - F(t)} \quad (95)$$

where  $f(t)$  is the residence time density function and  $F(t)$  is the corresponding distribution function.  $h(t)$  has the significance of the fractional rate at which particles which have been in the system a time  $t$  will escape from the system. This is plotted in Figure 3 for the density functions of Figure 2. In the graph,  $h_x(t)$  corresponds to  $f_x(t)$  and  $h_\varphi(t)$  corresponds to  $f_\varphi(t)$ . In a steady system, when the curve of  $h(t)$  decreases over some range, it is an indication that the flow pattern exhibits bypassing or stagnancy, since the tendency of a particle to leave the system is higher when it has been in the system a short time than it is at longer times. This effect is present in both  $h_x(t)$  and  $h_\varphi(t)$  (Figure 3), but is much more noticeable in  $h_x(t)$ . Thus the effect of the fluctuating flow rate is similar to that of bypassing.

We conclude this discussion of our illustrative example by making out the mean conversion for a first-order reaction. Here, following Equation 62, we have

$$v \frac{dx}{dt} = \varphi_a - w_a x - kx \quad (96)$$

and we seek the solutions of the stationary distribution Equations 68 for the two feed conditions:

$$\varphi_a = w_a x_0; \quad \alpha = 1, 2 \quad (97)$$

corresponding to a constant reactant inlet concentration, and

$$\varphi_a = \varphi \quad \alpha = 1, 2 \quad (98)$$

corresponding to a constant reactant feed rate. As before, we work with the moments

$$m_\alpha = \int x^\alpha p_\alpha(x) dx; \quad \alpha = 1, 2 \quad (99)$$

in terms of which we may express the mean outlet flow rate of unconverted reactant

$$\langle \psi \rangle = w_1 m_1 + w_2 m_2 \quad (100)$$

and the corresponding mean outlet concentration

$$\langle x \rangle = m_1 + m_2 \quad (101)$$

The main result is contained in the system of Equations 71, and solving them gives, for the different interpretations of fraction of reactant unconverted:

$$\frac{\langle \psi_x \rangle}{\bar{w} x_0} = \frac{[(\beta_1 w_1^2 + \beta_2 w_2^2)/v\bar{w}]k + (w_1 w_2/v^2) + (\bar{w}/v)(\lambda_1 + \lambda_2)}{k^2 + [(w_1/v) + (w_2/v) + \lambda_1 + \lambda_2]k + (w_1 w_2/v^2) + (\bar{w}/v)(\lambda_1 + \lambda_2)} \quad (102)$$

$$\frac{\langle \psi_\varphi \rangle}{\varphi} = \frac{(\bar{w}/v)k + (w_1 w_2/v^2) + (\bar{w}/v)(\lambda_1 + \lambda_2)}{k^2 + [(w_1/v) + (w_2/v) + \lambda_1 + \lambda_2]k + (w_1 w_2/v^2) + (\bar{w}/v)(\lambda_1 + \lambda_2)} \quad (103)$$

$$\frac{\bar{w} \langle x_\varphi \rangle}{\varphi} = \frac{(\bar{w}/v)k + (w_1 w_2/v^2) + (\bar{w}/v)(\lambda_1 + \lambda_2) + \beta_1 \beta_2 [(w_1/v) - (w_2/v)]^2}{k^2 + [(w_1/v) + (w_2/v) + \lambda_1 + \lambda_2]k + (w_1 w_2/v^2) + (\bar{w}/v)(\lambda_1 + \lambda_2)} \quad (104)$$

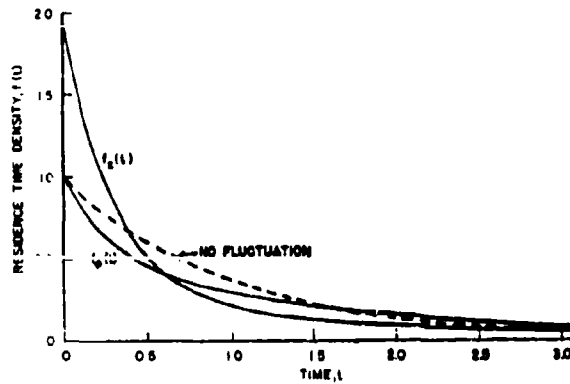


Figure 2. Illustrative residence time densities

Residence time density vs. time

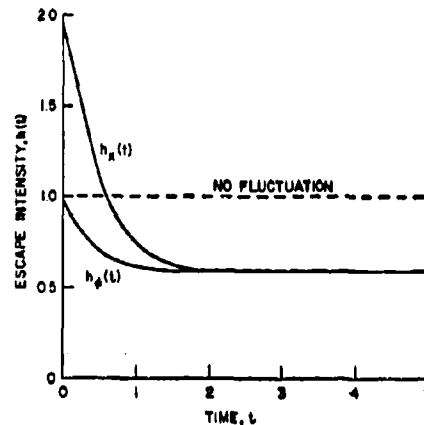


Figure 3. Illustrative escape intensities

Escape intensity vs. time

The result for  $\langle x_x \rangle/x_0$  is not quoted here, since it turns out to be identically equal to  $\langle \psi_x \rangle/\varphi$ . As in the tracer experiments for this example, this is not true in general, but is an accident of this particularly simple illustrative case.

Equations 102 and 103 give the fraction of reactant unconverted under the two different feed conditions being studied; Equation 104 does not quite do this. Still, as the switching rates  $\lambda_1 \lambda_2 \rightarrow \infty$ , all the equations coalesce to the common value

$$\frac{x}{x_0} = \frac{1}{1 + vk/\bar{w}} \quad (105)$$

which is the unconverted fraction for a steady flow  $\bar{w}$ . Figure 4 shows illustrative plots of the unconverted fraction from Equations 102 and 103, and the limiting value of 105. The

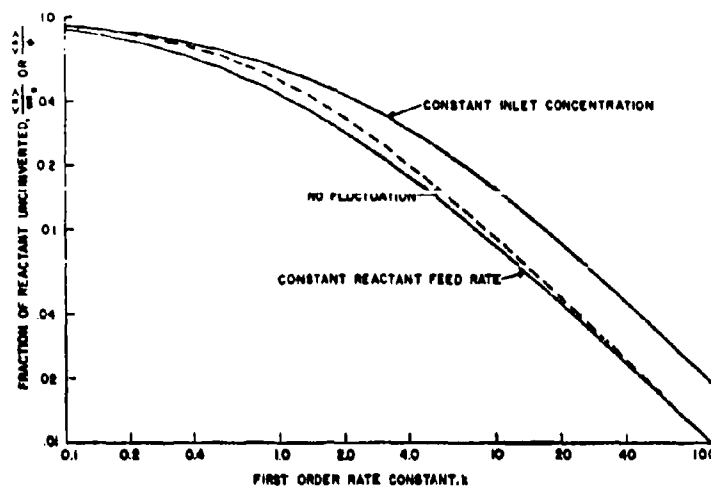


Figure 4. Illustrative behavior for first-order reaction

Fraction of reactant unconverted vs. first-order rate constant

numerical values are those chosen for the plots of Figure 2, and the first-order rate constant  $k$  is normalized on  $\bar{v}/v$ .

It may be seen from Figure 4, and directly from Equations 102 and 103, that the unconverted fractions based on constant inlet reactant concentrations and constant reactant feed rate straddle the limiting value of Equation 105

$$\frac{\langle \psi_w \rangle}{\varphi} < \frac{1}{1 + vk/\bar{v}} < \frac{\langle \psi_x \rangle}{\bar{v}x_0} \quad (106)$$

#### Appendix. Mean Residence Time

This Appendix aims at an intuitive proof that for a broad class of mixing systems, the mean residence time is the ratio of the mean working volume to the mean input-output flow rate. As a general matter, this is not an especially surprising result, although the point seems to arise from time to time in the discussion of particular mixing models. The proof is offered here as an intuitive base for the detailed calculations on the stochastic mixing models presented in this paper, although it applies to much more general mixing systems. Indeed, the argument is altogether model-free, and proceeds by a straightforward accounting for the sojourn time in the system of each material element passing through the system. We adduce no statistical considerations, nor any general considerations of stationarity, but instead carry out simple averaging in time, over what may be regarded as a very long transient from the moment the mixing vessel is brought (empty) on stream till it is retired (empty) from service.

Consider accordingly a mixing system of volume  $V$ , with inlet and outlet flow rates  $u$  and  $w$ , respectively, all varying with time in such a way that

$$\frac{dV}{dt} = u - w \quad (107)$$

The working fluid we take to be made up of identifiable material particles, each maintaining its own identity, and for convenience, we agree to measure  $V$ ,  $u$ , and  $w$  in particle units, so that  $V(t)$  is simply the number of particles in the system at time  $t$ , and  $u(t)$  and  $w(t)$  are, respectively, the numbers of particles per unit time entering and leaving the

system at time  $t$ . We imagine further the whole history of the mixing system spread over the (long) time interval  $t_0 < t < t_1$ , so that  $u = w = 0$  before  $t_0$  and after  $t_1$ , and suppose that over its life the system handles  $N$  particles, so that

$$\int_{t_0}^{t_1} u(t) dt = \int_{t_0}^{t_1} w(t) dt = N \quad (108)$$

Mean values here are simply time averages over the interval  $t_0, t_1$ , so that

$$\langle u \rangle = \langle w \rangle = \frac{N}{t_1 - t_0} \quad (109)$$

The time interval  $t_0, t_1$  represents the whole life of the mixing system, and not the much shorter duration of this or that tracer experiment. In the simplest situation of constant volume and flow rates, we might, for instance, have

$$u = \frac{N}{t_1 - t_0 - a}, \quad t_0 < t < t_1 - a$$

$$w = \frac{N}{t_1 - t_0 - a}, \quad t_0 + a < t < t_1$$

where  $a$  is the time needed to fill (or empty) the vessel.

Suppose the mixing system to have certain stagnant regions. Physically, such regions communicate very sluggishly with the main body of the system, and can introduce serious discrepancies between the ratio of volume to flow rate and the mean residence time as calculated from tracer experiments. We represent these stagnant regions here as zones that do not communicate with the main body of the system. Specifically, we consider that there is within the mixing system at all times a completely stagnant region of (constant) volume  $V_0$ . When the system is brought on stream at time  $t_0$ , and when it is removed from service at time  $t_1$ , we take it to be empty except for this volume  $V_0$ .  $V_0$  is then the common value of  $V$  at  $t_0$  and at  $t_1$ , and we see on integrating Equation 107 that

$$V(t) = V_0 + \int_{t_0}^t \{u(s) - w(s)\} ds$$

Integrating this now over the whole range  $t_0, t_1$  to form the

mean value of  $V$  gives

$$\langle V \rangle = V_0 + \frac{1}{t_1 - t_0} \int_{t_0}^{t_1} dt \int_{t_0}^t \{u(s) - w(s)\} ds$$

and interchanging the order of integration and applying Equation 108, we are left with

$$\langle V \rangle = V_0 + \frac{1}{t_1 - t_0} \left\{ \int_{t_0}^{t_1} s w(s) ds - \int_{t_0}^{t_1} s u(s) ds \right\} \quad (110)$$

Now in Equation 110, the integral of  $s \cdot u(s)$  simply cumulates the times at which all the particles enter the system, and the integral of  $s \cdot w(s)$ , the times at which they leave. Their difference is accordingly just the sum of the sojourn times in the system of all the particles that have passed through during its history, and if we denote the sojourn times of the individual particles by  $\theta_1, \theta_2$ , etc., we have

$$\langle V \rangle = V_0 + \frac{1}{t_1 - t_0} (\theta_1 + \theta_2 + \dots + \theta_N)$$

The mean sojourn time we identify simply as

$$\bar{\theta} = \frac{\theta_1 + \theta_2 + \dots + \theta_N}{N} \quad (111)$$

and, consulting Equation 109, we find

$$\langle V \rangle = V_0 + \langle w \rangle \bar{\theta} \quad (112)$$

Equation 112 is the result sought. For constant mixing volume  $V$ , and vanishing stagnant volume  $V_0$ , it reduces to the result in Equation 25. That the mean sojourn time,  $\bar{\theta}$ , should be computed from the residence time distribution  $f_x$ —that is, from the sojourn time distribution for a random particle, and not from the distributions  $f_p$  or  $f_0$  for particles entering or leaving at random times—is evidenced simply by the form of Equation 111, where each particle passing through the system is weighted equally in the evaluation of  $\bar{\theta}$ .

#### Nomenclature

$b_1, b_2$	= constants (Equation 98)
$f(t)$	= residence time density function
$F(t)$	= residence time distribution function
$\hat{f}(k)$	= Laplace transform of $f(t)$
$f_0(t)$	= residence time density function for particles chosen at a random time in outlet stream
$f_s(t)$	= true residence time density function
$f_p(t)$	= residence time density function for particles chosen at a random time in inlet stream
$f_{0p}(t)$	= residence time density function for particles chosen at a random time in outlet stream while being fed in inlet stream at a constant rate
$f_{ia}(t, \mathbf{x})$	= time rate of change of $x$
$h(t)$	= intensity function (Equation 95)
$k$	= reaction rate constant
$m_{ai}$	= partial moments of reactant concentration $(x_i)_a$
$p_a(t)$	= flow state probability distribution
$\hat{p}_a$	= stationary flow state distribution
$p_a^0$	= flow state distribution at instant an average particle enters
$p_a^s$	= flow state distribution at instant a particle leaves
$p_{ai}(t)$	= joint probability distribution of flow state and particle location
$p_{n+1}(t   \alpha)$	= conditional probability that particle has left

by time  $t$  given that flow state when it leaves is  $\beta$

$p_{n+1}^*(t)$	= joint probability of a particle chosen in outlet stream at a random time leaving in flow state $\alpha$ at a time less than $t$
$p_a(t, \mathbf{x})$	= joint probability distribution of flow state and concentration
$R(x_j)$	= reaction rate
$v$	= volume of single tank
$v_i$	= volume of tank $i$
$w$	= inlet and outlet flow rate
$w_a$	= inlet and outlet flow rate when flow state is $a$
$w_{ij}$	= flow rate from tank $i$ to tank $j$
$w_{i\alpha}$	= flow rate from tank $i$ to tank $j$ when flow state is $\alpha$
$\bar{w}$	= mean inlet flow rate
$x$	= single tank concentration
$x_i$	= concentration in tank $i$
$\mathbf{x}$	= set of concentrations, = $\{x_1, x_2, \dots, x_n\}$
$x_0$	= inlet concentration
$z$	= outlet concentration
$z_s(t)$	= tracer concentration response to an impulse in concentration
$z_p(t)$	= tracer concentration response to an impulse in flow rate
$z_x$	= outlet reactant concentration for constant inlet concentration
$z_w$	= outlet reactant concentration for constant inlet reactant flow rate

#### GREEK LETTERS

$\theta$	= mean residence time
$\theta_{ai}$	= partial mean residence time (Equation 21)
$\theta_p$	= see Equation 92
$\lambda_{a\beta}$	= switching rate
$\lambda_1$	= $\lambda_{12}$
$\lambda_2$	= $\lambda_{21}$
$\mu_{ai}(t)$	= partial mean concentration (Equation 47)
$\mu_1(t), \mu_2(t)$	= $\mu_{11}(t), \mu_{21}(t)$ for single tank
$\hat{\mu}_{ai}(t)$	= Laplace transform of $\mu_{ai}(t)$
$\pi_{a\beta}(\tau)$	= transition probability
$\rho(\tau)$	= autocovariance function
$\sigma_w^2$	= variance of flow rate
$\varphi$	= inlet reactant or tracer flow rate
$\varphi_{ai}(t)$	= inlet flow rate of tracer to tank $i$ when flow rate is $\alpha$
$\varphi_a(t)$	= $\varphi_{ai}(t)$ for single tank
$\psi$	= outlet reactant or tracer flow rate
$\psi_s(t)$	= outlet tracer flow rate response to concentration impulse
$\psi_p(t)$	= outlet tracer flow rate response to flow rate impulse

#### Literature Cited

- American Heart Association, New York, Symposium on the Use of Indicator-Dilution Techniques in the Study of the Circulation, 1962.
- Dankwerts, P. V., *Chem. Eng. Sci.* **8**, 93 (1958).
- Feller, W., "Introduction to Probability Theory and Its Applications," Vol. 2, Wiley, New York, 1960.
- Krambeck, F. J., Shinnar, R., Katz, S., *IND. ENG. CHEM. FUNDAMENTALS* **6**, 276 (1967).
- Kramers, H., Westerterp, K. R., "Elements of Chemical Reactor Design and Operation," Academic Press, New York, 1963.
- Naoi, P., Shinnar, R., *IND. ENG. CHEM. FUNDAMENTALS* **2**, 278 (1963).
- Zwietering, Th.N., *Chem. Eng. Sci.* **11**, 1 (1956).

RECEIVED for review March 10, 1968  
ACCEPTED March 3, 1969

Work supported by the Air Force Office of Scientific Research under AFOSR grant No. 921-67. Part of the research carried out by one of the authors (F. J. Krambeck) at The City University of New York in partial fulfillment of the requirements for the degree of doctor of philosophy.

**BLANK PAGE**

# Analysis of Some Random Blending Processes

F. J. KRAMBECK, R. SHINNAR and S. KATZ

*Department of Chemical Engineering, The City College of the City University of New York,  
New York, N.Y., U.S.A.*

A common problem in the design of mixing and blending equipment is the estimation of the size of the equipment needed to achieve a certain specification. If the statistical properties of the non-uniformities in the production lots to be blended are known one can calculate by known methods<sup>(1)</sup> the reduction in the variance of the product properties. Specifications however are normally given not in terms of a variance but in terms of limits. These can be estimated from the variance by assuming a Gaussian distribution. In this paper a method is discussed which allows one to calculate these limits directly for some blending problems in which the source of the nonuniformity is due to the production of an off-grade lot. This not only allows more accurate design procedures, but also gives some insights as to the magnitude of the error made by assuming a Gaussian distribution.

In a previous paper by one of the authors<sup>(1)</sup> the effect of a mixing tank on fluctuations in the feedstream compositions was discussed and methods were described which allow one to calculate some statistical properties of the output in terms of the statistical properties of the input. For example, one can use this method to calculate the correlation function of the output,  $\rho_c(\tau) = \langle c(t) c(t + \tau) \rangle$  in terms of  $\rho_{c_0}(\tau)$ , the correlation function of the feed stream. If the concentration is expressed relative to the mean, so that  $\langle c_0 \rangle$  and  $\langle c \rangle$  are zero,  $\rho_c(\theta)$  is the variance of the output. The method given in<sup>(1)</sup> can be applied to any system which can be reasonably described by a linearized model, as well as to blending processes.

Un problème courant dans la conception de l'outillage de malaxage et de mélange est l'estimé des dimensions de l'outillage qui doit répondre à des exigences spécifiques. Si l'on connaît les propriétés statistiques des facteurs de non-uniformité dans les portions des matériaux à mélanger, on peut calculer par des méthodes connues (référence 1) la diminution de la variance des propriétés du produit. Toutefois, on formule normalement les exigences en terme de limites plutôt que de variance et on peut les évaluer à partir de la variance en supposant l'existence d'une distribution de Gauss. On discute, dans ce travail, une méthode qui permet de calculer ces limites directement, dans le cas de certains problèmes de mélange où le manque d'uniformité est dû à la production d'une quantité de produit qui s'écarte de la qualité désirée. Ceci permet, non seulement l'obtention de procédés plus précis pour la conception, mais donne une idée de l'ampleur de l'erreur qui résulte de l'existence présumée d'une distribution de Gauss.

It often happens, however, that specifications are expressed in terms of limiting concentrations or limiting values of some other parameter, rather than in terms of a variance, and the method mentioned does not provide this kind of information, except for the special case where the probability distribution of the inlet concentration is Gaussian. In this special case the outlet concentration would also be Gaussian, and knowledge of the mean and variance determine the distribution completely. If the fluctuations in inlet concentration cannot be reasonably described by a Gaussian distribution, the above method cannot be used to determine confidence limits on the output.



In what follows a method is described which permits the computation of the complete probability distribution of the output of a blending tank for some specific, non-Gaussian inputs. It is interesting to note that in the cases studied the Gaussian approximation would be in appreciable error.

**Description of the Blending Process**

In some industrial processes the occurrence of off-grade batches cannot be prevented. Sometimes a certain amount of off-grade material is produced during the startup of a process. Often this off-grade material can be blended into the product provided its concentration does not exceed a certain limiting value. One way of dealing with such a situation is to provide an off-grade storage tank and feed the material slowly into the product stream. This possibility is discussed in reference<sup>(2)</sup>. If the process contains some large blending facilities one might consider the alternate possibility of feeding all the material into a single blending tank. This is the situation that will be studied here. It will be assumed that off-grade batches occur at random times, with the time intervals between them distributed exponentially. The capacity of the blending tank will be assumed large compared to the volume of off grade in a single batch, so that each batch can be considered a Dirac pulse in time. The product is fed to the tank and withdrawn continuously. The amount of offgrade contained in each pulse is also a random variable, with density function  $f(m)$ . In case the real problem does not involve impurities but rather a large deviation in some quantity like molecular weight, color, etc. one can always treat this deviation from the average in the same way that impurity concentration is treated here. We now proceed to set up the blending equations.

The pulses occur at a mean rate  $1/\theta$  and the number of pulses occurring in a fixed time interval is a Poisson random variable. The outlet concentration of impurity,  $x$ , then satisfies the equation

$$v \frac{dx}{dt} = \sum_i \delta(t - t_i) m_i - wx \dots (1)$$

where  $w$  is the total volumetric flow rate,  $v$  is the volume of the tank, and the  $t_i$  are the random pulse times. The pulse heights  $m_i$  are distributed according to  $f(m)$ . Thus in between pulses the concentration will satisfy

$$v \frac{dx}{dt} = -wx \dots (2)$$

while each pulse will cause an instantaneous surge in concentration by the amount  $m_i/v$ .

We define transition probabilities  $\pi(x \rightarrow y; \tau)$  so that the probability that the outlet concentration is in the interval  $(y, y + dy)$  at time  $t + \tau$  given that it was equal to  $x$  at time  $t$  is  $\pi(x \rightarrow y; \tau) dy$ . We also define the probability density function of outlet concentration,  $\phi(t, x)$ , so that the probability that the outlet concentration is in the interval  $(x, x + dx)$  at time  $t$  is  $\phi(t, x) dx$ . By writing the transition probabilities in the above form, we have assumed that the probability distribution at a later time,  $t + \tau$ , depends only on the state of the system at time  $t$  and not on any previous states of the system, and also that this dependence only involves the time interval between the two points of time in question rather than on the times measured from some absolute reference. These two assumptions classify the process as a stationary Markov process. Reflection will show that they are true for the present problem as stated. Any process of this type will satisfy the Chapman-Kolmogorov equation:

$$\phi(t + \tau, y) = \int dx \phi(t, x) \pi(x \rightarrow y; \tau) \dots (3)$$

(There is an extensive literature on the theory of Markov processes. See, for example, reference<sup>(3)</sup>).

The transition probabilities can be expressed for small time intervals as follows:

$$\pi(x \rightarrow y; \tau) = \left(1 - \frac{\tau}{\theta}\right) \delta\left[y - x + \frac{wx}{v} \tau + o(\tau)\right] + \frac{\tau}{\theta} v f\left[v(y - x) + o(1)\right] \dots (4)$$

The first term on the right hand side is the product of the probability of no pulse arriving in the interval  $\tau$ ,  $\left(1 - \frac{\tau}{\theta}\right)$ , times the  $\delta$ -function, which expresses the certainty of what will happen if no pulse arrives, namely that the concentration will change according to Equation (2). The second term is the product of the probability that a pulse will arrive, times the density function for  $y$  that will result from this occurrence. This is derived from the function  $f(m)$  by substituting  $v(y - x) + o(1)$  for  $m$ , since for a small enough time interval the change in concentration resulting from the pulse will be  $\frac{m}{v}$ . The function must be multiplied by  $v$  because  $dm = v dy$ .

We then expand the  $\delta$ -function in a power series in  $\tau$ .

$$\delta\left[y - x + \frac{wx}{v} \tau + o(\tau)\right] = \delta(y - x) - \frac{w}{v} x \left[\frac{d}{dx} \delta(y - x)\right] \tau + o(\tau) \dots (5)$$

and substitute (4) and (5) into (3) to find

$$\phi(t + \tau, y) = \phi(t, y) - \frac{\tau}{\theta} \phi(t, y) + \tau \frac{w}{v} \frac{d}{dy} [y \phi(t, y)] + \tau \frac{v}{\theta} \int dx \phi(t, x) f[v(y - x) + o(1)] + o(\tau) \dots (6)$$

Changing the integration variable and rearranging yields

$$\frac{\phi(t + \tau, y) - \phi(t, y)}{\tau} = -\frac{1}{\theta} \phi(t, y) + \frac{w}{v} \frac{d}{dy} [y \phi(t, y)] + \frac{1}{\theta} \int dm \phi\left(t, y - \frac{m}{v} + o(1)\right) f(m) + o(\tau) \dots (7)$$

and, as  $\tau \rightarrow 0$ , we find

$$\frac{\partial \phi(t, x)}{\partial t} = -\frac{1}{\theta} \phi(t, x) + \frac{w}{v} \frac{d}{dx} [x \phi(t, x)] + \frac{1}{\theta} \int \phi\left(t, x - \frac{m}{v}\right) f(m) dm \dots (8)$$

Setting  $\frac{\partial \phi}{\partial t} = 0$  yields the equation for the stationary probability distribution for the process:

$$\frac{d}{dx} [x \phi(x)] = \frac{v}{w\theta} \phi(x) - \frac{v}{w\theta} \int \phi\left(x - \frac{m}{v}\right) f(m) dm \dots (9)$$

**Moments of Outlet Concentration**

Let

$$\mu_k = \int x^k \phi(x) dx \text{ and } \lambda_k = \int m^k f(m) dm$$

Multiplying Equation (9) by  $x^k$  and integrating we find

$$-k \mu_k = \frac{v}{w\theta} \mu_k - \frac{v}{w\theta} \sum_{j=0}^k \binom{j}{k} \frac{\mu_j \lambda_{k-j}}{v^{k-j}}$$

or

$$\mu_k = \frac{v}{kw\theta} \sum_{j=0}^{k-1} \binom{k}{j} \frac{\mu_j \lambda^{k-j}}{v^{k-j}} \dots (10)$$

Equation (10) expresses the  $k^{\text{th}}$  moment of the outlet concentration in terms of the moments of the pulse height distribution and the first  $k-1$  moments of the concentration, so that the moments may be calculated in turn. For example:

$$\begin{aligned} \mu_1 &= \frac{\lambda_1}{w\theta} \\ \mu_2 &= \frac{\lambda_2}{2vw\theta} + \frac{\mu_1 \lambda_1}{w\theta} \\ &= \frac{\lambda_2}{2vw\theta} + \mu_1^2 \end{aligned}$$

Thus the variance of the outlet concentration is  $\frac{\lambda_2}{2vw\theta}$ .

The moments may also be found through a Laplace transform method. Taking Laplace transforms in Equation (9) we obtain

$$-s \frac{d\hat{\phi}}{ds} = \frac{v}{w\theta} \hat{\phi} - \frac{v}{w\theta} f\left(\frac{s}{v}\right) \hat{\phi} \dots (11)$$

where

$$\hat{\phi}(s) = \int_0^\infty e^{-sx} \phi(x) dx$$

which is solved to yield

$$\ln \hat{\phi}(s) = \frac{v}{w\theta} \int_0^\infty \frac{f(t) - 1}{t} dt \dots (12)$$

Since  $\mu_k = (-1)^k \frac{d^k \hat{\phi}(s)}{ds^k} \Big|_{s=0}$ , differentiation of Equation (12) gives the moments of  $\phi$  in terms of the moments of  $f$ .

**Distribution of Output for Exponentially Distributed Pulse Heights**

For exponentially distributed pulse heights we have

$$f(m) = \frac{1}{\lambda} e^{-\frac{m}{\lambda}} \dots (12a)$$

where here  $\lambda$  is the mean pulse height.

Taking the Laplace transform we find

$$\hat{f}(t) = \frac{1}{1 + \lambda t} \dots (13)$$

Substituting (13) into (12) yields

$$\hat{\phi}(s) = \left[ 1 + \frac{s\lambda}{v} \right]^{-\frac{v}{w\theta}}$$

which can be inverted to give the gamma distribution:

$$\phi(x) = \frac{(v/\lambda)^{\frac{v}{w\theta}}}{\Gamma\left(\frac{v}{w\theta}\right)} x^{\frac{v}{w\theta}-1} e^{-\frac{vx}{\lambda}} \dots (14)$$

The cumulative distribution function corresponding to this density is the incomplete gamma function (+):

$$\Phi(x) = \frac{1}{\Gamma\left(\frac{v}{w\theta}\right)} \int_0^{\frac{vx}{\lambda}} r^{\frac{v}{w\theta}-1} e^{-r} dr = P\left(\frac{v}{w\theta}, \frac{vx}{\lambda}\right) \dots (15)$$

The foregoing Equations, (14) and (15), give the probability distribution of outlet concentration. However, for the design of a blending tank, one must consider the fact that a pulse of impurity will produce a sudden jump in outlet concentration, and it is the height of this jump that one wishes to limit. Thus we consider the distribution of outlet concentration given that a pulse has just entered the system. Since the probability of a pulse occurring in a given time interval is independent of when the previous pulse occurred, it is also independent of the state of the system. Therefore the outlet concentration distribution just before a pulse occurs is the same as the previously computed distribution (14), (15). The distribution in concentration just

after a pulse is then that of the sum  $x + \frac{m}{v}$ .

The independence of the two random variables permits the calculation of the distribution of their sum by convolution:

$$\psi(x) = \int_0^x v f[v(x-\xi)] \phi(\xi) d\xi \dots (16)$$

(Equation (16) can also be derived by a more careful argument given in the appendix)

Substituting (14) and (12a) into (16) we obtain

$$\psi(x) = \frac{(v/\lambda)^{\frac{v}{w\theta} + 1}}{\Gamma\left(\frac{v}{w\theta} + 1\right)} x^{\frac{v}{w\theta}} e^{-\frac{vx}{\lambda}} \dots (17)$$

which is also a gamma distribution. The cumulative distribution now becomes

$$\Psi(x) = P\left(\frac{v}{w\theta} + 1, \frac{vx}{\lambda}\right) \dots (18)$$

The distribution characterized by  $\psi$  and  $\Psi$  may be called the distribution of surge concentrations. Roughly speaking, the distribution  $\Phi$  gives the fraction of total material which does not exceed a given limit, while the distribution  $\Psi$  gives the fraction of surges which will not exceed a given limit.

The moments of the outlet concentration distribution can be found from Equation (10). The moments of the pulse height distribution,  $f(m)$  are

$$\lambda_k = k! \lambda^k ; k = 1, 2, \dots$$

thus, substituting in (10),

$$\begin{aligned} \mu_k &= \frac{v}{kw\theta} \sum_{j=0}^{k-1} \binom{k}{j} \frac{\mu_j \lambda^{k-j}}{v^{k-j}} (k-j)! \\ &= \frac{v}{kw\theta} \sum_{j=0}^{k-1} \frac{k! \mu_j \lambda^{k-j}}{j! v^{k-j}} \end{aligned}$$

In particular, the mean and variance are

$$\begin{aligned} \mu_1 &= \frac{\lambda}{w\theta} \\ \sigma^2 &= \mu_2 - \mu_1^2 = \frac{\lambda^2}{vw\theta} \end{aligned}$$

Let us introduce the following dimensionless variables to reduce the number of parameters involved.

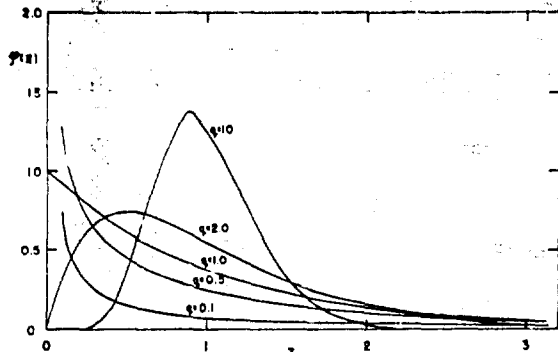


Figure 1—Probability density of outlet concentration for exponentially distributed pulse heights.

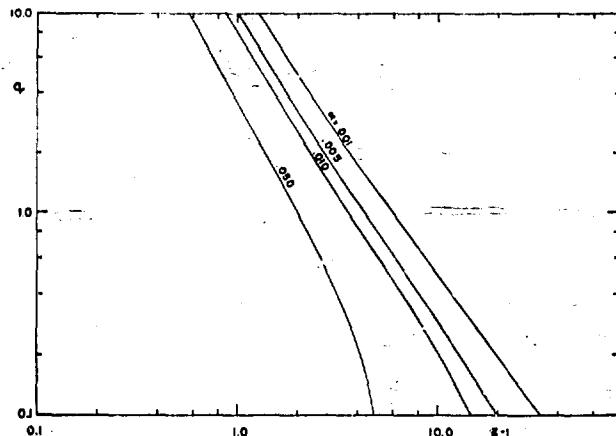


Figure 2—Design chart based on confidence limit of concentration for exponentially distributed pulse heights.

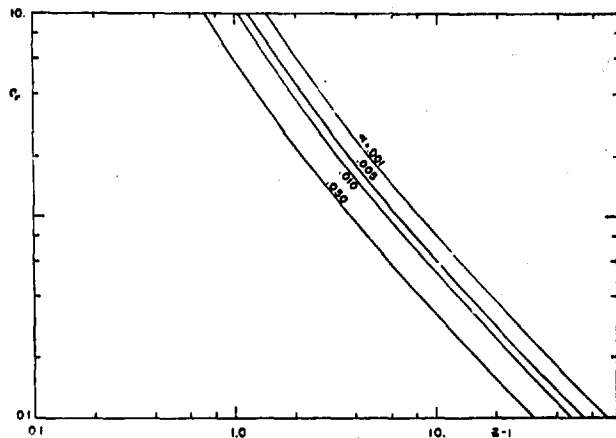


Figure 3—Design chart based on confidence limit of surge concentration for exponentially distributed pulse heights.

$$q = \frac{v}{w\theta}$$

$$z = \frac{w\theta x}{\lambda}$$

The parameter  $q$  is equal to the average number of pulses per residence time of the blender and  $z$  is a dimensionless concentration equal to the outlet concentration divided by the mean outlet concentration. In this way

$$\phi(z) = \frac{1}{\Gamma(q)} \int_0^{qz} t^{q-1} e^{-t} dt = P(q, qz)$$

and

$$\phi(z) = \frac{q^q}{\Gamma(q)} z^{q-1} e^{-qz}$$

The moments of the dimensionless distribution are

$$\mu_1 = 1$$

$$\sigma^2 = \frac{1}{q}$$

Figure 1 gives some curves of  $\phi(z)$  vs.  $z$  for typical values of the dimensionless pulse frequency,  $q$ . Figure 2 gives confidence limits for the dimensionless concentration at different values of  $q$ . The abscissa of the plot in Figure 2 is  $z - 1$ , where  $z$  is the value of dimensionless outlet concentration that has probability  $\alpha$  of being exceeded:

$$\alpha = 1 - \Phi(z) = 1 - P(q, qz)$$

The confidence limits on surge concentration are given in Figure 3. These curves are given by

$$\alpha = 1 - \Psi(z) = 1 - P(q + 1, qz)$$

It should be kept in mind when using plots that the limit on concentration will be exceeded a fraction  $\alpha$  of the time, while the limit on surge concentration will be exceeded for a fraction  $\alpha$  of the surges. This will obviously result in a much smaller amount of spoiled product.

#### Distribution of Output for Constant Pulse Heights

For equal pulse heights the function  $f$  is given by

$$f(m) = \delta(\lambda - m) \dots \dots \dots (19)$$

where  $\lambda$  is the pulse height. The Laplace transform is

$$\hat{f}(s) = e^{-\lambda s} \dots \dots \dots (20)$$

Substitution of (20) into (12) yields

$$\ln \hat{\phi}(s) = -\frac{v}{w\theta} \int_0^{s\theta} \frac{1 - e^{-\lambda t}}{t} dt$$

or

$$\ln \hat{\phi}(s) = -\frac{\tau}{w\theta} \left[ E_1 \left( \frac{\lambda s}{v} \right) + \ln \left( \frac{\lambda s}{v} \right) + \gamma \right] \dots \dots (21)$$

where

$$E_1(x) = \int_x^\infty \frac{e^{-t}}{t} dt \text{ and } \gamma \text{ is Euler's constant (ref. (4))}$$

Since (21) is difficult to invert, another method will be used to determine  $\phi(x)$ . However it will be useful to obtain a limiting form of  $\phi(x)$  as  $x \rightarrow 0$ . This is done by studying  $\phi(s)$  as  $s \rightarrow \infty$ :

$$\hat{\phi}(s) \rightarrow \left( \frac{\lambda}{v} e^\gamma \right)^{-\frac{v}{w\theta}} s^{-\frac{v}{w\theta}} ; s \rightarrow \infty$$

$$\therefore \phi(x) \rightarrow \frac{\left( \frac{\lambda}{v} e^\gamma \right)^{-\frac{v}{w\theta}}}{\Gamma \left( \frac{v}{w\theta} \right)} x^{\frac{v}{w\theta} - 1} ; x \rightarrow 0 \dots \dots (22)$$

To solve for  $\phi(x)$ , we substitute Equation (19) into equation (9):

$$\frac{d}{dx} [x\phi] = \frac{v}{w\theta} \phi - \frac{v}{w\theta} \phi \left( x - \frac{\lambda}{v} \right) \dots (23)$$

B.C:  $\phi(x) = 0$  when  $x < 0$

Equation (23) can be solved stepwise to yield

$$0 < x < \frac{\lambda}{v} :$$

$$\phi(x) = c_1 x^{\frac{v}{w\theta}} - 1$$

$$\frac{\lambda}{v} < x < \frac{2\lambda}{v} :$$

$$\phi(x) = c_1 x^{\frac{v}{w\theta}} - 1 \left[ 1 - \frac{v}{w\theta} \int_{\lambda/v}^x \xi^{-\frac{v}{w\theta}} \left( \xi - \frac{\lambda}{v} \right)^{\frac{v}{w\theta} - 1} d\xi \right]$$

etc.

(24)

From equation (22) we see that

$$c_1 = \frac{\left( \frac{\lambda e^\gamma}{v} \right)^{\frac{v}{w\theta}}}{\Gamma\left( \frac{v}{w\theta} \right)} \dots (25)$$

Since the integrals in (24) soon become unwieldy, the functions  $\phi$  and  $\Phi$  were computed numerically for some typical cases. For the case of constant pulse heights, the distribution of surge compositions is just

$$\psi(x) = \phi \left( x - \frac{\lambda}{v} \right)$$

and

$$\Psi(x) = \Phi \left( x - \frac{\lambda}{v} \right)$$

In this case the moments of  $f(m)$  are given by

$$\lambda_k = \lambda^k$$

The moments of the output concentration are

$$\mu_k = \frac{v}{kw\theta} \sum_{j=0}^{k-1} \binom{k}{j} \frac{\mu_j \lambda^{k-j}}{v^{k-j}}$$

In particular, the mean and variance are

$$\mu_1 = \frac{\lambda}{w\theta}$$

$$\sigma^2 = \mu_2 - \mu_1^2 = \frac{\lambda^2}{2vw\theta}$$

Again we introduce the dimensionless variables  $q$  and  $z$ , with the same significance as before. Then

$$0 < z < \frac{1}{q} :$$

$$\phi(z) = \frac{(qe^{-\gamma})^q}{\Gamma(q)} z^{q-1}$$

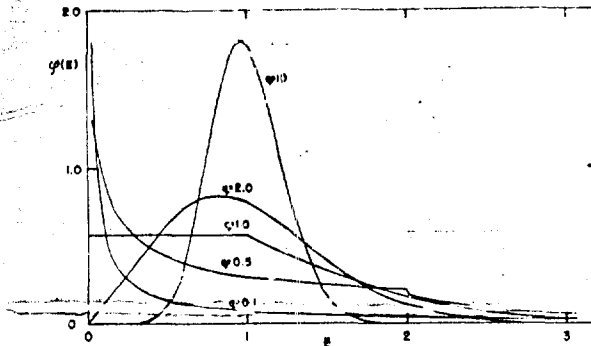


Figure 4—Probability density of outlet concentration for constant pulse heights.

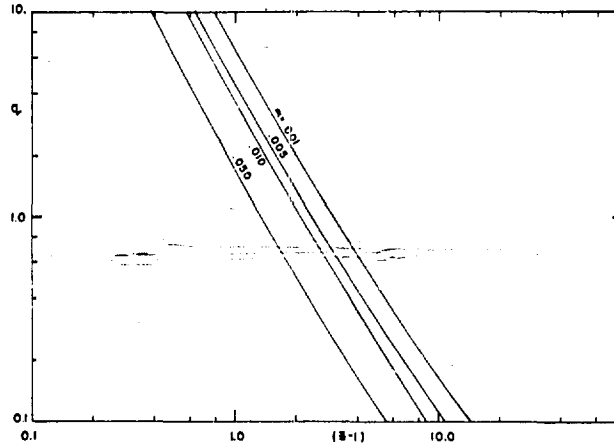


Figure 5—Design chart based on confidence limit of concentration for constant pulse height.

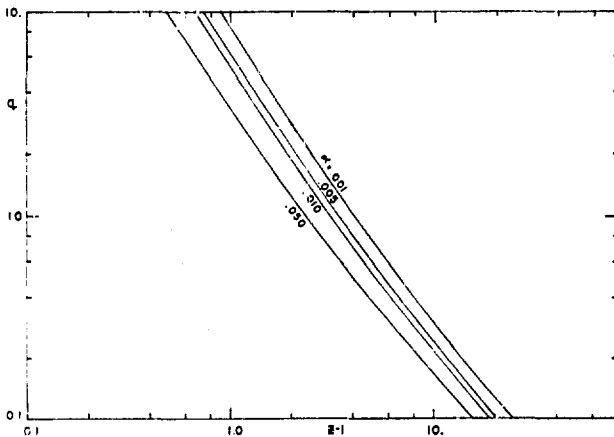


Figure 6—Design chart based on confidence limit of surge concentration for constant pulse heights.

$$\frac{1}{q} < z < \frac{2}{q} :$$

$$\phi(z) = \frac{(qe^{-\gamma})^q}{\Gamma(q)} z^{q-1} \left[ 1 - q \int_{1/q}^z \xi^{-q} \left( \xi - \frac{1}{q} \right)^{q-1} d\xi \right]$$

The moments are given by

$$\mu_1 = 1$$

$$\sigma^2 = \frac{1}{2q}$$

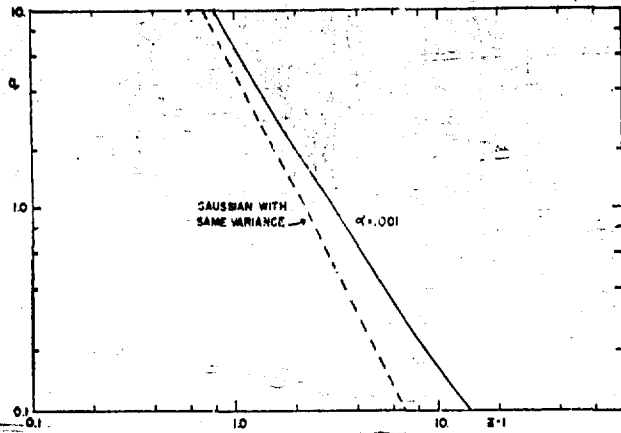


Figure 7—Comparison of confidence limits for constant pulse heights with Gaussian approximation.

One notes that for the same mean and an equal value of  $q$  the variance of outlet concentration for equal pulse heights is half of that for exponentially distributed heights. Figure 4 shows some typical curves of  $\phi(z)$  and Figure 5 shows the corresponding confidence limits. The confidence limits on surge concentration are given in Figure 6.

#### Comparison with the Gaussian Approximation

It was stated in the introduction that in the absence of any other method one can try to estimate the confidence limits by assuming that the distribution of output is approximately normal. In this case the confidence limit of  $z$  for  $\alpha = 0.001$  is  $\mu_1 + 3.09\sigma$ , where  $\sigma$  is the standard deviation, and  $\mu_1$  is the average value of  $z$  which is one. In the case of constant pulse heights,

$$\sigma = \frac{1}{\sqrt{2q}}, \text{ while in the case of exponentially distributed pulse}$$

heights,  $\sigma = \frac{1}{\sqrt{q}}$ . The actual confidence limit for constant

pulse height is compared with the Gaussian approximation in Figure 7, for  $\alpha = 0.001$ , and in Figure 8 with the exponentially distributed pulse height case. One notes that for high values of  $q$ , ( $q > 5$ ), the Gaussian approximation gives fairly close results whereas for low values of  $q$  the deviations are considerable. For  $q = 0.1$  the Gaussian approximation underestimates the upper concentration limit by about a factor of 2 for the constant pulse height case and 3 for the exponential pulse height case. Another type of comparison is illustrated by the following. Suppose it is desired to design a blending tank for offgrade lots such that the maximum outlet concentration of impurity is less than five times the average outlet concentration with a probability of 99.9%. The average outlet concentration is that which would result if the offgrade material were evenly distributed over the total production. In the exponentially distributed pulse height case the required value of  $q$  would be 1.26, while the Gaussian approximation gives .39. In the constant pulse height case the required value is .45 vs. the Gaussian prediction of .183. Thus the Gaussian approximation would predict a much smaller blender size.

In general one could conclude that in any case of a stochastic input where the input deviates strongly from a Gaussian distribution the assumption that the outlet concentration is Gaussian is only good if the time scale of the input fluctuations is small compared to the residence time of the tank.

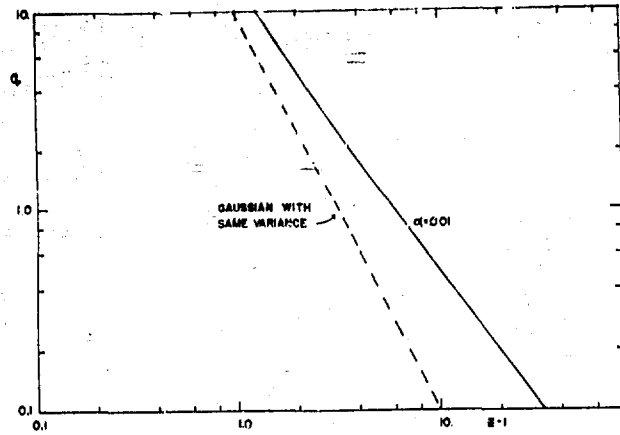


Figure 8—Comparison of confidence limits for exponentially distributed pulse heights with Gaussian approximation.

## APPENDIX

### Distribution of Surge Concentrations

Consider successive surge concentrations as points in a Markov chain. We define one-step transition probability densities  $\pi(x \rightarrow y)$  so that the probability that the surge concentration is in the interval  $(y, y + dy)$  given that the last surge was of height  $x$  is  $\pi(x \rightarrow y)dy$ . We may derive this density in terms of the density of pulse heights,  $f(m)$ , and the

density of times between surges,  $\frac{1}{\theta} e^{-t/\theta}$  as follows: Since the height of the last surge was  $x$ , the value of concentration just

before the next surge is  $x e^{-\frac{m}{v}t}$ , where  $t$  is the time between surges. The concentration is then increased by an amount

$\frac{m}{v}$ , so that the random variable  $Y$  depends on the variables  $t$  and  $m$  according to the equation

$$Y = x e^{-\frac{m}{v}t} + \frac{m}{v}$$

The joint density function of  $t$  and  $m$  is the product of the two respective densities,  $\frac{1}{\theta} e^{-t/\theta} f(m)$ . Thus

$$Pr \{ Y < y \} = \int_0^{\infty} \int_0^{\infty} \frac{1}{\theta} e^{-t/\theta} \int_0^{y - x e^{-\frac{m}{v}t}} f(m) dm dt$$

$$\frac{d}{dy} Pr \{ Y < y \} = \pi(x \rightarrow y) = \int_0^{\infty} \frac{1}{\theta} e^{-t/\theta} v f(y - x e^{-\frac{m}{v}t}) dt$$

The Chapman-Kolmogorov equation (for the stationary distribution)

$$\psi(y) = \int \psi(x) \pi(x \rightarrow y) dx$$

then becomes

$$\psi(y) = \int_0^{\infty} dx \int_0^{\infty} dt \psi(x) \frac{1}{\theta} v f(y - x e^{-\frac{m}{v}t}) e^{-t/\theta}$$

Taking Laplace transforms,

$$\hat{\psi}(s) = \frac{1}{\theta} \hat{f}\left(\frac{s}{v}\right) \int_0^{\infty} e^{-st} \hat{\psi}(se^{-\frac{v}{\theta}t}) dt$$

where

$$\hat{\psi}(s) = \int_0^{\infty} e^{-sx} \psi(x) dx$$

Let

$$u = se^{-\frac{v}{\theta}t} \quad \text{The expression then becomes}$$

$$\hat{\psi}(s) = \frac{v}{w\theta} s^{-\frac{v}{w\theta}} \hat{f}\left(\frac{s}{v}\right) \int_0^{\infty} u^{\frac{v}{w\theta}-1} \hat{\psi}(u) du$$

Differentiating,

$$\frac{d\hat{\psi}(s)}{ds} = \left\{ \frac{\hat{f}\left(\frac{s}{v}\right) - 1}{w\theta} + \frac{\hat{f}\left(\frac{s}{v}\right)}{v\hat{f}\left(\frac{s}{v}\right)} \right\} \hat{\psi}(s)$$

or

$$\ln \hat{\psi}(s) = \frac{v}{w\theta} \int_0^{\infty} \frac{\hat{f}(t) - 1}{t} dt + \ln \hat{f}\left(\frac{s}{v}\right)$$

Comparing with equation (2) we see that

$$\hat{\psi}(s) = \hat{f}\left(\frac{s}{v}\right) \hat{\psi}(s)$$

which gives

$$\psi(x) = \int_0^{\infty} v/v(x-\xi) \phi(\xi) d\xi$$

#### Nomenclature

- $f$  = pulse height probability density  
 $\hat{f}$  = Laplace transform of pulse height density

$m_i$  = pulse height of  $i^{\text{th}}$  pulse

$q$  = dimensionless tank volume (or pulse rate) =  $\frac{v}{w\theta}$

$s$  = Laplace transform variable

$t$  = time

$t_i$  = time of  $i^{\text{th}}$  pulse

$v$  = volume of tank

$w$  = volumetric flow rate

$x$  = concentration of impurity

$z$  = dimensionless impurity concentration

$\alpha$  = probability of exceeding confidence limit

$\theta$  = mean time between pulses

$\lambda$  = mean pulse height (=  $\lambda_1$ )

$\lambda_k$  =  $k^{\text{th}}$  moment of pulse height distribution

$\mu_k$  =  $k^{\text{th}}$  moment of outlet concentration distribution

$\pi$  = transition probability

$\rho$  = correlation function

$\sigma$  = standard deviation

$\phi$  = probability density of outlet concentration

$\Phi$  = distribution function of outlet concentration

$\psi$  = probability density of surge concentration

$\Psi$  = distribution function of surge concentration

#### Acknowledgments

The work reported here was supported in part under AFOSR Grant No. 921-65. Some of this work is part of the research carried out by one of the authors (F.J.K.) at the City University of New York in partial fulfillment of the requirements of the degree of Doctor of Philosophy.

#### References

- (1) Katz, S., "A Statistical Analysis of Certain Mixing Problems", Chem. Eng. Sci., 9, 61 (1958).
- (2) Shinnar, R., "Sizing of Storage Tanks for Off-Grade Material in a Blending Cascade", in publication.
- (3) Feller, W., "An Introduction to Probability Theory and its Applications", Volume II, John Wiley & Sons, Inc., New York (1966).
- (4) Abramowitz, M. and Stegun, I. A. (editors), "Handbook of Mathematical Functions", National Bureau of Standards, Applied Mathematics Series, 55 (June, 1964).

Manuscript received January 13; accepted April 5, 1967.  
 Based on a paper presented to the C.I.C. 16th Canadian Chemical Engineering Conference, Windsor, Ont., October 16-19, 1966.

★ ★ ★

**BLANK PAGE**

# Particulate Methods in Probability Systems

STANLEY GATE  
HEUT. SMOKE

A stochastic approach to particulate processing systems can give the investigator insight into underlying mechanisms and the nature of observed fluctuations in particle size and number

**C**louds of particles in chemical processing systems are perhaps one of the newer contexts in which probabilistic analyses come to the fore. But while the context may be new, the mathematical methods have much in common with studies in biological populations, on the one hand, and in classical statistical mechanics on the other.

The chemical processing context itself offers a good deal of variety. It includes, for example, problems in crystallization, in mineral flotation, and in fluid bed dynamics. In the realm of submicroscopic particles, there are polymerization problems. And if we permit a more abstract view of our particles, we find problems in turbulent mixing.

In these different cases, we look for the probability distributions associated with the particle populations—the distributions of population size and the joint distributions of population size and the appropriate measures of particle quality. We would like to know these distributions at single times as well as the corresponding joint distributions at two or more times. We begin the

The general mathematical background of this review is to be found in any one of a great number of books on probability theory. For the reader interested to learn or re-learn this subject, we are fortunate to be able to direct him to the very beautiful two-volume work of Feller (2), one of the great texts of this century. A rather shorter introduction to our part of the subject is given in the recent, crisp book of Karlin (3). And a treatment of Markov processes with a good many physical applications may be found in the book of Bharucha-Reid (1).

- (1) Bharucha-Reid, A. T., "Elements of the Theory of Markov Processes and their Applications," McGraw-Hill, New York, N. Y., 1960.
- (2) Feller, William, "An Introduction to Probability Theory and Its Applications," Wiley, New York, N. Y., Vol. 1, 1950; Vol. 2, 1966.
- (3) Karlin, Samuel, "A First Course in Stochastic Processes," Academic Press, New York, N. Y., 1966.



search, mathematically speaking, with some plausible guess at the random mechanism underlying the population changes. This tentative specification of the mechanism always contains rate parameters describing the short-term changes in the system, and while these can rarely be directly measured, we may estimate them, if we can push the mathematical work through to the end, by comparing the final calculated probability distributions with appropriate measurements on the actual particle populations.

For example, in studying a continuous crystallizer, we might postulate a random nucleation mechanism forming new particles at some average rate, a random takeoff mechanism withdrawing particles at some average fractional rate, and a deterministic growth mechanism. What we would hope to learn from the analysis would be how the growth rate and the average nucleation and takeoff rates affect the joint distributions of particle count and size. Many polymerization problems could be studied in an entirely similar way; the particles would be growing radicals, and account would be taken of suitable termination mechanisms.

To take a slightly different example, in studying a flotation cell, we might postulate random feed-takeoff mechanisms for air bubbles and for mineral particles, and a random collision mechanism whereby particles are attached to bubbles. What we would hope to learn would be how the average rates of takeoff, withdrawal, and attachment affect the joint distributions of free particle count and air bubble count and loading. The average rates appearing in the underlying random mechanisms need not of course be constant, but may depend on the particle quality itself, or on associated environmental factors. Thus, a crystal growth rate may well depend on the crystal size as well as on the solute concentration, and in a flotation cell the average rate of attachment of particle to air bubble will likely depend on how heavily the bubble is already loaded.

To ask for the full history of the probability distributions of particle count and quality is, in most cases, to ask for more than we can reasonably expect to get. That is, the technical problems that arise in bridging the gap from a postulated random mechanism to a full knowledge of the probability distributions are often so formidable that we must content ourselves with partial information. Sometimes this partial information is found by simplifying the random mechanisms to the point where more tractable mathematical problems emerge. But more often we are not willing to accept a perhaps oversimplified mechanism, and we look instead for partial information in the form of suitable averages of the underlying random process—means,

variances, covariances. We are particularly willing to settle for this kind of summary information for large populations, where an intuitive reliance on limit theorems leads us to expect that variances will be of the same order of magnitude as means and standard deviations, accordingly, small fractions of the corresponding means.

Also, for large populations, an older point of view asserts itself—that we need not bother explicitly with random mechanisms at all, but may simply describe the macroscopic performance of our systems phenomenologically. From this point of view, we simply introduce plausible rate mechanisms for the processes of interest and embody them in conservation laws for the system properties we are trying to follow. True, we no longer have a hold on the statistical fluctuations of our systems, but we have good reason to believe that these are small anyway. This is, of course, a familiar procedure in the study of conventional transport phenomena, and in our problems, just as in thermodynamic fluctuation theory, we find a very illuminating methodological connection between the phenomenological laws, on the one hand, and the statistical underpinning on the other. The connection is through a kind of repeated averaging on the underlying random process. This averaging, repeated at every instant of time, leads to equations that we may identify with the phenomenological equations; the average rates associated with the underlying random mechanisms appear as the instantaneous phenomenological rates. What comes out of the solution of these equations is not necessarily the true average of the underlying random process, but for large populations it is not usually essentially different, and we are often most willing to settle for it.

Now the bulk of our engineering applications in the study of dispersed systems is in situations where the number of particles is always, in fact, large, and we may ask what in these cases is the point of a probabilistic analysis. The chief technical reason is that from a probabilistic study we may learn just how large a population we really need before we can properly say that deterministic phenomenological equations describe its behavior satisfactorily. This will especially be the case in systems having a certain linear character, where the results of repeated averaging are in fact equal to the true means, no matter what the population size. Here we will often be able to compute variances and see under just what circumstances the standard deviation becomes a sufficiently small fraction of the mean.

In other cases, repeated averaging will not lead precisely to the true means for small populations, and here we will commonly have to rely on semi-intuitive judgments of the population size necessary to reduce variances to a low enough level so that we may properly equate the two after all. In this general connection, we might note that there are situations where statistical fluctuations are important even though the population sizes are large; these large fluctuations turn out, on analysis, to be due to too close a statistical relationship between successive influences on the population, or to be the effects of very rare events, perhaps as arising from an

---

**AUTHORS** *Stanley Katz and Reuel Shinnar are both Professors of Chemical Engineering at The City College, City University of New York. This review was presented at the 34th Chemical Engineering Symposium of the ACS Division of Industrial and Engineering Chemistry held at MIT in December 1967.*

initially small population size. There is every reason to believe that for a vigorous random mechanism operating on populations that are and have been large, statistical fluctuations are in fact unimportant.

Apart from this technical reason for undertaking a probabilistic analysis of a dispersed system with a large number of particles, there is the matter of a certain conceptual convenience in formulating equations for the system behavior. Here we focus on situations where the number of particles is always so large—an emulsion polymerization, for example—that statistical fluctuations in the population as a whole play no role at all. If we wish to study, say, the polymer molecular weight distribution, we might develop the appropriate working equations in terms of macroscopic balances on the population of emulsion particles—introducing instantaneous phenomenological rates for the capture of primary radicals by emulsion particles, and so on.

It would, however, be very natural to interpret the fraction of emulsion particles containing a certain number of growing radicals as the probability that a given particle contains that number of radicals, to interpret the capture rate of primary radicals per particle as the average rate associated with the random arrival of radicals in a given particle, and so on. With this interpretation, we might well find it much more convenient simply to formulate the probability equations for a single emulsion particle than to set up the deterministic equations for the whole population of particles. Especially if the differential equations that arise call for the application of boundary conditions, the form of these boundary conditions might be seen much more clearly from probabilistic considerations. From this point of view, the probability machinery furnishes a conceptual guide to the construction of suitable phenomenological equations, probability distributions for the single particle appearing simply as a shorthand for number fractions over the whole universe of particles.

Now the entire program, as sketched out in the foregoing, has a technical language and a variety of technical methods in terms of which we may try to implement it, and for our purposes, we may take this technical apparatus to be that of Markov processes. It is not that all random processes are Markov, but rather that, allowing full freedom in specifying the states of our systems, we may describe a great many—perhaps all—of our particulate systems in terms of Markov processes. We begin the study of a Markov process by specifying the probabilities of the short-time transitions from one state to another. This specification, which contains the average rates associated with the underlying random mechanism, is summarized in a linear operator on functions of state, the generator of the Markov process.

With the generator in hand, we may set up equations describing the transition probabilities in general, and, in sufficiently simple cases and with luck, proceed to solve them. These transition probabilities, once known, furnish the complete probabilistic description of the system. With them, we may carry forward any initial probability distribution in time, carry out averaging

procedures to find the time history of mean and variance, evaluate two-time probability distributions and the associated covariances, and so on. If we cannot evaluate the transition probabilities in general, we can go back to the equations describing them and try to rework them into simpler, self-contained equations for summary quantities of interest such as means, variances, covariances.

For systems in which we deal always with a large number of particles, we might not be interested in the detailed probability structure, and might prefer instead to set up the repeated averaging procedure noted above, and use it as a guide to the construction of phenomenological equations. These phenomenological equations might of course be derived directly as macroscopic particle balances, but the probabilistic formulation may serve as a useful guide to our physical intuition, and will in any case show directly how the average rates associated with the underlying random mechanisms are to be interpreted as the instantaneous phenomenological rates at which processes transpire.

We may now set down the plan of this review. Following a sketch of the basic mathematical machinery for Markov processes, we set up the repeated averaging procedure noted earlier and show, by way of illustration, how it may be applied to lead to the familiar phenomenological equations for a crystallizer and to a set of perhaps less familiar equations for a mineral flotation cell. Then we illustrate the nature of statistical fluctuations in small populations, in contexts drawn from studies in chemical kinetics and general particle population studies. Following this, we illustrate the nature of some problems arising in particle interactions by way of a familiar model for turbulent mixing. These are the main technical points of this review, and we close with a discussion of the conceptual convenience often found in describing the behavior of particulate systems probabilistically, even when populations are large and deterministic descriptions open to us: this discussion is illustrated by application to an emulsion polymerization study.

It should perhaps be noted that while this review does not contain any new results, neither does it systematically survey the existing literature. It offers instead simply one point of view on the role of probability methods in formulating and studying problems in particulate systems. There are accordingly no formal references made here to the existing literature, but our friends and colleagues will surely recognize how much we have learned from their work, and how freely we have made use of it.

### Markov Processes

We sketch out here, for later reference, the basic mathematical machinery of Markov processes. To keep the ideas as concrete as possible, we restrict ourselves to three special cases: discrete state processes, continuous jump processes, and diffusional processes. These examples do not begin to exhaust the variety of

the chemical processing applications, but they may serve to illustrate adequately the underlying mathematical ideas. Further, we restrict ourselves, this time for conciseness, to stationary Markov processes, that is, those for which the transition probabilities between two states at two times depend only on the time difference. Again, this excludes many applications in which the particle environment is changed systematically with time, but we hope it will be fairly clear how the machinery is to be extended to cover such cases.

By way of introduction to what follows, we may note that our summary of the properties of Markov processes is grounded in the generator,  $\mathcal{G}$ , of the process, and its adjoint  $\mathcal{G}^*$ . Both are linear operators, taking as their domains of operation suitable functions of the state of the process. They appear variously as matrices, as integral operators, or as differential operators, depending on the topology of the state space and the nature of the process. The adjoint operator,  $\mathcal{G}^*$ , appears in the Kolmogorov forward equation. This is the equation describing the history of the single-time probability distribution of the process, and is accordingly the important working equation in most of our applications. The generator  $\mathcal{G}$ , itself, appears in the Kolmogorov backward equation. From the point of view of the mathematical structure of the process, the backward equation plays a more fundamental role than the forward. But in our applications, it appears primarily as the carrier of the method of repeated averaging noted earlier, to be applied to the development of phenomenological equations for the system under study.

We begin now with discrete state processes and let the integer  $i$  serve to index the states; in a typical application,  $i$  might be a particle population count. We shall discuss such processes in some detail, as serving to illustrate the methodology in the simplest context. The underlying random mechanism for such processes we take in the following form: the system, in state  $i$ , will in a short time  $t$  leave it with probability  $\alpha_i t$ ; the system, leaving state  $i$ , will go to state  $j$  with probability  $\beta_{ij}$ —i.e.,  $\alpha_i$  is the average jump rate from state  $i$ , and  $\alpha_i \beta_{ij}$  is the average jump rate from  $i$  to  $j$ . Here,  $\beta_{ii} = 0$  and  $\sum_j \beta_{ij} = 1$ . If we denote the transition probability from  $i$  to  $j$  in time  $t$  by  $p_{ij}(t)$ , we find that we have specified the short-time behavior of  $p_{ij}$ .

$$p_{ij}(t) \sim \begin{cases} 1 - \alpha_i t, & j = i \\ \alpha_i \beta_{ij} t, & j \neq i \end{cases} t \downarrow 0 \quad (1)$$

Equations such as Equation 1 are sometimes written

$$p_{ij}(dt) = \begin{cases} 1 - \alpha_i \cdot dt, & j = i \\ \alpha_i \beta_{ij} \cdot dt, & j \neq i \end{cases}$$

to emphasize the fact that the transition time  $dt$  is short, but we shall not use this convention here.

Now the general behavior of the transition probabilities of a Markov process is regulated by the Chapman-Kolmogorov equation

$$p_{ij}(t+s) = \sum_k p_{ik}(t)p_{kj}(s); \quad t, s \geq 0 \quad (2)$$

which describes the independence of past and future characterizing such processes. To find the general behavior of the system, we would want to solve the Chapman equation, Equation 2, subject to the short-time condition, Equation 1. This task is facilitated by developing differential equations in the  $p_{ij}$  from Equation 2. We begin by letting  $s \downarrow 0$  in Equation 2—small last step—and applying Equation 1. What emerges is

$$\frac{dp_{ij}(t)}{dt} = -p_{ij}(t)\alpha_j + \sum_k p_{ik}(t)\alpha_k\beta_{kj} \quad (3)$$

i.e., Kolmogorov's forward equation (the familiar Fokker-Planck equation) in the transition probabilities. The short-time behavior, Equation 1, is subsumed in the coefficients of Equation 3 and gives rise also to the initial condition

$$p_{ij}(0) = \delta_{ij} \quad (4)$$

A perhaps less familiar equation in the transition probabilities is found by letting  $t \downarrow 0$  in Equation 2—small first step—and applying Equation 1. This leads to Kolmogorov's backward equation

$$\frac{dp_{ij}(s)}{ds} = -\alpha_i p_{ij}(s) + \alpha_i \sum_k \beta_{ik} p_{kj}(s) \quad (5)$$

together with the initial condition Equation 4.

The structure of the forward and backward equations emerges a little more clearly if we recognize their right-hand sides as matrix products. If we introduce the matrix elements

$$g_{ij} = \begin{cases} -\alpha_i; & j = i \\ \alpha_i \beta_{ij}; & j \neq i \end{cases}$$

so that the short-time transition probabilities, Equation 1, may be written

$$p_{ij}(t) \sim \delta_{ij} + g_{ij}t; \quad t \downarrow 0$$

then the forward equation, Equation 3, becomes

$$\frac{dp_{ij}(t)}{dt} = \sum_k p_{ik}(t)g_{kj} \quad (6)$$

and the backward equation, Equation 5, becomes

$$\frac{dp_{ij}(t)}{dt} = \sum_k g_{ik} p_{kj}(t) \quad (7)$$

The matrix

$$\mathcal{G} = (g_{ij})$$

is the generator of the Markov process. It serves as a linear operator on functions of state, that is, on vectors  $u_i$ . We might illuminate the central role of the generator by noting that the forward or backward equations, together with the initial condition, Equation 4, have the formal matrix solution

$$p_{ij}(t) = (e^{\mathcal{G}t})_{ij}$$

The generator also appears in a natural way in the evaluation of conditional means (conditional expectations) of functions of state. If we take an initial vector

$u_i(0)$  and form its conditional expectation at a later time  $t$

$$u_i(t) = \sum_j p_{ij}(t)u_j(0)$$

we find from the backward equation, Equation 7, that this conditional expectation satisfies

$$\frac{du_i}{dt} = \sum_k g_{ik}u_k = (\mathcal{G}u)_i \quad (8)$$

The differential equation, Equation 8, will, with suitable choice of vectors  $u_i$ , serve as the basis for the method of repeated averaging to be discussed below. Since  $\sum_k g_{ik} = 0$ , we see that  $\mathcal{G}u$ , or rather  $u + \mathcal{G}u$ , is of the nature of a smoothed version of  $u$ , so that a solution of Equation 8 really represents a kind of continued smoothing.

If, leaving conditional expectations apart, we wish to study directly the evolution of an initial probability distribution in time, we turn to the forward equation. An initial probability distribution  $v_j(0)$  develops at a later time  $t$  into

$$v_j(t) = \sum_i v_i(0)p_{ij}(t)$$

and we see from Equation 6 that this distribution satisfies

$$\frac{dv_j}{dt} = \sum_k v_k g_{kj} = (\mathcal{G}^*v)_j \quad (9)$$

As a matrix,  $\mathcal{G}^*$  is simply the transpose of  $\mathcal{G}$ . As an operator,  $\mathcal{G}^*$  is adjoint to  $\mathcal{G}$  in the sense that

$$\sum_i v_i(\mathcal{G}u)_i = \sum_j (\mathcal{G}^*v)_j u_j$$

for any vectors  $u, v$ .

It might be noted that Equation 9 is just of the form of the forward equation, Equation 6, and Equation 8 is just of the form of the backward equation, Equation 7. Accordingly, if we could find analytical solutions of either of them that were general enough to satisfy the different initial conditions, we would have in hand the complete probabilistic picture of the process. The applications being as complicated as they are, we very rarely succeed in doing this. Instead, we try to distill from Equation 9 simpler equations for summary properties of the distribution  $v_j$ , such as the leading moments, and only infrequently compute a detailed distribution. Alternatively, we go over to the phenomenological point of view and look for suitable vectors  $u_i$  which, taken to Equation 8, will form a tractable self-contained set of equations in what we may hopefully interpret as mean values of quantities of interest. In this connection, we may note that the mean value of a vector  $u$

$$\langle u \rangle = \sum_k v_k u_k$$

where  $v_k$  is the single-time probability distribution, satisfies, according to Equation 9, the differential equation

$$\frac{d\langle u \rangle}{dt} = \sum_k v_k \sum_j g_{kj} u_j = \langle \mathcal{G}u \rangle$$

This is not quite the backward equation, Equation 8, but if  $\mathcal{G}$  has an appropriately simple character, we may find that the mean values of suitable vectors  $u$  satisfy something very much like the backward equation, and, in fact, turn out to be equal to the corresponding conditional expectations.

This concludes our discussion of discrete state processes. We turn next to a brief sketch of continuous jump processes. We restrict for convenience to one dimension and let  $x$  serve as the index of states. An application of these jump processes will appear below in the discussion of a familiar method for agglomerative mixing. The underlying random mechanism for such processes we take in the following form: the system, in state  $x$ , will in a short time  $t$  make a jump with probability  $\alpha(x)t$ ; the system, leaving state  $x$ , will jump to the interval  $y, y + dy$  with probability  $\beta(x,y)dy$ ; the system, between jumps, will change state continuously according to the differential equation  $dx/dt = f(x)$ . That is,  $f(x)$  is the translation rate at state  $x$ ,  $\alpha(x)$  is the average jump rate from state  $x$ , and  $\alpha(x)\beta(x,y)$  is the average jump rate density from  $x$  to  $y$ . Here,  $\int \beta(x,y)dy = 1$ . If we denote the transition probability density from  $x$  to  $y$  in time  $t$  by  $p(x,y;t)$ , we find that we have specified the short-time behavior of  $p$  in the form

$$p(x,y;t) \sim [1 - t\alpha(x)]\delta[y - x - tf(x)] + t\alpha(x)\beta(x,y); \quad t \downarrow 0$$

The Chapman-Kolmogorov equation, here appearing as,

$$p(x,y;t+s) = \int p(x,z;t)p(z,y;s)dz \quad (10)$$

then leads, as for discrete processes, to a forward equation

$$\frac{\partial p(x,y;t)}{\partial t} = -\frac{\partial}{\partial y} \{p(x,y;t)f(y)\} - p(x,y;t)\alpha(y) + \int p(x,z;t)\alpha(z)\beta(z,y)dz \quad (11)$$

and to a backward equation

$$\frac{\partial p(x,y;t)}{\partial t} = f(x)\frac{\partial p(x,y;t)}{\partial x} - \alpha(x)p(x,y;t) + \alpha(x)\int \beta(x,z)p(z,y;t)dz \quad (12)$$

together with the initial condition

$$p(x,y;0) = \delta(y - x) \quad (13)$$

From Equations 11 and 12, we may extract, as before, the generator  $\mathcal{G}$  and its adjoint

$$(\mathcal{G}u)(x) = f(x)\frac{du(x)}{dx} - \alpha(x)u(x) + \alpha(x)\int \beta(x,z)u(z)dz \quad (14)$$

$$(\mathcal{G}^*v)(y) = -\frac{d}{dy} [v(y)f(y)] - v(y)\alpha(y) + \int v(z)\alpha(z)\beta(z,y)dz \quad (15)$$

Here  $\mathcal{G}^*$  is adjoint to  $\mathcal{G}$  in the sense that

$$\int v(x)(\mathcal{G}u)(x)dx = \int (\mathcal{G}^*v)(y)u(y)dy \quad (16)$$

With  $\mathcal{G}^*$ , we may follow the evolution in time of an initial probability density  $v(y; 0)$ . This density evolves in a time  $t$  into

$$v(y; t) = \int v(x; 0) p(x, y; t) dx \quad (17)$$

which, according to the forward equation, Equation 11, satisfies

$$\frac{\partial v}{\partial t} = \mathcal{G}^* v \quad (18)$$

With  $\mathcal{G}$ , we may follow the conditional expectation of an initial vector  $u(x; 0)$ . This conditional expectation is

$$u(x; t) = \int p(x, y; t) u(y; 0) dy \quad (19)$$

and, according to the backward equation, Equation 12, satisfies

$$\frac{\partial u}{\partial t} = \mathcal{G} u \quad (20)$$

The use of Equations 18 and 20 in the applications follows that of the corresponding equations, Equations 9 and 8, developed for discrete processes, and the discussion made there applies here as well.

This concludes our sketch of jump processes, and we turn finally to diffusional processes. Again, we restrict ourselves, for convenience, to one dimension and let  $x$  serve as the index of states. Here, we characterize the underlying random mechanism for the process by thinking of the system as being continuously shocked in such a way that a jump from  $x$  in a short time  $t$  has mean  $f(x)t$  and mean square  $k^2(x)t$ . That is, we take the transition probability density  $p(x, y; t)$  from  $x$  to  $y$  in time  $t$  to have the short-time behavior

$$\left\{ \begin{array}{l} \int (y-x) p(x, y; t) dy \sim f(x)t \\ \int (y-x)^2 p(x, y; t) dy \sim k^2(x)t \end{array} \right\} \downarrow 0 \quad (21)$$

A model for such a process may be formed in a way familiar from Brownian motion studies by taking

$$\frac{dx}{dt} = f(x) + k(x)w(t)$$

where  $w$  is a white noise with unit spectral density, that is to say, where

$$\langle w(t) \rangle = 0, \quad \langle w(t)w(t+s) \rangle = \delta(s)$$

the pointed brackets denoting mean values. Other models will appear below in connection with population size problems.

The Chapman-Kolmogorov equation has the standard one-dimensional form, Equation 10, and we may recover from it, by consulting the short-time behavior, Equation 21, a forward equation in  $p$

$$\frac{\partial p(x, y; t)}{\partial t} = - \frac{\partial}{\partial y} [p(x, y; t)f(y)] + \frac{1}{2} \frac{\partial^2}{\partial y^2} [p(x, y; t)k^2(y)] \quad (22)$$

and a backward equation

$$\frac{\partial p(x, y; t)}{\partial t} = f(x) \frac{\partial p(x, y; t)}{\partial x} + \frac{1}{2} k^2(x) \frac{\partial^2 p(x, y; t)}{\partial x^2} \quad (23)$$

together with the standard initial condition, Equation 13. We may accordingly recognize the generator  $\mathcal{G}$  and its adjoint as

$$(\mathcal{G}u)(x) = f(x) \frac{du(x)}{dx} + \frac{1}{2} k^2(x) \frac{d^2u(x)}{dx^2} \quad (24)$$

$$(\mathcal{G}^*v)(y) = - \frac{d}{dy} [v(y)f(y)] + \frac{1}{2} \frac{d^2}{dy^2} [v(y)k^2(y)] \quad (25)$$

where  $\mathcal{G}^*$  is adjoint to  $\mathcal{G}$  in the familiar one-dimensional sense of Equation 16. With  $\mathcal{G}$  and  $\mathcal{G}^*$  in hand, we may develop working equations for probability densities and conditional expectations just as before. Thus, a density,  $v$ , defined according to Equation 17, satisfies a forward equation, Equation 18, while a conditional expectation  $u$ , defined according to Equation 19, satisfies a backward equation, Equation 20.

With diffusional processes, the question of boundary conditions comes up, as indeed it may also for the translational aspects of the continuous jump processes. The general guide here seems to be that if a transition into a forbidden zone is possible, it must be guarded against by imposing a suitable condition at the zone boundary. Consider, for illustration, a population problem modeled diffusively, where we wish to forbid transitions to negative population size  $x$ . It would be natural to impose on the transition probability density  $p(x, y; t)$  the boundary condition

$$\frac{\partial p(x, y; t)}{\partial x} = 0; \quad x = 0 \quad (26)$$

drawn from the behavior of a reflecting barrier in a random walk. This would amount to attaching the boundary condition

$$\frac{du(x)}{dx} = 0; \quad x = 0 \quad (27)$$

to the definition, Equation 24, of the generator, and accordingly the boundary condition

$$v(y)f(y) - \frac{1}{2} \frac{d}{dy} [v(y)k^2(y)] = 0; \quad y = 0 \quad (28)$$

to the definition, Equation 25, of its adjoint. This last amounts to saying that the transition probability density  $p$  also satisfies the boundary condition

$$p(x, y; t)f(y) - \frac{1}{2} \frac{\partial}{\partial y} [p(x, y; t)k^2(y)] = 0; \quad y = 0 \quad (29)$$

The boundary condition, Equation 29, would have to be attached to the forward equation, Equation 22, in the transition probability density, and the condition, Equation 26, to the backward equation, Equation 23. Similarly, the boundary condition, Equation 27, would have to be attached to the working backward equation, Equation 20, for conditional expectations, and the condi-

tion, Equation 28, attached to the working forward equation, Equation 18, for probability densities. Indeed, the condition, Equation 28, turns out to be just what is needed to preserve the normalization of  $v$  in Equation 18.

### Repeated Averaging

We discuss here the construction of phenomenological equations associated with a Markov process. In a macroscopic view of the process, these are deterministic conservation equations in quantities of interest. From the point of view of the underlying random structure, they are equations in suitable conditional expectations. The generator of the Markov process, which we have seen above to be of the nature of a smoothing operator, will accordingly play a central role in the development, and since the phenomenological equations will be of the general form of Equation 20, we see that what is involved in their solution is really a kind of continued averaging. Our task here will be to develop these phenomenological equations from the Markov process, discuss them as macroscopic conservation equations, and see how the elementary average rates of random change subsumed in the generator are interpreted macroscopically as instantaneous deterministic rates of change in the system.

To illustrate the ideas as concretely as may be, we proceed by example, considering first a crystallizer with random formation and discharge of particles together with deterministic growth of existing particles, and second a mineral flotation cell with random attachment of particles to vacant sites on air bubbles. It will emerge from the discussion that the conditional expectations appearing in the phenomenological equations will sometimes be precisely equal to the true mean values, sometimes not—as an engineering matter, this seems to depend on whether the particles in the system interact or not. We will, however, argue on semi-intuitive grounds that even when the two are not equal, they become approximately equal for populations that are and remain large. Indeed our argument will be that in such cases, variances and covariances become small, distributions become singular, and the processes involved become essentially deterministic. However, to illustrate the uncertain character of this reasoning, we discuss briefly some problems in population size, too simple to be of any engineering interest, but which show that this method of repeated averaging may falsify essential features of the system behavior even when the populations are large.

**Crystallizer.** We turn now to a consideration of the crystallizer. We consider a mixed continuous crystallizer with clear feed, and, for convenience, take the chemical environment to be constant. The underlying random mechanism of the process we take in the following form: in a short time,  $t$ , a new particle, of vanishingly small size, will be formed with probability  $Bt$ ; in a short time,  $t$ , any given particle will be discharged with probability  $Dt$ ; a particle of size  $x$  in the system at the rate  $dx/dt = G(x)$ . If we describe the sta-

system at any moment by the number  $m$  of particles present, together with their sizes  $x_1, x_2, \dots, x_m$  (say, oldest first), we see that we have specified the short-time behavior of the transition probability  $p(mx_1 \dots x_m, ny_1 \dots y_n; t)$  from state  $m, x_1, \dots, x_m$  to state  $n, y_1, \dots, y_n$ . Taking  $p$  to be a probability in  $n$  jointly with a probability density in  $y_1, y_2, \dots, y_n$ , we may write:

$$p(mx_1 \dots x_m, ny_1 \dots y_n; t) \sim \\ Bt \delta_{n,m+1} \delta(y_1 - x_1) \dots \delta(y_m - x_m) \delta(y_{m+1}) + \\ Dt \sum_{j=1}^m \delta_{n,m-1} \delta(y_1 - x_1) \dots \delta(y_{j-1} - x_{j-1}) \times \\ \delta(y_j - x_{j+1}) \dots \delta(y_{m-1} - x_m) + [1 - (B + mD)t] \delta_{nm} \times \\ \delta[y_1 - x_1 - G(x_1)t] \dots \delta[y_m - x_m - G(x_m)t]; \quad t \downarrow 0$$

Now all this represents a rather more complicated situation than in any of the Markov processes sketched out earlier. Still, we may apply the same basic machinery, and extract from it a knowledge of the generator  $\mathcal{G}$  for the process in hand. We find

$$(\mathcal{G}u)(mx_1 \dots x_m) = \sum_{j=1}^m G(x_j) \times \\ \frac{\partial u(mx_1 \dots x_m)}{\partial x_j} + Bu(m+1, x_1 \dots x_m, 0) + \\ D \sum_{j=1}^m u(m-1, x_1 \dots x_{j-1} x_{j+1} \dots x_m) - \\ (B + mD)u(mx_1 \dots x_m) \quad (30)$$

With  $\mathcal{G}$  in hand, we are ready, in principle, to set up and try to solve the equations for the underlying probability distributions. Or, turning aside from such an ambitious effort, we may look instead for suitable functions of the system state—i.e., of  $mx_1 \dots x_m$ , for which we may construct self-contained phenomenological equations of the form of Equation 20. A natural function of this kind is the number distribution of crystal sizes in the system:

$$F(x) = \sum_{j=1}^m \Delta(x - x_j) \quad (31)$$

where  $\Delta$  is the Heaviside unit step function. Applying Equation 30, we find that

$$(\mathcal{G}F)(x) = -G(x) \frac{dF(x)}{dx} - DF(x) + B\Delta(x)$$

so that the conditional expectation of Equation 31—we may denote this  $F(x,t)$ —satisfies

$$\frac{\partial F}{\partial t} = -G(x) \frac{\partial F}{\partial x} - DF + B\Delta(x)$$

Finally, introducing in place of the number distribution  $F$  its density  $f = \partial F / \partial x$ , we find the more familiar equation

$$\frac{\partial f}{\partial t} + \frac{\partial}{\partial x} [G(x) \cdot f] = B \cdot \delta(x) - D \cdot f \quad (32)$$

Indeed, Equation 32 is of the usual form of the phenomenological equation for a continuous mixed

crystallizer, and if we interpret  $fdx$  as the number of crystals per unit working volume with sizes in the range,  $x, x + dx$ , we may identify  $B$  as the rate of nucleus formation per unit volume and  $1/D$  as the nominal residence time in the crystallizer. Now Equation 32 has been developed for a conditional expectation, not for a true mean value based on how the underlying probability distributions evolve in time. In this case, a calculation will show that the true mean value satisfies the same differential equation, although this would no longer be so if we introduced particle interactions, say by way of a supersaturation-dependent crystal growth rate, and the associated solute balance. But here, with the mean number density,  $f$ , of crystal sizes satisfying Equation 32, we may confidently expect that for large crystal populations, there will be no appreciable statistical fluctuations in  $f$ , and accordingly that Equation 32, viewed as a deterministic phenomenological equation, will, in fact, give a satisfactory complete description of the process. (The fluctuations to be expected in over-all particle count will be discussed in the next section of this review.) However, while we may be very willing to use analogous equations in more difficult cases, we should bear in mind that they will not necessarily describe the true mean values of interest, but only related conditional expectations.

**Flotation cell.** This concludes our discussion of the crystallizer, and we turn next to a consideration of a mineral flotation cell. We consider, for convenience, a simple experimental situation: a mixed batch cell with particles all of one size and an equal likelihood of attachment to a vacant site on an air bubble, the bubbles themselves being well mixed throughout the working volume. We may accordingly describe the random mechanism underlying the process as follows: in a short time  $t$ , a bubble, particle-free, will be introduced with probability  $Bt$ ; in a short time,  $t$ , any given bubble, with its particle loading, will be discharged with probability  $Dt$ ; in a short time,  $t$ , any given particle will attach itself to any given bubble already carrying  $n$  particles with probability  $A_n t$ , where  $n$  may be 0, 1, 2, etc. If we describe the state of the system at any moment by the number,  $u$ , of free particles present together with the numbers  $x_0, x_1, x_2$ , etc., of bubbles carrying 0, 1, 2 particles, etc., we see that we have specified the short-time behavior of the transition probability  $p(ux_0x_1 \dots, y_0y_1 \dots; t)$  from state  $u, x_0, x_1, \dots$  to state  $v, y_0, y_1, \dots$ :

$$p(ux_0x_1 \dots, y_0y_1 \dots; t) \sim Bt \delta_{vu} \delta_{y_0x_0} \prod_{m \neq 0} \delta_{y_m, x_m} + \sum_n Dx_n t \cdot \delta_{v, u-1} \delta_{y_n, x_n-1} \prod_{m \neq n} \delta_{y_m, x_m} + \sum_n A_n ux_n t \cdot \delta_{v, u+1} \delta_{y_n, x_n+1} \prod_{m \neq n, n+1} \delta_{y_m, x_m} + \{1 - (B + \sum_n Dx_n + \sum_n A_n ux_n)t\} \delta_{vu} \prod_m \delta_{y_m, x_m}; \quad t \downarrow 0$$

Now the variables of state  $u, x_n$ , are integers, so that we have here a multidimensional version of the discrete state process of Equations 1 through 9. We may accordingly recover, as there, the generator of the process in the form:

$$\begin{aligned} (\mathcal{G}\phi)(ux_0x_1x_2 \dots) = & B \cdot \phi(u, x_0 + 1, x_1, x_2 \dots) + \\ & Dx_0 \cdot \phi(u, x_0 - 1, x_1, x_2 \dots) + Dx_1 \phi(u, x_0, x_1 - 1, x_2 \dots) + \\ & \dots + A_0 ux_0 \phi(u - 1, x_0 - 1, x_1 + 1, x_2 \dots) + \\ & A_1 ux_1 \phi(u - 1, x_0, x_1 - 1, x_2 + 1 \dots) + \dots - \\ & (B + \sum_n Dx_n + \sum_n A_n ux_n) \phi(ux_0x_1x_2 \dots) \quad (33) \end{aligned}$$

With  $\mathcal{G}$  in hand, we are ready, in principle, to try for the whole probability history of the flotation process. However, the interaction between particles and bubbles makes this an especially ambitious task, and we turn instead, as for the crystallizer, to the search for suitable functions of state whose conditional expectations will satisfy self-contained sets of equations of the form of Equation 20, here taken in the representation, Equation 8. The state variables themselves are such functions, and bringing  $u, x_0, x_1, x_2, \dots$  in turn to Equation 33, we find

$$\left\{ \begin{aligned} \frac{du}{dt} &= - \sum_n A_n ux_n \\ \frac{dx_0}{dt} &= B - Dx_0 - A_0 ux_0 \\ \frac{dx_n}{dt} &= -Dx_n + A_{n-1} ux_{n-1} - A_n ux_n; \quad n \neq 0 \end{aligned} \right. \quad (34)$$

We may readily identify Equation 34 as a set of phenomenological equations for the performance of the flotation cell. If we interpret the variables per unit working volume, so that  $u$  is the number density of free particles in the cell and  $x_n$  the number density of bubbles carrying  $n$  particles, then we may interpret the  $A_n$  as rate constants for the attachment of particles to bubbles,  $B$  as a feed rate of bubbles, and  $1/D$  as the average residence time of bubbles in the cell. It should be noted here that the actual mean values of the quantities  $u, x_n$  as the underlying probability distributions evolve in time do not satisfy these phenomenological equations, as the analogous mean values do for the crystallizer—the bubble-particle interactions stand in the way. Indeed, an attempt to construct working equations for the true mean values (we denote them here by pointed brackets) leads to

$$\left\{ \begin{aligned} \frac{d\langle u \rangle}{dt} &= - \sum_n A_n \langle ux_n \rangle \\ \frac{d\langle x_0 \rangle}{dt} &= B - D\langle x_0 \rangle - A_0 \langle ux_0 \rangle \\ \frac{d\langle x_n \rangle}{dt} &= -D\langle x_n \rangle + A_{n-1} \langle ux_{n-1} \rangle - A_n \langle ux_n \rangle; \quad n \neq 0 \end{aligned} \right.$$

These differ from the phenomenological Equations 34 only in that their right-hand sides involve mean values of products,  $\langle ux_n \rangle$ , rather than products of mean values,  $\langle u \rangle \langle x_n \rangle$ . Now  $\langle ux_n \rangle$  differs from  $\langle u \rangle \langle x_n \rangle$  just by the covariance between  $u$  and  $x_n$ , and this covariance is bounded in absolute value by the product of the standard deviations of  $u$  and  $x_n$ . Accordingly, if the appro-

appropriate populations are large, so that the standard deviations are small fractions of the corresponding means, the mean values  $\langle ux_n \rangle$  become approximately equal to the products  $\langle u \rangle \langle x_n \rangle$ , and we may not only confidently identify the conditional expectations in Equations 34 with the true mean values, but also argue that, the statistical fluctuations being negligible, the deterministic phenomenological Equations 34 give an essentially complete description of the process.

The approximate equality of  $\langle ux_n \rangle$  with  $\langle u \rangle \langle x_n \rangle$  for large populations may be described as a kind of asymptotic orthogonality of the random quantities  $u$  and  $x_n$ , and the verbal arguments we have just made represent an attempt to deal on intuitive grounds with the mathematical question of specifying the conditions under which  $u$  and  $x_n$  will be approximately orthogonal. This is a characteristic question in the study of systems of interacting particles, and we shall return to it, in a somewhat sharpened form, where the issue is independence rather than simple orthogonality, in a later section of this review.

This concludes our discussion of the flotation cell, and we turn finally to two simple examples of population growth which show some of the pitfalls in the use of this method of repeated averaging.

**Examples of population growth.** We consider first a linear birth process where, in a short time  $t$ , a population of size  $i$  jumps to size  $i + 1$  with probability  $Bit$ . If we characterize the state of the system at any moment by its population size, then the machinery of the discrete states processes (Equations 1 through 9) applies directly. We find

$$p_{ij}(t) \sim Bit \delta_{j,i+1} + (1 - Bit) \delta_{ji}; \quad t \downarrow 0$$

so that

$$(\mathcal{G}u)_i = Bi(u_{i+1} - u_i) \quad (35)$$

Taking for  $u_i$  the population size  $i$  itself, we find according to Equation 8 that its conditional expectation satisfies

$$\frac{di}{dt} = Bi \quad (36)$$

This is of the expected exponential form, and we have no hesitation in identifying it as a phenomenological equation in the deterministic population size,  $i$ . Further, a straightforward calculation shows that the actual mean value of the random population size, as the underlying distribution evolves in time, satisfies just this same equation, Equation 36.

So far, so good, but if we consider instead a quadratic birth process, where, in a short time  $t$ , the population size jumps from  $i$  to  $i + 1$  with probability  $Bi^2t$  something much more dramatic happens. Formally, the machinery works as before. We find

$$(\mathcal{G}u)_i = Bi^2(u_{i+1} - u_i)$$

and, taking for  $u_i$  the population size  $i$  itself, we see from Equation 8 that its conditional expectation satisfies

$$\frac{di}{dt} = Bi^2 \quad (37)$$

Again, we would not hesitate to identify this as a phenomenological equation in the deterministic population size,  $i$ . But now the conditional expectation behaves rather differently from the true mean value of the underlying random birth process. The conditional expectation equation, Equation 37, starting from an initial population size  $i_0$ , has the solution

$$i = \frac{i_0}{1 - Bi_0 t}$$

Thus, according to Equation 37, the population grows hyperbolically, exploding at the time  $t = 1/Bi_0$ . Now this is a very short time if  $i_0$  is large, but a careful analysis of the underlying random process, nevertheless, shows a finite probability of having an infinite number of births in every time interval. Consequently, right from the outset, there is a finite probability of having an infinite population, and the true mean population size is infinite. Before taking too seriously the practical implications of this divergence between conditional expectation and true mean, we should note that this is a very unrealistic example, and that suitable constraints on the birth process, designed to mitigate its explosive behavior, would likely serve also to bring the conditional expectation of population more into line with its true mean.

### Small Populations

We present here three examples to illustrate the nature of the statistical fluctuations to be expected in small populations. One is of a first-order decay process, and may be taken to apply to first-order chemical kinetics or to simple radioactive decay. Another is the linear birth process that was discussed briefly in the preceding section. The last is of a combined birth and death process and may apply to a study of particle populations in a mixed vessel, or perhaps to growing radical populations in an emulsion particle.

We turn accordingly to the first-order decay process, where, in a particle population, any given particle disappears in a short time  $t$  with probability  $Dt$ . We may interpret  $D$  as a radioactive decay constant, or as a first-order chemical rate constant. The size  $i$  may be taken to index the state of the process, and the machinery of the discrete state processes sketched in Equations 1 through 9 applies directly. We have the generator in the form

$$\begin{cases} (\mathcal{G}u)_0 = 0 \\ (\mathcal{G}u)_i = Di(u_{i-1} - u_i); \quad i \neq 0 \end{cases} \quad (38)$$

and its adjoint

$$(\mathcal{G}^*v)_j = -Djv_j + D(j+1)v_{j+1}$$

We may accordingly set up the forward and backward equations (Equations 3 and 5) for the transition probabilities  $p_{ij}$ , and see that they have the solution in simple binomial form



$$p_{i,j}(t) = \begin{cases} \binom{i}{j} (e^{-Dt})^j (1 - e^{-Dt})^{i-j}; & j = 0, 1, 2, \dots, i \\ 0; & j = i + 1, i + 2, \dots \end{cases} \quad (39)$$

From Equation 39, we may follow the probability history of any initial population. If we take a population initially of size  $N$ , so that its initial probability distribution is

$$v_j(0) = \delta_{jN}$$

we may see that it evolves into

$$v_j(t) = \binom{N}{j} (e^{-Dt})^j (1 - e^{-Dt})^{N-j} \quad (40)$$

satisfying a forward equation

$$\frac{dv_j}{dt} = -Djv_j + D(j+1)v_{j+1} \quad (41)$$

of the form of Equation 9. From Equation 40, we find the mean population size to be

$$\mu = Ne^{-Dt}$$

This satisfies the differential equation

$$\frac{d\mu}{dt} = -D\mu$$

which may indeed also be developed directly from Equation 41. We see, incidentally, on consulting Equations 38 and 8, that the conditional expectation of the population size also satisfies just this differential equation, so that the method of repeated averaging would give us the true mean for this process, although this would not necessarily be true for more complicated decay mechanisms.

We may also calculate the variance  $\sigma^2$  of a population initially of size  $N$ —either directly from Equation 40, or by developing a differential equation in  $\sigma^2$  from Equation 41. We find in any case

$$\sigma^2 = Ne^{-Dt}(1 - e^{-Dt})$$

and from this we may infer something about the statistical fluctuations in population size. We see, for example, that

$$\frac{\sigma}{N} = \sqrt{\frac{e^{-Dt}(1 - e^{-Dt})}{N}}$$

is uniformly small for large  $N$ , so that the fluctuations in an initially large population are always small compared to the initial size. More revealing is the ratio

$$\frac{\sigma}{\mu} = \sqrt{\frac{e^{Dt} - 1}{N}}$$

This increases exponentially with  $t$  no matter what the size of  $N$ , but for large  $t$  it behaves as follows:

$$\frac{\sigma}{\mu} \sim \frac{1}{\sqrt{N}}; \quad t \uparrow \infty$$

Thus, the ratio  $\sigma/\mu$  is asymptotically independent of the initial population size  $N$ , depending only on the decreasing mean,  $\mu$ ; as long as  $\mu$  remains sizable, the relative fluctuations will be correspondingly small.

Finally, with the transition probabilities, Equation 39, and the single-time probability distribution, Equation 40, in hand, we can readily assemble the joint distribution of the population sizes at the two times  $t, t + s$ . The results are not worth quoting in any detail, but we may, by way of illustration, give the correlation coefficient between the two populations. For an aged system—large  $t$ —this turns out to be simply  $e^{-Ds/2}$ .

This concludes our discussion of the first-order decay process, and we turn next to the linear birth process. This process was discussed briefly in the preceding section of this review; with birth rate  $B$  and population size  $i$ , it has the generator Equation 35. We shall not describe this process in as great detail as the first-order decay, but simply quote some key results on means and variances that seem to cast some light on the role of a continually large population size in ensuring that statistical fluctuations stay small. These results are all readily derivable by straightforward calculation from the discrete process machinery of Equations 1 through 9. We have, for a population initially of size  $N$ , that the growing population size has mean

$$\mu = Ne^{Bt}$$

and variance

$$\sigma^2 = Ne^{2Bt}(1 - e^{-Bt})$$

so that

$$\frac{\sigma}{\mu} = \sqrt{\frac{1 - e^{-Bt}}{N}}$$

For large  $t$ ,  $\sigma/\mu$  becomes simply  $1/\sqrt{N}$ , and two points emerge. The first is that if the population is initially large, and hence always large, the statistical fluctuations are, as we expect, small compared to the mean. The second, and more surprising, is that if the population is initially small, say  $N = 1$ , the fluctuations are of the same order of magnitude as the mean, even though the mean itself increases without bound as time progresses.

To mitigate this surprise, we should, however, note that while these large fluctuations might be expected in, say, a particle break-up process (and of course biological processes of various kinds), they would not arise in a process whereby new particles are formed, or appear, at a rate independent of the population size. If we take, as in a Poisson process, a new particle to appear in a short time  $t$  with probability  $Bt$ , and, as before, index the population size on  $i$ , we find for the generator

$$(G_u)_t = B \cdot (u_{i+1} - u_i)$$

in contrast with Equation 35. Calculations of mean and variance, for a population initially of size 0, then lead to

$$\mu = \sigma^2 = Bt$$

so that

$$\frac{\sigma}{\mu} = \frac{1}{\sqrt{\mu}}$$

which becomes quite satisfactorily small as soon as  $\mu$  reaches a sizable value.

At this point we might mention one well-known physical example for a process involving large numbers which shows significant statistical fluctuations. Consider again a crystallization, but now let us assume that we are dealing with a case where primary homogeneous formation of nuclei is a very rare event. In the presence of crystals, most of the nucleation will be secondary nucleation due to break-off of dendritic growth on the surface of a growing crystal. A melt or a solution might be heavily undercooled before the first crystal appears, but once it appears, nucleation and formation of new particles are almost explosive and may lead to almost instantaneous solidification of the melt. While the final number of crystals is large, the total number of crystals will show significant fluctuations with time as the experiment is repeated.

This concludes our discussion of the linear birth process, and we turn finally to our particle birth and death process. We describe the underlying random mechanism of the process as follows: in a short time,  $t$ , a new particle appears with probability  $Bt$ ; in a short time,  $t$ , any given existing particle disappears with probability  $Dt$ . For a particle population problem in a mixed vessel, we might interpret  $B$  as the particle feed or production rate, and  $1/D$  as the mean residence time of particles in the vessel. In the context of an emulsion polymerization, where we study the population of growing radicals,  $B$  might be the arrival rate of primary radicals in an emulsion particle, and  $D$  a rate constant for the escape or spontaneous termination of growing radicals. As before, the population size,  $i$ , may be taken to index the state of the process, and the machinery of the discrete state process sketched in Equations 1 through 9 applies directly. The transition probability  $p_{ij}(t)$  has the short-time behavior:

$$p_{ij}(t) \sim Bt \delta_{j,i+1} + Dit \delta_{j,i-1} + (1 - Bt - Dit)\delta_{ji}; \quad t \downarrow 0 \quad (42)$$

and we may recover the generator of the process in the form

$$(\mathcal{G}u)_i = B \cdot (u_{i+1} - u_i) + Di(u_{i-1} - u_i) \quad (43)$$

and its adjoint as

$$\begin{cases} (\mathcal{G}^*v)_0 = -Bv_0 + Dv_1 \\ (\mathcal{G}^*v)_j = B(v_{j-1} - v_j) + D(j+1)v_{j+1} - D_jv_j; \\ j \neq 0 \end{cases} \quad (44)$$

We shall quote here only a few illustrative results readily derivable from Equations 43 and 44. The probability distribution  $v_j$  of the population size, once the process has settled down into a state of statistical

equilibrium, satisfies, according to Equation 9, the equation

$$(\mathcal{G}^*v)_j = 0$$

and is seen to be of the familiar Poisson form

$$v_j = e^{-B/D} \frac{(B/D)^j}{j!}$$

This has mean  $\mu$  and variance  $\sigma^2$  both equal to  $B/D$ , so that

$$\frac{\sigma}{\mu} = \frac{1}{\sqrt{\mu}}$$

and we may accordingly expect that small populations will exhibit pronounced fluctuations about their means. The conditional expectation of the population size, as computed from Equation 5, will incidentally be equal to the true mean,  $\mu$ , for this process—although this would not necessarily be true for more complicated particle disappearance mechanisms. Finally, we may derive from the forward equations, Equation 3 or 6, in the transition probabilities differential equations in the lagged covariances for this process, and find, for example, that at statistical equilibrium the correlation coefficient between the population sizes at times  $t$  and  $t+s$  is just  $e^{-Ds}$ , entirely independent of  $B$ .

We might also note here that birth and death processes of this kind can also usefully be modeled in terms of the diffusional processes sketched in Equations 21 through 29. From the short-time transition probability behavior, Equation 42, we may see that

$$\left. \begin{aligned} \langle j-i \rangle &\sim (B-Di)t \\ \langle (j-i)^2 \rangle &\sim (B+Di)t \end{aligned} \right\} t \downarrow 0$$

Accordingly, consulting Equation 21, we find from Equation 24 the generator

$$(\mathcal{G}u)(i) = (B-Di) \frac{du(i)}{di} + \frac{1}{2} (B+Di) \frac{d^2u(i)}{di^2} \quad (45)$$

and from Equation 25 its adjoint

$$\begin{aligned} (\mathcal{G}^*v)(j) &= -\frac{d}{dj} [v(j) \cdot (B-Dj)] + \\ &\quad \frac{1}{2} \frac{d^2}{dj^2} [v(j) \cdot (B+Dj)] \end{aligned} \quad (46)$$

Here  $i$  and  $j$  are continuous variables representing the population size. To keep the population size positive, we would want to apply boundary conditions in the manner of Equations 27 and 28, that is, to attach to Equation 45 the boundary condition

$$\frac{du(i)}{di} = 0; \quad i = 0 \quad (47)$$

and to Equation 46 the boundary condition

$$\begin{aligned} v(j) \cdot (B-Dj) - \frac{1}{2} \frac{d}{dj} [v(j) \cdot (B+Dj)] &= 0; \\ j = 0 \end{aligned} \quad (48)$$

With the generator given by Equations 45 and 47 and its adjoint by Equations 46 and 48, we would be prepared to begin a study of the population process according to this diffusional model.

### Particle Interactions

Almost all of our examples up to this point have dealt with particles that behaved quite independently of each other, and this was for the good reason that problems involving significant particle interactions are commonly very difficult. We propose here to discuss what seems to us to be a key difficulty in treating clusters of interacting particles. The difficulty is, of course, simply that the particles do interact, so that the properties of the individual particles are not statistically independent. This difficulty has already come up in our earlier discussion of the mineral flotation cell, but rather than return to this earlier discussion, we shall illustrate it anew in terms of a familiar agglomerative model for turbulent mixing, which brings us to the difficulty in a sharper, more transparent form.

According to this model, the turbulent mass is divided up into  $N$  equally sized droplets, the particles, which undergo binary collisions at the average rate  $NA$ , where  $A$  is a measure of the mixing intensity—*i.e.*, in a short time  $t$ , any given particle pair will collide with probability  $2At/(N-1)$ , so that some pair will collide with probability  $NAt$ . The colliding particles merge, equalize concentrations, and immediately separate. If we denote the concentrations of some key substance in the individual droplets by  $x_1, x_2, \dots, x_N$ , then the vector  $x = (x_1, x_2, \dots, x_N)$  may be taken to represent the state of the system, and we find a multidimensional version of the jump process, Equations 10 through 20, with

$$\alpha(x) = NA$$

$$\beta(x, y) = \frac{2}{N(N-1)} \sum_{m < n} \delta\left(y_m - \frac{x_m + x_n}{2}\right) \times \delta\left(y_n - \frac{x_m + x_n}{2}\right) \times \prod_{l \neq m, n} \delta(y_l - x_l)$$

We may also introduce a translation rate into the process by imagining a chemical reaction going on in the system, the concentrations  $x_m$  in the individual droplets continuously changing according to the rate equation  $dx_m/dt = R(x_m)$ ,  $m = 1, 2, \dots, N$ .

Now we find on applying the machinery of Equations 10 through 20 that the probability density of system states as defined in Equation 17—we denote it here  $v^{(N)}(y; t) = v^{(N)}(y_1, y_2, \dots, y_N; t)$ —satisfies the equation

$$\begin{aligned} \frac{\partial v^{(N)}(y; t)}{\partial t} &= (\mathcal{G}^* v^{(N)})(y; t) = \\ &= \sum_m \frac{\partial}{\partial y_m} [R(y_m) v^{(N)}(y; t)] - NAv^{(N)}(y; t) + \\ &= \frac{2A}{N-1} \sum_{m < n} \iint v^{(N)}(y_1, \dots, x_m, \dots, x_n, \dots, y_N; t) \times \\ &= \delta\left(y_m - \frac{x_m + x_n}{2}\right) \delta\left(y_n - \frac{x_m + x_n}{2}\right) \times dx_m dx_n \quad (49) \end{aligned}$$

The solution of Equation 49 would certainly tell us a very great deal about how the system evolves in time from some initial state. But quite apart from the difficulty in solving it, it would tell us rather more than we want to know—all the information we really want about the system is contained in the one-dimensional marginal distribution for a typical particle, and indeed in the leading moments of this one-dimensional margin. Besides, we would be hard put to assign a numerical value to  $N$ , which we think of rather vaguely as large.

Accordingly, we recognize first that if  $v^{(N)}$  is symmetrical in the  $y$ 's, so is  $\mathcal{G}^* v^{(N)}$ , so that, according to Equation 49, a distribution initially symmetrical stays symmetrical. We then proceed to integrate out  $y_2, y_3, \dots, y_N$  in Equation 49, hoping to obtain an equation for the typical single particle distribution

$$v^{(1)}(y_1; t) = \int \dots \int v^{(N)}(y; t) dy_2 dy_3 \dots dy_N$$

what emerges is

$$\begin{aligned} \frac{\partial v^{(1)}(y_1; t)}{\partial t} &= - \frac{\partial}{\partial y_1} [R(y_1) v^{(1)}(y_1; t)] - 2Av^{(1)}(y_1; t) + \\ &= 2A \iint v^{(2)}(x_1, x_2; t) \delta\left(y_1 - \frac{x_1 + x_2}{2}\right) dx_1 dx_2 \quad (50) \end{aligned}$$

But this involves the typical two-particle distribution

$$v^{(2)}(y_1, y_2; t) = \int \dots \int v^{(N)}(y; t) dy_3 \dots dy_N$$

If we try to close matters off by integrating out only  $y_3, \dots, y_N$  in Equation 49, we find an equation very much like Equation 50 with  $v^{(2)}$  in the derivative terms and the three-particle distribution  $v^{(3)}$  in the integral. We cannot, that is to say, develop self-contained equations in the lower order marginal distributions and must either return to the full equation, Equation 49, or make some judicious approximation to close off the hierarchy of lower order equations.

Now we may make an intuitive interpretation of Equation 50 in terms of macroscopic variables, in a way suggested by the variables appearing in our earlier discussion of the flotation unit. Without bothering about the repeated averaging machinery, we may renormalize the probability distributions— $v^{(1)}$  to the total number of particles,  $v^{(2)}$  to its square—divide up the concentration space into cells, and interpret the integrals of the renormalized distributions over these cells as the actual numbers of particles and particle pairs with concentrations in the appropriate ranges. If the particle population is large and the cells are sufficiently broad so that there is a large number of particles in each cell, these cell counts will be random variables with small variances and hence small covariances, just as the particle and bubble counts in the flotation unit were. We may then argue, as there, that for a typical cell pair

$$\int_{a_1}^{b_1} \int_{a_1}^{b_1} v^{(2)}(x_1, x_2; t) dx_1 dx_2 = \int_{a_1}^{b_1} v^{(1)}(x_1, t) dx_1 \times \int_{a_1}^{b_1} v^{(1)}(x_2, t) dx_2$$

so that, if the cells are in fact not too broad, we have in general

$$v^{(2)}(x_1, x_2; t) dx_1 dx_2 = v^{(1)}(x_1; t) dx_1 \cdot v^{(1)}(x_2; t) dx_2$$

This relation may then be returned to Equation 50 to give a self-contained equation in  $v^{(1)}$ .

There are, of course, formidable difficulties in making this line of argument precise. We don't attempt to do this here, but simply point out that very much the same difficulties arise in the kinetic theory of gases in making a systematic development of the Boltzmann equation. The questions there, however, are commonly posed in a somewhat different mathematical way—*i.e.*, one recognizes that the foregoing intuitive argument leads to the statement that the concentrations  $x_1, x_2, \dots, x_N$  for the particles in the system are independent by pairs. Accordingly, one sets it down as such:

$$v^{(2)}(x_1, x_2; t) = v^{(1)}(x_1; t) v^{(1)}(x_2; t) \quad (51)$$

and recovers from Equation 50—the  $v$ 's are probability densities again—

$$\frac{\partial v^{(1)}(y_1; t)}{\partial t} = - \frac{\partial}{\partial y_1} \{R(y_1) v^{(1)}(y_1; t)\} - 2 A v^{(1)}(y_1; t) + 2 A \int \int v^{(1)}(x_1; t) v^{(1)}(x_2; t) \times \delta\left(y_1 - \frac{x_1 + x_2}{2}\right) dx_1 dx_2 \quad (52)$$

a self-contained working equation in  $v^{(1)}$ . One realizes, of course, that the statement, Equation 51, is not under all circumstances true, and asks various mathematical questions aimed at clarifying the conditions when it is true. We might perhaps close this discussion with one of them. If Equation 49 is solved for an initial distribution in which the  $y$ 's are independent, what are the conditions under which the  $y$ 's remain independent in the solution—*i.e.*, under what conditions does independence preserve itself in time? Our intuitive answer would be: when the population is large.

### Problem Formulation

The technical part of this review being completed, we devote this final section to a consideration of why we should formulate engineering systems probabilistically at all. It goes without saying that if the process exhibits fluctuations in the macroscopic scale—imperfect reproducibility, in experimental terms—that it may be very useful to describe it in terms of a random mechanism rather than to look for a very fine grained deterministic description. In our applications these large-scale fluctuations are usually associated with small particle populations. Our point here is that even for large populations, where the over-all behavior is quite deterministic, there is often a certain conceptual convenience in making a probabilistic formulation at the single particle level, interpreting the single particle probability distributions in terms of number fractions for the whole ensemble of particles. We proceed, as throughout, by example, contenting ourselves here with the single example of the study of molecular weight distribution

74

in an emulsion polymerization system. This situation would seem to be rather complicated to formulate in terms of over-all deterministic balances for the emulsion system as a whole.

We turn accordingly to the consideration of an emulsion polymerization system and focus attention on a single emulsion particle. For reasons of analytic simplicity, we take the particle to be in a fixed chemical environment and ignore variations in its size and in its monomer concentration. We can then describe the underlying random mechanism affecting it in terms of three parameters,  $B, G, D$ : in a short time,  $t$ , a primary free radical enters with probability  $Bt$ ; the molecular weight of a free radical grows at the rate  $G$ ; in a short time,  $t$ , any two growing radicals terminate, by combination, with probability  $Dt$ . The parameters  $B, G, D$  have, of course, a direct interpretation in terms of macroscopic rate constants. If we describe the state of the emulsion particle at any moment by the number  $m$  of free radicals present, together with their sizes  $x_1, x_2, \dots, x_m$  (say, oldest first), we see that we have specified the short time transition probability  $p(mx_1 \dots x_m, ny_1 \dots y_n; t)$  from state  $m, x_1, \dots, x_m$  to state  $n, y_1, \dots, y_n$  in time  $t$ . Taking  $p$  to be a probability in  $n$  jointly with a probability density in  $y_1, \dots, y_n$ , we have

$$p(mx_1 \dots x_m, ny_1 \dots y_n; t) \sim Bt \cdot \delta_{n, m+1} \cdot \delta(y_1 - x_1) \dots \delta(y_m - x_m) \delta(y_{m+1}) + Dt \cdot \delta_{n, m-2} \cdot \sum_{i < j} \delta(y_1 - x_1) \dots \delta(y_{i-1} - x_{i-1}) \delta(y_i - x_{i-1}) \delta(y_{i+1} - x_{i+1}) \dots \delta(y_{j-2} - x_{j-1}) \times \delta(y_{j-1} - x_{j+1}) \dots \delta(y_{m-2} - x_m) + \left[ 1 - Bt - \binom{m}{2} Dt \right] \delta_n \delta(y_1 - x_1 - Gt) \dots \delta(y_m - x_m - Gt); t \downarrow 0$$

We may note that we have taken the molecular weight of a primary radical to be vanishingly small.

This process is, mathematically speaking, a rather more complicated version of the crystallizer process discussed earlier. It is not specifically included in our sketch of Markov processes, but an application of the same general machinery will yield its generator. It will be convenient first to symmetrize the short time transition probabilities in the  $x$ 's and  $y$ 's. Since we are concerned here only with the forward equation which governs the single-time probability distribution, we quote simply the adjoint of the generator for the symmetrized process:

$$(\mathcal{G}^*v)(n, y_1 \dots y_n) = - G \sum_j \frac{\partial v(n, y_1 \dots y_n)}{\partial y_j} + \frac{B}{n} \sum_j v(n-1, y_1 \dots y_{j-1}, y_{j+1} \dots y_n) \delta(y_j) + \binom{n+2}{2} D \int \int v(n+2, y_1 \dots y_n, r, s) dr ds - \left[ B + \binom{n}{2} D \right] v(n, y_1 \dots y_n)$$

where it is understood that  $v$  is symmetric in the  $y$ 's.

We are concerned here, in fact, only to find the distribution of states after the process has settled down into statistical equilibrium. Denoting this by  $v(n, y_1 \dots y_n)$ —symmetrized in the  $y$ 's—we note that according to Equation 9 or any of its continuous analogs, it satisfies

$$\mathfrak{G}^*v = 0$$

This really concludes the probabilistic part of the story. It remains only to reduce the equations describing the equilibrium distribution,  $v$ , to a convenient working form. This can readily be done by introducing the marginal distributions:

$$\begin{aligned}\theta_n &= \int v(n, y_1 \dots y_n) dy_1 \dots dy_n \\ \varphi_n(y_1) &= \int v(n, y_1 \dots y_n) dy_2 \dots dy_n \\ \psi_n(y_1, y_2) &= \int v(n, y_1 \dots y_n) dy_3 \dots dy_n\end{aligned}$$

where  $\theta_n$  is the probability of having  $n$  radicals present,  $\varphi_n$  is the joint distribution of radical count and molecular weight of a typical radical, and so on. We recover, after some calculation, a difference equation in  $\theta_n$

$$0 = (\theta_{n-1} - \theta_n) + \frac{D}{B} \left[ \binom{n+2}{2} \theta_{n+2} - \binom{n}{2} \theta_n \right] \quad (53)$$

ordinary differential equations in the  $\varphi_n(y)$

$$\begin{aligned}\frac{G}{B} \frac{d\varphi_n}{dy} &= \frac{1}{n} [\theta_{n-1} \delta(y) - \varphi_{n-1}] + (\varphi_{n-1} - \varphi_n) + \\ &\frac{D}{B} \left[ \binom{n+2}{2} \varphi_{n+2} - \binom{n}{2} \varphi_n \right] \quad (54)\end{aligned}$$

and partial differential equations in the  $\psi_n(y_1, y_2)$

$$\begin{aligned}\frac{G}{B} \left( \frac{\partial \psi_n}{\partial y_1} + \frac{\partial \psi_n}{\partial y_2} \right) &= \\ \frac{1}{n} [\varphi_{n-1}(y_1) \delta(y_2) + \varphi_{n-1}(y_2) \delta(y_1) - 2\psi_{n-1}] + \\ (\psi_{n-1} - \psi_n) + \frac{D}{B} \left[ \binom{n+2}{2} \psi_{n+2} - \binom{n}{2} \psi_n \right] \quad (55)\end{aligned}$$

The probability density for the molecular weight of the combined product can be expressed as

$$f(z) = \frac{\sum_n \binom{n}{2} \iint \psi_n(y_1, y_2) \delta(y_1 + y_2 - z) dy_1 dy_2}{\sum_n \binom{n}{2} \theta_n}$$

and this suggests that we introduce the functions

$$\rho_n(z) = \iint \psi_n(y_1, y_2) \delta(y_1 + y_2 - z) dy_1 dy_2$$

which, according to Equation 55, satisfy the ordinary differential equations

$$\begin{aligned}2 \cdot \frac{G}{B} \frac{d\rho_n}{dz} &= \frac{2}{n} [\varphi_{n-1}(z) - \rho_{n-1}] + \\ (\rho_{n-1} - \rho_n) + \frac{D}{B} \left[ \binom{n+2}{2} \rho_{n+2} - \binom{n}{2} \rho_n \right] \quad (56)\end{aligned}$$

The solution to Equation 53 being known,

$$\theta_n = \frac{1}{n! \sqrt{2}} \left( \frac{2B}{D} \right)^{n/2} \frac{I_{n-1} \left( \sqrt{\frac{8B}{D}} \right)}{I_1 \left( \sqrt{\frac{16B}{D}} \right)}$$

with

$$\sum_n n \theta_n = \sqrt{\frac{B}{D}} \frac{I_0 \left( \sqrt{\frac{16B}{D}} \right)}{I_1 \left( \sqrt{\frac{16B}{D}} \right)}$$

and

$$\sum_n \binom{n}{2} \theta_n = \frac{B}{2D}$$

we may readily undertake to organize first the numerical solution of Equation 54, and then of Equation 56.

It turns out to be convenient to work with the cumulative distributions of the tails. Letting

$$\Phi_n(y) = \int_y^\infty \varphi_n$$

$$P_n(y) = \int_y^\infty \rho_n$$

we find from Equation 54

$$\begin{cases} \frac{G}{B} \frac{d\Phi_n}{dy} = \left( 1 - \frac{1}{n} \right) \Phi_{n-1} - \Phi_n + \\ \frac{D}{B} \left[ \binom{n+2}{2} \Phi_{n+2} - \binom{n}{2} \Phi_n \right]; & y > 0 \\ \Phi_n(0) = \theta_n \end{cases}$$

and from Equation 56

$$\begin{cases} 2 \cdot \frac{G}{B} \frac{dP_n}{dy} = \frac{2}{n} \Phi_{n-1} + \left( 1 - \frac{2}{n} \right) P_{n-1} - P_n + \\ \frac{D}{B} \left[ \binom{n+2}{2} P_{n+2} - \binom{n}{2} P_n \right]; & y > 0 \\ P_n(0) = \theta_n \end{cases}$$

It is then a straightforward matter to truncate these systems of equations at some value of  $n$  past which  $\theta_n$  is negligibly small and to organize a direct numerical solution. The tails distribution of the product molecular weight

$$F(y) = \int_y^\infty f$$

can be recovered from these solutions in the form

$$F(y) = \frac{2D}{B} \sum_n \binom{n}{2} P_n(y)$$



**BLANK PAGE**

## A stochastic model for fluidized beds†

FREDERICK J. KRAMBECK,‡ STANLEY KATZ and REUEL SHINNAR

Department of Chemical Engineering, The City College, The City University of New York, New York, U.S.A.

(First received 13 August 1968; in revised form 7 March 1969)

**Abstract**—A mathematical model for gas-fluidized beds is proposed that allows for a randomly fluctuating flow pattern. It is shown how mean first-order conversion is related to contact time distribution for arbitrary models of this type. A simplified version of the model is then studied, and it is found that the effect of fluctuating flow is similar to that of stagnancy in steady systems. This effect is inconsistent with the usual steady-state models, but it is shown that some published data on conversion in fluidized beds [6] exhibit this effect.

### 1. INTRODUCTION

ONE OF the readily observable features of the flow pattern in fluidized beds is its fluctuating character. The various elements of dense-phase fluid are intermittently exposed to bubbles of different gas composition. Since one is normally interested in the average behavior of the beds, rather than in the details of the fluctuations, it is usual to represent such systems by steady-state models. It is the purpose of this paper to investigate by help of a simple model the effects that stochastic fluctuations might have on the behavior of the bed.

Of course, with the present state of knowledge, it is rather difficult to determine the parameters of even steady-state models accurately, or to choose between different models. Thus it is unlikely that this can be done with a stochastic model either. It is, however, of some interest to determine properties of stochastic models appropriate to fluidized beds to gain an understanding of how and under what conditions these unsteady properties might affect the behavior of the bed as a chemical reactor.

Now every turbulent reactor is an unsteady system. The reason that in many situations we can neglect this unsteady behavior is the fact that the time scale of the fluctuations is often small as compared to the time scale of the system.

The output of the system for steady input might therefore be almost completely deterministic and we can deal with the system as a steady system.

This assumption might be correct in high narrow fluidized beds as used in pilot plants or where vertical pipe heat exchangers are used to break up the bubbles in large beds but should not hold for large scale unbaffled fluidized beds. The time scale of the internal mixing processes and the gas residence time are here of the same order of magnitude. Gas bubbles are often large especially in the upper part of the bed and the local concentration of bubbles exhibits fluctuations, the time scale of which has the same order of magnitude as the residence time. The concentration fluctuations in the dense phase should therefore undergo similar fluctuations which might effect the behavior of the bed as a reactor and might be important in its control.

As will be shown in this paper the inclusion of the unsteadiness of the reactor explains some puzzling phenomena (see for example [6]) and it is hoped that it might be helpful for a better understanding of the fluidized bed.

The kind of model to be considered is similar to that described in [1]. This consists of a network of ideally stirred tanks interconnected by flows which fluctuate randomly in time. The new

†Presented at A.I.Ch.E. Annual Meeting, New York, November 1967.

‡Present address: Mobil Research, Princeton, N.J. 08540, U.S.A.



feature to be considered here is the presence of two types of tanks corresponding to zones in the dense phase and the bubble phase of fluidized beds. It should be noted that such a model with steady flows can be used to approximate arbitrarily closely any other steady-state two-phase model of the fluidized bed.

It is often assumed that the dense phase is either completely well mixed or that it is in plug flow but, again, that lateral mixing is complete. On the other hand, the contact with large bubbles assures good instantaneous mixing only in the immediate neighborhood of the bubble. As said before, the time scale of the mixing in the dense phase is of the same order of magnitude as that of the fluctuation in bubble concentration, and therefore it may not be desirable to assume that the dense phase is well mixed. On the other hand, every part of the dense phase comes into contact with bubbles, so that the dense phase would be homogeneous in some time-averaged sense. Now the model mentioned before describes a different physical situation where the dense phase is well mixed or at least can be described by a network of a few well stirred tanks but the transfer rate to those tanks fluctuates with time. But if we consider the total physical effect of the fluctuations on the local behavior in the dense phase we note that this model captures the basic physics of this unsteady behavior and should at least predict correctly in what way this unsteady nature of the transport processes might interact with the kinetic behavior of the reactor.

## 2. SOME PROPERTIES OF THE GENERAL MODEL.

The analytical structure of the stochastic mixing models was developed, and various properties were derived, in reference [1]. Here we derive some new results which are required for the application of these models to heterogeneous systems.

In general, the model consists of  $n$  ideally mixed tanks which are interconnected by flow streams in some arbitrary manner. The interconnecting flow rates are allowed to fluctuate

randomly in time with a definite probabilistic structure, that of a discrete-state Markov process. The tanks are taken to be of constant volume, and the fluid is assumed incompressible. The system of tanks will be assumed here to possess only a single inlet stream and a single outlet stream, although more general situations may be treated. The new feature introduced here is the special consideration of some subset of the tanks as an "active region" of the model, corresponding to the dense phase of a fluidized bed. Thus when the model is viewed as a chemical reactor, only the fluid contained in the active region of the system at any instant will undergo reaction.

It was shown in [1, 2] how the random walk of a single fluid molecule through the system may be described analytically, and how various properties of this random walk may be related to tracer response statistics and first-order reaction behavior. Thus the expected response to a certain tracer experiment is equal to the residence time density function, and the mean conversion for a first-order reaction as a function of the rate coefficient is just the Laplace transform of this function. In order to extend such results to the present situation a new random variable, the contact time, is introduced. For the random walk of a single fluid molecule through the system, this is defined as the total time spent by the molecule in the active region during its sojourn through the system. This will, in general, be less than the residence time of the molecule, defined here as the time spent in the system as a whole.

We denote the number of tanks in the model by  $n$ , the volume of the  $i$ th tank by  $v_i$ , and the volumetric flow rate from the  $i$ th tank to the  $j$ th tank by  $w_{j|i\alpha}$ , where  $\alpha$  is the state of the underlying Markov process, called the flow state. The flow rate from the inlet stream to tank  $i$  is called  $w_{0|i\alpha}$ , and the flow rate from the  $i$ th tank to the exit stream is called  $w_{i|n-1,\alpha}$ . It is convenient to define quantities of the form  $w_{i|\alpha}$  so that

$$w_{i|\alpha} = - \sum_{j=1}^{n+1} w_{j|i\alpha} = \sum_{j=0}^n w_{j|i\alpha} \quad (1)$$

## A stochastic model for fluidized beds

The total inlet flow rate (equal to the total outflow) will be denoted  $w_a$ . Then:

$$w_a = \sum_{i=1}^{n+1} w_{0ia} = \sum_{i=0}^n w_{i,n+1,a} \quad (2)$$

Note that direct bypassing,  $w_{0,n+1,a}$ , is allowed for.

The flow state transitions are governed by a switching matrix  $\lambda_{\alpha\beta}$  such that, for small time intervals  $\tau$ ,

$$\pi_{\alpha\beta}(\tau) = \delta_{\alpha\beta} + \lambda_{\alpha\beta}\tau + o(\tau) \quad (3)$$

where  $\pi_{\alpha\beta}(\tau)$  is the probability of transition from state  $\alpha$  to state  $\beta$  in a time interval  $\tau$ , and the function  $o(\tau)$  has the property

$$\lim_{\tau \rightarrow 0} \left\{ \frac{o(\tau)}{\tau} \right\} = 0.$$

The matrix  $\lambda_{\alpha\beta}$  has the properties

$$\lambda_{\alpha\beta} \geq 0; \quad \alpha \neq \beta \quad (4)$$

$$\sum_{\beta} \lambda_{\alpha\beta} = 0; \quad \text{all } \alpha.$$

We now consider the random passage of a single particle of fluid through the system. In heterogeneous reaction systems the important property of the single particle random passage is the contact time distribution, where contact time is defined as the total length of time a particle spends in the "active" part of the system during its passage. In the two-phase model of the fluidized bed, this would be the dense phase residence time distribution. The variation of contact time,  $\theta$ , with clock time,  $t$ , is given by

$$\frac{d\theta}{dt} = \chi_i(\alpha, j) \quad (5)$$

where  $A$  is the set of active states for the particles, and

$$\chi_i(\alpha, j) = \begin{cases} 1; & (\alpha, j) \in A \\ 0; & (\alpha, j) \notin A \end{cases} \quad (6)$$

Using the methods of reference [1], it can be

shown that if  $P_{\alpha i}(t, \theta)d\theta$  is defined as the joint probability that the particle is in state  $(\alpha, i)$  where  $\alpha$  is the flow state and  $i$  is the tank number, and that the contact time is between  $\theta$  and  $\theta + d\theta$ ,

$$\begin{aligned} \frac{\partial P_{\beta j}(t, \theta)}{\partial t} = & -\chi_i(\beta, j) \frac{\partial P_{\beta j}(t, \theta)}{\partial \theta} \\ & + \sum_{i=1}^n \frac{w_{i\beta}}{v_i} P_{\beta i}(t, \theta) + \sum_{\alpha} \lambda_{\alpha\beta} P_{\alpha j}(t, \theta) \end{aligned} \quad (7)$$

and

$$\frac{\partial P_{\alpha i}(t, \theta)}{\partial t} = \sum_{\beta} \sum_{j=1}^n \frac{w_{i,\beta+1,\alpha}}{v_i} P_{\beta j}(t, \theta) \quad (8)$$

where the suffix  $\alpha$  denotes the outlet state:  $\alpha = U\{(\alpha, n+1)\}$ . The initial distribution,  $P_{\alpha i}(0, \theta)$ , is given by (see [2])

$$\begin{aligned} P_{\alpha i}(0, \theta) = & \bar{P}_{\alpha} \frac{w_{0i\alpha}}{\bar{w}} \delta(\theta) \\ P_{\alpha i}(0, \theta) = & \sum_{\alpha} \bar{P}_{\alpha} \frac{w_{0,\beta+1,\alpha}}{\bar{w}} \delta(\theta) \end{aligned} \quad (9)$$

The differential Eqs. (7) and (8) together with initial conditions (9) give the  $P_{\alpha i}(t, \theta)$  completely. The contact time density function,  $f_i(\theta)$ , is then given by

$$f_i(\theta) = \lim_{t \rightarrow \infty} P_{\alpha i}(t, \theta). \quad (10)$$

It is not necessary to solve (7) and (8) completely to determine this function, however. Thus, integrating (7) and (8) from  $t = 0$  to  $t = \infty$ ,

$$\begin{aligned} \chi_i(\beta, j) \frac{dg_{\beta j}(\theta)}{d\theta} = & \bar{P}_{\beta} \frac{w_{0i\beta}}{\bar{w}} \delta(\theta) \\ & + \sum_{i=1}^n \frac{w_{i\beta}}{v_i} g_{\beta i}(\theta) + \sum_{\alpha} \lambda_{\alpha\beta} g_{\alpha j}(\theta) \end{aligned} \quad (11)$$

$$f_i(\theta) = \sum_{\beta} P_{\beta} \frac{w_{0,\beta+1,i}}{\bar{w}} \delta(\theta) + \sum_{\alpha} \sum_{j=1}^n \frac{w_{i,\beta+1,\alpha}}{v_i} g_{\alpha j}(\theta) \quad (12)$$

where  $g_{\beta j}(\theta) = \int_0^{\infty} P_{\beta j}(t, \theta) dt$ . The initial conditions for the system of equations (11) are

I. J. KRAMBECK, S. KATZ and R. SHINNAR

$$\chi_i(\beta, j)g_{ij}(0) = 0. \quad (13)$$

In this way, the function  $f_i(\theta)$  can be found by solving the system of ordinary differential and algebraic Eq. (11), rather than the system of partial differential Eq. (7).

It is of some interest to calculate the mean contact time,  $\bar{\theta} = \int_0^\infty \theta f_i(\theta) d\theta$ . In the Appendix, it is shown that

$$\bar{\theta} = \frac{1}{\bar{w}} \sum_{j=1}^n \sum_{\beta} \chi_i(\beta, j) \bar{P}_{\beta} v_j \quad (14)$$

where  $\bar{P}_{\beta}$  is the stationary probability distribution of flow states, which satisfies

$$\sum_{\alpha} \lambda_{\alpha\beta} \bar{P}_{\alpha} = 0; \text{ all } \beta. \quad (15)$$

and  $\bar{w}$  is the mean total inlet flow rate:

$$\bar{w} = \sum_{\beta} \bar{P}_{\beta} w_{\beta}. \quad (16)$$

If a set  $A$  consists of certain tanks in the model independently of flow state, then

$$\chi_A(\beta, j) = \sum_{k \in A} \delta_{jk} \quad (17)$$

and

$$\bar{\theta} = \frac{1}{\bar{w}} \sum_{k \in A} v_k. \quad (18)$$

In other words, the mean contact time is equal to the volume of the active region divided by the mean total inlet volumetric flow rate. This result is independent of whether the inlet flow rate or the internal flow rates fluctuate. It may be noted that if the set  $A$  includes all the tanks Eq. (18) will give the mean residence time.

This concludes our discussion of a single fluid particle through the system, and we turn now to the other point of view of individual tank concentrations. This is formulated in terms of the joint probability,  $P_{\alpha}(t, x) dx$ , of the flow state being  $\alpha$  and the concentrations of the individual tanks,  $(x_1, \dots, x_n) = x$ , being in the volume  $dx$  containing  $x$ . Using a slight modification of the derivation in [1] we arrive at

$$\frac{\partial P_{\beta}(t, x)}{\partial t} + \sum_{j=1}^n \frac{\partial}{\partial x_j} \left[ \left\{ \frac{w_{j\beta}}{v_j} x_0 + \sum_{i=1}^n \frac{w_{i\beta}}{v_i} - \chi_i(\beta, j) k x_j \right\} P_{\beta}(t, x) \right] = \sum_{\alpha} \lambda_{\alpha\beta} P_{\alpha}(t, x). \quad (19)$$

It has been assumed in (19) that a first-order reaction occurs in the active region of the model only, with rate coefficient  $k$ . After a time, a stationary probability distribution will be approached. This can be calculated by setting the time derivative in (19) equal to zero.

It is possible to calculate the first moments of  $P_{\alpha}(t, x)$  without solving (19), however. Thus if we define  $\mu_{\beta j} = \int x_j P_{\beta}(t, x) dx$  we find, as in [1],

$$\frac{d\mu_{\beta j}}{dt} = \bar{P}_{\beta} \frac{w_{j\beta}}{v_j} x_0 + \sum_{i=1}^n \frac{w_{i\beta}}{v_i} \mu_{\beta i} - \chi_i(\beta, j) k \mu_{\beta j} + \sum_{\alpha} \lambda_{\alpha\beta} \mu_{\alpha j}. \quad (20)$$

Here, again, we calculate the stationary values of  $\mu_{\beta j}$  by setting the time derivative in (20) equal to zero. The mean outlet flow rate of unconverted reactant is given by

$$\langle \psi \rangle = \sum_{\beta} \sum_{j=1}^n w_{j, n+1, \beta} \mu_{\beta j} + \sum_{\beta} \bar{P}_{\beta} w_{0, n+1, \beta} x_0. \quad (21)$$

If the Laplace transforms of Eqs. (11) and (12) are compared with (20) and (21), it is found that, for the stationary value of  $\langle \psi \rangle$ ,

$$\frac{\langle \psi \rangle}{\bar{w} x_0} = f_c(k) \quad (22)$$

where  $f_c(k) = \int_0^\infty e^{-k\theta} f_i(\theta) d\theta$ . Thus we may conclude that the Laplace transform of the contact time distribution is equal to the mean unconverted fraction of reactant when the inlet concentration is constant and stationary conditions have been achieved.

### 3. SIMPLIFIED MODEL

#### (a) Description

The general model described in the previous section has great flexibility, and by using sufficient tanks and connections one could

undoubtedly match it to any experimental data. Before undertaking such a project, however, it would be useful to have some feeling for how the fluctuating mixing flows affect the properties of such models. For this purpose a very simple model of the previous type will be postulated, on a largely intuitive basis, and its properties will be investigated.

Various steady-state models of fluidized beds have been proposed based on the two-phase picture of such systems. Common to these models is the assumption, based on observation, that the particulate phase behaves as an incompressible fluid whose volume is the same as that of the bed at incipient fluidization, and that the amount of gas passing through the bed in the form of bubbles is just the excess of the total gas flow over that at incipient fluidization. The models differ in the assumed mixing between and within the phases. For the purposes of this study, the simplified model shown in Fig. 1 will be assumed. In this model the particulate phase is assumed to be of constant volume and well-mixed. The quantity  $v_2$  is the interstitial volume of this phase. The total flow rate,  $w$ , is constant with time, as is the fraction of the total flow which travels in the form of bubbles,  $r$ . The bubble phase is assumed to be of constant volume,  $v_1$ , and is also well-mixed. The mixing flow rate,  $w_m$ , is assumed to fluctuate with

time, however. It may be noted that while the assumption of perfect mixing in the particulate phase seems reasonable, on the basis of the observed uniformity of temperature in such systems, that of perfect mixing in the bubble phase seems doubtful. In fact it is often assumed that the bubble phase is in a condition of plug flow. It will be shown, however, that many properties of the system are independent of this assumption, so it will be made for convenience. The assumption that the bubble phase is of constant volume results from defining the boundaries of the reactor appropriately.

The equations of change for the system of Fig. 1 are

$$v_1 \frac{dx_1}{dt} = rwx_0 - [rw + w_m]x_1 + w_mx_2 \quad (23)$$

$$v_2 \frac{dx_2}{dt} = (1-r)wx_0 + w_mx_1 - [(1-r)w + w_m]x_2 - v_2 R(x_2)$$

$$Z = rx_1 + (1-r)x_2 \quad (24)$$

where  $R(x)$  is the reaction rate expression. It is assumed, as before, that only one reaction occurs and that it occurs only in the particulate phase. The concentrations of reactant in the bubble phase and the particulate phase are  $x_1$  and  $x_2$  respectively. For tracer experiments,  $R(x)$  is just zero. The quantity  $Z$  is the outlet concentration.

#### (b) Steady flow behavior

Before discussing the effects of fluctuations in  $w_m$  on the system behavior, it is useful to first derive some properties of the system with constant  $w_m$ . Under this condition the model is just another in the general category previously mentioned, but the effect of fluctuations can only be made clear by comparison with this steady behavior. Also, by analyzing the steady model from the point of view developed for the stochastic models some interesting results are discovered.

Because the reaction takes place, in the model, only in tank 2, the residence time distribution of

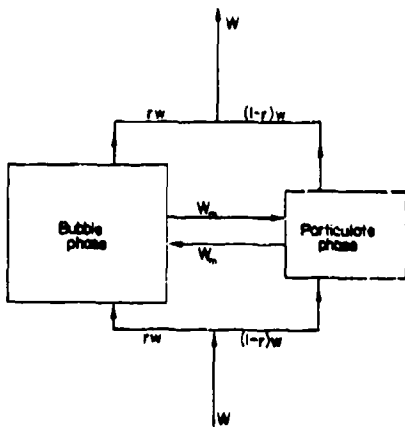


Fig. 1.

the system is of minor importance compared to the contact time distribution of gas particles with the particulate phase. One of the difficulties with using tracer experiments to study the properties of such systems is the fact that an experiment performed with a tracer that does not interact with the solid particles can furnish information only about the residence time distribution and not about the contact time distribution. It is therefore interesting to compare the two distributions.

The residence time density function is obtained by solving Eq. (11) with all the states included in the set  $A$ . This is found to be

$$f(t) = w \left[ \frac{r^2}{v_1} + \frac{(1-r)}{v_2} \right] \frac{b_1 e^{b_1 t} - b_2 e^{b_2 t}}{b_1 - b_2} - \left\{ w^2 \left[ \frac{r^2}{v_1^2} + \frac{(1-r)^2}{v_2^2} \right] + w w_m \left[ \frac{1}{v_1} - \frac{(1-r)}{v_2} \right]^2 \right\} \times \frac{e^{b_1 t} - e^{b_2 t}}{b_1 - b_2} \quad (25)$$

where  $b_1$  and  $b_2$  are the two roots of

$$b^2 + \left[ \frac{rw}{v_1} + \frac{(1-r)}{v_2} w + \frac{w_m}{v_1} + \frac{w_m}{v_2} \right] \times b + \frac{r(1-r)w^2}{v_1 v_2} + \frac{w w_m}{v_1 v_2} = 0. \quad (26)$$

The corresponding distribution function,  $F(t)$ , is just the integral of Eq. (25). This is plotted in Fig. 2 for typical values of the parameters. The value of  $r=0.9$  corresponds to a ratio  $u/u_0$

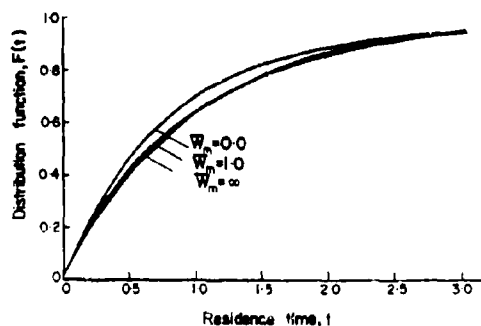


Fig. 2.

of 10, where  $u_0$  is the superficial gas velocity at incipient fluidization, and  $u$  is the superficial gas velocity at the system conditions. The ratio of the two volumes corresponds to a porosity of 0.5 in the particulate phase, and ratio of bed height to bed height at incipient fluidization,  $H/H_0$ , of 2. These values are thought to be typical of commercial fluidized beds. The values  $v_1 + v_2 = w = 1$  are chosen by assuming appropriate scale factors. Under these conditions the mean residence time is equal to one.

The three curves shown are for three values of the mixing flow rate,  $w_m$ , covering the range from zero to infinity. It is seen that the residence time distribution is only slightly affected by changes in  $w_m$ .

The contact time density function is calculated in the same way, with only tank 2 included in the set  $A$ . The result is,

$$f_c(\theta) = r_b \delta(\theta) + \frac{w'}{v_2} (1-r_b)^2 e^{-\left(\frac{w'}{v_2}(1-r_b)\theta\right)} \quad (27)$$

where  $r_b$  is given by

$$r_b = \frac{r^2 w'}{r w' + w'_m} \quad (28)$$

The quantity  $r_b$  above is just the fraction of gas which bypasses the particulate phase entirely, and thus has a zero contact time. When  $w_m = 0$ , it is seen that  $r_b = r$ , meaning that when there is no mixing between the phases, all the gas that passes through the system in the form of bubbles bypasses the particulate phase completely. The corresponding distribution function,  $F_c(\theta)$ , which is just the integral of (27), is plotted in Fig. 3 for the same system as was used in Fig. 2. For these values, the mean contact time,  $v_2 w'$ , is equal to 0.333. Comparison of Figs. 2 and 3 shows quite clearly that while the mixing rate,  $w_m$ , has only a slight effect on the residence time distribution, it has a pronounced effect on the contact time distribution.

An additional factor which makes the estimate of the transfer rate even more difficult, is the fact that it is also sensitive to our assumptions as to the nature of the mixing processes within the phases.

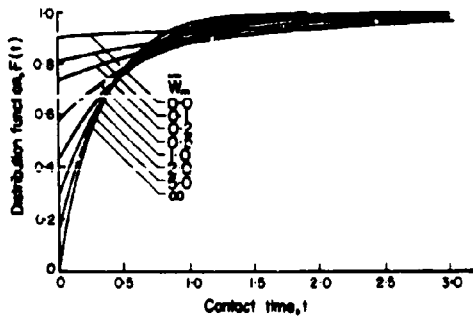


Fig. 3.

The contact time distribution of this system is closely related to its reaction behavior. Thus the conversion for a single first-order reaction is just the Laplace transform of  $f_i(\theta)$ . The conversion and selectivity of complex first-order systems are also determined by this function. Finally, for many reactions, the method of Zwietering and Dankwerts[3, 4] can be used to find bounds on conversion on the basis of  $f_i(\theta)$ . Since such large differences in  $f_i(\theta)$ , as shown in Fig. 3, are consistent with such slight differences in  $f(t)$ , the residence time distribution, it must be concluded that measurements of  $f(t)$ , that is tracer experiments performed with non-interacting tracer, where the tracer is introduced in the inlet and is measured in the outlet stream, provide a very poor basis on which to construct a model of the system's reactor performance.

The steady conversion for a first-order reaction catalyzed by the solid particles can be calculated from Eqs. (20) and (21), or by taking the Laplace transform of  $f_i(\theta)$ . The resulting fraction of unconverted reactant is then given by

$$\frac{Z}{x_0} = r_b + \frac{(1-r_b)^2}{1-r_b + k \frac{v_2}{w}} \quad (29)$$

It is interesting to note that this expression is identical to that derived by Davidson and Harrison[5] by assuming plug flow in the bubble phase and complete mixing in the particulate phase. Only the expression for  $r_b$ , the bypass fraction, in terms of the system parameters is different,

being given in their work by

$$r_b = re^{-N} \quad (30)$$

where  $N$  is the number of transfer units. In fact as long as the flows are steady, it can be shown that the contact time distribution for the well-mixed particulate phase is given by Eq. (27) regardless of the nature of the mixing processes in the bubble phase. This is seen by noting that whenever the set of states  $A$  consists of only a single state, the system of Eq. (11) reduces to a single linear differential equation. Its solution must then be of the form

$$f_i(\theta) = r_b \delta(\theta) + ae^{b\theta} \quad (31)$$

where  $a$  and  $b$  are constants. It is known, however, that the integral of  $f_i(\theta)$  is one, and that the mean contact time is  $w/v_2$ . These two conditions determine  $a$  and  $b$ .

This fact points up another difficulty in using tracer experiments for studying such systems, namely, that while the reactor performance is relatively insensitive to the nature of the mixing in the bubble phase, the residence time distribution is just as sensitive to these mixing processes as to those occurring within the particulate phase and between the two phases, so that different assumptions about the mixing in the bubble phase would allow very different conclusions about the particulate phase and the interphase mixing, based on such experiments. On the other hand, for purposes of studying the reaction behavior of such models, the assumption used here, that the bubble phase is well-mixed is seen to be of minor importance.

The unconverted fraction given by Eq. (29) is plotted in Fig. 4. It is seen there that the mixing rate,  $w_m$ , has a very large effect on first-order conversion, substantiating the conclusion about the importance of this parameter. At each value of  $w_m$  the unconverted fraction approaches an asymptotic value as  $k$ , the rate constant, goes to infinity. This value is just  $r_b$ , the bypass fraction.

Another point that emerges is that Eq. (27) for the contact time distribution contains only

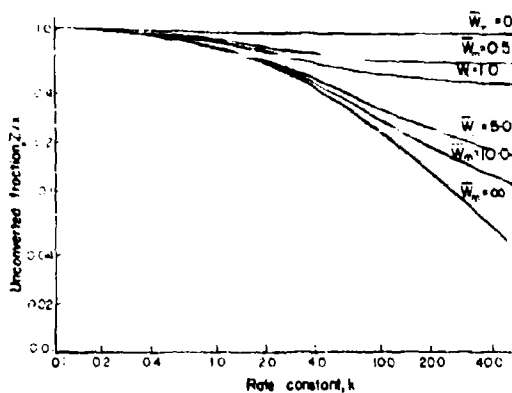


Fig. 4.

one unknown parameter,  $r_b$ . In general,  $w$  and  $v_2$  will be known in advance. Thus, if one is willing to assume that the particulate phase is well mixed and that the fluctuations in the rate of exchange between the two phases is unimportant, a determination of the single quantity  $r_b$  can be used to estimate the contact time distribution. This quantity can be measured by carrying out a fast reaction in the system or by using a tracer that is completely absorbed on the solid particles.

(c) Behavior with fluctuating flow

It will now be assumed that the mixing flow,

$$r_b = \frac{r^2 w}{r w + \bar{w}_m} \left\{ \frac{1}{\bar{P}_1 \bar{P}_2 \epsilon^2} \left[ 1 - \frac{1}{[r w + \bar{w}_m] [r w + \bar{w}_m + \epsilon (\bar{P}_2 - \bar{P}_1) + v_1 (\lambda_1 + \lambda_2)]} \right] \right\} \quad (34)$$

$w_m$  fluctuates by switching between two values,  $w_{m1}$  and  $w_{m2}$ . Under these conditions, the equations for the contact time distribution, (11) and (12), become

$$f_c(\theta) = \frac{r w}{v_1} g_{11}(\theta) + \frac{r w}{v_1} g_{21}(\theta) + \frac{(1-r)w}{v_2} g_{12}(\theta) + \frac{(1-r)w}{v_2} g_{22}(\theta) \quad (32)$$

and

$$0 = \bar{P}_1 r \delta(\theta) - \left[ \frac{r w}{v_1} + \frac{w_{m1}}{v_1} + \lambda_1 \right] g_{11}(\theta) + \lambda_2 g_{21}(\theta) + \frac{w_{m1}}{v_2} g_{12}(\theta)$$

$$0 = \bar{P}_2 r \delta(\theta) + \lambda_1 g_{11}(\theta) - \left[ \frac{r w}{v_1} + \frac{w_{m2}}{v_1} + \lambda_2 \right] g_{21}(\theta) + \frac{w_{m2}}{v_2} g_{22}(\theta)$$

$$\frac{d g_{12}(\theta)}{d \theta} = \bar{P}_1 (1-r) \delta(\theta) + \frac{w_{m1}}{v_1} g_{11}(\theta) - \left[ \frac{(1-r)w}{v_2} + \frac{w_{m1}}{v_2} + \lambda_1 \right] g_{12}(\theta) + \lambda_2 g_{22}(\theta)$$

$$\frac{d g_{22}(\theta)}{d \theta} = \bar{P}_2 (1-r) \delta(\theta) + \frac{w_{m2}}{v_1} g_{21}(\theta) + \lambda_1 g_{12}(\theta) - \left[ \frac{(1-r)w}{v_2} + \frac{w_{m2}}{v_2} + \lambda_2 \right] g_{22}(\theta) \quad (33)$$

with  $g_{12}(0) = g_{22}(0) = 0$ . To find the residence time distribution the zeros on the left of the first two equations of (33) are replaced by  $d g_{11}/d \theta$  and  $d g_{21}/d \theta$  respectively.

It is found again that  $f_c(\theta)$  contains an atom of probability at zero contact time which is the bypass fraction of the system. For the fluctuating case, this fraction is given by

where  $\epsilon = w_{m1} - w_{m2}$  and  $\bar{w}_m$  is the mean mixing flow. Comparison of (34) with (28) shows that the bypass fraction with fluctuations is always greater than that without for the same mean mixing rate, and that at high switching rates ( $\lambda_1 + \lambda_2 \rightarrow \infty$ ) the two become equal. To illustrate the effect of fluctuations on  $r_b$ , this quantity is plotted for some values of the parameters in Figs. 5 and 6. In Fig. 5, the quantity  $\epsilon/\bar{w}_m$  has been given its maximum allowable value. In

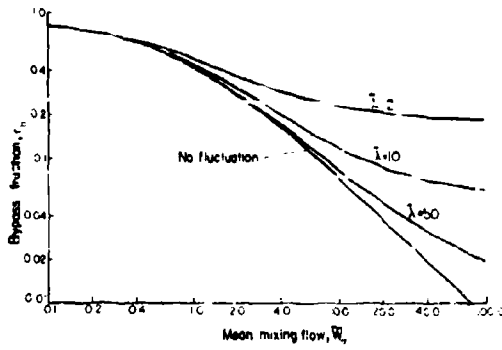


Fig. 5.

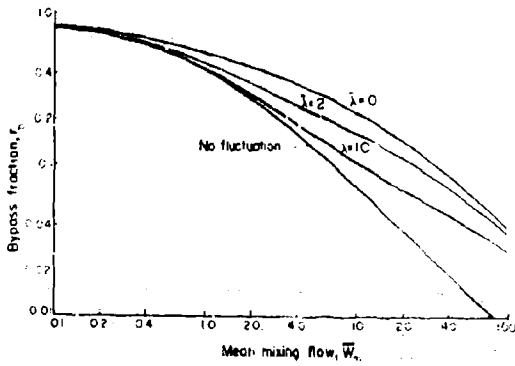


Fig. 6.

Thus the fact that the curves in Fig. 5 approach asymptotic values depends on the fact that complete cutoff occurs in one of the flow states. Otherwise  $r_b$  would approach zero.

When complete cutoff does not occur, it is seen from Eq. (34) that the ratio of  $r_b$  to the value of  $r_b$  with steady flow, as given by Eq. (28), becomes constant under the above conditions. Thus

$$\lim_{\epsilon \rightarrow 0} \left\{ \frac{r_b(rw + \bar{w}_m)}{r^2 w} \right\} = \frac{1 + \left( \frac{\epsilon}{\bar{w}_m} \right) (\bar{P}_2 - \bar{P}_1)}{1 + \frac{\epsilon}{\bar{w}_m} (\bar{P}_2 - \bar{P}_1) - \bar{P}_1 \bar{P}_2 \left( \frac{\epsilon}{\bar{w}_m} \right)^2} \quad (37)$$

One notes that, according to (37), the bypass fraction approaches an asymptote that is independent of switching rate. In Fig. 6,  $\epsilon/\bar{w}_m$  has been taken as 1.8, with the rest of the parameters the same as those in Fig. 5. Again the effect of the fluctuations on  $r_b$  is appreciable. For smaller values of  $\epsilon/\bar{w}_m$ , the effect of fluctuations on  $r_b$  is much smaller. Thus if  $\epsilon/\bar{w}_m = 10$  per cent the ratio given by (37) will be  $\approx 1$  per cent.

From the discussion in the previous section about the behavior of the system with steady flow, it is clear that changes in  $r_b$  have a large effect on the reactor performance. Thus the fluctuations will have an effect on the reactor performance by changing  $r_b$ . However, when a model is set up for a particular unit, the parameter  $r_b$  will be fixed by experimental means, since it is so important. One would then be interested in how the fluctuations would affect reactor performance once  $r_b$  is fixed.

Figures 7 and 8 illustrate the effect of fluctuations on the contact time distribution with  $r_b$  fixed. The distribution has been plotted in the

general, to keep the flow rates positive,

$$-\frac{1}{\bar{P}_2} \leq \frac{\epsilon}{\bar{w}_m} \leq \frac{1}{\bar{P}_1} \quad (35)$$

In the case shown,  $\bar{P}_1 = \bar{P}_2 = \frac{1}{2}$ , so  $\epsilon/\bar{w}_m$  has been taken as 2. It is seen that curves of  $r_b$  vs.  $\bar{w}_m$  appear to approach asymptotes. Inspection of Eq. (58) shows that, if  $\epsilon/\bar{w}_m$  is held constant,

$$\lim_{\epsilon \rightarrow 0} \langle r_b \rangle = \begin{cases} \frac{r \left[ 1 + \frac{\epsilon}{\bar{w}_m} (\bar{P}_2 - \bar{P}_1) \right]}{2 + \frac{\epsilon}{\bar{w}_m} (\bar{P}_2 - \bar{P}_1) + \frac{v_1}{rV} (\lambda_1 + \lambda_2)}; & \frac{\epsilon}{\bar{w}_m} = \frac{1}{\bar{P}_1} \text{ or } -\frac{1}{\bar{P}_2} \\ 0; & -\frac{1}{\bar{P}_2} < \frac{\epsilon}{\bar{w}_m} < \frac{1}{\bar{P}_1}. \end{cases} \quad (36)$$



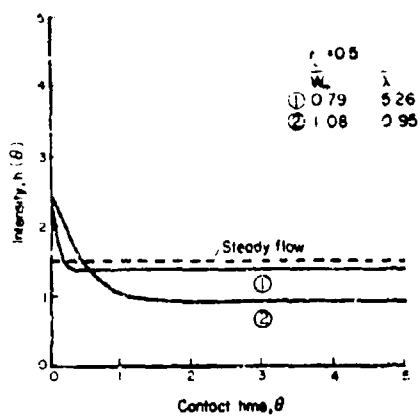


Fig. 7.

form of  $h_c(\theta)$ , the contact time intensity function [9], where

$$h_c(\theta) = \frac{f_c(\theta)}{1 - F_c(\theta)} \quad (38)$$

In Fig. 7 the parameters were chosen to keep  $r_b = 0.5$ , while in Fig. 8,  $r_b = 0.05$ . The effect of fluctuations on the contact time distribution is larger for 0.5, than for  $r_b = 0.05$ . In both cases, the effect is to decrease the value of  $h(\theta)$  for large  $\theta$ , which means that within the particulate phase itself there is a stagnancy (or bypassing) effect, in addition to the direct bypassing due to the bubbles.

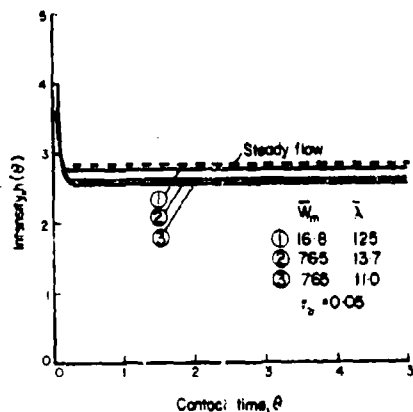


Fig. 8.

The behavior of the fluctuating system with first-order reaction is analyzed in terms of first moments by applying Eqs. (20) and (21), and in terms of second moments by similar methods, as explained in [1].

The mean outlet concentration and the coefficient of variation,  $= \sigma/\mu$ , are shown in Fig. 9 for the same parameter values as used in Fig. 8. It is seen that the fluctuations have the effect of decreasing mean conversion, and that the coefficient of variation of the output can be quite large, especially for high reaction rates. Since the determination of the mean bypass fraction involves an experiment with high reaction rates ( $K \rightarrow \infty$ ), whatever fluctuations there are would make themselves quite noticeable in the course of this experiment.

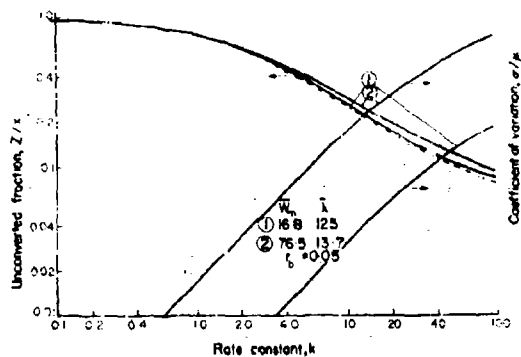


Fig. 9.

4. DISCUSSIONS

The contact time distribution for fluidized beds was first defined by Orcutt, Davidson and Pigford [6]. These authors made the contact time dimensionless by dividing by its mean value, so that the resulting distribution has a mean of unity. It was then suggested that this distribution be measured by carrying out a first-order reaction in the bed so as to determine the Laplace transform of the density function. The rate constant was made dimensionless in such a way that the resulting group,  $K$ , is equivalent to  $k\bar{\theta}$ , as defined in the present study, under the usual assumption that the rate of reaction on a

given mass of catalyst and at a given gas composition will be the same in the dense phase of a fluidized bed as it is in a packed bed. Thus a plot of unconverted fraction of reactant vs.  $K$  should be the Laplace transform of a density function with unit mean.

Actually, the numerical inversion of an experimentally measured Laplace transform can be subject to large errors. Since the contact time distribution cannot be measured directly, it is probably more useful to think in terms of its Laplace transform. It is not necessary to invert the transform in order to calculate conversion and selectivity for first-order reaction systems, for example, since such reaction schemes can be mathematically decoupled [7, 8]. Also, the very fact that the measured rate data can be interpreted as the Laplace transform of a valid density function places some restrictions on its structure. It must be completely monotone, for example. Because it is so closely related to actual conversion data, it seems that the function  $\hat{f}(k)$  is a more useful way to characterize fluidized bed reactors than results of tracer experiments, especially since these are rather insensitive to the interphase mixing.

The only situation that comes to mind in which it would be more desirable to have the contact time density  $f(\theta)$  rather than its transform is where the method of Danckwerts and Zwietering [3, 4] is to be used to predict bounds on conversion for nonlinear reactions. Even then one can use the transform to derive one of the bounds, that of complete segregation, as long as the batch conversion data can be approximated by a sum of exponentials. Thus if  $c(t)$  is the unconverted fraction for a batch reaction, the limiting unconverted fraction for complete segregation is

$$\frac{Z}{x_0} = \int_0^\infty c(\theta) f(\theta) d\theta \quad (39)$$

where  $f(\theta)$  is the contact time distribution. Then, if

$$c(t) = \sum_i a_i e^{-b_i t} \quad (40)$$

it is seen that

$$\frac{Z}{x_0} = \sum_i a_i \hat{f}(b_i) \quad (41)$$

where the time  $t$  in  $c(t)$  has been scaled by the mean contact time. It is not clear how the other extreme, maximum mixedness, could be calculated from the transform, however.

It was noted that the effect of fluctuations on contact time distribution is to decrease the values of the intensity function,  $h(\theta)$ , at large values of  $\theta$ . Such a shape for  $h(\theta)$  indicates that the tail of the contact time distribution has more weight than it would for the case of ideal mixing in the particulate phase with no fluctuation, a condition which for steady flows is termed stagnancy [10]. This results in high values for the higher moments of the contact time distribution. The corresponding effect on the Laplace transform of the distribution can be seen by expanding it in Taylor series:

$$\hat{f}(K) = \sum_{i=0}^{\infty} \frac{\mu_i}{i!} K^i \quad (42)$$

where  $\mu_i = \int_0^\infty \theta^i f(\theta) d\theta$ . Thus

$$\hat{f}(K) = 1 - K + \frac{1}{2}(1 + \sigma^2)K^2, \dots \quad (43)$$

The effect of stagnancy, then, on  $\hat{f}(K)$  is to increase it, at least in some region near  $K=0$ . This result is borne out in Fig. 9 (note that abscissa on Fig. 9 is equal to  $3K$ ). This argument does not imply that  $\hat{f}(K)$  will increase at all values of  $K$ , but in fact it does in Fig. 9.

One can also put the above argument in a somewhat different form. If the tail of the distribution has a strong weight this is just another way of saying that a small fraction of the gas has residence time considerably longer than that expected in a stirred tank. In a steady flow situation this is often caused by a stagnant region in the flow in which particles become trapped. Such a stagnancy can be easily recognized from the fact that the intensity function has a decreasing region (9). We note that the unsteady flow has the same effect on the contact time distribu-

tion as stagnancy has in steady flow. Now in order to detect the effect of this on  $f(t)$  one needs a very accurate measurement of the tail. If our experimental method is such that we just measure the main part of the curve (such as in a pulse) we often do not detect this tail. We then find that the average value of the contact (or residence) time is less than its expected value, namely volume divided by flow rate.

It has often been assumed in theoretical work that the state of axial mixing in the dense phase is somewhere between that of complete mixing and plug flow. In a steady state model, this results in a contact time distribution with variance less than that for steady complete mixing in the dense phase, with the same bypass fraction. The stagnancy effect discussed above, however, results in a variance greater than that for steady complete mixing in the dense phase with the same bypass fraction. The existence of stagnancy is thus inconsistent with steady state models using an axial diffusion coefficient in the dense phase. It is consistent, however, with the observation of Rowe [9], that the axial dispersion in a fluidized bed is due to batches of the solid being carried up in the wakes of individual bubbles rather than intimate mixing throughout the bed. This allows the possibility that certain zones of the dense phase will be relatively stagnant for short time periods.

It would be interesting to test experimentally whether such a stagnancy effect exists. A method for doing this is arrived at as follows: For steady flow and complete mixing, the unconverted fraction is given by

$$\varphi = r_b + \frac{(1-r_b)^2}{1-r_b+K} \quad (44)$$

solving for  $r_b$  gives

$$r_b = \frac{\varphi K - (1-\varphi)}{K - (1-\varphi)} \quad (45)$$

A plot of the right hand side of (45) against  $K$  will be horizontal for complete mixing and steady flow, will be above its asymptotic value at low  $K$  values if stagnancy is present, and will

be below if the axial diffusion coefficient model is correct. In fact,

$$\lim_{K \rightarrow 0} \left\{ \frac{\varphi K - (1-\varphi)}{K - (1-\varphi)} \right\} = \frac{\sigma^2 - 1}{\sigma^2 + 1} \quad (46)$$

where  $\sigma^2$  is the variance of the contact time distribution. This was tried with some data from the literature in Fig. 10 in which some of the experimental results of [6] are plotted. It can be seen that the presence of stagnancy is clearly indicated.

In [6] it was noted by the authors that the average contact time as measured from the slope of  $\varphi(K)$  was too low. There are two possible explanations for this. Either the reaction rate is lower than in a packed bed, which is hard to believe, or part of the bed is inactive. Now in a fluidized bed the solids are well agitated, and at first it is hard to conceive of any inactive region. But the mixing processes of the solid phase have the same time scale as the contact time of the gas, and with respect to this time scale the solids are not well mixed. If we consider a region of the dense phase, then, it experiences periods of intimate contact with the gas phase followed by periods of very little contact with the gas phase. The time scale of the fluctuations is of the same order of magnitude as the residence time. Over one residence time the total fraction of dense phase in intimate contact with the bubble phase might be only half. This effect is clearly borne out by Orcutt's experiments [6]

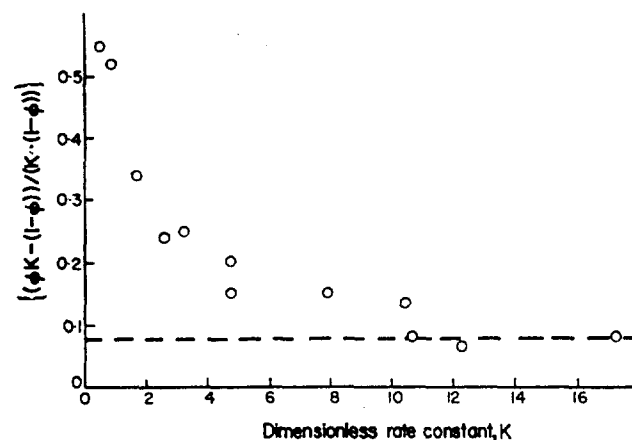


Fig. 10. Conversion data exhibiting stagnancy (Orcutt; 6 in. dia., 0.46 ft sec., 24 in. packed height,  $V/V_0 = 33$ ).

and might change from bed to bed. It is regrettable that similar results for large beds are not available.

In the context of our simplified model, the effect of a fluctuating exchange rate would also express itself in a variance larger than unity. This is, however, a result of our assumption that the dense phase is well mixed. If we would assume that the dense phase is better represented by two stirred tanks in series, each of them having a fluctuating exchange with the gas phase, then the variance of the contact time distribution can be less than unity.  $h(t)$  will, however, still have a decreasing region and again we might, under some conditions, note a reduced apparent average contact time. The effect of the fluctuations on performance should decrease if the bubbles are small as compared to bed height, and should be largest in large reactors with no internal structures to reduce bubble size.

While our crude model at this stage may not represent a reactor accurately, it still allows us to estimate the effect of the unsteady nature of the transport processes on the performance of the reactors. We may evaluate the behavior of any chemical reaction system in the above model by numerical methods and compare it to a steady-state model. While the parameters of the model are not known they can be estimated from measurements of the transform of the contact time distribution as outlined in [6].

Such model studies could be important for scaling as one can quite safely assume that, during scaling, the size of the bubbles relative to the bed height is going to increase and therefore the relative time scale of the fluctuations is also going to increase. These effects are, therefore, going to be more important in a full-sized plant than in a pilot plant, and studies of this model could indicate for what reactions this might be of importance.

##### 5. CONCLUSIONS

Certain average properties of quite general two-phase fluidized bed models are independent of the presence of fluctuations. The dense phase residence time or contact time distribution will

have a mean value given by the dense-phase gas volume divided by the mean volumetric inlet flow rate, and the mean unconverted fraction with a first-order reaction is just the Laplace transform of the dense-phase residence time density function.

Consideration of a very simple example of such two-phase models indicates that the tracer response of the system is quite insensitive to certain parameters of the model, so that measured tracer response curves carry little information about them. It was found that fluctuating behavior has a large effect on the bypass fraction, which is an important parameter for a catalytic reactor. Also, if the parameters of the model are adjusted so as to keep the bypass fraction constant, fluctuations cause a change in the dense-phase residence time distribution and in the mean first-order conversion which are similar to the effects of stagnancy in a steady flow model. The average contact time as measured by the conversion at low values of  $k$  will appear to be lower than its real average as defined by the void volume of the dense phase divided by the total flow rate. This behavior is in good agreement with some experimental data on contact time distributions, and provides a reasonable explanation for them. This does not, of course, verify that the model is adequate under the given conditions, since this would require that the experimental data exhibit fluctuations of the size predicted, and data on such fluctuations are not available.

The proposed model could be of use in situations where the fluctuating output is important and a dynamic model of these is desired, or where a simple model of a fluidized bed is needed exhibiting the basic feature of the unsteady nature of the transport processes. In either case experimental data would be required to fix the values of certain parameters. If, however, we just intended to estimate what effects this unsteadiness has on conversion or control, estimates on the parameters of the model are accessible and in that respect the model could hopefully be of use even in the absence of more accurate data.

**Acknowledgments**—This work has been supported by the Air Force Office of Scientific Research AFOSR Grant No. 921-67. Some of this work is part of the research carried out by one of the authors (F. J. Krambeck) at the City University of New York in partial fulfillment of the requirement of the degree of doctor of philosophy.

## NOTATION

$A$	set of active states
$f(t)$	residence time density
$f_c(\theta)$	contact time density
$F_c(\theta)$	contact time distribution
$R_{xi}(\theta)$	$\int_0^x P_{xi}(t, \theta) dt$
$\hat{R}_{xi}(k)$	$\int_0^x e^{-k\theta} R_{xi}(\theta) d\theta$
$h_c(\theta)$	contact time intensity function (Eq. (38))
$k$	rate constant
$K$	dimensionless rate constant, $k\bar{\theta}$
$\bar{P}_x$	stationary flow state distribution
$P_{oi}(t)$	probability of having left the system at time $t$
$P_{xi}(t, \theta) d\theta$	joint distribution of flow state, particle position, and accumulated contact time at time $t$
$P_{oi}(t, \theta) d\theta$	joint probability of having left the system by time $t$ with contact time in $(\theta, \theta + d\theta)$
$P_x(t, x) dx$	joint probability distribution of flow state and concentration
$r$	fraction of total gas flow traveling as bubbles
$r_b$	bypass fraction
$R_i(x_i)$	reaction rate in tank $i$

$v_i$	volume of tank $i$
$w$	total inlet flow rate
$w_x$	total inlet flow rate when flow state is $x$
$\bar{w}$	mean inlet flow rate
$w_{i,n}$	mixing flow rate (simplified model)
$w_{n,1}, w_{m,2}$	mixing flow rate in states 1 and 2
$\bar{w}_m$	mean mixing flow rate (simplified model)
$w_{ijx}$	flow rate from tank $i$ to tank $j$ when state is $x$
$x_i$	concentration in tank $i$
$x_0$	inlet concentration
$Z$	outlet concentration

## Greek symbols

$\delta_{ij}$	Kronecker delta
$\epsilon$	$w_{m1} - w_{m2}$
$\theta$	contact time
$\bar{\theta}$	mean contact time
$\lambda_{\alpha\beta}$	switching rate
$\lambda_1$	switching rate, $\lambda_{12}$
$\lambda_2$	switching rate, $\lambda_{21}$
$\bar{\lambda}$	mean switching rate, $\frac{1}{2}(\lambda_1 + \lambda_2)$
$\mu$	mean value
$\mu_{oi}$	partial moments (Eq. (20))
$\pi_{\alpha\beta}(\tau)$	transition probability (Eq. (3))
$\sigma$	standard deviation
$\phi$	unconverted fraction
$\chi_A(\alpha, i)$	characteristic function of $A$
$\psi$	outlet reactant flow rate

## REFERENCES

- [1] KRAMBECK F. J., SHINNAR R. and KATZ S., *Ind. Engng Chem. Fundls* 1967 6 276.
- [2] KRAMBECK F. J., SHINNAR R. and KATZ S., *Ind. Engng Chem. Fundls* (in press)
- [3] ZWEITERING TH. N., *Chem. Engng Sci.* 1959 11 10.
- [4] DANCKWERTS P. V., *Chem. Engng Sci.* 1958 8 93.
- [5] DAVIDSON J. F. and HARRISON D., *Fluidized Particles*, Cambridge University Press 1963.
- [6] ORCUTT J. C., DAVIDSON J. F. and PIGFORD R. L., *Chem. Engng Prog. Symp. Ser.* 1962 58 No. 381.
- [7] WEI J. and PRATER C. D., *The Structure and Analysis of Complex Reaction Systems*, Vol. 13, pp. 203-392, Academic Press 1962.
- [8] WEI J., *Can. J. Chem. Engng* 1965 44 51.
- [9] ROWE P. N., *Chem. Engng Prog. Symp. Ser.* 1962 58 1.
- [10] NAOR P. and SHINNAR R., *Ind. Engng Chem. Fundls* 1963 2 278.

## APPENDIX

## MEAN CONTACT TIME

To derive Eq. (14) for the mean contact time, we begin by summing the system (11) over  $\beta$  and  $j$  to give

$$\sum_{\beta} \sum_{j=1}^n \chi_{\beta}(\beta, j) \frac{dR_{\beta j}(\theta)}{d\theta} = \delta(\theta) - \sum_{\beta} \bar{P}_{\beta} \frac{w_{\beta, n-1, \beta}}{\bar{w}} \delta(\theta) + \sum_{\beta} \sum_{i=1}^n \sum_{j=1}^n \frac{w_{i\beta}}{v_i} R_{\beta i}(\theta). \quad (A1)$$

## A stochastic model for fluidized beds

Then, using (2) and (12), we find

$$\sum_{\beta} \sum_{j=1}^n \chi_{\beta}(j) \frac{dF_{\beta}(j, \theta)}{d\theta} = \delta(\theta) - F_{\beta}(j, \theta) \quad (\text{A2})$$

Integrating (A2) with initial conditions (13) gives

$$1 - F_{\beta}(j, \theta) = \sum_{\beta} \sum_{j=1}^n \chi_{\beta}(j) g_{\beta}(j, \theta) \quad (\text{A3})$$

and integrating again gives

$$\theta = \sum_{\beta} \sum_{j=1}^n \chi_{\beta}(j) \theta_{\beta j} \quad (\text{A4})$$

where  $\theta_{\beta j} = \int_0^{\theta} g_{\beta}(j, \theta) d\theta$ . Thus the mean contact time,  $\theta$ , can be expressed as a sum of individual contact times,  $\theta_{\beta j}$ , for the states making up the set  $\mathcal{A}$ . The  $\theta_{\beta j}$  are calculated by

integrating Eq. (11):

$$\chi_{\beta}(j) \{ \lambda_{\beta j} (\infty)^{-1} - g_{\beta}(j, 0) \} = P_{\beta} \frac{v_{\beta j}}{u} + \sum_{i=1}^n \frac{v_{\beta i}}{v_i} \theta_{\beta i} + \sum_{\alpha} \lambda_{\alpha i} \theta_{\alpha i} \quad (\text{A5})$$

or

$$\sum_{i=1}^n \frac{v_{\beta i}}{v_i} \theta_{\beta i} + \sum_{\alpha} \lambda_{\alpha i} \theta_{\alpha i} = -P_{\beta} \frac{v_{\beta j}}{v_j} \quad (\text{A6})$$

By inspection, it is seen that the solution to (A6) is

$$\theta_{\beta j} = P_{\beta} \frac{v_j}{v_j} \quad (\text{A7})$$

when Eqs. (2) and (4) are taken into account. Substituting (A7) in (A4) gives Eq. (14).

**Résumé**—On propose un modèle mathématique pour des couches de gaz fluidisées permettant un courant présentant des fluctuations au hasard. On démontre la relation d'une conversion moyenne de premier ordre à la distribution des temps de contact, pour des modèles arbitraires de ce type. Une version simplifiée du modèle est ensuite étudiée et on trouve que l'effet du courant de fluctuation est similaire à celui de la stagnation dans les systèmes stables. Cet effet est contradictoire aux modèles habituels à l'état stable, mais l'on montre que certaines informations publiées sur la conversion des couches fluidisées [6] présentent cet effet.

**Zusammenfassung**—Es wird ein mathematisches Modell für durch Gas betätigte Wirbelschichten vorgeschlagen, das ein zufälliges Schwankungen unterworfenen Strömungsbild in Betracht zieht. Die Beziehung der durchschnittlichen Umsetzung einer Reaktion erster Ordnung zur Verteilung der Berührungszeit für willkürlich gewählte Modelle dieser Art wird gezeigt. Es wird dann eine vereinfachte Version des Modells untersucht, und es wird festgestellt, dass der Effekt einer schwankenden Strömung ähnlich dem einer Stagnation in stationären Systemen ist. Dieser Effekt ist mit den üblichen Modellen des stationären Zustandes unvereinbar, doch wird gezeigt, dass verschiedene über die Umsetzung in Wirbelschichten gemachte Angaben [6] diesen Effekt aufzeigen.

Reprinted From . . .

# AICHE JOURNAL

## SCALE-UP CRITERIA FOR STIRRED TANK REACTORS

J. J. Evangelista, Stanley Katz,  
and Reuel Shinnar

*The City College, CUNY, New York, New York*

# Scale-up Criteria for Stirred Tank Reactors

J. J. EVANGELISTA, STANLEY KATZ, and REUEL SHINNAR

The City College, CUNY, New York, New York

A method is derived for the design of stirred tank reactors for homogeneous reactions. A simple mixing model proposed previously by Curl (4) is used to compute the effects of finite mixing time on complex chemical reactions. It is also shown how the parameters of the model can be obtained by tracer experiments, or estimated theoretically by the assumption of isotropic turbulence. It is shown that in many practical cases the assumption of ideal mixing is a good approximation. However, the effects of imperfect mixing are more likely to be felt in a large reactor than in a pilot plant. Some quantitative examples are discussed. Methods are derived to compute the average outlet concentration for complex systems such as autothermic reactions, polymerization, crystallization, etc.

In a number of recent publications the effect of mixing on homogenous chemical reactions is discussed. In this paper an attempt is made to summarize this work into a design and scale up procedure for stirred tank reactors. The method as described is limited to reactants which completely mix though it can be extended to certain heterogeneous reaction systems.

Now in any such scale up problem the first question that one has to answer is what are the dangers involved. If there is only a simple one path reaction, then the only question is how much is the conversion affected, and this can be relatively easily handled either by safety factors or by some of the estimation procedures described in the following. The more complex and challenging case is the one in which the product quality itself might be affected by the scale up, and in this case there is no way of compensating for our lack of precise knowledge by a larger reactor volume. This is true especially in complex reactions, where side reactions might be favored by local overconcentrations. Other systems very sensitive to local overconcentration are systems involving nucleation, such as crystallization and certain polymerization processes.

The problem of scaling up a homogeneous reaction is therefore basically to evaluate the effect of mixing on the reaction. The first question that we have to ask ourselves is what changes when we scale up. One property we want to maintain during scale up is a similarity in the basic flow regime. It was shown in previous work (8, 9) that this criterion can be fulfilled by choosing the size of the pilot plant or bench reactor such that the Reynolds number is large ( $> 10^4$  or preferably  $10^5$ ). This ensures that the average velocity distribution is a function of space coordinates only and fairly independent of Reynolds number, resulting in a similarity in the overall velocity distribution between geometrically similar reactors. The second criterion commonly used and explained elsewhere (5, 9) is that the energy input per unit volume should be constant, as this gives a similarity of the turbulent flow regime in the high wave number range of the turbulent velocity spectrum. This is important for heterogeneous systems, as the velocity field that a single particle sees around its periphery remains constant during scale up. It was pointed out that the time scale of mixing changes during scale up at constant energy input per unit volume. To keep this time constant during scale up of geometrically similar vessels (with large Reynolds numbers) one would have to keep the agitator speed constant. For homogeneous reactions the overall mixing time is really the important criterion, and as long as we can keep both the Reynolds number high and the revolutions per minute constant, then we could scale up with considerable confidence. This is however in most cases impractical. At constant revolutions per minute the Reynolds number increases linearly with the characteristic length  $L$  and the energy input per

unit volume increases proportionally to  $L^2$ . If we want to keep the Reynolds number above  $10^4$  in the small vessel we either have a relatively small scale up ratio or we end up with an unrealistic energy consumption in the large vessel. We therefore often have to live with the fact that during scale up the mixing time increases and try to estimate this effect in a quantitative way. These considerations apply not only for the design of continuous reactors but also to the design of batch reactors, if one of the reactants is added continuously.

Zweitering (17) has shown that if the reaction is of  $n$ th order and the feed is premixed one can estimate bounds on the conversion. One bound (a maximum for  $n > 1$  and a minimum for  $n < 1$ ) is the case of maximum segregation, where all particles are assumed to mix only with particles having the same age and waiting time, the other bound is the case of maximum mixedness, which in the case of a stirred reactor with a Poisson residence time distribution is the same as the ideally mixed reactor. Obviously for a first-order reaction the conversion is independent of mixing and depends only on residence time distribution. For more complex reactions these limiting cases do not result in any bounds on conversion, and other methods to obtain these bounds for more complex systems have been proposed (15). While these methods are not rigorous they still give a fairly good estimate of the bounds.

Such bounding is especially useful if the bounds are close together. This indicates that the system is insensitive to mixing and can be scaled up quite safely. However, in the cases where it matters most, namely, in complex reactions, nucleation, etc., the bounds are very far apart, and thus bounding methods based on residence time distribution alone are not very useful. Luckily most agitated reactors are, in their behavior, very close to ideally stirred tanks. Mixing times in most reactors are measured in seconds whereas residence times are normally measured in minutes or hours. Unless we deal with a system sensitive to mixing or with very large reactors, it is very hard to measure any deviations from complete mixing [see for example (16)]. We therefore normally deal with the case of a reactor which at least in the pilot plant is very close to ideal mixing and our main problem is to estimate

1. How large is the deviation from ideal mixing likely to become in the large scale reactor?
2. How sensitive is the process to small deviations from complete mixing?

A quantitative approach to these two problems is outlined in the following sections.

## THE MODEL

The mixing model for a stirred tank reactor used here



is the one used by Curl (4), Spielman and Levenspiel (11), Kattan and Adler (18), and others in this and related contexts. Briefly, it regards the reacting mass as made up of a large number of equally-sized parcels of material (particles), which from time to time undergo independent pair collisions, equalize concentrations, and then separate. Between collisions, each parcel of fluid behaves like a little batch reactor. Fresh material is fed at a constant rate, and the withdrawal takes a representative cut of the contents of the vessel. One speaks of these particles as though they had a definite material identity. This is reasonable for dispersed phase systems but here where we are dealing with homogenous phase systems, they might perhaps be better regarded for the present purpose as primitive representations of turbulent eddies.

If we consider, for concreteness, a single reaction where the concentration  $c$  of reagent behaves in batch according to

$$\frac{dc}{dt} = r(c) \quad (1)$$

then we may describe the contents of the reactor at any time  $t$  by the concentration distribution  $p(c, t)$  of particles at that time. Technically speaking,  $p$  is a probability density in  $c$ , with  $\int_a^b p(c, t) dc$  giving the proportion of

particles having concentration between  $a$  and  $b$  at time  $t$ . The distribution  $p$ , according to what has been said, satisfies the integro-differential equation (4)

$$\begin{aligned} \frac{\partial p(c, t)}{\partial t} + \frac{\partial}{\partial c} \{r(c)p(c, t)\} = & \alpha \{p_0(c, t) - p(c, t)\} \\ & + 2\beta \left\{ \int \int p(c', t)p(c'', t) \delta\left(\frac{c' + c''}{2} - c\right) dc' dc'' \right. \\ & \left. - p(c, t) \right\} \quad (2) \end{aligned}$$

where  $p_0(c, t)$  is the concentration distribution for the feed,  $1/\alpha$  the nominal residence time of material in the tank, and  $\beta$  a measure of the agglomerative mixing intensity. The mean concentration of reagent in the vessel and outlet is simply the first moment of  $p$ , and this is the working measure of overall reactor performance for a given kinetic system. Information about the random fluctuations in a turbulent mixing system is given by the higher moments.

It should be noted that the concentration variable  $c$  in Equation (2) may be scaled in any one of a number of convenient ways, provided only that the basic property of averaging on agglomeration is preserved. Thus, we may write (2) with yield, conversion, extent of reaction, and so on, in place of  $c$ . Further, when there is more than one reaction going on, so that the kinetics are described by several simultaneous equations in place of Equation (1), we find natural generalizations of (2). Thus, with two independent reactions whose progress variables (say) follow the kinetic scheme

$$\begin{aligned} \frac{dx}{dt} &= r(x, y) \\ \frac{dy}{dt} &= s(x, y) \end{aligned} \quad (3)$$

we have

$$\frac{\partial p(x, y, t)}{\partial t} + \frac{\partial}{\partial x} \{r(x, y)p(x, y, t)\}$$

$$\begin{aligned} + \frac{\partial}{\partial y} \{s(x, y)p(x, y, t)\} = & \alpha \{p_0(x, y, t) - p(x, y, t)\} \\ & + 2\beta \left\{ \int \int \int \int p(x', y', t)p(x'', y'', t) \right. \\ & \delta\left(\frac{x' + x''}{2} - x\right) \delta\left(\frac{y' + y''}{2} - y\right) dx' dy' dx'' dy'' \\ & \left. - p(x, y, t) \right\} \quad (4) \end{aligned}$$

Calculations of reactor performance according to Equations (2) and (4) for some common one and two reaction schemes will be found below.

The basic equation in  $p$  may be applied as well in the study of certain polymerization reactions, where we are concerned, to describe the molecular weight distribution. In a homogeneous radical polymerization, for example, we are concerned to describe the concentration of initiator (catalyst)  $i(t)$ , of monomer  $m(t)$ , of growing radicals having molecular weight between  $r$  and  $r + dr$ ,  $\phi(r, t)dr$ , and of terminated polymer having molecular weight between  $r$  and  $r + dr$ ,  $\psi(r, t)dr$ . Assuming termination by combination, the batch performance of such a polymerization system may be described following reference 19 by

$$\begin{aligned} \frac{\partial \phi(r, t)}{\partial t} + Gm \frac{\partial \phi(r, t)}{\partial r} &= \nu B i(t) \delta(r) - D \phi(r, t) \int \phi dr \\ \frac{\partial \psi(r, t)}{\partial t} &= \frac{D}{2} \int \phi(r', t) \phi(r - r', t) dr' \\ \frac{di(t)}{dt} &= -B i(t) \\ \frac{dm(t)}{dt} &= -Gm(t) \int \phi dr \end{aligned}$$

Here, the molecular weight is reckoned in monomer units,  $\nu$  is the number of radicals formed by each molecule of decomposing initiator, and  $B, G, D$  are rate constants for initiation, propagation, and termination, respectively. Again, introducing the moments of the size distributions

$$x_i = \int r^i \phi dr, y_j = \int r^j \psi dr$$

we find, (19) a set of batch kinetic equations in these moments and the concentrations  $i, m$ :

$$\begin{aligned} \frac{dx_0}{dt} &= \nu B i - D x_0^2 \\ \frac{dx_1}{dt} &= G m x_0 - D x_0 x_1 \\ \frac{dx_2}{dt} &= 2G m x_1 - D x_0 x_2 \\ \frac{dy_0}{dt} &= \frac{D}{2} x_0^2 \\ \frac{dy_1}{dt} &= D x_0 x_1 \\ \frac{dy_2}{dt} &= D (x_0 x_2 + x_1^2) \end{aligned}$$

$$\begin{aligned} \frac{dt}{dt} &= -Bt \\ \frac{dm}{dt} &= -Cm\alpha \end{aligned} \quad (5)$$

These serve as an eight dimensional version of (3), and we have corresponding to them an eight dimensional version of (4) in the distribution  $p(x_0, x_1, x_2, y_0, y_1, y_2, m, t)$ . From the distribution  $p$ , we may recover, say, the weight average molecular weight of radical together with polymer as

$$\frac{\int (x_2 + y_2) p dx_0 dx_1 dx_2 dy_0 dy_1 dy_2 dt dm}{\int (x_1 + y_1) p dx_0 dx_1 dx_2 dy_0 dy_1 dy_2 dt dm}$$

Entirely similar considerations may be applied to the study of such particulate systems as crystallization reaction.

Now the methods of solution of Equations (2) and (4) that are developed below apply regardless of the number of independent reaction variables, provided only that the kinetic expressions may be taken as polynomials in these reaction variables. They may accordingly furnish a useful guide to how the mixing interacts with strong nonlinearities in the kinetics, as in the crystallization nucleation rate, or with an independently varied critical feed stream, as in the initiator feed to polymerization reactors. We do not however present any results along these lines here, but reserve these studies for later report.

Solutions to Equation (2) for several simple reactions have been published (4, 7, 11). In the literature (11) a Monte Carlo method was used and (7) a direct numerical method was employed. A method will be described in this paper which allows one to obtain the moments of  $p(c)$  in a simpler way.

The authors want in no way to imply that the above model represents the real mixing processes in a turbulent reactor. These are far more complex and defy as yet an analytical description. The above model has, however, one important similarity to turbulent mixing. As will be shown below a concentration disturbance (in the absence of reaction) as computed from this model shows the same sort of decay as in isotropic turbulence, the variance (or the second moment) of the concentration in fluctuations in both cases decreasing exponentially with time. We furthermore do not claim that it is possible to predict a conversion accurately if  $\beta/\alpha$  is not very large. Our claim that this simplified model is useful in design is based on the fact that the behavior of the conversion with respect to  $\beta/\alpha$  reaches an asymptotic value for high values of  $\beta/\alpha$ . As long as  $\beta/\alpha$  during scale up stays large enough so that we remain in a region where our results are insensitive to  $\beta/\alpha$ , we have good justification to assume that a real mixing process will also be insensitive to mixing in the same range of mixing times. In the design of real stirred tank reactors we mostly deal with small deviations from complete mixing. To say that the results are insensitive to the value of  $\beta/\alpha$  provided  $\beta/\alpha$  is large enough is the same as assuming the vessel is ideally mixed. The method described above allows one to estimate the mixing intensity required to approach ideal mixing. Now even if the vessel is not ideally mixed, and the results depend on  $\beta/\alpha$ , as long as the deviations from ideal mixing are small, the above method should estimate these effects fairly accurately. The question that we still have to answer is how can we relate  $\beta/\alpha$  to an experimentally measurable quantity, or how can we estimate it in the absence of suitable measurements.

INTERPRETATION OF TRACER EXPERIMENTS

We are concerned here to attach an empirical interpretation to the mixing intensity parameter  $\beta$  of Equation (2) and its higher-dimensional analogues. This interpretation is to be found in the analysis of tracer mixing experiments, and we accordingly begin by writing (2), without the kinetic term, in the form

$$\begin{aligned} \frac{\partial p(c, t)}{\partial t} &= \alpha \{ p_0(c, t) - p(c, t) \} \\ &+ 2\beta \left\{ \iint p(c', t) p(c'', t) \right. \\ &\left. + \left( \frac{c' + c''}{2} - c \right) dc' dc'' - p(c, t) \right\} \end{aligned} \quad (6)$$

We may note at once that the information we want is contained in the statistical fluctuations of concentration about its mean. As far as mean values go, the mixing system (without reaction) behaves like a completely mixed vessel with input-output time constant  $\alpha$ .

Indeed, if we denote the mean concentration by

$$\mu(t) = \int c p(c, t) dt$$

we find from (6) that  $\mu$  satisfies the ordinary differential equation

$$\frac{d\mu}{dt} = \alpha(\mu_0 - \mu) \quad (7)$$

independent of  $\beta$ , where

$$\mu_0(t) = \int c p_0(c, t) dc$$

is the mean of the feed distribution  $p_0$ . And if we put a step of tracer into the feed of an initially tracer-free vessel, so that

$$p_0(c, t) = \delta(c - c_0); t > 0 \quad (8)$$

and

$$\mu(c) = 0 \quad (9)$$

we find from (7) that the mean tracer concentration in the vessel and its outlet is

$$\mu(t) = c_0(1 - e^{-\alpha t}) \quad (10)$$

the familiar stirred tank exponential response.

The first measure of the concentration fluctuation is given by its variance

$$\sigma^2(t) = \int \{c - \mu(t)\}^2 p(c, t) dc$$

and we find from Equations (6) and (7) that it satisfies the differential equation

$$\frac{d\sigma^2}{dt} = \alpha(\mu_0 - \mu)^2 + \alpha(\sigma_0^2 - \sigma^2) - \beta\sigma^2 \quad (11)$$

where

$$\sigma_0^2(t) = \int \{c - \mu_0(t)\}^2 p_0(c, t) dc$$

is the variance of the feed distribution. Again, with a step of tracer (8) in the feed of a vessel that is initially tracer-free, so that we have, besides, (9), the initial condition

$$\sigma^2(0) = 0 \quad (12)$$

we find by solving (11) and consulting (10) that the variance of tracer concentration in the vessel and its outlet

$$\sigma^2(t) = \alpha c_0^2 e^{-\alpha t} \frac{e^{-\alpha t} - e^{-\beta t}}{\beta - \alpha} \quad (13)$$

With careful monitoring of an output line, the expression for the variance in (13) may serve as a guide to the estimation of  $\beta$ . This variance rises from 0 to a maximum at

$$t = \frac{1}{\beta - \alpha} \ln \frac{\beta + \alpha}{2\alpha}$$

before decaying again to 0, and, with  $\alpha$  known, the bare location of this maximum will give some estimate of  $\beta$ , even without detailed knowledge of the variance history.

The step input experiments described above furnish perhaps the most convenient means for an empirical determination of  $\beta$ , although the underlying Equation (6) can readily be made to yield results appropriate to quite different experimental situations. Indeed, the most direct way of visualizing the effect of  $\beta$  is via a batch experiment with no input-output at all. If, in (6), we drop the input-output terms, we are left with (4)

$$\frac{\partial p(c, t)}{\partial t} = 2\beta \left\{ \iint p(c', t) p(c'', t) \delta \left( \frac{c' + c''}{2} - c \right) dc' dc'' - p(c, t) \right\} \quad (14)$$

and we may see from this equation that the mean tracer concentration is constant

$$\frac{d\mu}{dt} = 0$$

and that the variance decays according to

$$\frac{d\sigma^2}{dt} = -\beta\sigma^2 \quad (15)$$

Thus, in a pure batch experiment, where a quantity of tracer is injected initially into some portion of the vessel, the resulting inhomogeneity in the distribution of tracer in the vessel decays, as far as variance goes, according to

$$\sigma^2(t) = \sigma^2(0) e^{-\beta t}$$

that is, simply with the time constant  $\beta$ . According to this direct interpretation,  $\beta$  can be related to the characteristics of the turbulent flow in the vessel, and we shall review below these relations and their implication for the transiation of  $\beta$  from one scale of operation to another.

In order to get an experimental measurement of  $\beta$  we can therefore perform three types of experiments. One is to introduce an amount of tracer and measure the decay of the concentration fluctuations. The second is to introduce a step in tracer concentration and perform the same measurement. The third is in the case of multiple feeds to introduce a tracer in one of the feed streams only and measure the variance of the concentration fluctuations over the vessel at steady state. (The latter can also readily be computed.) In each case we need a method which is able to measure concentration fluctuations on a very small scale.

Two methods have been recently developed which should make an important contribution to our understanding of the mixing process in stirred tanks. One developed by Kim and Wilhelm (5) is based on the scattering of light due to gradients in the refractive index. The second by Bradley (2) uses fiber optics and colored tracers. As yet there have been very few actual studies

and it is hoped that in the near future more measurements will be available, enabling one to correlate  $\beta$  with agitator design.

It may be noted finally that each value of the mixing intensity  $\beta$  corresponds to a definite value of Zweitering's degree of segregation (17) in the reactor. Indeed, if we denote the degree of segregation by  $s$ , we have simply

$$s = \frac{\alpha}{\alpha + \beta}$$

with vanishing  $\beta$  giving complete segregation, and infinite  $\beta$ , complete mixing. Thus, an estimate of the degree of segregation, obtained perhaps by studying a particular reaction system (not first order), can be translated directly into an estimate of  $\beta$ .

#### APPLICATION OF TURBULENCE THEORY

The work of Batchelor (1) and Corrsin (3) and others on the application of the theory of turbulence to the scale-up of stirred tank reactors leads directly to an estimate of the mixing intensity  $\beta$  in terms of the large-scale properties of the turbulence. Accordingly, we recapitulate the basic results here, and discuss their bearing on the practical estimation of  $\beta$ . The analysis is all for a homogenous isotropic turbulence.

The development begins with the standard partial differential equation for Fick's law diffusion superimposed on turbulent convection in an isolated system, from which one argues in the usual way that

$$\frac{d\bar{c}^2}{dt} = -2D (\text{grad } c)^2$$

Here  $D$  is the molecular diffusivity,  $c$  is a concentration fluctuation, and the overbar denotes an average so that  $\bar{c}^2$  is simply the variance  $\sigma^2$  of concentration in a batch experiment. The mean square gradient in concentration fluctuation is related back to  $\sigma^2$  by introducing a microscale  $l_m$  for the turbulent mixing, according to which the mean square components of the concentration gradient all have the common value

$$\frac{1}{2} \frac{\partial \bar{c}^2}{\partial x} = \frac{1}{2} \frac{\partial \bar{c}^2}{\partial y} = \frac{1}{2} \frac{\partial \bar{c}^2}{\partial z} = \frac{\bar{c}^2}{l_m^2}$$

so that

$$(\text{grad } c)^2 = 6 \frac{\bar{c}^2}{l_m^2}$$

and

$$\frac{d\bar{c}^2}{dt} = -\frac{12D}{l_m^2} \bar{c}^2$$

This represents a simple exponential decay in variance, and consulting (15), we see that

$$\beta = \frac{12D}{l_m^2} \quad (16)$$

Information about the turbulent velocity field itself is however more naturally expressed in terms of the Taylor (dissipation) microscale  $l_m$  and of a corresponding Reynolds number  $R$ . The characteristic velocity appearing in this Reynolds number is the root mean square velocity fluctuation  $u$ . For an isotropic turbulence, this root mean square fluctuation is the same in each coordinate direction.

$$u_x = u_y = u_z = \frac{u}{\sqrt{3}}$$

and the appropriate Reynolds number is accordingly defined as

$$R = \frac{1}{\sqrt{3}} \frac{l_d u}{\nu} \quad (17)$$

where  $\nu$  is the (molecular) kinematic viscosity of the working fluid. The two microscales are related (approximately) by the fact that

$$\frac{l_m^2}{l_d^2} = \frac{2D}{\nu} \quad (18)$$

this relation being valid for  $R$  large, but  $D/\nu$  not too large. We may note, as a guide, that diffusivities in water are of the order of  $10^{-4}$  to  $10^{-5}$  sq. cm./sec., while the kinematic viscosity  $\nu$  is  $10^{-2}$  sq. cm./sec. In most practical liquid reaction problems  $D/\nu$  is less than or equal to unity. [Should  $D/\nu$  be large the literature (1) shows how the following analysis might be modified.]

Now the Taylor microscale  $l_d$  may be related to a characteristic linear dimension  $L$  of the mixing system as a whole (the paddle diameter, say, or the vessel diameter itself) by taking

$$\frac{l_d}{L} = \frac{A}{R}$$

or, applying the definition (17) of the Reynolds number  $R$ ,

$$\frac{l_d}{L} = \sqrt{3} \frac{A\nu}{l_d u} \quad (19)$$

Here  $A$  is an empirical parameter, independent of the scale of the mixing system, but varying from one mixing configuration to another. One would expect  $A$  to depend, for example, on the physical properties of the working fluid, on the shape of the stirrer in a mixed vessel, and on the ratio of stirrer diameter to vessel diameter, but to have the same value for geometrically similar mixing systems working on the same fluid.

The Taylor microscale  $l_d$  may also be related to the power input to the turbulent fluid. Using a conservative numerical factor, one takes the energy dissipation per unit mass of fluid to be  $10/3 \nu u^2/l_d^2$ , and, with an empirical efficiency factor  $\eta$ , one may identify this as the actual power input  $\epsilon$  to the mixing system per unit mass of working fluid

$$\epsilon = \frac{10}{3} \frac{\eta \nu u^3}{l_d^2} \quad (20)$$

The efficiency  $\eta$  measures that fraction of the power input to the system which goes directly to the turbulent velocity field (and is only later dissipated as heat), as distinct from that fraction which goes directly to heat. One would expect  $\eta$  also to be independent of the scale of the mixing system, but varying from one mixing configuration to another.

The basic physical relations in question are now contained in (17), (19), (20), and these may be solved directly for  $u$ ,  $l_d$ ,  $l_m$ . One finds

$$\left. \begin{aligned} u &= \left( \frac{0.27A^2}{\eta^3} \right)^{1/6} (\epsilon L)^{1/3} \\ l_d &= (10.0 A^2 \eta)^{1/6} \left( \frac{\nu^2 L^2}{\epsilon} \right)^{1/6} \\ l_m &= (80.0 A^2 \eta)^{1/6} \left( \frac{D^2 L^2}{\epsilon} \right)^{1/6} \end{aligned} \right\} \quad (21)$$

and, consulting (16)

$$\beta = \left( \frac{21.6}{A^2 \eta} \right)^{1/3} \left( \frac{\epsilon}{L^2} \right)^{1/3} \quad (22)$$

The first inference commonly drawn from (22) is that in order to keep the same reactor mixing properties on scale up, one should maintain similarity, and also keep the ratio  $\epsilon/L^2$  constant. In geometrically similar vessels, as  $\epsilon$  is proportional to  $N^3 L^2$ , this means keeping the agitator speed  $N$  constant during scale up. Also, since  $\epsilon$  is the power input per unit mass, keeping  $\epsilon/L^2$  constant amounts to making the actual power input proportional to  $L^3$ , a demand which often results in uncommonly high power requirements. More realistically, we may use (22) to give a numerical estimate of  $\beta$  for a specified reactor size  $L$  and power input per unit mass  $\epsilon$ , and then use the methods developed below to estimate the effect of this  $\beta$  on the reaction system in hand. To do this requires of course a knowledge of the constant  $A^2 \eta$ , but since this is scale-free, it can be estimated economically in small scale by means of the tracer experiments discussed above.

The dependence of  $\beta$  on  $\epsilon$  and  $L$  shown in (22) might of course also have been obtained by a straightforward dimensional argument. But the analysis based on turbulence theory leads also to some idea of the actual numerical magnitudes involved that may serve as a useful guide to practice in the absence of the tracer experiments suggested above. From work in wind tunnels and in pipe flows, Corrsin cites the (approximate) values

$$A \sim 20, \eta \sim 1/2$$

so that (22) gives

$$\beta \sim \frac{1}{2} \left( \frac{\epsilon}{L^2} \right)^{1/3} \quad (23)$$

In a typical commercial application, with  $L = 100$  cm.,  $\epsilon = 2 \times 10^4$  sq. cm./sec.<sup>3</sup> (1 h.p./100 gal. of water), Equation (23) gives  $\beta \sim .63$  1/sec. It may be noted that with these same numerical values, (21) gives for the root mean square velocity fluctuation,  $u \sim 340$  cm./sec., a plausible figure for the circulation velocity in the vessel (which in this context we identify with the turbulent velocity fluctuation).

In agitated vessels both  $A$  and  $\eta$  should strongly depend on agitator design and one would need more accurate studies before one could really predict  $A$  and  $\eta$  on the basis of the geometrical design of the vessel.

There are several studies available on the effect of agitator design on overall mixing time. Van De Vusse (13) measured mixing time by observing the disappearance of large scale refractive index gradients via a Schlieren method. While this is not the same as the tracer experiment described in this section, we can still get an estimate of  $\beta$ , by writing

$$\beta = \frac{m}{\tau_m}$$

where the constant of proportionality  $m$  depends on the sensitivity of the method used to determine the time of complete mixing ( $m$  should vary from 1 to 5). Choosing  $m = 1$  gives a real lower bound on  $\beta$ , and this is exactly what is needed in our case.

For a baffled completely stirred turbo or paddle mixer, Van De Vusse recommends a scale up equation derived by dimensional arguments which is exactly equivalent to Equation (22). If one compares values of  $\beta$  estimated from Van De Vusse's work to Equation (23) one finds that the values from (23) are too high. However, one should remember that Van De Vusse measured disappearance of a dye, and that by choosing  $\beta = 1/\tau_m$ , we made a very conservative estimate of  $\beta$ . In view of this

the experimental results are really in surprisingly good agreement with our *a priori* estimate.

Van De Vusse's data correlate well with

$$\beta \sim 0.1 \left( \frac{c}{L^2} \right)^{1/3}$$

As said before the constant in this correlation strongly depends on agitator design and should preferably be either measured or in the absence of more accurate data estimated from the literature (13). In case a high value of  $\beta$  is desirable strong emphasis should be given to correct agitator design and correct placement of the feed pipes. Multiple agitators and multiple feed points can increase the value of  $\beta$  considerably.

**CALCULATION OF REACTOR PERFORMANCE**

We are concerned here to establish a systematic way of solving Equation (2) and its higher-dimensional analogues such as Equation (4) under conditions of steady state reactor operation. These equations seem in general to be very difficult to solve, and since our interest commonly centers on high mixing rates, we proceed by expansion in powers of  $\alpha/\beta$ . What results is a succession of linear integral equations in the successive contributions to the overall  $p$ , and while these don't seem to be easily solvable either, they do lead to sets of linear algebraic equations in the moments of the successive contributions to  $p$ . The procedure closes, that is, it gives at each level of approximation a self-contained set of equations in a finite number of leading moments, provided the rate expressions (1), (3) and so on are polynomials. The resulting linear equations in the moments can be solved by standard means. The overall average reactor performance is found finally by adding up the contributions to the first moments of  $p$ .

We begin with the one dimensional Equation (2). We drop the time dependence, introduce a neutral variable  $x$  to stand for concentration, yield or whatever, and divide through by the input-output time constant  $\alpha$  to find for the distribution  $p$

$$\frac{d}{dx} \{f(x)p(x)\} = p_0(x) - (1 + \lambda)p(x) + \lambda \int \int p(x')p(x'') \delta\left(\frac{x'+x''}{2} - x\right) dx'dx'' \quad (24)$$

Here  $p_0(x)$  represents the feed distribution, commonly  $\delta(x - x_0)$  for a suitable  $x_0$ ,  $f(x)$  is the rate expression normalized on  $\alpha$ , and

$$\lambda = \frac{2\beta}{\alpha} \quad (25)$$

is a dimensionless mixing intensity. The first result we want from (24) is an overall average material balance. If we denote the moments of  $p$  by

$$\mu_n = \int x^n p(x) dx$$

and those of  $p_0$  by

$$\mu_{n,0} = \int x^n p_0(x) dx$$

we find this material balance by multiplying (24) through by  $x$  and integrating

$$- \int f(x) p(x) dx = \mu_{1,0} - \mu \quad (26)$$

We note also here that  $p(x)$  is to be a properly normalized probability density, so that

$$\int p(x) dx = 1 \quad (27)$$

If  $f$  is a polynomial of degree  $N$ , then (26) furnishes an overall relation among the first  $N$  moments of  $p$ . In particular, for a first order reaction with rate constant  $k$ , where  $x$  is the concentration of reagent so that  $f(x) = -kx/\alpha$ , we find for the mean reagent concentration in vessel and outlet the standard result:

$$\mu = \frac{\mu_{1,0}}{1 + \frac{k}{\alpha}}$$

(independent of the mixing intensity  $\beta$ ), where  $\mu_{1,0}$  is the mean reagent concentration in the feed.

In general, however,  $p$  (but not  $p_0$ ) and its moments depend on the mixing intensity, and we proceed by expanding (24), (26), (27) in powers of  $1/\lambda$ . We remind ourselves that in almost all practical applications  $\lambda$  is huge as compared to unity, and we therefore expect such an expansion to converge fairly rapidly.

We write formally

$$p(x) = \sum_{j=0}^{\infty} \frac{1}{\lambda^j} p^{(j)}(x) \quad (28)$$

and

$$\mu_n = \sum_{j=0}^{\infty} \frac{1}{\lambda^j} \mu_n^{(j)} \quad (29)$$

so that

$$\mu_n^{(j)} = \int x^n p^{(j)}(x) dx \quad (30)$$

Bringing (28) to (24) and equating coefficients in  $\lambda$  gives for  $p^{(0)}$

$$p^{(0)}(x) - \int \int p^{(0)}(x')p^{(0)}(x'') \delta\left(\frac{x'+x''}{2} - x\right) dx'dx'' = 0 \quad (31)$$

for  $p^{(1)}$

$$p^{(1)}(x) - 2 \int \int p^{(0)}(x')p^{(0)}(x'') \delta\left(\frac{x'+x''}{2} - x\right) dx'dx'' = p_0(x) - p^{(0)}(x) - \frac{d}{dx} \{f(x)p^{(0)}(x)\} \quad (32)$$

and for the higher  $p^{(j)}$

$$p^{(j)}(x) - 2 \int \int p^{(0)}(x')p^{(j)}(x'') \delta\left(\frac{x'+x''}{2} - x\right) dx'dx'' = \sum_{i=1}^{j-1} \int \int p^{(i)}(x')p^{(j-i)}(x'') \delta\left(\frac{x'+x''}{2} - x\right) dx'dx'' - p^{(j-1)}(x) - \frac{d}{dx} \{f(x)p^{(j-1)}(x)\}; j = 2, 3, \dots \quad (33)$$

Similarly, bringing (28) and (29) to (26) and equating coefficients in  $\lambda$  gives in  $p^{(0)}$

$$\mu_1^{(0)} - \int f(x)p^{(0)}(x) dx = \mu_{1,0} \quad (34)$$

and in the higher  $p^{(j)}$

$$\mu_1^{(j)} - \int f(x)p^{(j)}(x) dx = 0; j = 1, 2, \dots \quad (35)$$

Finally from (27), we have that

$$\mu_0^{(0)} = 1 \quad (36)$$

while

$$\mu_0^{(j)} = 0; \quad j = 1, 2, \dots \quad (37)$$

Now the equation (31) in  $p^{(0)}$  simply represents the behavior of the perfectly mixed reactor (infinite  $\beta$ ), and its solution is

$$p^{(0)}(x) = \delta[x - \mu_1^{(0)}] \quad (38)$$

which satisfies the normalization (36). The mean value  $\mu_1^{(0)}$  is determined by the overall material balance (34)

$$\mu_1^{(0)} - f[\mu_1^{(0)}] = \mu_{1;0} \quad (39)$$

With  $p^{(0)}$  in hand, we may attack the equation (32) in the first correction  $p^{(1)}$  by taking partial moments (30), that is, by multiplying through by successive powers of  $x$  and integrating. We find, taking due account of (37), linear algebraic equations in the  $\mu_n^{(1)}$  of the form

$$\left(1 - \frac{1}{2^{n-1}}\right) \mu_n^{(1)} - \frac{1}{2^{n-1}} \sum_{m=1}^{n-1} \binom{n}{m} [\mu_1^{(0)}]^{n-m} \mu_m^{(1)} \\ = \mu_{n;0} - [\mu_1^{(0)}]^n + n[\mu_1^{(0)}]^{n-1} f[\mu_1^{(0)}]; \quad n = 2, 3, \dots \quad (40)$$

there being no information in the moment equations for  $n = 1$ . This loss of information is however made up by the overall material balance (35) for  $j = 1$ .

$$\mu_1^{(1)} - \int f(x) p^{(1)}(x) dx = 0 \quad (41)$$

If  $f$  is a polynomial of degree  $N$ , Equation (41) is another independent relation among the first  $N$  moments of  $p^{(1)}$ , and taking it together with the Equations (40) for  $n = 2, 3, \dots, N$ , we find a set of  $N$  linear algebraic equations in  $\mu_1^{(1)}, \dots, \mu_N^{(1)}$  which can be solved by standard numerical means. With these first  $N$  moments in hand, as many further moments as desired can be generated by taking (40) for  $n = N + 1, N + 2$ , etc., in turn.

The same procedure applies to the higher  $p^{(j)}$  of (33). Taking moments, we find a set of algebraic equations very much like (40), indeed having the same left hand sides

$$\left(1 - \frac{1}{2^{n-1}}\right) \mu_n^{(j)} - \frac{1}{2^{n-1}} \sum_{m=1}^{n-1} \binom{n}{m} [\mu_1^{(0)}]^{n-m} \mu_m^{(j)} \\ = \sum_{i=1}^{j-1} \sum_{m=1}^{n-1} \binom{n}{m} \mu_m^{(i)} \mu_{n-m}^{(j-i)} \\ - \mu_n^{(j-1)} + n \int x^{n-1} f(x) p^{(j-1)}(x) dx \\ n = 2, 3, \dots \\ j = 2, 3, \dots \quad (42)$$

the right hand sides for each  $j$  involving moments of the earlier  $p^{(i)}$ . Again, there is no information in the moment equations for  $n = 1$ , but if  $f$  is a polynomial of degree  $N$ , we find for each  $j$  a closed set of equations in  $\mu_1^{(j)}, \mu_2^{(j)}, \dots, \mu_N^{(j)}$  by taking Equation (42) for  $n = 2, 3, \dots, N$  together with (35). As before, once the first  $N$  moments of  $p^{(j)}$  have been found, as many higher moments as desired can be generated by taking (42) for  $n = N + 1, N + 2$  etc. It should be noted that the integral term on the right hand side of (42) leads to a certain cascading in the number of earlier moments required as we go to successive values of  $j$ . Thus, with  $f$  of degree  $N$ , we need:  $2N - 1$  moments of  $p^{(1)}$  to find  $N$  moments of  $p^{(2)}$ ;  $3N - 2$  moments of  $p^{(1)}$  to find  $(2N - 1)$  moments of  $p^{(2)}$  to find  $N$  moments of  $p^{(3)}$ ; etc. But since higher

moments can be found at will, this causes no special difficulty. Finally, having evaluated the partial moments for as many  $j$  as desired, we may see explicitly the effect of the mixing intensity on the overall performance of the reactor from (29).

$$\mu_1 = \mu_1^{(0)} + \frac{1}{\lambda} \mu_1^{(1)} + \frac{1}{\lambda^2} \mu_1^{(2)} + \dots \quad (43)$$

This completes our solution of the one-dimensional equation (24). Entirely similar considerations apply to the higher dimensional versions of (2) such as (4). For the working equation, we have in place of (24)

$$\sum_{r=1}^R \frac{\partial}{\partial x_r} \{f_r(x) p(x)\} = p_0(x) - (1 + \lambda) p(x) \\ + \lambda \int \int p(x') p(x'') \delta \left( \frac{x' + x''}{2} - x \right) dx' dx'' \quad (44)$$

where  $x$  stands for  $(x_1, x_2, \dots, x_R)$ ,  $dx$  for the volume element  $dx_1, dx_2, \dots, dx_R$ , and the  $\delta$ -symbol for the appropriate product of  $\delta$ -functions. The moments of  $p$  are now multidimensional, and we denote them

$$\mu_{n_1 n_2 \dots n_R} = \int x_1^{n_1} x_2^{n_2} \dots x_R^{n_R} p(x) dx$$

with

$$\mu_{n_1 n_2 \dots n_R; 0} = \int x_1^{n_1} x_2^{n_2} \dots x_R^{n_R} p_0(x) dx$$

There are now  $R$  overall material balances in place of (26)

$$- \int f_1(x) p(x) dx = \mu_{10 \dots 0} - \mu_{10 \dots 0} \\ - \int f_R(x) p(x) dx = \mu_{00 \dots 10} - \mu_{00 \dots 10} \quad (45)$$

and these determine entirely the average behavior of the system for first order kinetics. The single normalization condition (27) stands.

The expansion (28) applied to (44) leads to (31) for  $p^{(0)}$ , to

$$p^{(1)}(x) - 2 \int \int p^{(0)}(x') p^{(1)}(x'') \delta \left( \frac{x' + x''}{2} - x \right) dx' dx'' \\ = p_0(x) - p^{(0)}(x) - \sum_{r=1}^R \frac{\partial}{\partial x_r} \{f_r(x) p^{(0)}(x)\} \quad (46)$$

for  $p^{(1)}$ , and to

$$p^{(j)}(x) - 2 \int \int p^{(0)}(x') p^{(j)}(x'') \delta \left( \frac{x' + x''}{2} - x \right) dx' dx'' \\ = \sum_{i=1}^{j-1} \int \int p^{(i)}(x') p^{(j-i)}(x'') \delta \left( \frac{x' + x''}{2} - x \right) dx' dx'' \\ - p^{(j-1)}(x) - \sum_{r=1}^R \frac{\partial}{\partial x_r} \{f_r(x) p^{(j-1)}(x)\}; \quad j = 2, 3, \dots \quad (47)$$

for the higher  $p^{(j)}$ . The moment expansions

$$\mu_{n_1 n_2 \dots n_R} = \sum_{j=0}^{\infty} \frac{1}{\lambda^j} \mu_{n_1 n_2 \dots n_R}^{(j)} \quad (48)$$

with

$$\mu_{n_1 n_2 \dots n_R}^{(j)} = \int x_1^{n_1} x_2^{n_2} \dots x_R^{n_R} p^{(j)}(x) dx \quad (49)$$

applied to the material balance (45) give  $R$  equations in  $p^{(0)}$

$$\mu_{10 \dots 0} - \int f_1(x) p^{(0)}(x) dx = \mu_{10 \dots 0} - \mu_{10 \dots 0}$$

$$\mu_{00\dots 1}^{(0)} - \int f_R(x) p^{(0)}(x) dx = \mu_{00\dots 1;0} \quad (50)$$

and  $R$  equations in each of the higher  $p^{(j)}$

$$\begin{aligned} \mu_{10\dots 0}^{(j)} - \int f_1(x) p^{(j)}(x) dx &= 0 \\ \mu_{00\dots 1}^{(j)} - \int f_R(x) p^{(j)}(x) dx &= 0 \end{aligned} \quad j = 1, 2, \dots \quad (51)$$

Finally, the moment expansions applied to the normalization (27) give

$$\mu_{00\dots 0}^{(0)} = 1 \quad (52)$$

and

$$\mu_{00\dots 0}^{(j)} = 0; \quad j = 1, 2, \dots \quad (53)$$

The Equation (31) in  $p^{(0)}$  is solved just as for one dimension. We have

$$p^{(0)}(x) = \delta(x_1 - \mu_{10\dots 0}^{(0)}) \dots \delta(x_R - \mu_{00\dots 1}^{(0)}) \quad (54)$$

satisfying the normalization (52), with the  $R$  first moments determined by the  $R$  material balances (50).

$$\begin{aligned} \mu_{10\dots 0}^{(0)} - f_1[\mu_{10\dots 0}^{(0)}, \dots, \mu_{00\dots 1}^{(0)}] &= \mu_{10\dots 0;0} \\ \mu_{00\dots 1}^{(0)} - f_R[\mu_{10\dots 0}^{(0)}, \dots, \mu_{00\dots 1}^{(0)}] &= \mu_{00\dots 1;0} \end{aligned} \quad (55)$$

For the first correction  $p^{(1)}$ , we take moments. We find from (46)

$$\begin{aligned} \mu_{n_1 n_2 \dots n_R}^{(1)} - \frac{1}{2^{n_1 + \dots + n_R - 1}} \sum_{m_1=0}^{n_1} \binom{n_1}{m_1} [\mu_{10\dots 0}^{(0)}]^{n_1 - m_1} \dots \sum_{m_R=0}^{n_R} \binom{n_R}{m_R} [\mu_{00\dots 1}^{(0)}]^{n_R - m_R} \mu_{m_1 m_2 \dots m_R}^{(1)} \\ = \mu_{n_1 n_2 \dots n_R; 0} - [\mu_{10\dots 0}^{(0)}]^{n_1} \dots [\mu_{00\dots 1}^{(0)}]^{n_R} \\ + n_1 [\mu_{10\dots 0}^{(0)}]^{n_1 - 1} \dots [\mu_{00\dots 1}^{(0)}]^{n_R} \\ f_1[\mu_{10\dots 0}^{(0)}, \dots, \mu_{00\dots 1}^{(0)}] + \dots \\ + n_R [\mu_{10\dots 0}^{(0)}]^{n_1} \dots [\mu_{00\dots 1}^{(0)}]^{n_R - 1} \\ f_R[\mu_{10\dots 0}^{(0)}, \dots, \mu_{00\dots 1}^{(0)}] \end{aligned} \quad n_1 + n_2 + \dots + n_R > 1 \quad (56)$$

Again, the leading term in the sum on the left hand side disappears by virtue of the normalization (53), and we find no information in the equations for  $n_1 + n_2 + \dots + n_R = 1$ . Assuming these  $f_r$  to be polynomials, each of degree  $\leq N$  in each argument, this deficiency is made up as in the 1 dimensional case by taking the Equations (56) with  $n_1, n_2, \dots, n_R$  each running from 0 to  $N$  (but excluding  $n_1 + n_2 + \dots + n_R = 0, 1$ ), and adjoining to them the  $R$  balance equations (51) for  $j = 1$ . What results is a self-contained set of  $NR + R - 1$  linear algebraic equations in the leading moments of  $p^{(1)}$ . Even in complex cases, this is by no means a very large number for standard numerical methods. Thus, for the polymerization kinetics (5), with  $N = 2$  and  $R = 8$ , we would have only 23 equations.

The procedure may as before be extended to the higher  $p^{(j)}$  by taking moments in (47). We find

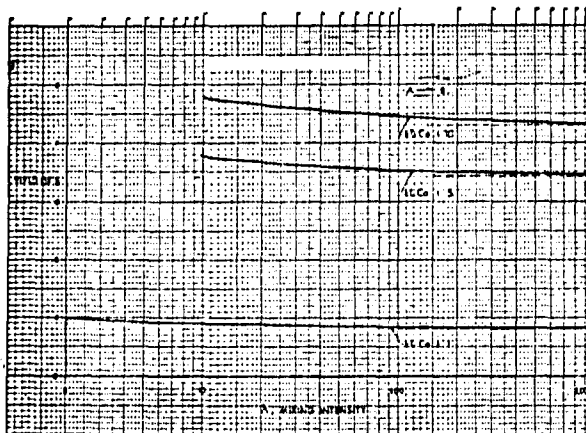


Fig. 1. Second order reactions;  $2A \rightarrow 2B$ . ----- Asymptotic values.

$$\begin{aligned} \mu_{n_1 n_2 \dots n_R}^{(j)} - \frac{1}{2^{n_1 + \dots + n_R - 1}} \sum_{m_1=0}^{n_1} \binom{n_1}{m_1} (\mu_{10\dots 0}^{(0)})^{n_1 - m_1} \dots \sum_{m_R=0}^{n_R} \binom{n_R}{m_R} (\mu_{00\dots 1}^{(0)})^{n_R - m_R} \mu_{m_1 m_2 \dots m_R}^{(j)} \\ = \sum_{i=1}^{j-1} \frac{1}{2^{n_1 + \dots + n_R}} \sum_{m_1=0}^{n_1} \binom{n_1}{m_1} \dots \sum_{m_R=0}^{n_R} \binom{n_R}{m_R} \mu_{m_1 \dots m_R}^{(i)} \mu_{n_1 - m_1 \dots n_R - m_R}^{(j-i)} \\ + \sum_{r=1}^R n_r \int x_1^{n_1} \dots x_r^{n_r - 1} \dots x_r^{n_r} f_r(x) p^{(j-1)}(x) dx \end{aligned} \quad n_1 + n_2 + \dots + n_R > 1 \quad j = 2, 3, \dots \quad (57)$$

and for polynomial  $f_r$  these equations can again be closed off by applying the overall balance (51) and the normalization condition (53). There is again, as we take successive values of  $j$ , a cascading requirement for the number of moments of the earlier  $p_j$ , but these can as before be generated in turn once each basic set of equations for the leading moments has been solved. Finally, having evalu-

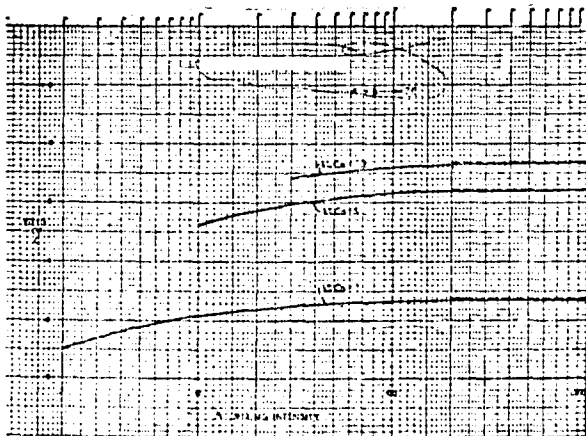


Fig. 2. Bimolecular reactions;  $A + B \rightarrow 2C$ . Separate feeds for A and B,  $p_0(x, y) = 1/2[\delta(x-2)\delta(y) + \delta(x)\delta(y-2)]$ ,  $C_0 = 1/2x_0 = 1/2y_0 = 1$ . ----- Asymptotic values.

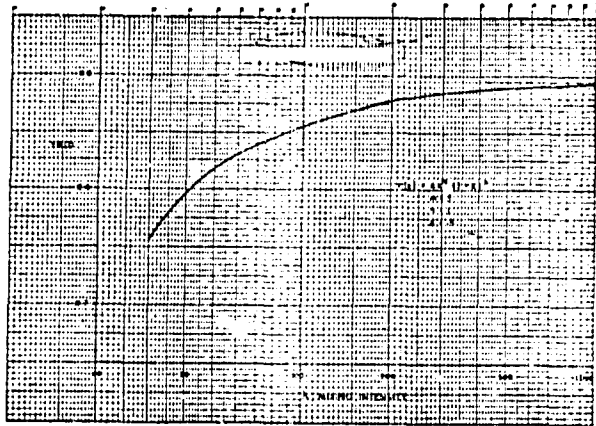


Fig. 3. Adiabatic reactions;  $x$  = concentration of product, yield =  $x$  averaged over contents of vessel. ----- Asymptotic values.

ated the partial moments for as many  $f$  as desired, we may see explicitly the effect of the mixing intensity on the overall reactor performance by assembling the  $R$  first moments from (48).

$$\mu_{10} \dots 0 = \mu_{10}^{(0)} + \frac{1}{\lambda} \mu_{10}^{(1)} + \frac{1}{\lambda^2} \mu_{10}^{(2)} + \dots$$

$$\mu_{00} \dots 1 = \mu_{00}^{(0)} + \frac{1}{\lambda} \mu_{00}^{(1)} + \frac{1}{\lambda^2} \mu_{00}^{(2)} + \dots \quad (58)$$

This concludes our development of the solution to the reactor performance equations for high mixing intensity, and the series expansions and moment methods developed here are applied below to the calculation of reactor behavior for some common reaction systems. It might be noted that similar results can be developed for low mixing intensity by expanding the basic equations in powers of  $\beta/\alpha$ , that is, in powers of the  $\lambda$  of (25) rather than  $1/\lambda$ . What results is a hierarchy of differential rather than integral equations in the successive contributions to  $p$ , the leading term being that corresponding to a completely segregated reactor. Moment methods are no longer appropriate, and indeed the successive (linear) differential equations can readily be solved: directly, for the one-dimensional case; via characteristics, for higher dimension. The methods are quite straightforward, and the results are

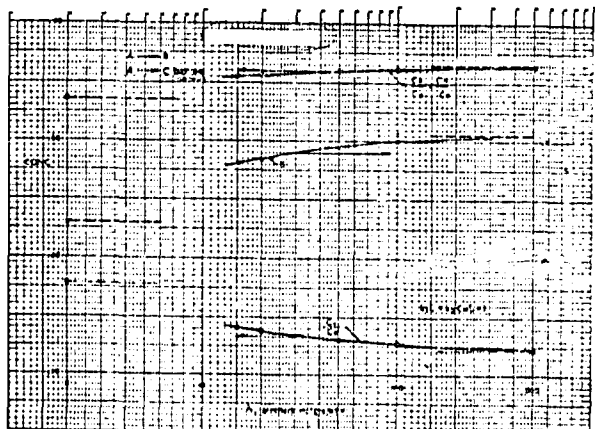


Fig. 4. Parallel reactions;  $A \rightarrow B$ ; rate constant  $k_1$ ,  $2A \rightarrow 2C$ ; rate constant  $k_2$ .  $S = C_B/C_0 - C_A$ , selectivity. ----- Asymptotic values.

not quoted here. In practical design problems  $\lambda$  is almost invariably large as compared to unity, and the results for small values of  $\lambda$  are therefore of little interest in our context.

#### DISCUSSION AND EXAMPLES

One can now summarize the preceding discussions into a design procedure for stirred tank reactors.

The first and most important point is to determine whether deviations from complete mixing will have a detrimental effect. Quite often the opposite is true. Thus for example in a homogeneous premixed second-order reaction a degree of segregation different from zero would improve conversion. Several authors have therefore pointed out that assuming complete mixing will lead to an overestimate of the required volume. The authors do not agree to this as in our experience most agitated vessels are very close to complete mixing. It is not practical to control the mixing so that it should be incomplete, while maintaining good agitation heat transfer. If no agitation is necessary then we should a priori use a plug flow reactor in such a case. If mixing is necessary and it is further desirable to minimize the variance of the residence time distribution then this can be achieved by using a cascade of stirred tanks or similar devices. Therefore the main problem in designing or scaling up a stirred tank reactor is to decide whether small deviations from complete mixing have a detrimental effect or not.

In Figure 1 the effect of  $\lambda = 2\beta/\alpha$  on conversion is plotted for some typical cases of a second-order reaction. We note that for values of  $\lambda$  larger than 100 the conversion is already insensitive to variation of  $\lambda$ . This is not the case for  $\lambda$  close to unity, but in stirred tank reactors such low values are quite uncommon. Consider again a practical example. For a 10 liter vessel with a standard turbine agitator and power input the low estimate of  $\beta$  according to the literature (13) would be 0.05 to 0.1 sec.<sup>-1</sup>. A value of  $\lambda$  of 5 would mean a residence time of 50 sec. For a 10,000 liter vessel the lowest estimate of  $\beta$  under the same condition would be 0.01 to 0.02 and a value of  $\lambda = 5$  would correspond to 250 sec. residence time.

As we stated already our main problem in the design and scale up of stirred tank reactors concerns reactions on which a too low value of  $\lambda$  is detrimental. The simplest such case would be a reaction whose total order is less than unity. Such reactions are very scarce in liquid homogenous systems and again the effect of  $\lambda$  is small.\*

Another fairly simple case is where two reactants enter the vessel in two separate feed pipes. In Figure 2 the conversion for a simple irreversible second-order reaction with separate feeds is plotted as a function of  $\lambda$ . Again the effect is small for values of  $\lambda$  over 100.

Here however, in very large vessels the effect would lead to a significant reduction of  $\lambda$  and should be evaluated quantitatively.

A second case with similar features is an autothermic reaction, in which a cold feed is introduced into a hot reaction mixture. Again in this case incomplete mixing always reduces the conversion. In Figure 3 a numerical example of the effect of  $\lambda$  on one typical autothermic reaction is given. In computing the effect of  $\alpha$  on the reaction we made use of a method introduced by Spalding (10), namely the fact that for most exothermic adiabatic reac-

\* Several authors have discussed the case of a zero order reaction. The assumption of a zero order reaction is however a simplified description of the limiting reaction velocity of catalytic reaction at high pressures. These reactions are not zero order at high conversions, where the effect of  $\lambda$  would be noticeable. Furthermore, our method (as well as Zwietering's) does not apply to heterogeneous catalytic reactions.



tions the effect of conversion on reaction rate can with sufficient accuracy be described by

$$\frac{dx}{dt} = A(1-x)^n(x+\epsilon)^m \quad (59)$$

The constants  $n$  and  $m$  are determined by a best fit to the actual reaction rate dependence which normally contains an exponential term, such as

$$\frac{dx}{dt} = A(1-x)^n e^{-E/RT} = A(1-x)^n e^{-E/RT_0}(1+\alpha x) \quad (60)$$

Spalding has shown that for most exothermic reactions the mistake made in writing (59) instead of an Arrhenius relation is small. Equation (59) has the advantage that it can be treated by the moment method of the preceding section.

A low value of  $\lambda$  leads always to a lower conversion and the effect is quite pronounced. However for values of  $\alpha$  larger than 100 the effect of  $\beta$  again becomes small.

These last cases are examples of a broad class of cases in which the only effect of a low value of  $\alpha$  is a reduced conversion. We can always compensate for this by a larger residence time, and in fact we might want to compare the cost of intense mixing to the cost of an increased residence time. A quantitative evaluation, similar to the one in the examples given, will lead to a conservative design procedure as long as we use a conservative estimation procedure for  $\lambda$ .

A simple example of the second class of problems in which a low value of  $\lambda$  might change the quality of the product is given in Figure 4, where the reaction is assumed to consist of two parallel reactions of different order [for an example see (14)]. As the undesired reaction is of a higher order, the concentration of the reactant should be as low as possible everywhere. A low value of  $\lambda$  will therefore favor the undesirable side reaction.

If the side product is not separated, and the conversion is high the reduction of  $\lambda$  due to scale up might have a serious effect. One notes here, that just increasing the residence time without changing the intensity of agitation will not be sufficient, as the side reaction will occur in the concentrated region near the inlet. There is a whole class of reactions of this type, and what complicates this case further is the fact that in many cases the exact mechanism and kinetics of all the possible side reactions is unknown. As another example of this type one might mention reactions in which the pH is controlled by acid addition and where high pH in the nonmixed region might cause side reactions.

If the kinetics of all possible undesired side reactions is at least approximately known then the above methods can be used to estimate the minimum value of  $\lambda$  necessary to guarantee the specifications. Sometimes it might turn out to be impractical to obtain a sufficiently high value of  $\lambda$  in a very large tank and several parallel smaller reactors might provide simpler and cheaper solution.

One might also want to investigate ways of increasing  $\lambda$  by improving both the design of the agitator and the design of the feed distribution. It is unfortunate that we do not possess sufficiently accurate data for the effect of the feed distribution on agitator design. But it is apparent that using multiple agitators (single or multiple shaft) and multiple feed injection for each agitator, we can considerably increase  $\lambda$  without increasing the energy consumption.

Similar considerations apply to the case of systems with nucleation, in which the effect of  $\lambda$  might be the most pronounced, as even with relatively very low concentration

fluctuations all the nucleation might occur in the small unmixed region. This will be discussed in detail in a future paper.

One last and somewhat discouraging conclusion that we can draw from the above discussion is that direct empirical evaluation of the effect of agitator design on complex reactions is impossible in the pilot plant. If a reaction is sensitive to mixing time then this sensitivity is a strong function of  $\beta$  and therefore a reaction might be insensitive to agitator design in the pilot plant while it is very sensitive to correct agitator design in the large scale plant. This by the way is true of other systems sensitive to agitator design (9).

#### ACKNOWLEDGMENT

The work reported here was supported under AFOSR Grant No. 821-67. Some of the work reported here is a part of the research carried out by J. J. Evangelista in partial fulfillment of the requirements for the Ph.D. at The City University of New York.

#### NOTATION

- $A$  = empirical parameter appearing in Equation (19)
- $A$  = rate constant in autothermic reaction expression
- $a, b$  = bounds on concentration
- $B$  = rate constant for initiation step in polymerization scheme
- $C_A$  = outlet concentration of A
- $C_B$  = outlet concentration of B
- $C_C$  = outlet concentration of C
- $c$  = concentration
- $c', c''$  = dummy variables
- $C_0$  = concentration of A in feed
- $D$  = molecular diffusivity
- $D$  = rate constant for termination step in polymerization scheme
- $f$  = rate expression
- $f_r$  = rate expression,  $r = 1, 2, \dots, R$
- $G$  = rate constant for propagation step in polymerization scheme
- $i(t)$  = initiator concentration
- $k$  = reaction rate constant
- $L$  = characteristic length of the mixing system
- $l_d$  = Taylor (dissipation) microscale
- $l_m$  = microscale for turbulent mixing
- $m$  = constant of proportionality
- $m$  = exponent in approximate rate expression for autothermic reaction
- $m(t)$  = monomer concentration
- $N$  = agitator speed, rev./min.
- $N$  = degree of polynomial  $f$
- $n$  = exponent in approximate rate expression for autothermic reaction
- $n_r$  = integer in moment definition;  $r = 1, 2, \dots, R$
- $p$  = concentration distribution
- $p_0$  = concentration distribution for the feed
- $p^j$  =  $j$ th term in expansion of  $p$
- $R$  = Reynolds number
- $R$  = number of independent concentration variables
- $r$  = batch rate expression
- $r$  = linear dimension of crystal
- $r$  = molecular weight
- $s$  = degree of segregation
- $s$  = batch rate expression
- $t$  = time
- $u$  = root mean square of velocity fluctuation
- $u_x$  =  $x$ -component of  $u$
- $u_y$  =  $y$ -component of  $u$
- $u_z$  =  $z$ -component of  $u$

- $x$  = cartesian coordinate  
 $x$  = progress variable  
 $\tau$  =  $j$ th moment of size distribution of growing polymer chains  
 $x', x''$  = dummy variables  
 $y$  = cartesian coordinate  
 $y$  = progress variable  
 $y_j$  =  $j$ th moment of size distribution of terminated polymer  
 $y', y''$  = dummy variables  
 $z$  = cartesian coordinate

#### Greek Letters

- $\alpha$  = inverse of nominal residence time  
 $\beta$  = measure of agglomerative mixing intensity  
 $\epsilon$  = actual power input to mixing system per unit mass of fluid  
 $\eta$  = empirical efficiency parameter  
 $\lambda$  = mixing inequality parameter,  $= 2\beta/\alpha$   
 $\mu$  = mean concentration  
 $\mu_0$  = mean feed concentration  
 $\mu_n$  =  $n$ th moment of  $p$   
 $\mu_{n0}$  =  $n$ th moment of  $p_0$   
 $\mu_{n1}$  =  $n$ th moment of  $p^1$   
 $\nu$  = kinematic viscosity of working fluid  
 $\nu$  = number of radicals formed by each molecule of decomposing initiator  
 $\sigma^2$  = variance of concentration distribution  
 $\sigma_0^2$  = variance of feed distribution  
 $\tau$  = mean residence time  
 $\tau_m$  = mixing time

- $\dagger$  = concentration distribution of growing polymer chains  
 $\psi$  = concentration distribution of terminated polymer

#### LITERATURE CITED

1. Batchelor, G. K., *J. Fluid Mech.*, **5**, 113 (1959).
2. Brodkey, R. S., and J. O. Nye, *Rev. Sci. Instr.*, **34**, 1080 (1963).
3. ———, and J. Lee, *AIChE J.*, **10**, 167 (1964).
4. Corrsin, S., *ibid.*, **3**, 329 (1957); **10**, 670 (1964).
5. Curl, R. L., *AIChE J.*, **9**, 175 (1963).
6. ———, Y. C., and R. H. Wilhelm, Preprint 26B, Fifty-sixth Annual Meeting of the AIChE, Houston, Texas.
7. Rietema, K., *Advan. Chem. Eng.*, **5**, (1964).
8. Shain, S., *AIChE J.*, **12**, 806 (1966).
9. Shtinnar, R., *J. Fluid Mech.*, **10**, Pt. 2, 259 (1961).
10. ———, and J. M. Church, *Ind. Eng. Chem.*, **52**, 253 (1960); **53**, 479 (1961).
11. Spalding, D. B., *Combustion Flame*, **1**, 287, 296 (1957).
12. Spielman, L. A., and O. Levenspiel, *Chem. Eng. Sci.*, **20**, 241 (1965).
13. Tadmor, Z., and A. Biesenberger, *Ind. Eng. Chem. Fundamentals*, **5**, 336 (1966).
14. Von de Vusse, J. G., *Chem. Eng. Sci.*, **4**, 178, 209 (1955).
15. *ibid.*, **17**, 507, 1962.
16. Weinstein, H., and R. J. Adler, *Chem. Eng. Sci.*, **22**, 65 (1967).
17. Warrell, G. R., and L. C. Eagleton, *Can. J. Chem. Eng.*, **43**, 254 (Dec. 1964).
18. Zwietering, Th. N., *Chem. Eng. Sci.*, **11**, No. 1, 1 (1959).
19. Kattan, A., and R. J. Adler, *AIChE J.*, **13**, 589 (1967).
20. Saidel, G. M., and S. Katz, *ibid.*, **319** (1967).

Manuscript received October 11, 1967; revision received June 28, 1968; paper accepted July 18, 1968

Reprinted from  
**Twelfth Symposium (International) on Combustion**

© 1969 The Combustion Institute  
Union Trust Bldg. Pittsburgh, Penna.

PRINTED IN THE UNITED STATES OF AMERICA

## THE EFFECT OF IMPERFECT MIXING ON STIRRED COMBUSTION REACTORS

JOHN J. EVANGELISTA, REUEL SHINNAR, AND STANLEY KATZ

*Department of Chemical Engineering, The City College, City University of New York, New York City*

Mixed gas reactors, even when special pains have been taken to ensure good mixing, often depart quite noticeably from the ideal of instantaneous mixing on the micro-scale. The present paper offers a quantitative measure of the extent of this departure, and shows how it is related to the reactor performance.

The intensity of the mixing is characterized by a single parameter that measures the time scale of decay of nonuniformities in composition in the reactor. This is related to the design parameters of a gas reactor by dimensional arguments drawn from the theory of isotropic turbulence. The analysis of reactor performance is carried out in terms of a coalescence model for the micro-mixing that incorporates this time scale. The mixing model is borrowed from chemical engineering studies.

Calculations are presented for adiabatic reaction systems, showing the shift in the effective reaction-rate curve, and especially the reduction in blow-out limit, with decreasing mixing intensity. Such calculations permit one to see how high a mixing intensity is needed to approximate perfect mixing, and how this level depends on the reaction kinetics.

### 1. Introduction

The concept of an ideally stirred reactor has had several important applications in combustion. A spherical adiabatic combustor has been introduced by Longwell to study the kinetics of fast reactions,<sup>1</sup> and in the interpretation of the data one normally assumes that the reactor is ideally mixed. It has also been observed<sup>2-4</sup> that an ideally stirred tank might be a useful simplified description of some industrial combustors. The concept of an ideally stirred reactor has also contributed considerably to our understanding of the stability and control of autothermic reactors.<sup>2,5</sup>

It is quite obvious that a perfectly stirred reactor is an ideal concept that can be only approached, but not reached, since real mixing processes occur at a finite rate. In Longwell's spherical reactor, considerable effort went into the design to approach instantaneous mixing. This is not true in industrial combustors, where the mixing is much less intense. The question then arises as to what effect the imperfect mixing has on the performance of such a reactor, and a general discussion of this point is given in Refs. 2 and 3. It has been shown further<sup>13</sup> that, even for a small spherical reactor as used in kinetic studies, mixing processes are important. Thus, the blow-out velocity was shown to be considerably influenced by injector design, and some empirical

correlations based on pressure drop were suggested to compensate for this effect.

Real stirred reactors may also deviate from the ideal by having residence-time distributions that are not in the (Poisson) exponential form. Such deviations are reported in Ref. 16. It is the authors' experience that, by suitable placement of inlet and outlet, it is almost always possible to achieve a residence-time distribution closely approaching that of a stirred tank. The present paper, accordingly, confines itself to the situation where perfect mixing at the macro-scale has been essentially achieved, and develops methods that permit one to make quantitative estimates of the effect of imperfect mixing at the micro-scale.

Admittedly, turbulent combustion is a very complex process and cannot be given a complete analytical description. However, in a well-designed reactor, mixing intensities are very high and the mixing time is very short as compared to the residence time. In a previous publication,<sup>6</sup> it was shown that a rather simple stochastic mixing model allows one to simulate the basic features of the real turbulent mixing process. For such an ideal turbulent mixing process, it is possible to compute both the steady and the dynamic behavior of many complex reaction systems, and for small deviations from complete mixing, one can reasonably hope that the results of such computation will predict quite well how

far the performance of the actual combustor should deviate from an ideal one. From this, one gets reasonable estimates as to the mixing intensity required to achieve conditions close to ideal mixing. In Ref. 6, this was applied to the behavior of reactors stirred by turbines commonly used in the chemical industry. In particular, it was shown that the mixing intensity necessary to approach ideal mixing strongly depends upon the kinetics of the reaction. The same method is applied here to combustion reactors.

## 2. The Mixing Processes

While there is a considerable body of experimental investigations on the mixing performance of mechanical agitators, there are few data on the quantitative aspects of mixing in gas reactors of the Longwell type. It has been shown<sup>14</sup> that considerable recirculation exists. Furthermore, mixing of a jet introduced into a stagnant fluid has been studied extensively. Now, it was shown<sup>6</sup> in that, for mechanically agitated reactors, purely theoretical estimates of the mixing time are in reasonably good agreement with the experimental results. It is therefore reasonable to hope that the same methods should lead to reasonable estimates in the present case.

The mixing pattern can be divided into two parts. One is the macro-motion of the fluid, introduced by the jets, that should cause a circulation in the reactor. The second is the dissipation of local concentration fluctuations by turbulence. One of the first conditions for good over-all mixing is that the jets have sufficient energy so that their penetration length into the reactor is very large as compared to reactor diameter, so that the turbulent energy is not dissipated near the entrance of the jet. In a highly agitated reactor, the turbulent motion on a small scale becomes quite uniform and locally isotropic.<sup>15</sup> For such cases, one can estimate the mixing time by the methods derived by Batchelor<sup>8</sup> and Corrsin.<sup>11</sup> These methods lead to an exponential decay in the variance of an initial concentration non-uniformity in the vessel, and we identify the characteristic time of this decay with the micro-mixing time.

The turbulence theory estimate of the micro-mixing time we quote from Corrsin,<sup>11</sup> as reworked in Ref. 6. It appears first that, if a nonuniformity in concentration is described by its variance  $\sigma^2$ , that is, by the mean-square departure of the concentration from its average value, then a homogeneous isotropic turbulent mixing gives rise to an exponential decay in  $\sigma^2$ . That is, there is associated with the turbulent system a mixing

rate (intensity)  $\beta$ , such that

$$d\sigma^2/dt = -\beta\sigma^2.$$

An initial nonuniformity  $\sigma_0^2$  thus decays in time according to

$$\sigma^2(t) = \sigma_0^2 \exp(-\beta t),$$

and we may regard  $1/\beta$  as a micro-mixing time.

For a fully developed turbulence, Corrsin estimates the mixing intensity  $\beta$  in the form

$$\beta = \text{const. } (\epsilon/L^2)^{1/3}, \quad (2.1)$$

where  $\epsilon$  is the power input per unit mass of working fluid, and  $L$  a characteristic linear dimension of the mixing system as a whole. The constant in (2.1) is a mixture of empirical parameters, involving an estimate of the Taylor micro-scale of the turbulent velocity field, and an estimate of how efficiently the power input is transformed into the kinetic energy of the turbulent fluid. This constant may be expected to be independent of the scale of the mixing system, but to vary from one mixing configuration to another. One would expect it to depend, for example, upon the physical properties of the gas, the shape of the vessel, and the configuration of inlet jets and outlet ports, but to have the same value for geometrically similar mixing systems working on the same gas.

The form of (2.1), of course, might also have been obtained by a straightforward dimensional argument. But the analysis based on turbulence theory leads also to some idea of the actual numerical magnitudes involved that may serve as a useful guide to practice. From work in wind tunnels and in pipe flows, Corrsin finds (approximately)

$$\beta \approx \frac{1}{2} (\epsilon/L^2)^{1/3}. \quad (2.2)$$

This concludes Corrsin's argument from turbulence theory, which applies very generally, regardless of the source of the energy that supports the turbulence. For mixing of a gas reactor by its feed jets, we may rework it into a more convenient form. Suppose, accordingly, the vessel is fed by a system of jets at inlet velocity  $v$ , through a total cross-section area  $S$ . The energy input per unit mass in the reactor may then be written

$$\epsilon = Sv \cdot \frac{1}{2} v^2 / \frac{1}{6} \pi L^3. \quad (2.3)$$

(We take  $L$  to be an equivalent spherical diameter for the vessel.) We may also identify the flow rate per unit volume of reactor (reciprocal mean

residence time) as

$$\alpha = Sv/\frac{1}{4}\pi L^3. \quad (2.4)$$

Eliminating  $v$  and  $\epsilon$  among (2.2)–(2.4) gives

$$\beta/\alpha \approx \frac{1}{4}(L^2/S)^{2/3}, \quad (2.5)$$

which relates the mixing intensity  $\beta$  directly to the jet design parameter  $L^2/S$ .

A good many different designs of spherical reactors have been used for kinetic studies, with reported values of  $L^2/S$  ranging from 30 to 3000. The values of  $\beta/\alpha$  estimated from (2.5) would accordingly vary approximately from 2.5 to 50. In deriving (2.5), the fluid was assumed to be incompressible, but compressibility effects can readily be introduced. One should also note that, in comparing differently sized reactors with the same mean residence time (that is, the same  $\alpha$ ), constant  $L^2/S$  (constant  $\beta/\alpha$ ) requires  $v/L$  to remain constant. Thus, the necessary pressure drop through the injector increases with increasing reactor size. For short residence times, it is much easier to achieve high mixing rates in a small reactor, provided of course the size is large enough to ensure a highly turbulent flow.

The above dimensional considerations lead to quite reliable relations for comparison of geometrically similar reactors of different size at high Reynolds number. They also allow some estimate of the highest mixing rates possible under optimum design conditions.

It must be noted that the empirical constant  $\frac{1}{4}$  in (2.5) cannot be taken as anything more than a rough indication of order of magnitude. Its real value will depend strongly upon the geometrical design, and  $\beta/\alpha$  therefore will depend not only upon  $L^2/S$  but also upon the number and location of the jets. The constant in (2.5) should be determined at need for a given mixing configuration by suitable tracer experiments. Some of these are discussed in Sec. 3.

### 3. The Reactor Model

The reactor model used here is a coalescence model introduced by Curl,<sup>12</sup> and used by him and others in studies of mixed reactor performance, and of two-phase mixing. Briefly, it regards the reacting mass as made up of a large number of equally sized parcels of material ("particles"), that from time to time undergo independent pair collisions, equalize concentrations, and then separate. Between collisions, each parcel of fluid behaves like a little batch reactor. Fresh material is fed at a constant rate, and the withdrawal takes

a representative cut of the contents of the vessel. While, in two-phase mixing studies, these particles may have a definite material identity, they might perhaps better be regarded for the present purpose as primitive representations of turbulent eddies.

If we consider, for concreteness, a single reaction where the concentration  $c$  of reagent behaves in batch according to

$$dc/dt = r(c), \quad (3.1)$$

then we may describe the contents of the reactor at any time  $t$  by the concentration distribution  $p(c, t)$  of particles at that time. Technically speaking,  $p$  is a probability density in  $c$ , with

$$\int_a^b p(c, t) dc$$

giving the proportion of particles having concentration between  $a$  and  $b$  at time  $t$ . The distribution  $p$ , according to what has been said, satisfies the integro-differential equation

$$\begin{aligned} & [\partial p(c, t)/\partial t] + (\partial/\partial c)\{r(c)p(c, t)\} \\ &= \alpha\{p_0(c, t) - p(c, t)\} + 2\beta \left\{ \iint p(c', t)p(c'', t) \right. \\ & \quad \left. \times \delta[\frac{1}{2}(c' + c'') - c] dc' dc'' - p(c, t) \right\}, \quad (3.2) \end{aligned}$$

where  $p_0(c, t)$  is the concentration distribution for the feed,  $1/\alpha$  the nominal residence time of material in the tank, and  $\beta$  a measure of the coalescence rate (mixing intensity). The mean concentration of reagent in the vessel and outlet is simply the first moment of  $p$ , and this is the working measure of over-all reactor performance for a given kinetic system. Information about the random fluctuations in a turbulent mixing system is given by the higher moments. As indicated in Ref. 6, a similar equation can be developed for the appropriate multi-dimensional distribution  $p$  when several reactions are going on simultaneously.

The parameter  $\alpha$  in (3.2) is just the flow rate per unit reactor volume, as in Sec. 2, and it will appear that the mixing intensity  $\beta$  also has the same meaning as in Sec. 2. These points emerge from a consideration of conceptual tracer experiments on the model. We give only a sketch of the results here, since they are worked out in detail in Ref. 6.

The connection of the  $\beta$  of (3.2) with that of Sec. 2 may be seen by adapting (3.2) to the situation of an isolated vessel ( $\alpha = 0$ ) with no

chemical reaction going on ( $r = 0$ ), but with the mixing intensity maintained somehow at the level  $\beta$ . If we define the mean concentration by

$$\bar{c}(t) = \int cp(c, t) dc,$$

and the variance by

$$\sigma^2(t) = \int (c - \bar{c})^2 p(c, t) dc,$$

the reduced form of (3.2) gives: first, that  $\bar{c}$  is, as it must be, constant; and second, that

$$d\sigma^2/dt = -\beta\sigma^2,$$

so that the variance of an initial inhomogeneity in concentration decays exponentially, and this  $\beta$  may be identified with the  $\beta$  of (2.2) or of (2.5).

A more reasonable kind of tracer experiment for gas reactors is one in which a step in tracer concentration is switched into the feed line of a tracer-free vessel at time 0, and the resulting tracer concentration measured at the outlet. This we may analyze by suppressing the reaction term in (3.2), taking the inlet concentration distribution in the form

$$p_0(c, t) = \delta(c - c_0) \quad t > 0,$$

and taking the initial concentration distribution in vessel and outlet to be

$$p(c, 0) = \delta(c).$$

We find then:

$$\bar{c}(t) = c_0[1 - \exp(-\alpha t)]$$

$$\sigma^2(t) = \alpha c_0^2 \exp(-\alpha t)$$

$$\times \{[\exp(-\alpha t) - \exp(-\beta t)]/(\beta - \alpha)\}.$$

The exponential response for  $\bar{c}$  indicates that the vessel is, on the macro-scale, well-mixed, with input-output time constant  $\alpha$ . The response for  $\sigma^2$  contains information about  $\beta$ , and, with careful monitoring of an output line, as perhaps with the colored tracers and fiber optics techniques of Brodkey,<sup>9,10</sup> it may serve as a guide to the measurement of  $\beta$ . Thus,  $\sigma^2$  rises from 0 to a maximum at

$$t = (\beta - \alpha)^{-1} \ln [(\beta + \alpha)/2\alpha]$$

before decaying again to 0, and, with  $\alpha$  known, the

bare location of this maximum will give some estimate of  $\beta$ , even without detailed knowledge of the variance history.

We turn now to a consideration of methods of solving (3.2) so as to ascertain the effect of  $\beta$  on the reactor performance. We are concerned here only with single reactions, and we work accordingly in terms of the conversion  $x$  rather than the concentration  $c$ . In place of (3.1), we write

$$dx/dt = r(x), \quad (3.3)$$

and, in place of (3.2),

$$\begin{aligned} & [\partial p(x, t)/\partial t] + (\partial/\partial x)\{r(x)p(x, t)\} \\ & = \alpha\{\delta(x) - p(x, t)\} + 2\beta \left\{ \iint p(u, t)p(v, t) \right. \\ & \quad \left. \times \delta[\frac{1}{2}(u+v) - x] du dv - p(x, t) \right\}, \quad (3.4) \end{aligned}$$

where the inlet distribution  $\delta(x)$  represents a feed of unconverted material.

The rate function  $r(x)$  in (3.3) represents the reaction rate normalized on the inlet concentration of reagent. For  $n$ th order isothermal kinetics, we have accordingly

$$r(x) = k \cdot (1 - x)^n. \quad (3.5)$$

Allowing dependence on temperature in the usual Arrhenius form, we have

$$r = A \exp(-E/RT) \cdot (1 - x)^n,$$

where  $T$  is the absolute temperature, and  $E$  the activation energy. For adiabatic operation, temperature may be directly related to conversion in the usual way, and we find

$$\begin{aligned} r(x) = A \exp\left(\frac{-E/RT_i}{1 + [(T_f - T_i)/T_i] \cdot x}\right) \\ \cdot (1 - x)^n, \quad (3.6) \end{aligned}$$

where  $T_i$  is the inlet temperature, and  $T_f$  the temperature reached at complete conversion. The rate expression (3.6) is analytically rather intractable, and for exothermic reactions, where  $E/RT_i$  may be of the order of 20 to 80, and  $(T_f - T_i)/T_i$  of the order of 2 to 6, Spalding<sup>7</sup> has suggested that it may be usefully approximated in the form

$$r(x) = k \cdot (x + \epsilon)^m \cdot (1 - x)^n. \quad (3.7)$$

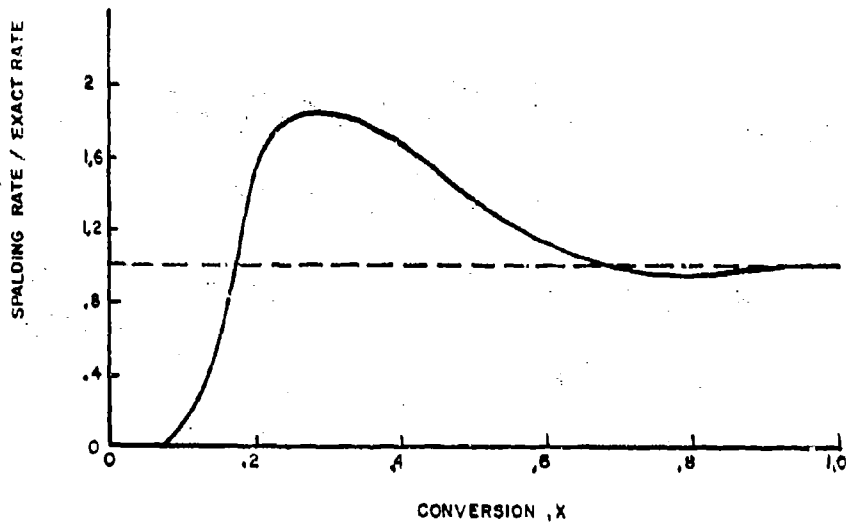
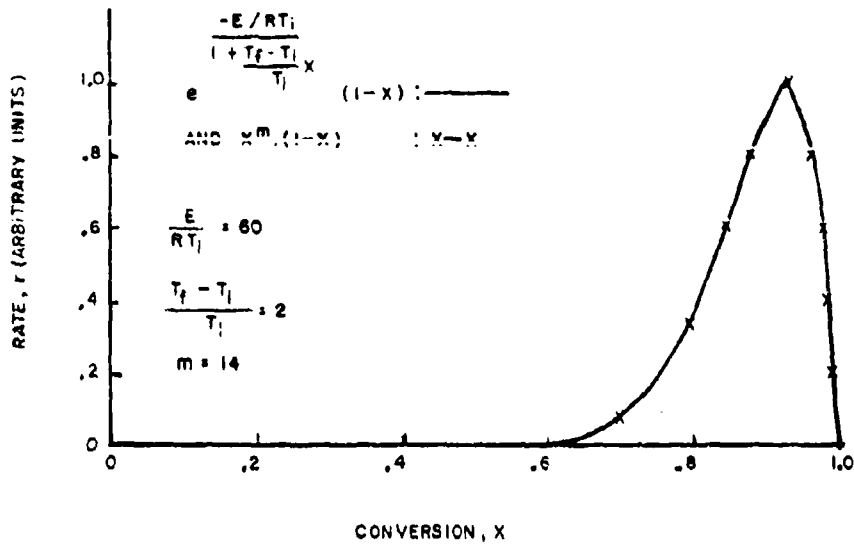


FIG. 1. Approximate rate expressions.

The parameter  $\epsilon$  might be taken equal to zero

$$r(x) = k \cdot x^m \cdot (1 - x)^n \quad (3.8)$$

if one were not especially interested in capturing the low conversion behavior. A comparison be-

tween (3.6) and (3.8) in a representative situation is shown in Fig. 1.

With any of the forms [(3.5), (3.7), (3.8)], the rate expression  $r(x)$  may be written

$$r(x) = k \cdot f(x),$$



where, provided  $m$  and  $n$  are whole numbers,  $f$  is a polynomial in  $x$ . Equation (3.4) may then be written

$$\alpha^{-1}[\partial p(x, t)/\partial t] + (k/\alpha)(\partial/\partial x)\{f(x)p(x, t)\} \\ = \delta(x) - p(x, t) + (2\beta/\alpha) \left\{ \iint p(u, t)p(v, t) \right. \\ \left. \times \delta[\frac{1}{2}(u+v) - x] du dv - p(x, t) \right\}. \quad (3.9)$$

With  $t$  scaled on  $\alpha^{-1}$ , the behavior of the system for any given form of  $f(x)$  is seen to be controlled by the dimensionless mixing intensity  $\beta/\alpha$  and the dimensionless flow rate  $\alpha/k$ . The polynomial character of  $f$  greatly simplifies the solution of (3.9). The results discussed in Sec. 4 are all for the kinetic form (3.8).

Since our interest centers in high values of the mixing intensity  $\beta$ , our principal method of dealing with (3.9) is by expansion in powers of  $1/\beta$ . We work with the steady-state solutions, and give only a sketch of the methods here, since they are laid out in detail in Ref. 6. It is convenient to take the expansion in the form

$$p(x) = p^{(0)}(x) + (\alpha/2\beta)p^{(1)}(x) + \dots, \quad (3.10)$$

where  $p^{(0)}(x)$  is the distribution in the ideally mixed limit (infinite  $\beta$ )

$$p^{(0)}(x) = \delta(x - \xi),$$

with  $\xi$  given by solving

$$f(\xi) = (\alpha/k)\xi. \quad (3.11)$$

We may work in turn with the stable and the unstable solutions of (3.11). In any case, the distribution  $p^{(1)}$  is characterized in terms of its moments

$$\mu_n^{(1)} = \int x^n p^{(1)}(x) dx, \quad n = 1, 2, \dots$$

and, when  $f$  is a polynomial of degree  $N$ , we find, on bringing (3.10) to (3.9), a set of linear algebraic equations in these moments

$$\left(1 - \frac{1}{2^{n-1}}\right) \mu_n^{(1)} - \frac{1}{2^{n-1}} \sum_{m=1}^{n-1} \binom{n}{m} \xi^{n-m} \mu_m^{(1)} \\ = (n-1)\xi^n, \quad n = 2, 3, \dots, N$$

which, together with the over-all material balance

$$\int f(x)p^{(1)}(x) dx = (\alpha/k)\mu_1^{(1)},$$

forms a self-contained system in  $\mu_1^{(1)}, \mu_2^{(1)}, \dots, \mu_N^{(1)}$  that can be readily solved by standard numerical methods. In Ref. 6, it is shown how the expansion (3.10) can be carried to terms of higher order in  $\alpha/\beta$ , and how the whole procedure can be extended to situations where several reactions are proceeding simultaneously.

The method sketched above produced the body of results discussed in Sec. 4. However, these results were spot-checked to estimate the range of validity of the expansion (3.10), and to test the dynamic stability of the solutions by another method formally independent of the size of the mixing intensity  $\beta$ . This method consists of developing moment equations from (3.9), and closing them off into a self-contained set by assuming a suitable function form for  $p$ . It proceeds by taking moments

$$\mu_n(t) = \int x^n p(x, t) dx$$

in Eq. (3.9)

$$\alpha^{-1}(d\mu_n/dt) = n(k/\alpha) \int x^{n-1} f(x)p(x, t) dx - \mu_n \\ + (2\beta/\alpha) \left\{ \frac{1}{2^n} \sum_{m=0}^n \binom{n}{m} \mu_m \mu_{n-m} - \mu_n \right\}. \\ n = 1, 2, \dots. \quad (3.12)$$

For polynomial  $f$ , the integral term on the right-hand side of Eq. (3.12) is a linear combination of moments, in general, of order  $> n$ . However, the order can be reduced by imagining a convenient functional form for  $p$ , and expressing higher moments in terms of lower in a way suggested by this form. A suitable functional form here is the  $B$ -function distribution

$$p(x, t) = [x^{a(t)-1}(1-x)^{b(t)-1}] / \{B[a(t), b(t)]\}$$

with

$$\mu_n = [B(a+n, b)] / [B(a, b)],$$

so that all moments of order  $> 2$  may be expressed in terms of  $\mu_1, \mu_2$ . This moment-closing approximation can be brought to Eq. (3.12), and gives, on dropping the time term, algebraic equations for the steady-state mean and variance. Transient solutions and linearized stability analyses were also carried out in this way.

It may be noted here that we do not suggest

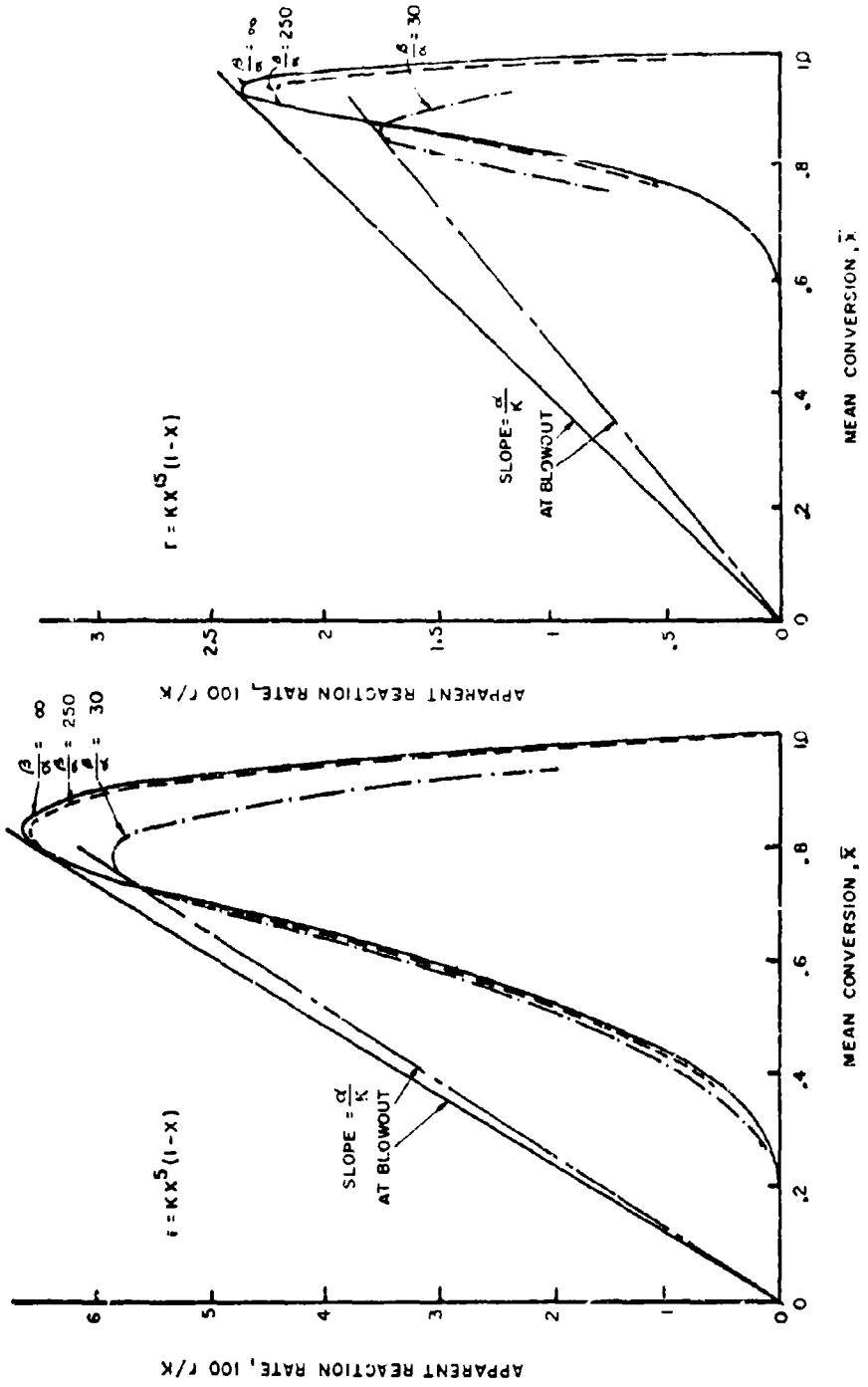


Fig. 2. Effect of mixing intensity on apparent reaction rate; various mixing intensities of  $\beta/\alpha$ ; various kinetic parameters  $m$ .

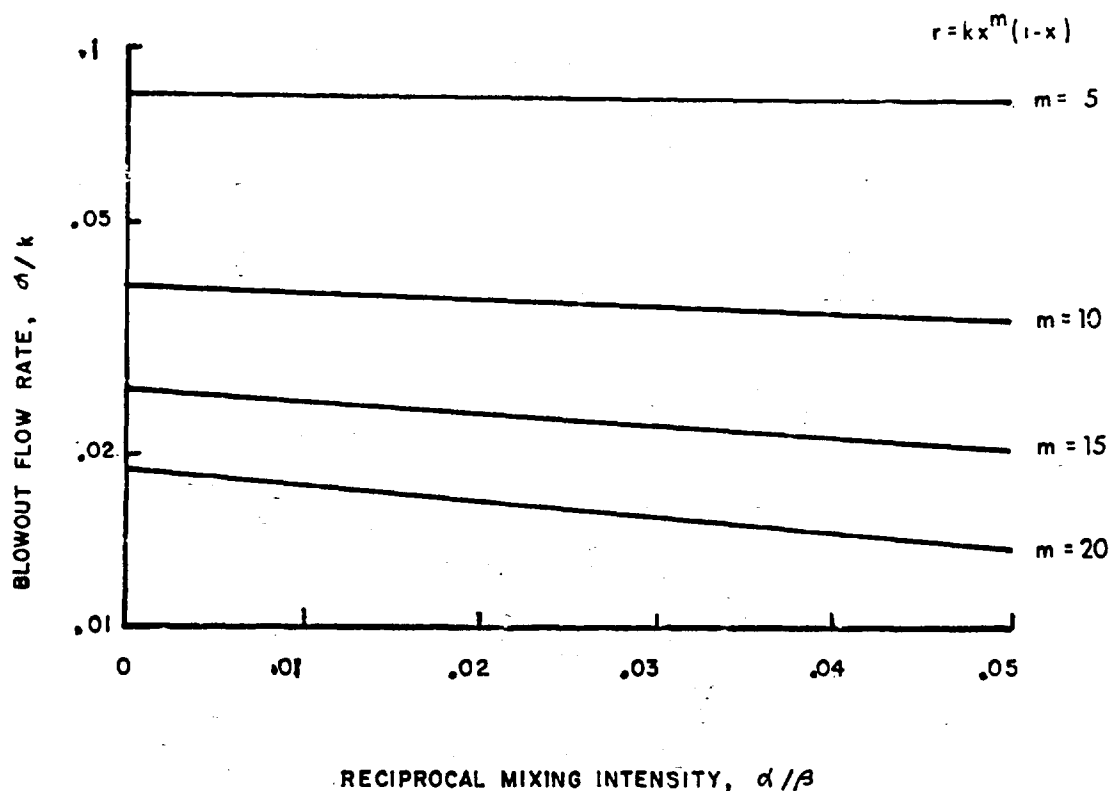


FIG. 3. Effect of mixing intensity on blow-out limit; various kinetic parameters ( $m$ ).

that the model discussed in the foregoing represents the real mixing processes in a turbulent reactor. These are far more complex, and defy as yet an analytical description. However, the model has one important similarity to turbulent mixing—the exponential decay of an initial concentration inhomogeneity. We do not believe that the model will predict conversion accurately unless  $\beta/\alpha$  is very large (or very small). However, conversion goes asymptotically to the limit of ideal mixing as  $\beta/\alpha$  goes to infinity, and we think that the model captures enough of the basic physical behavior of the mixing to tell us how large  $\beta/\alpha$  need be to validate the assumption of perfect mixing, and in what way departures from this level are likely to damage the reactor performance.

#### 4. Applications

For any given form of reaction rate, it is possible once and for all to compute the effect of imperfect mixing, and exhibit it in a generalized form, by plotting the conversion as a function of the mixing intensity  $\beta/\alpha$ , for different levels of the throughput  $\alpha/k$ . (Here, the mixing intensity  $\beta$  is normalized on the reciprocal mean residence time  $\alpha$ , and  $\alpha$  itself (which measures the throughput) is normalized on the kinetic parameter  $k$  that

serves as a time constant for the reaction.) However, autothermic reaction rates may depend upon composition in so many different forms that we give here only the results for one typical class of cases. These results are based on the Spalding approximation for exothermic reaction rates discussed in Sec. 3, according to which the reaction rate under adiabatic conditions can be expressed as a function of conversion  $x$  in the form

$$r(x) = kx^m(1-x)^n.$$

Figures 2-4 show the results of a number of calculations based on the approximate kinetics over a range of values of  $n$ , and with  $m = 1$ . Similar curves, of course, can be developed for higher values of  $n$ .

Figure 2 shows how the effective reaction rate curve, taken in the dimensionless form  $r(x)/k$ , is shifted under the influence of the mixing intensity  $\beta/\alpha$ . These curves are obtained by calculating the average conversions according to the methods of Sec. 3, and plotting them along lines whose slope is the corresponding  $\alpha/k$ . Three steady states are obtained for each operating condition, the intermediate one being unstable just as for complete mixing (and the lowest representing, to this kinetic approximation, no conversion). For each

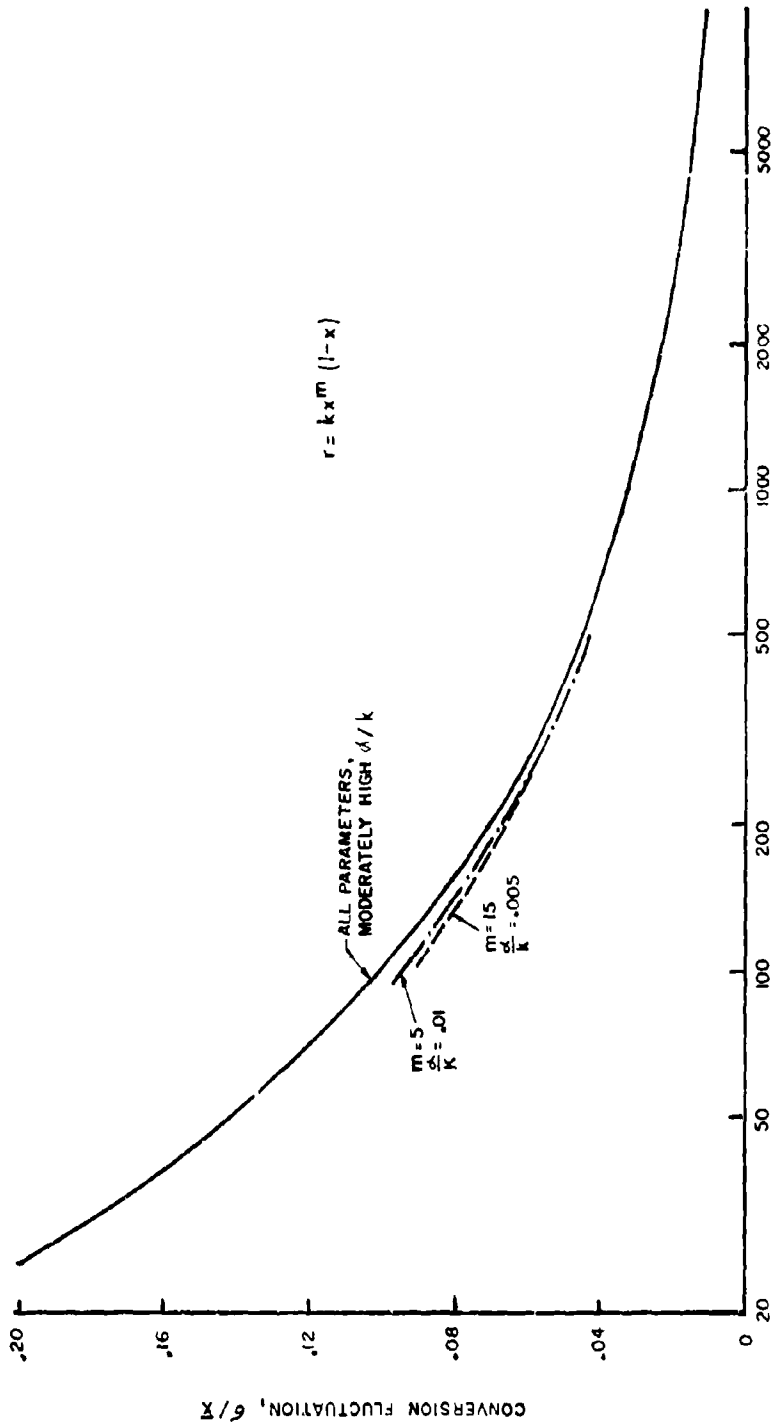


Fig. 4. Effect of mixing intensity on fluctuations in conversion; various throughput rates to  $k$ , various kinetic parameters  $m$ .

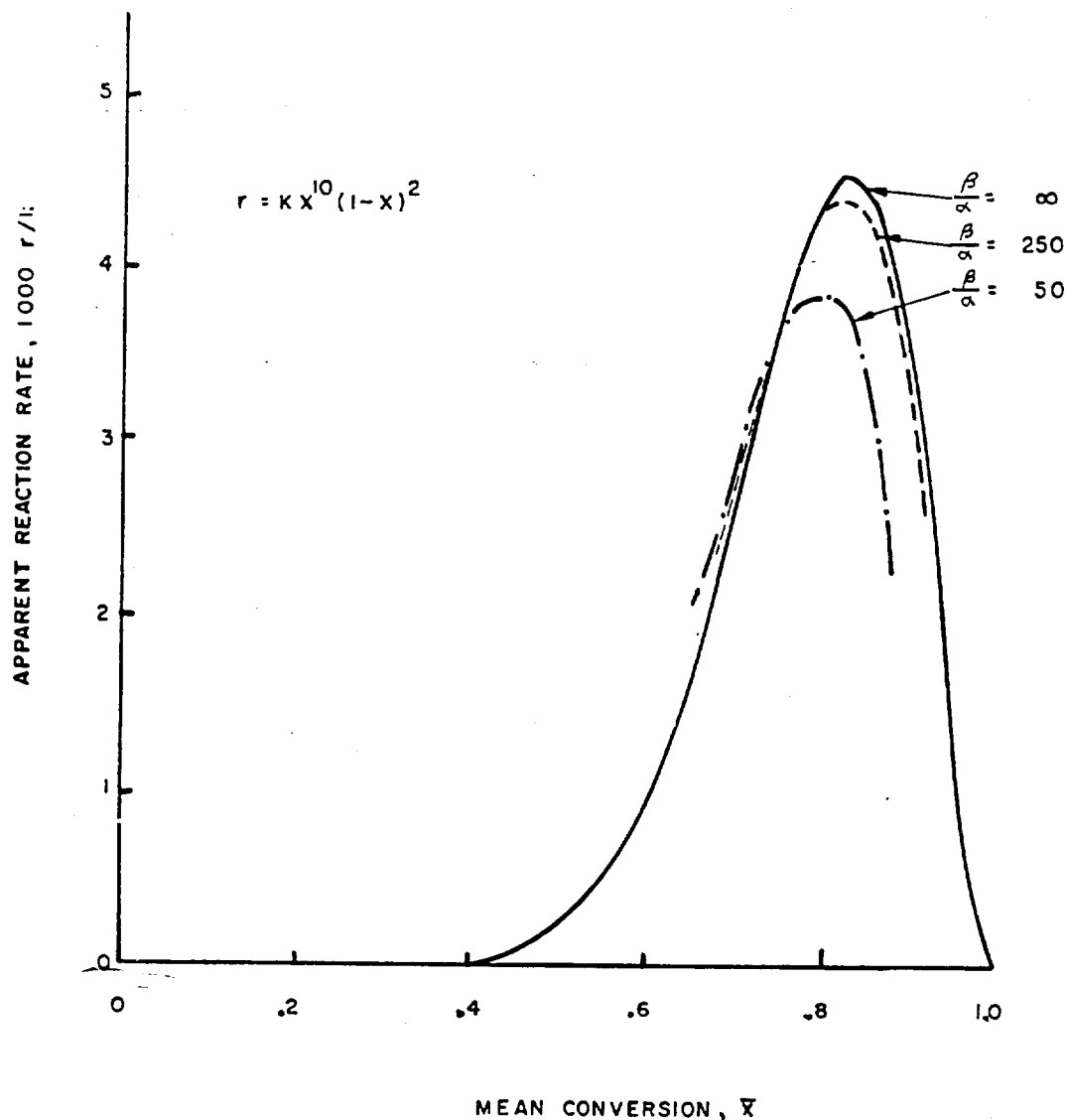


Fig. 5. Effect of mixing intensity on apparent reaction rate—second-order kinetics; various mixing intensities ( $\beta/\alpha$ ).

$\beta/\alpha$ , the resulting curve then has the same character as  $r(x)/k$  for ideal mixing (infinite  $\beta$ ), in that its intersections with lines of slope  $\alpha/k$  give the average steady conversions. One notes that, for high values of  $\beta/\alpha$ , the curve approaches the curve for infinite mixing. The value of  $\beta/\alpha$  for which the mixing, for practical purposes, becomes ideal, increases with increasing  $m$ . The averaged reaction rate is also much more sensitive to mixing for high values of  $\alpha$ . That means that, near the critical flow rate at which the reaction extinguishes, the system is most sensitive to mixing, which is in good agreement with the experimental evidence. Figure 5 shows a corresponding family of curves for one example of an autothermic second-order reaction. The effects are seen to be similar.

In Fig. 3, the critical value of  $\alpha/k$  at blowout is plotted as a function of  $\beta/\alpha$  for different values of  $m$ . One notes again that the larger  $m$  (or the steeper the dependence of reaction rate upon conversion), the stronger the effect of  $\beta/\alpha$ . However, for  $\beta/\alpha > 30$ , the mistake made is relatively small, and in the most sensitive case ( $m = 20$ ) does not exceed 20 per cent. Nevertheless, the dependence of the blowout limit upon the reaction kinetics does indicate that attempts to correlate it with parameters of injector design, such as the pressure drop, should be viewed with some caution. Further, the fact that the reactor is insensitive to mixing for a specific reaction at one mixing rate, does not guarantee the same independence for other reactions at this mixing rate. However, the results of Figs. 2 and 3 should

provide some good guidelines in this direction. It may be noted that a comparison of the values of  $\beta/\alpha$  from Fig. 3 with the values predicted in Sec. 2 for some typical Longwell reactors indicates that, while some designs seem to approach the desired level, some of the injector designs reported in the literature seem to have mixing rates considerably below the desired level.

There are two general conclusions that one can draw from the above results. One is that quite high mixing intensities or pressure drops are needed for exothermic reactions to approach conditions of ideal mixing. But, with a well-designed reactor, such mixing rates are still feasible. Further research on the mixing reaction patterns in such reactors would be very worthwhile. As pointed out previously, we have little experimental information about mixing rates in such reactors. It would be useful, first of all, to test various mixing configurations by standard tracer experiments to see how well their residence-time distributions approximate that of a stirred tank. This would not give any information about the micro-mixing rates, but fortunately there are now experimental tracer techniques available<sup>9,10</sup> to carry out this more delicate measurement, and comparison of different designs along these lines would be very valuable.

A second general conclusion can also be drawn by invoking the results of Sec. 2. That is, since according to (2.5), keeping  $\beta/\alpha$  constant at different reactor sizes requires keeping  $L^2/S$  constant, and since, according to (2.4), keeping  $\alpha$  constant requires keeping  $Sv/L^3$  constant, it follows (as noted earlier) that, in scaling up in such a way as to keep the same  $\alpha$  and  $\beta$ , we must also keep the same  $v/L$ . The pressure drop needed to achieve the desired level of  $\beta/\alpha$  will then increase with reactor size, and one should accordingly use as small a reactor as will not give excessive heat losses (or too low a Reynolds number).

In Fig. 4, the variance of the conversion is shown as a function of  $\beta/\alpha$ . (Only the stable steady-state points are considered.) The standard deviation, normalized on the mean conversion, is essentially independent of the kinetic parameters and the flow rate over the whole working range; examples of departure from this standard form for very low values of  $\alpha/k$  are shown for representative values of  $m$ . One notes also that, for high but realizable values of  $\beta/\alpha$ , the variance becomes so small that our original assumption that the reactor is mixed really applies. For lower values of  $\beta/\alpha$ , the variance starts to increase rapidly. If the variance becomes very large, our model really does not apply because then the reaction becomes localized and flame fronts may start to exist. The model has the interesting feature that it predicts a change from mixed

combustion to highly localized combustion at lower mixing rates. The model can also be used to investigate the dynamic stability of the reactor under conditions of incomplete mixing. These effects will be discussed in more detail in a future paper.

#### ACKNOWLEDGMENTS

The work reported here was supported under Air Force Office of Scientific Research Grant No. AF-AFOSR-921-67. Some of this work represents a part of the research carried out by one of the authors (J.J.E.) in partial fulfillment of the requirements for the degree of Doctor of Philosophy at the City University of New York.

#### REFERENCES

1. LONGWELL, J. P. AND WEISS, M. A.: *Ind. Eng. Chem.* 47, 1634 (1955).
2. VULIS, L. A.: *Thermal Regimes of Combustion*, p. 155, McGraw-Hill, 1961.
3. ESSENHIGH, R. H.: Technical Report FS67-1(W), Combustion Laboratory, Pennsylvania State University, March 1967.
4. BEER, J. M. AND LEE, K. B.: *Tenth Symposium (International) on Combustion*, p. 1187, The Combustion Institute (1965).
5. ARIS, R. AND AMUNDSON, N. R.: *Chem. Eng. Sci.* 7, 121 (1958).
6. EVANGELISTA, J. J., KATZ, S., AND SHINNAR, R.: *Scale-up Criteria for Stirred Tank Reactors*, presented at Symposium on Mixing, Joint Meeting I.M.I.Q.-A.I.Ch.E., Mexico City (September 1967); *A.I.Ch.E. J.*, in press.
7. SPALDING, P. B.: *Combust. Flame* 1, 287, 296 (1951).
8. BATCHELOR, G. K.: *J. Fluid Mech.* 5, 113 (1959).
9. BRODKEY, R. S. AND NYE, J. O.: *Rev. Sci. Instr.* 34, 1086 (1963).
10. BRODKEY, R. S. AND LEE, J.: *A.I.Ch.E. J.* 10, 187 (1964).
11. CORRSIN, S.: *A.I.Ch.E. J.* 3, 329 (1957).
12. CURL, R. L.: *A.I.Ch.E. J.* 9, 175 (1963).
13. CLARKE, E., ODGERS, J., STRINGER, W., AND HARRISON, A. J.: *Tenth Symposium (International) on Combustion*, p. 1151, The Combustion Institute, 1965; *Seventh Symposium (International) on Combustion*, p. 664, Butterworth, 1959.
14. *Seventh Symposium (International) on Combustion*, p. 730, The Combustion Institute (1959). Butterworth, 1959.
15. SHINNAR, R.: *J. Fluid Mech.* 10, 259 (1961).
16. BARTOK, W., HEATH, C. E., AND WEISS, M. A.: *A.I.Ch.E. J.* 6, 685 (1960).

## COMMENTS

*G. G. de Soete*, Institut Français du Pétrole. The determination of kinetic parameters by the stirred-reactor method must deal with a supplementary difficulty: the mixing process which does not exist in the laminar premixed flame methods. The paper shows the strong effect of mixing time and reaction kinetics, but it is not clearly pointed out whether the influence of the residence time/mixing time ratio on the measured rate constant should be expected only on the pre-exponential factor, or could result also in an *apparent* change in the measured value of the average activation energy. If the latter, great attention should be paid to the interpretation of over-all activation energies obtained by stirred-reactor methods; in particular, the well-mixedness should be carefully proved out.

*The Authors*. Departure from perfect mixing certainly does affect the measurement of activation energy. The apparent reaction-rate curves in the text show that, as the mixing intensity decreases, the curves broaden somewhat and shift down toward lower conversion, thus giving the effect of a reduced activation energy. We hope to explore these effects more fully in further work.

*W. A. Sirignano*, Princeton University. Two characteristic times were mentioned in the presentation: a residence time and a mixing time. Actually, a third time appears, that must be important: the chemical reaction time. When the reaction time is considerably longer than the mixing time, the reactor is essentially perfectly mixed. On the other hand, when the mixing time is considerably longer than the reaction time, mixing is the rate-controlling factor and reaction may be considered as instantaneous. Does your

analysis predict these conclusions, which one obtains intuitively?

*The Authors*. These conclusions are implicit in the coalescence model, and can be exhibited by expanding the working equations in powers (and reciprocal powers) of the mixing time/reaction time ratio, with the residence time/reaction time ratio treated as a parameter. The emphasis in the text being slightly different, the results there are developed instead from expansions in powers of the mixing time/residence time ratio, with the reaction time/residence time ratio varied as a parameter.

*J. Swithenbank*, Sheffield University. I would like to draw attention to the important connection between the theoretical study contained in this paper and the design of practical combustion systems. This arises as a result of the applicability of the treatment to real, incompletely mixed systems. Optimization of the combustor design then may be obtained by minimizing the pressure energy required by the stabilizer in order to stir (i.e., generate turbulence in) the combustor. This can be carried out by an energy balance as shown in Swithenbank and Chigier (this Symposium), which is complementary to this paper. These considerations lead to the need both for accurate measurements of flame turbulence intensities, in excess of 100%, and clarification of the position regarding flame-generated turbulence. I would suggest that systems in which the total pressure loss due to the baffle aerodynamics is large compared to the pressure loss due to heat addition (i.e., most practical systems) have a negligible contribution to stirring by flame-generated turbulence.

## Combustion of Ammonium Perchlorate—Some Negative Conclusions

JOSEPH WENOGRAD\*

*University of Hartford, Hartford, Conn.*

AND

REUEL SHINNAR†

*City College of the City University of New York,  
New York, N.Y.*

**D**ESPITE the considerable technological importance of ammonium perchlorate composite solid propellants, and despite a broad international effort to comprehend the mechanism of their combustion, there does not exist today a generally acceptable theory of the burning process. The

Received December 27, 1966; revision received January 12, 1968. R. Shinnar was supported by AFOSR Grant 931-65.

\* Associate Dean, School of Arts and Sciences. Associate Fellow AIAA.

† Professor of Chemical Engineering. Member AIAA.

*Reprinted from AIAA JOURNAL*



conceptual models that have been evaluated, with varying degrees of rigor, may be divided into two broad classes: 1) those in which the rate-controlling processes are presumed to occur at or below the propellant surface and to be part of the vaporization process and 2) those in which the rate-controlling processes are presumed to occur in the gas-phase flame which consumes the vapors that emanate from the propellant surface. Theories of the latter class are older, more fully developed mathematically, more fully tested experimentally, and more generally accepted by those conducting research in this field. The authors of this Note disagree with this "orthodox" interpretation of the available evidence and wish to present arguments that throw the credibility of such mechanisms into doubt.

For didactic purposes, attention will be focused on the combustion of ammonium perchlorate, either pure or with minor percentages of impurities. This is done because the combustion of this rather weakly exothermic material presents an amazingly valid simulation of the combustion of strongly exothermic composite propellants,<sup>1</sup> because it is a pure crystalline material whose thermodynamic properties are fairly well established, and because its physico-chemical and combustion characteristics have been investigated widely. As in the case of composite propellants, the combustion rate of ammonium perchlorate is accelerated by the presence of minor amounts of catalysts and by increased ambient pressure.

The presumption that the rate of propagation of a combustion wave through solid ammonium perchlorate depends on the rate of reactions in the gas-phase flame zone, requires an acceptance of the applicability of the thermal theory of laminar flame propagation<sup>2,3</sup> to this specific situation. The theory is widely accepted and well tested and must be a good representation of many combustion processes.

The application of laminar flame theory to the combustion of a substance in a condensed phase is postulated on the assumption that the rate of energy supply from the flame is sufficient to supply the latent heat of vaporization. Johnson and Nachbar<sup>4</sup> have provided an analytical solution for this specific case of a laminar flame. In some instances, as in the classical study of the combustion of nitroglycerine by Belayev,<sup>5</sup> this procedure seems to work. The vaporization of nitroglycerine, at atmospheric pressure, satisfies the required conditions.

In the case of ammonium perchlorate, however, this assumption appears to fail. Levy and Friedman<sup>6</sup> and many others have studied the combustion of ammonium perchlorate. The adiabatic flame temperature is approximately 1000°C, and the temperature at the solid surface is several hundred degrees lower. At these temperatures the bulk of the energy transfer within a one-dimensional flame zone would be conductive rather than radiative. Levy and Friedman have calculated the magnitude of energy feedback necessary to vaporize sufficient ammonium perchlorate to support an experimentally observed burning velocity of 1 cm/sec at 1500 psi. This calculation was based on the assumption that the vaporization process involves the formation of ammonia and perchloric acid, a reaction that is endothermic by 56-60 kcal/mole. On the basis of purely thermochemical considerations and mass continuity they show that the energy flux at the surface must be 1300 cal/cm<sup>2</sup> sec or 32 Btu/in.<sup>2</sup> sec. This is an immense conductive heat flux.

Since the total temperature rise from the surface to the flame temperature is of the order of several hundred degrees, and since the thermal conductivity of the gas is of order  $2 \times 10^{-4}$  cal/cm°C sec, they concluded that the flame zone thickness would have to be of order 0.2-1.0  $\mu$ .

If the average gas velocity in this region is about 30 cm/sec then the residence time in the reaction zone has a magnitude less than  $3 \times 10^{-6}$  sec. Thus, the reaction has to be extremely fast. The number of collisions experienced by a

particle passing through the reaction zone would be less than  $10^6$ . A simple, one-stage, bimolecular reaction with an activation energy of less than 25,000 cal/mole and a steric efficiency of unity could occur in this time. However, any more complex mechanisms involving unstable intermediates or active radicals becomes virtually impossible in this time scale. It is very difficult to believe that the gas-phase reaction among the decomposition products of ammonium perchlorate could be a simple bimolecular reaction without intermediate steps. If the reaction cannot occur with the required speed, then the flame will not be thin enough to support the reaction wave.

A more serious argument against the application of gas-phase flame theory to ammonium perchlorate combustion can be made in consideration of the strong catalytic effect of copper chromite reported by Levy and Friedman,<sup>6</sup> and many others. One-half percent of this additive, which has a particle size of 10  $\mu$ , doubles the burning rate and even smaller quantities have significant effects. With a concentration of  $\frac{1}{2}\%$ , the average distance between catalyst particles would be 50  $\mu$ , about 50 times the thickness of the postulated flame.

The catalyst could affect the reaction rate either homogeneously or heterogeneously. In order for homogeneous catalysis to occur, there would have to be an appreciable concentration of copper chromite in the gas phase. Even if copper chromite were volatile under the surface conditions, which it is not, the geometry of the flame is such that mixing would be negligible. The diffusivity of the gases in the flame would be of order  $10^{-2}$  cm<sup>2</sup>/sec. The lateral diffusion distance during the  $10^{-6}$  sec residence time in the flame would be about 1  $\mu$ . This is clearly not enough if the average interparticle distance is 50  $\mu$ . Since homogeneous catalysis is implausible, heterogeneous catalysis should be considered. Again, the transport processes necessary to affect a flame of the postulated geometry are simply not available. There is not enough time for an appreciable amount of the gas to reach the catalyst surface. Even if there were, the heterogeneous reaction would have to be very fast indeed to accelerate a process which occurs in  $10^{-6}$  seconds without a catalyst.

The strong catalytic action of a heterogenous solid catalyst leads to an almost insoluble conflict when considered in light of a one-dimensional flame model and a reaction zone 1- $\mu$  thick. It is necessary to change the dimensions of the process by at least one or two orders of magnitude before reasonable results are obtained. The combustion of ammonium perchlorate must therefore be far more complex than the simple normally accepted laminar flame mechanism<sup>1,4</sup> would indicate.

These considerations indicate that the heat transferred back from the gas phase must be considerably smaller than normally assumed. It must then be presumed either that the heat of evaporation of AP is very small or that heat is generated during the decomposition of the solid either at the surface or below it. Such exothermic reactions could occur in the liquid layer observed by Hightower and Price.<sup>7</sup> Part of this heat could also be generated by a low-temperature decomposition reaction below the surface. Such low-temperature decomposition reaction could well be catalyzed by copper chromite.

The purpose of this Note is neither to establish an alternative mechanism for the burning of ammonium perchlorate nor to claim that the gas-phase flame is of no importance. Gas-phase flames certainly exist and may play an important role in the combustion process. This Note is intended to show that although the presently accepted theory has achieved some success in fitting burning rate vs pressure data it leads to some quite unreasonable assumptions as to the magnitude of thermal gradients, reaction rates, and transport processes. This is especially true if the effect of heterogenous catalysts on the burning rate are considered. It is therefore highly unlikely that the burning of pure AP is governed solely by an endothermic evaporation followed by an exothermic reaction in the gas phase close to the surface.

## References

- <sup>1</sup> Adams, G. K., Newman, B. H., and Robins, A. B., "The Combustion of Propellants Based upon Ammonium Perchlorate," *Eighth Symposium (International) on Combustion*, Williams and Wilkins, Baltimore, Md., 1962, p. 693.
- <sup>2</sup> Evans, M. W., *Chemical Reviews*, Vol. 51, 1952, p. 363.
- <sup>3</sup> Zeldovitch, Y. B. and Frank-Kamenetsky, D. A., *Comptes Rendus de l'Academie des Sciences URSS*, Vol. 19, 1938, p. 693.
- <sup>4</sup> Johnson, W. E. and Nachbar, W., "Deflagration Limits in the Steady Linear Burning of a Monopropellant with Application to Ammonium Perchlorate," *Eighth Symposium (International) on Combustion*, Williams and Wilkins, Baltimore, Md., 1962, p. 678.
- <sup>5</sup> Belayev, A. T., *Acta Physicochim, URSS*, Vol. 8, 1933, p. 783.
- <sup>6</sup> Levy, J. B. and Friedman, R., "Further Studies of Pure Ammonium Perchlorate Deflagration," *Eighth Symposium (International) on Combustion*, Williams and Wilkins, Baltimore, Md., 1962, p. 663.
- <sup>7</sup> Hightower, J. D. and Price, E. W., "Combustion of Ammonium Perchlorate," *11th Symposium on Combustion*, Combustion Institute, Pittsburgh, 1967, p. 463.

THE EFFECTS OF PERTURBATIONS IN  
FLOW-RATE ON A STIRRED COMBUSTOR

BY

Frederick J. Krambeck\*\*

Stanley Katz\*

and

Reul Shinnar\*

\* City University of New York

\*\* Mobil Research and Development Corp.,  
Princeton, New Jersey

THE EFFECT OF PERTURBATIONS IN FLOW-RATE  
ON A STIRRED COMBUSTOR

1. Introduction

The effects of random fluctuations in gas flow-rate on the performance of a well-stirred combustor will be studied by means of an idealized model. Such a model can be applied, for example, to automotive exhaust gas afterburners, where the fluctuations in flow rate are quite substantial, to the recirculation zone behind a flame holder, where the fluctuations arise from flow disturbances and turbulence, or to the design of stirred combustors for chemical kinetic measurements, where one would like to estimate the effects of flow perturbations on the accuracy of measured reaction rates. In addition, if one thinks of a turbulent flame as a large ensemble of such reactors, it is possible that some insight as to the effects of turbulent fluctuations on complex kinetics, apparent activation energies, etc. may be obtained from consideration of the statistics of this model.

2. The Model

The model consists of a well-stirred vessel of volume  $v$  with an inlet and outlet volumetric flow rate equal to  $w$ . This flow rate fluctuates randomly between the two fixed values  $w_1$  and  $w_2$  according to the probability structure of a Markov process. This is a special case of a model treated at length in [1]. Other aspects are presented in [2,3,4]. Denoting the probability that  $w=w_1$  by  $\pi_1$  and the probability that  $w=w_2$  by  $\pi_2$ , this implies that  $\pi_1$  and  $\pi_2$  evolve with time

according to the equation

$$\begin{aligned} \frac{d\pi_1}{dt} &= \lambda_2 \pi_2 - \lambda_1 \pi_1 \\ \frac{d\pi_2}{dt} &= \lambda_1 \pi_1 - \lambda_2 \pi_2 \end{aligned} \quad (1)$$

where  $\lambda_1$  and  $\lambda_2$  are the mean switching rates in the respective directions.

A material balance on the reactor gives an equation of change of the form

$$\frac{dx}{dt} = f(w, x) \quad (2)$$

where  $x$  is the concentration of reactant. We now define functions  $p_1(x)$  and  $p_2(x)$  so that the joint probability that  $w=w_1$  and  $x$  is in the interval  $(x, x+dx)$  is given by  $p_1(x) dx$ .

These then satisfy

$$\begin{aligned} \frac{d}{dx}[f(w_1, x) p_1(x)] &= -\lambda_1 p_1(x) + \lambda_2 p_2(x) \\ \frac{d}{dx}[f(w_2, x) p_2(x)] &= \lambda_1 p_1(x) - \lambda_2 p_2(x) \end{aligned} \quad (3)$$

We have assumed here that the process has reached its stationary probability distribution. The overall probability density function is just given by  $p_1(x) + p_2(x)$ .

Adding the two equations in (3) together, we find

$$\frac{d}{dx}[f_1(x) p_1(x) + f_2(x) p_2(x)] = 0$$

where  $f_1(x) = f(w_1, x)$ . Thus

$$f_1(x) p_1(x) + f_2(x) p_2(x) = c$$

where  $c$  is some constant independent of  $x$ .

If the expected value of  $f(w, x)$  is finite, it must happen that  $c=0$ , since

$$\begin{aligned} \langle f(w, x) \rangle &= \int_{-\infty}^{\infty} [f_1(x) p_1(x) + f_2(x) p_2(x)] dx \\ &= \int_{-\infty}^{\infty} c dx \end{aligned} \quad 119$$

Then

$$f_1(x)p_1(x) = -f_2(x)p_2(x) \quad (4)$$

Substituting (4) into (3),

$$\frac{d}{dx}[f_1(x)p_1(x)] + \left[ \frac{\lambda_1}{f_1(x)} + \frac{\lambda_2}{f_2(x)} \right] f_1(x)p_1(x) = 0 \quad (5)$$

Since  $p_1$  and  $p_2$  are probabilities they must be non-negative.

Then (4) implies that  $p_1(x)$  and  $p_2(x)$  can differ from zero only at points where  $f_1(x)$  and  $f_2(x)$  differ in sign. Defining

$g(x) = |f_1(x)p_1(x)| = |f_2(x)p_2(x)|$ , (5) becomes

$$\frac{dg}{dx} + \left[ \frac{\lambda_1}{f_1(x)} + \frac{\lambda_2}{f_2(x)} \right] g = 0$$

or

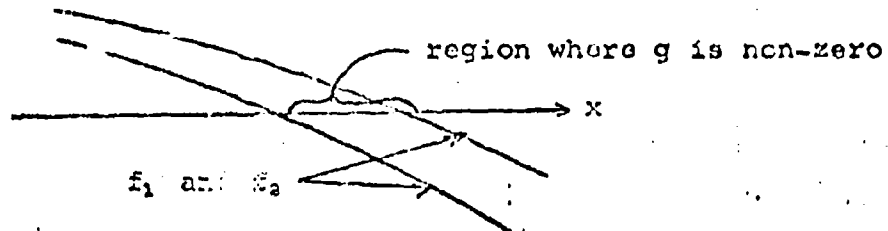
$$\frac{d}{dx}[\ln g] = - \left[ \frac{\lambda_1}{f_1(x)} + \frac{\lambda_2}{f_2(x)} \right] \quad (6)$$

To find boundary conditions on  $g$  to use with (6), consider the points where either  $f_1(x)$  or  $f_2(x)$  passes through zero.

Since  $p_1(x) = \frac{g(x)}{|f_1(x)|}$  is a probability density it must be integrable. Unless  $|f_1'(x)| = \infty$  at the point where  $f(x) = 0$ , an unusual situation,  $g(x)$  must approach zero at such a point.

Thus equation (6) is applied to regions on the  $x$ -axis over which  $f_1$  and  $f_2$  are of opposite sign. The values of  $g$  at the end points of such a region, which are necessarily zeros of either  $f_1$  or  $f_2$ , are zero. In fact, a further condition must be satisfied by  $f_1$  and  $f_2$  over the region. Since  $g \rightarrow 0$  at each singular point (i.e. a zero of either  $f_1$  or  $f_2$ ),  $\ln g \rightarrow -\infty$ . Thus  $\frac{d}{dx} \ln g$  must  $\rightarrow +\infty$  at the left end of the region and  $\rightarrow -\infty$  at the right end, so that the function that goes to zero at the left

end (either  $f_1$  or  $f_2$ ) must be positive in the region and that which goes to zero at the right end must be positive over the region. Therefore, in any region of the  $x$ -axis where  $g(x)$  is non-zero, the functions  $f_1(x)$  and  $f_2(x)$  must appear as in the sketch:



Physically, the points where  $f_1$  or  $f_2$  pass through zero are steady states when the flow is fixed at  $w_1$  or  $w_2$  respectively. The requirement that the slopes of  $f_1$  and  $f_2$  be negative at these points for solutions to exist between them is just the same as the conditions for stability of these steady states. At the stationary condition, then, the system will oscillate in a region bounded by stable steady states corresponding to the two different flow rates.

Some additional qualitative information on the shape of the probability density function may be inferred from the behavior of equation (6) near the ends of a stable region. Near the roots of  $f_1$ ,

$$f_1(x) \approx f_1'(a_1)(x-a_1)$$

where  $a_1$  is the root in question. If  $a_1$  is a stable root, then  $f_1'(a_1)$  will be negative. For value of  $x$  near  $a_1$ , equation (6) then becomes

$$\frac{d}{dx} \ln g \approx \frac{-\lambda_1}{f_1'(a_1)(x-a_1)}$$

since  $\lambda_2/f_2(x)$  will be negligible compared to  $\lambda_1/f_1'(a_1)(x-a_1)$ .

This gives

$$g(x) \approx c_1 |x-a_1|^{\frac{\lambda_1}{f_1'(a_1)}}$$

Then, as  $x \rightarrow a_1$

$$p_1(x) \rightarrow \frac{c_1}{|f_1'(a_1)|} |x-a_1|^{x-1}$$

$$p_2(x) \rightarrow 0$$

where  $a_2$  is a root of  $f_2$ .

$$p_2(x) = \frac{C_2}{|f_2(a_2)|} (x-a_2)^{s-1}$$

Here  $r$  and  $s$  are given by

$$r = \frac{\lambda_1}{|f_1(a_1)|} \quad s = \frac{\lambda_2}{|f_2(a_2)|} \tag{7}$$

Thus we see that the probability density,  $p_1(x) + p_2(x)$ , will have an infinity at  $x=a_1$  if  $r < 1$  and a zero at  $x=a_1$  if  $r > 1$ . It will have an infinity at  $x = a_2$  if  $s < 1$  and a zero there if  $s > 1$ . In the fortuitous case where  $r = 0$  or  $s = 0$ , the density will approach a non-zero constant at the respective point.

### 3. Results for Simple Kinetics

While we are interested primarily in the behavior of the model in the case of an adiabatic, exothermic reaction, we first derive the results for simpler reactions for comparison. Thus for an isothermal first order reaction, the right hand side of equation (2) becomes

$$f(w,x) = \frac{w}{v} (x_0 - x) - kx \tag{8}$$

where  $x_0$  is the inlet concentration and  $k$  is the rate coefficient.

Defining a new variable  $y$  by

$$y(x) = \frac{x - \frac{w_1 x_0}{w_1 + kv}}{\frac{w_2 x_0}{w_1 + kv} - \frac{w_1 x_0}{w_1 + kv}}$$

The solution to equation (3) is

$$p_1(y) = \frac{y^{r-1} (1-y)^s}{B(r,s+1)} \quad \bar{p}_1$$
  
$$p_2(y) = \frac{y^r (1-y)^{s-1}}{B(r+1,s)} \quad \bar{p}_2 \tag{9}$$



where

$$r = \frac{\lambda_1}{w_1 + k}, \quad s = \frac{\lambda_2}{w_2 + k}, \quad \bar{p}_1 = \frac{\lambda_1}{\lambda_1 + \lambda_2}, \quad \bar{p}_2 = \frac{\lambda_2}{\lambda_1 + \lambda_2}$$

and where  $B(r, s)$  is the beta function:

$$B(r, s) = \int_0^1 t^{r-1} (1-t)^{s-1} dt$$

Some typical curves for  $p_1(x) + p_2(x)$  calculated from (9) are shown in Figure 1. In performing the calculation the time has been scaled so that  $v/\bar{w}$ , the residence time, is unity.

The parameters used are defined as follows:

$$\bar{w} = \bar{p}_1 w_1 + \bar{p}_2 w_2$$

$$\bar{\lambda} = \frac{1}{2}(\lambda_1 + \lambda_2)$$

$$c = (w_2 - w_1) / \bar{w}$$

For the second-order isothermal case, the right hand side of equation (2) becomes

$$f(w, x) = \frac{v}{V} (x_0 - x) - kx^2 \quad (10)$$

This can be rewritten in the form

$$f(w_1, x) = -k(x - a_1)(x + b_1)$$

$$f(w_2, x) = -k(x - a_2)(x + b_2)$$

Solving equation (3) then gives

$$p_1(x) = \frac{c_1}{k} \frac{|x - a_1|^{r-1} |x - a_2|^s}{|x + b_1|^{r-1} |x + b_2|^s} \quad (11)$$

$$p_2(x) = \frac{c_1}{k} \frac{|x - a_1|^r |x - a_2|^{s-1}}{|x + b_1|^r |x + b_2|^{s-1}}$$

where  $c_1$  is a normalization constant calculated numerically.

Curves calculated from (10) look quite similar to those calculated from (9). An example is given in [1].

#### 4. Results for Combustion

We now consider an exothermic reaction under adiabatic conditions. For this situation both the material and energy

balance must be considered. The material balance is, for constant inlet concentration  $x_0$ ,

$$v \frac{dx}{dt} = w(x_0 - x) - v R(x, T) \tag{12}$$

and the energy balance is

$$v \frac{dT}{dt} = w(T_0 - T) + v \frac{\Delta T^*}{x_0} R(x, T) \tag{13}$$

where  $T$  is temperature,  $R(x, T)$  is the reaction rate, and  $\Delta T^*$  is the temperature increase resulting from complete conversion. Multiplying (12) by  $\frac{\Delta T^*}{x_0}$  and adding to (13),

$$v \frac{d}{dt} \left[ \frac{x \Delta T^*}{x_0} + T \right] = w \left\{ [\Delta T^* + T_0] - \left[ \frac{x \Delta T^*}{x_0} + T \right] \right\} \tag{14}$$

Since  $w$  is always positive, the quantity  $\left[ \frac{x \Delta T^*}{x_0} + T \right]$  will approach  $[\Delta T^* + T_0]$  monotonically, even though  $w$  fluctuates, so that after a long time, when the process becomes stationary,

$$T = T_0 + \Delta T^* \left( 1 - \frac{x}{x_0} \right)$$

or, scaling  $x$  so that  $x_0 = 1$ ,

$$T = T_0 + \Delta T^* (1 - x) \tag{15}$$

Actually, can be shown using the general stability criterion for Markov Processes [5] that (15) would be true for the stationary solution even if one of the states of  $w$  were negative, provided only that

- $\frac{w_1}{v} < \frac{1}{2}(\lambda_1 + \lambda_2)$
- $\frac{w_2}{v} < \frac{1}{2}(\lambda_1 + \lambda_2)$
- $\frac{w}{v} < \frac{2w_1 w_2}{v^2 (\lambda_1 + \lambda_2)}$

These relations are automatically true if  $w_1$  and  $w_2$  are both positive. The reaction rate,  $R(x, T)$ , may be taken as

$$R(x, T) = \frac{E}{RT^2} x \tag{16}$$

Substituting (15) into (16),

$$R(x,T) = k_0 e^{-\left[\frac{E}{RT} - \frac{A}{T}\right]} x^n \quad (17)$$

where

$$\alpha = \frac{E}{RT_0} \quad , \quad \theta = \frac{AT}{T_0}$$

Thus, for this case,

$$f(w,x) = \frac{w}{v} (1-x) - k x^n \exp\left[-\frac{E}{RT} + \frac{AT}{T_0}\right] \quad (18)$$

The interesting feature of this system is the existence of multiple roots of  $f_1(x)$  and  $f_2(x)$ , allowing the possibility of disjoint regions of non-zero probability. Figure 2, for example, shows a case where both  $f_1(x)$  and  $f_2(x)$  have three roots. In this case the entire probability distribution would be contained in two small regions. One region is bounded by the smallest root of  $f_1(x)$  and the smallest root of  $f_2(x)$ , and the other by the largest root of  $f_1(x)$  and the largest root of  $f_2(x)$ . The latter two points are very close together and also very close to  $x=1$ , so that they cannot be seen distinctly on the graph. Note that there will be no probability of being between the two middle roots, since  $f_1(x)$  and  $f_2(x)$  cross the axis with positive slope at these points. The middle roots of the two curves represent unstable steady states of the system with constant flow rates. The relative weights of the two regions are arbitrary, depending on the initial probability distribution of the system. The fact that the probability of being anywhere between the two regions is zero, together with the fact that the concentration varies continuously with time, shows that once the concentration is within one of the

two stable regions, it will never leave that region.

The stable region at low concentration, or high conversion, corresponds to an ignited state of a combustion process, while the stable region at high concentration, or low conversion, corresponds to an unignited state. Thus, under conditions where each of the allowable flow rates through the stirred reactor result in both ignited and unignited steady states when held steady, the probability distribution will be concentrated over two stable regions. If the system is once ignited it will not become extinguished, and if it is not ignited it will not spontaneously ignite.

A more interesting situation arises when the parameter values are such that  $f_1(x)$  has only a low-concentration (ignited) root and  $f_2(x)$  has only a high-concentration (extinguished) root. This will be illustrated with a concrete example, namely, the oxidation of CO in automotive exhaust gas afterburner. Reaction rate expressions for this process are given by Kozlov [6]. For exhaust gas conditions we may approximate his equations (roughly) by

$$\frac{d[\text{CO}]}{dt} = -3.16 \times 10^8 [\text{CO}] \exp\left(-\frac{32,200}{RT}\right) \quad (19)$$

(i.e.  $k_\infty = 3.16 \times 10^8$ ,  $E = 32,200$ ). Assuming  $T_0 = 1000^\circ\text{F}$  and  $\Delta T^* = 440^\circ\text{F}$ , which would typically occur under light-load engine conditions, we find  $\alpha = 20$  and  $\theta = 0.3$ . ... Scaling the time by the residence time of the combustor, the  $k$  of equation (18) is equal to  $k_\infty \tau$ , where  $\tau$  is the residence time.

Probability densities that result from the above parameter values are shown in Figure 3 for a residence time of

127 msec. and for two different values of the fluctuation rate  $\bar{\lambda}$ . A value of  $\bar{\lambda}=1$  implies that the flow switches, on the average, once per residence time. It can be seen that at this particular condition the shape of the probability density is quite sensitive to the fluctuation rate. In the absence of fluctuations, the parameter values used give two stable steady states:  $x = .205$  and  $x = .759$ . It can be seen that as the fluctuation rate increases the probability density curve develops peaks in the area of these points.

To compare the properties of our model to those of a steady flow system, it is useful to compute the mean outlet concentration. In doing so, one must distinguish between the time-averaged and the flow-averaged value. The time-average is given by

$$\langle x \rangle = \int x [p_1(x) + p_2(x)] dx \quad (20)$$

and the flow-average by

$$\langle x \rangle = \frac{1}{w} \int x [w_1 p_1(x) + w_2 p_2(x)] dx \quad (21)$$

It is the flow-averaged value that determines the conversion efficiency for CO oxidation, while the time-average is the value that would be measured by a probe at the outlet.

Curves similar to those in Figure 3 were calculated for different residence times. The flow-average concentrations obtained from these are plotted in Figure 4. The curve for steady flow is also given for comparison. It can be seen that the main effect of the fluctuations is to smear out the region of blowout, making it more gradual. In addition, as the fluctuation rate decreases the blowout point is shifted somewhat

# NOT REPRODUCIBLE

towards higher residence times (lower flow rates). In the region of low conversion the fluctuations improve the performance somewhat. In a practical design, one which gives high conversion, the fluctuations will always decrease conversion, however. The magnitude of this decrease can be kept small by a design which operates far from blowout.

Another question of some interest concerns the errors that result in measured reaction rates due to flow perturbations. To assess this effect an Arrhenius plot was constructed for the same conditions as Figure 4. This is shown in Figure 5, where  $\ln(k_a/k_m)$  is plotted against  $E/R\langle T \rangle$ . Here  $k_a$  is the apparent rate coefficient. Curves are shown both for time-average and flow-average data. It can be seen that if the data covers a sufficiently large range the errors in measured rate will be small for the particular conditions used.

## 5. Closure

Thus we have seen how this idealized model can be used to evaluate the effects of flow-rate perturbations on the performance of a well-mixed combustor. It must be emphasized, however, that conclusions drawn in this manner depend strongly on the assumption of perfect mixing. Thus one must use caution in applying this procedure to situations where departures from perfect mixing may be more important than fluctuations in flow rate. It can be seen that if the data covers a sufficiently large range the errors in measured rate will be small for the particular conditions used.

## References

1. F. J. Krambeck, "Stochastic Mixing Models for Turbulent Reactors", Ph.D. Thesis, City University of New York (1968).
2. F. J. Krambeck, R. Shinnar and S. Katz, "Stochastic Mixing Models for Chemical Reactors", I/EC Fundamentals 6, 276 (1967).
3. F. J. Krambeck, S. Katz and R. Shinnar, "Interpretation of Tracer Experiments in Systems with Fluctuating Throughput", I/EC Fundamentals 8, 431 (1969).
4. F. J. Krambeck, S. Katz and R. Shinnar, "A Stochastic Model for Fluidized Beds", Chem. Eng. Sci. 24, 1497 (1967).
5. I. Ia. Kats and N. N. Krasovskii, "On the Stability of Systems with Random Parameters", PMM 24, 809-823 (1960).
6. G. I. Kozlov, "On High Temperature Oxidation of Methane", Seventh Symposium (International) on Combustion, 142-149 (1958).

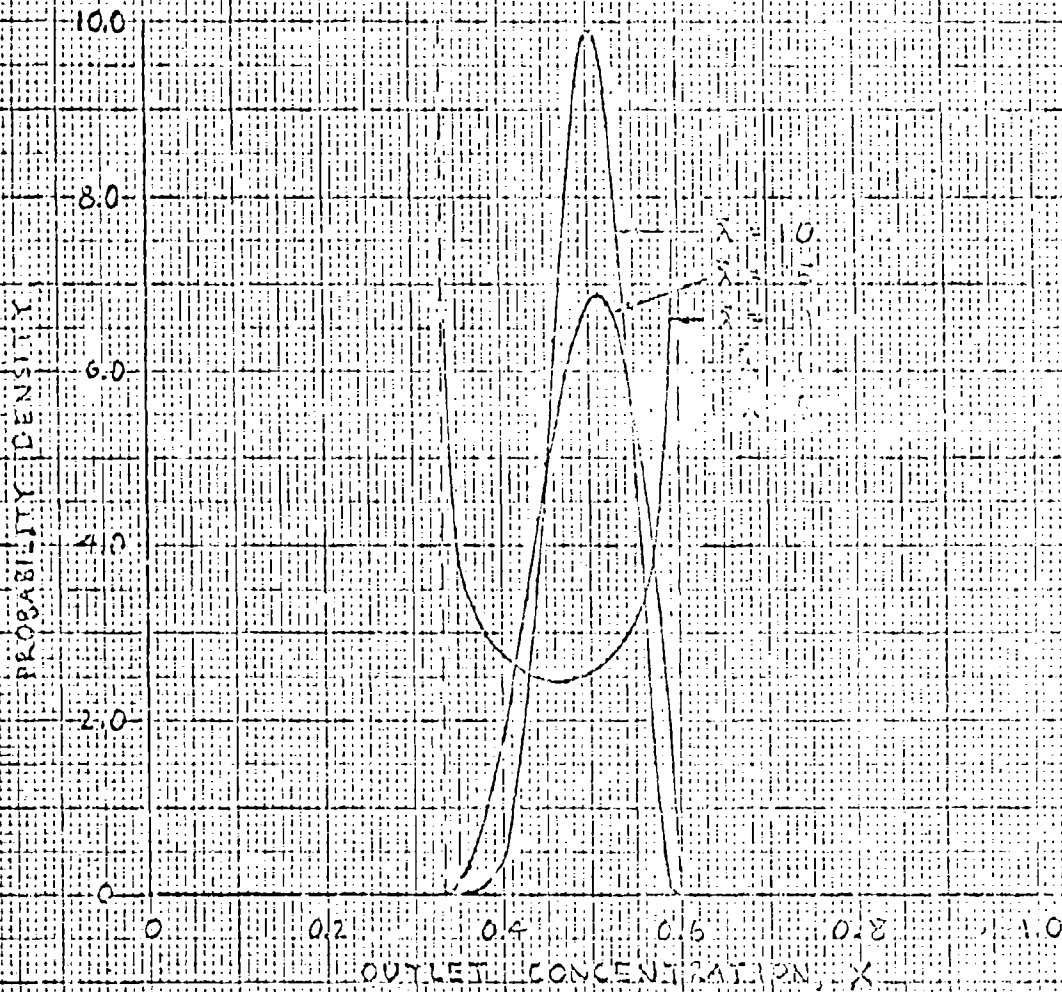
Acknowledgments - This work has been supported by the Air Force Office of Scientific Research AFOSR Grant No. 921-67

PROBABILITY DENSITY OF OUTLET CONCENTRATION  
FOR FIRST ORDER REACTION (3)  
(TYPICAL VALUES)

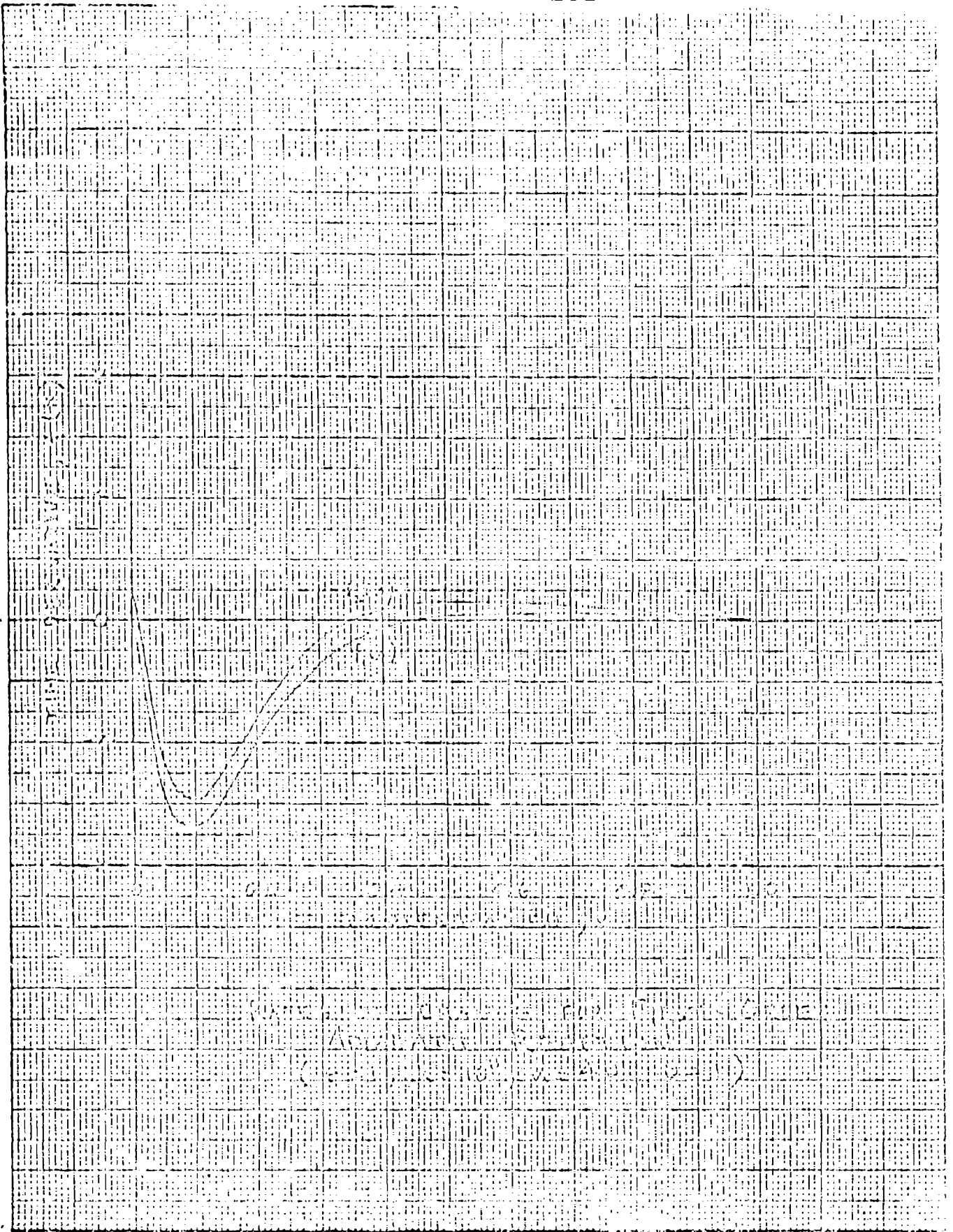
$$\lambda_1 = \lambda_2$$

$$C = 1$$

$$t = 1$$







REL. HUM. TEMP. (C)

$\frac{d \ln p}{dT} = \frac{L}{RT^2}$   
 $\ln p = -\frac{L}{RT} + C$   
 $\ln p = -\frac{L}{R} \cdot \frac{1}{T} + C$   
 $\ln p = -\frac{L}{R} \cdot \frac{1}{T} + C$   
 $\ln p = -\frac{L}{R} \cdot \frac{1}{T} + C$

Fig. 1. Relative humidity as a function of temperature.

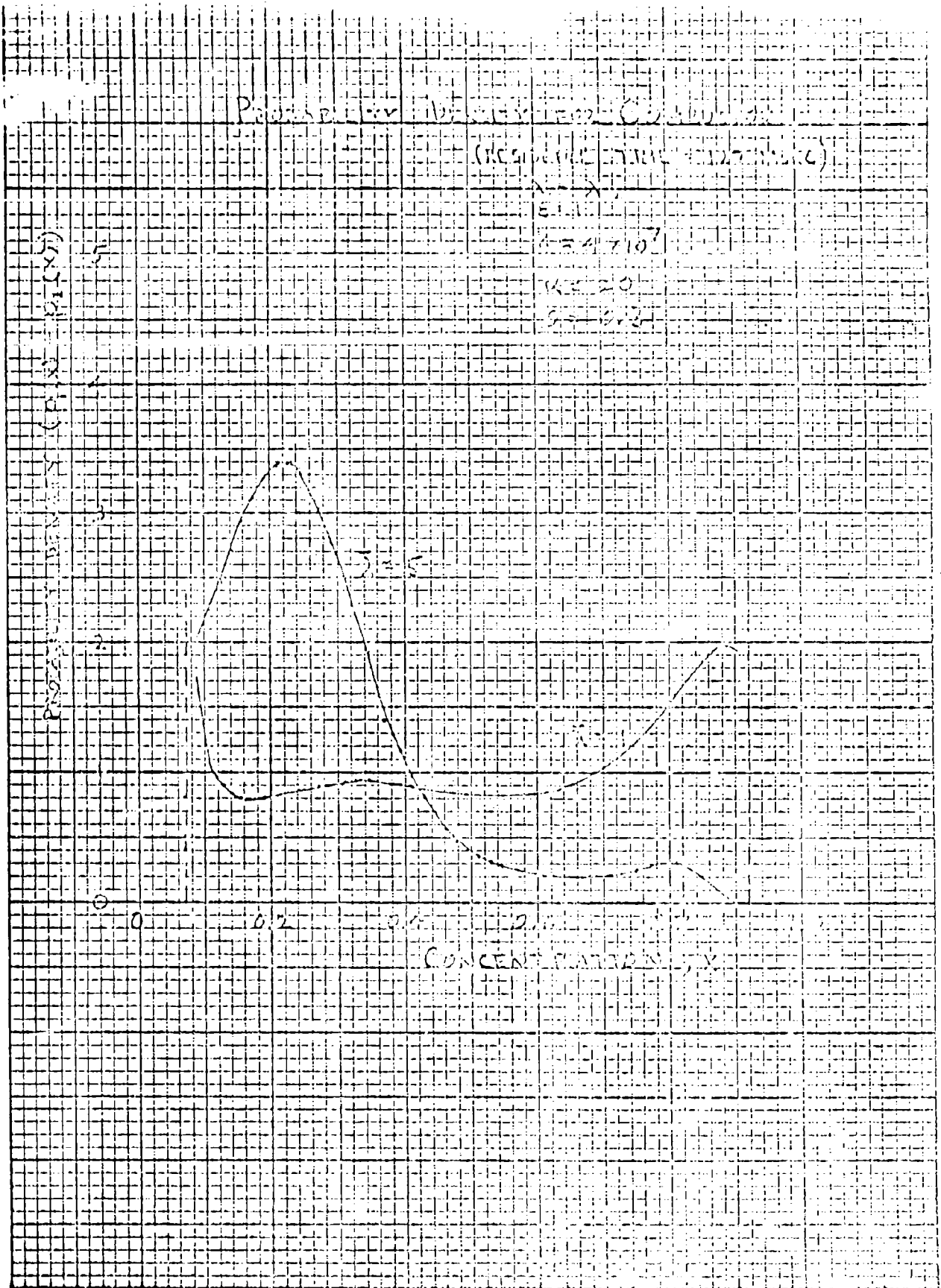
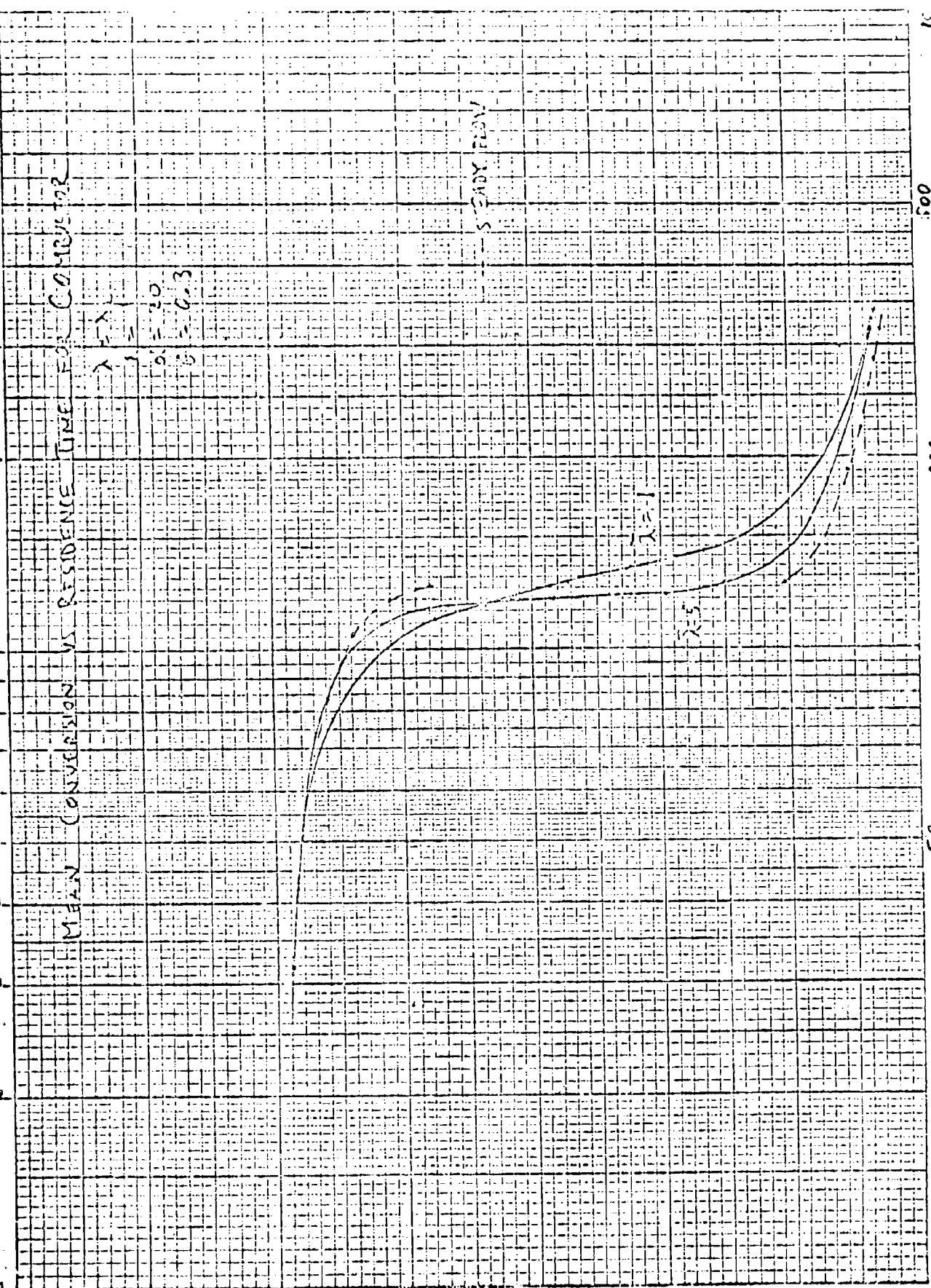


Figure 2

MEAN CONVERSION VS RESIDENCE TIME FOR COMPLET

$\lambda = 1$   
 $\lambda = 2$   
 $\lambda = 3$

STEADY STATE



RESIDENCE TIME

20

50

100

200

500

1000

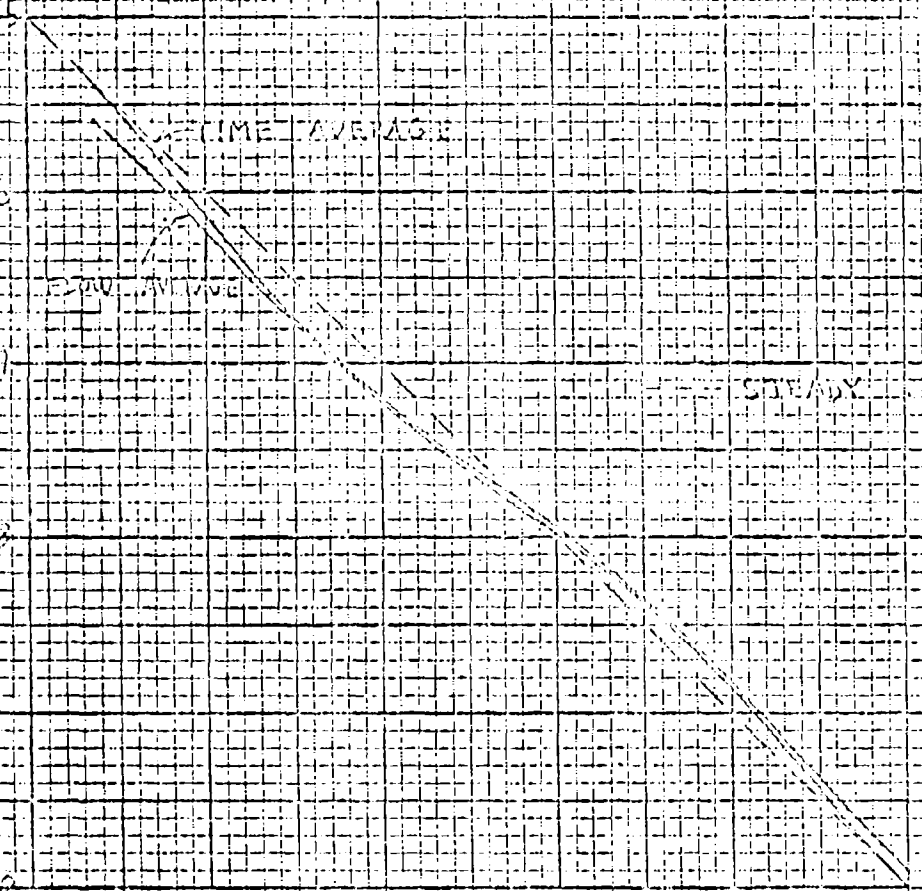
1000  
500  
200  
100  
50  
20

ABUNDANCE PRODUCTION (0.5-1.5-2.0)

$\ln(R_{10}/R_{20})$

TIME AVERAGE

STEADY STATE



15 16 17 18 19 20

$\ln(R_{10}/R_{20})$